Thesis submitted for the degree of

Doctor of Philosophy

at the University of Leicester

by

Kwame S. Amaning, BSc, MSc

University of Leicester

October 2002

ProQuest LLC
789 East Eisenhower Parkway
P.O. Box 1346
Ann Arbor, MI 48106-1346

FOR MY PARENTS AND ALL THE FAMILY

THE CONSEQUENCES OF TYROSINE MODIFICATION IN SIGNALLING PROTEINS

Kwame S. Amaning, University of Leicester, Leicester, LEI 9HN

ABSTRACT

Nitric oxide is a ubiquitous signalling molecule that plays a key role in cell physiology. Nitric oxide can react with a number of agents *in vivo* to form reactive species capable of modifying a range of biomolecules. The formation of nitrotyrosine in cells and tissues exposed to reactive nitrogen species is well documented, however, the mechanisms through which this modification affects cell function continue to be elucidated. SH2 domains are the major endogenous receptors that mediate protein-protein interactions between phosphotyrosine containing proteins and their intracellular binding partners. The interaction between a nitropeptide and the SH2 domain of the Src kinase Fyn has been investigated. Using nuclear magnetic resonance and a fluorescence resonance energy transfer based assay the dissociation constants of the high affinity phosphopeptide was determined as 40 nM, whilst the affinity of the nitropeptide and the non-modified peptide for the protein was markedly weaker (0.7 mM and 1.4 mM respectively). The chemical shift changes observed on binding of the nitropeptide, as visualised using heteronuclear single quauntum correlation spectroscopy, were similar to those generated on the binding of the phosphopeptide to ^{15}N labelled SH2 domain. Using computer modelling, the weak binding of the nitropeptide was rationalised on the basis of a lack of key interactions between the nitrotyrosine moiety and residues that form the phosphotyrosine binding pocket of the SH2 domain. The affinity of the peptides for Fyn SH2 domains was also demonstrated in the immunoprecipitatated Fyn derived from Jurkat cells. There is evidence to suggest that *in vivo* protein-bound nitrotyrosine is reduced to aminotyrosine. In addition, therefore, the aminotyrosine containing peptide was investigated as being a possible substrate for Src kinase, with provisional evidence suggesting that the aminopeptide might undergo phosphorylation by Src.

THESIS ASSOCIATED PUBLICATIONS

Abstract

The binding of peptide motifs containing modified tyrosine residues to the SH2 domain of Fyn. Amaning K., Jones D. J. L., Lamb J., H., Lord G., Roberts G. C. K., Shuker D. E. G. (2001) Toxicology. **164**, 198

Paper

Amaning, K.S., Roberts G.C.K., and Shuker, D.E.G. A nitropeptide fails to bind to the SH2 domain of Fyn. A possible role for reactive nitrogen species in Src kinase mediated carcinogenesis. *Manuscript in preparation.*

ACKNOWLEDGEMENTS

I would firstly like to thank my supervisors, D. Shuker and G. Roberts for their guidance and support over the past four years. Their infectious enthusiasm for science and their wealth of knowledge has been the tonic that has guided me through some trying times. I would also like to thank S. Prigent for her help and advice.

I would like to thanks all the members of BMI and Biological NMR for creating environments that were a joy to work in. In particular I would like to thank the mass spectrometrists (Don, Jon and Gwyn) for the analyses they conducted. Ian and particularly Igor are thanked for their assistance and patience in guiding me through the NMR; as are Mags and Carol, for the time they spent assisting me.

I am indebted to I. Campbell for the gifts of the Fyn expression plasmid and the NMR assignments.

Additional thanks go to all those who have attempted (and on the whole succeeded) in keeping me happy and smiling over the recent years through. You are too many to name individually but your encouragement and support was greatly appreciated. I will mention Syrup (enough said!!) Dani and in particular Bob, who has and continues to look out for me. Thanks to Lu for always being there.

Finally, to my rocks: my parents, brothers, sister and the little ones.

CONTENTS

ABBREVIATIONS

AngII - Angiotensin II

aTyr - 3-aminotyrosine

BSA - Bovine serum albumin

CE - Capillary Electrophoresis

cNOS - Constitutive nitric oxide synthase

cGMP - Cyclic guanylate monophosphate

ESI MS - Electrospray ionisation tandem mass spectrometry

FAB - Fast atom bombardment

FYB - Fyn binding protein

GDP - Guanylate diphosphate

GTP - Guanylate triphosphate

HPA - *p*-hydroxyphenylacetate

HPLC - High Preformance Liquid Chromatography

HSQC - Hetronuclear single quantum correlation

iNOS - Inducible nitric oxide synthase

IPTG - Isopropyl-D-thiogalactopyanoside

ITC - Isothermal Calorimetry

K_d - Dissociation constant

MPT - Mitochondrial permeability transition

MHC - Major histocompatibility complex

MS - Mass spectrometry

NanoES - Nanoelectrospray ionisation

NO - Nitric oxide

NO_x - Nitrogen Oxides

nTyr - 3-nitrotyrosine

$ONOO^-$ - Peroxynitrite

PARS - Poly ADP ribosyl synthetase

PLC - Phospholipase C

PMSF - Phenylmethyl-sulfonylfluoride

PTK - Protein tyrosine kinases

pTyr - Phosphotyrosine

PTB - Phosphotyrosine binding domain

PPHN - Persistent Pulmonary Hypertension of the Newborn

RNS - Reactive nitrogen species

RTK - Receptor tyrosine kinase

SAP - SLAM-associated protein

SH - Src Homology

SLAM - Signalling lymphocyte-associated molecule

SOD - Superoxide dismutase

SPR - Surface Plasmon Resonance

TCR - T cell receptor

TNM - Tetranitromethane

TB - Terffic Broth

XO - Xanthine oxidase

CHAPTER 1:

INTRODUCTION

INTRODUCTION

Since being identified as endothelial derived relaxing factor in 1987 (Ignarro et al., 1987), nitric oxide has been established as playing a fundamental role in the biochemistry and physiology of the central and peripheral nervous systems, the immune and cardiovascular systems (Bredt and Snyder, 1994; Schmidt and Walter, 1994). Although many of the mechanisms through which NO and its derivatives exert their biological effects are known, advances continue to be made in establishing how reactive nitrogen species (RNS: that is any reactive species containing both nitrogen and oxygen only) act as effectors in biological systems. Reactive nitrogen species are known modulators of signal transduction processes (Darley-Usmar et al., 1997; Lander, 1997). The work described in this thesis is concerned with the consequences of a modification known to occur in proteins on exposure to RNS; expressly, the consequence of this modification on a specific aspect of cell signalling. It is beyond the scope of this introduction to provide detailed accounts of all the roles played by NO and signal transduction in the cell biology; it is limited to an overview of those facets of NO biology and cell signalling that are relevant to the work detailed in this thesis.

HUMAN EXPOSURE TO REACTIVE NITROGEN SPECIES

Human exposure to RNS can occur by exogenous and endogenous routes. Oxides of nitrogen are ubiquitous pollutants of the atmosphere, however, the epithelial lung fluid contains an array of antioxidants capable of detoxifying the nitrogen oxides, thus protecting the underlying epithelia. These defences are likely to be breached by the acute exposures encountered during smoking, with levels of NO_x exceeding 10000 ppb. The endogenous component of human exposure to RNS is derived from nitric oxide (NO). NO is a diatomic, hydrophobic free radical that is synthesised *in vivo* and has multifarious roles. A significant proportion of the total body burden of RNS is derived from NO, although diet, in the form of nitrates also contributes to the *in vivo* burden (Oldreive and Rice-Evans, 2001). This section gives a brief outline of exposure to NO derived from endogenous and therapeutic sources.

The *In vivo* formation of nitric oxide

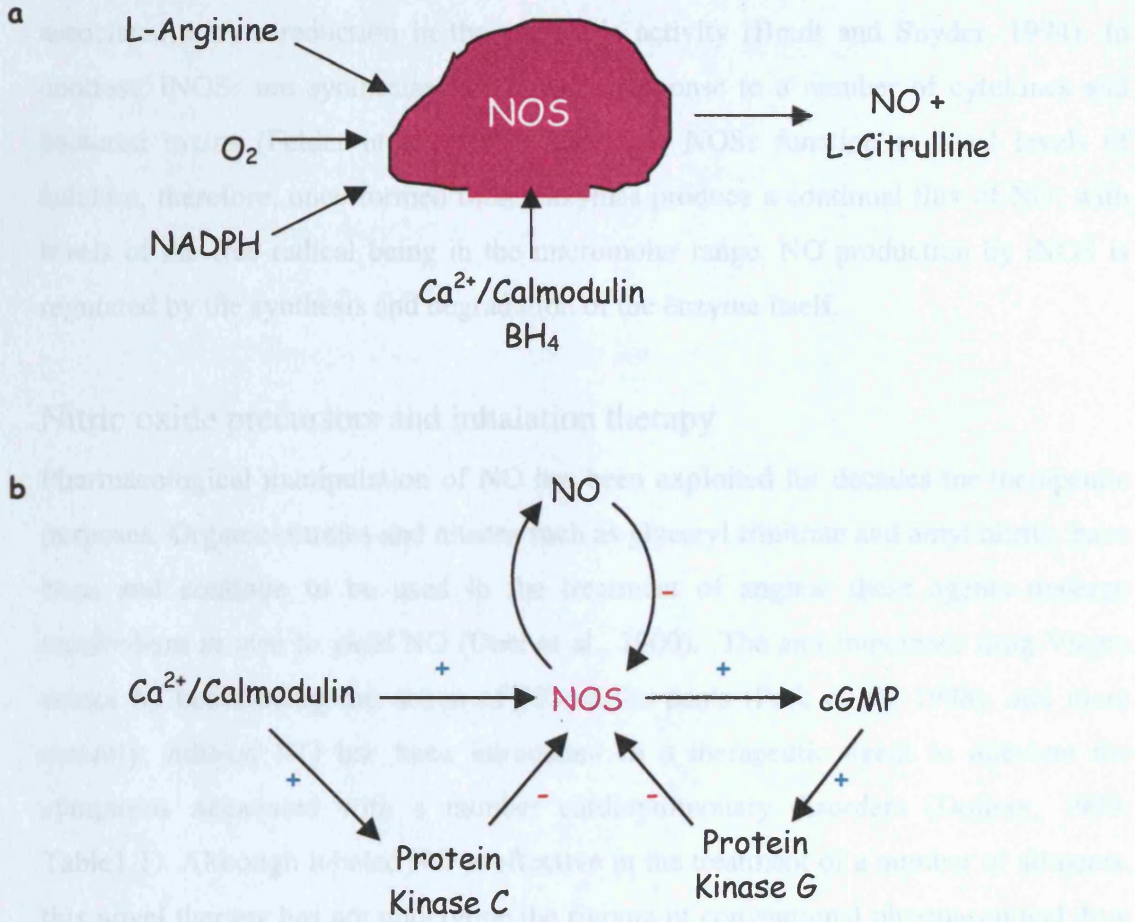

Figure 1.1. The synthesis of NO by nitric oxide synthase and mechanisms of enzyme regulation. (a) NOS utilises the molecular oxygen, and NADPH, to oxidise the amino acid L-Arginine to L-citrulline with the concomitant production of NO. The enzyme is dependent on intracellular calcium levels, as well as tetrahydrobiopterin. (b) Second messengers play a key role in modulating the activity of NOS. NO itself has inhibitory effects on the NOS, whilst calcium and cGMP activate kinases that inhibit the enzyme through phosphorylation.

Nitric oxide is synthesised *in vivo* by nitric oxide synthases. Three isoforms of the enzyme are currently known: neuronal, endothelial and inducible isoforms. All three of these isotypes catalyse the oxidation of L-arginine to L-citrulline with the concomitant formation of NO (Figure 1.1a). The production of NO by the constitutive endothelial and neuronal isoforms of the enzyme is dependent on transient increases in intracellular calcium. Consequently, NO is produced in short 'puffs', with

nanomolar levels being generated by these isozymes. In addition to calcium, and indeed NO itself, other second messengers regulate the activity of cNOS through phosphorylation of NOS (Figure 1.1b), with this post-translational modification being associated with a reduction in the enzyme's activity (Bredt and Snyder, 1994). In contrast, iNOSs are synthesised *de novo* in response to a number of cytokines and bacterial toxins (Felder et al., 1993). Inducible NOSs function at basal levels of calcium, therefore, once formed these enzymes produce a continual flux of NO, with levels of the free radical being in the micromolar range. NO production by iNOS is regulated by the synthesis and degradation of the enzyme itself.

Nitric oxide precursors and inhalation therapy

Pharmacological manipulation of NO has been exploited for decades for therapeutic purposes. Organic nitrates and nitrites such as glyceryl trinitrate and amyl nitrite, have been and continue to be used in the treatment of angina; these agents undergo metabolism *in vivo* to yield NO (Doel et al., 2000). The anti-impotence drug Viagra works by potentiating the action of NO in the penis (Park et al., 1998), and more recently, inhaled NO has been introduced as a therapeutic agent to alleviate the symptoms associated with a number cardiopulmonary disorders (Dollery, 1995; Table1.1). Although inhaled NO is effective in the treatment of a number of ailments, this novel therapy has not undergone the rigours of conventional pharmaceutical drug testing, and as such, chronic adverse effects of this treatment might yet be realised. Molecular aberrations in subjects, particularly neonates, undergoing inhaled NO therapy may manifest as serious injuries later in life. Shedding light on the mechanisms of NO induced toxicity may provide an indication of the potential adverse effects of inhaled NO therapy.

Table 1.1. The Indications for which inhaled NO is used (Dollery, 1995).

Condition
• Persistent pulmonary hypertension of the newborn.
• Congenital heart disease.
• Respiratory distress syndrome of the newborn.
• Bronchopulmonary dysplasia.
• Primary pulmonary hypertension.
• Adult respiratory distress syndrome.
• Cardiopulmonary bypass.
• Asthma
• Chronic obstructive pulmonary disease.

MOLECULAR INTERACTIONS OF NITRIC OXIDE

NO and its secondary products react with a number of biomolecules, accounting for both its pharmacological and toxicological profiles (Figure 1.2) (reviewed Halliwell et al., 1999; Murphy et al., 1998; Patel et al., 1999; Pfeiffer et al., 1999; and Wink and Mitchell, 1998). The transient release of NO by cNOSs is utilised for biochemical activity through the signalling molecule's interaction with haem and thiol centres. NO not utilised for biochemical purposes will primarily be oxidised to nitrate and nitrite and excreted in urine (Feldman et al., 1993). Conversely, the levels of NO released by the inducible form of the enzyme are capable of overwhelming the cell's defence mechanisms, resulting in interactions from which cell and tissue damage can result.

At low concentrations, the prominent interactions of NO are those with transition metal centres and free radicals (Patel et al., 1999). The interaction of NO with the haem centre of guanylate cyclase accounts for its physiological effects such as regulation of vascular tone and neuromodulation. The bacteriocidal activity of NO can also be attributed to its binding to the haem groups and inhibiting key enzymes such as aconitase and complex I and II of the mitochondrial electron transport chain (Feldman et al., 1993).

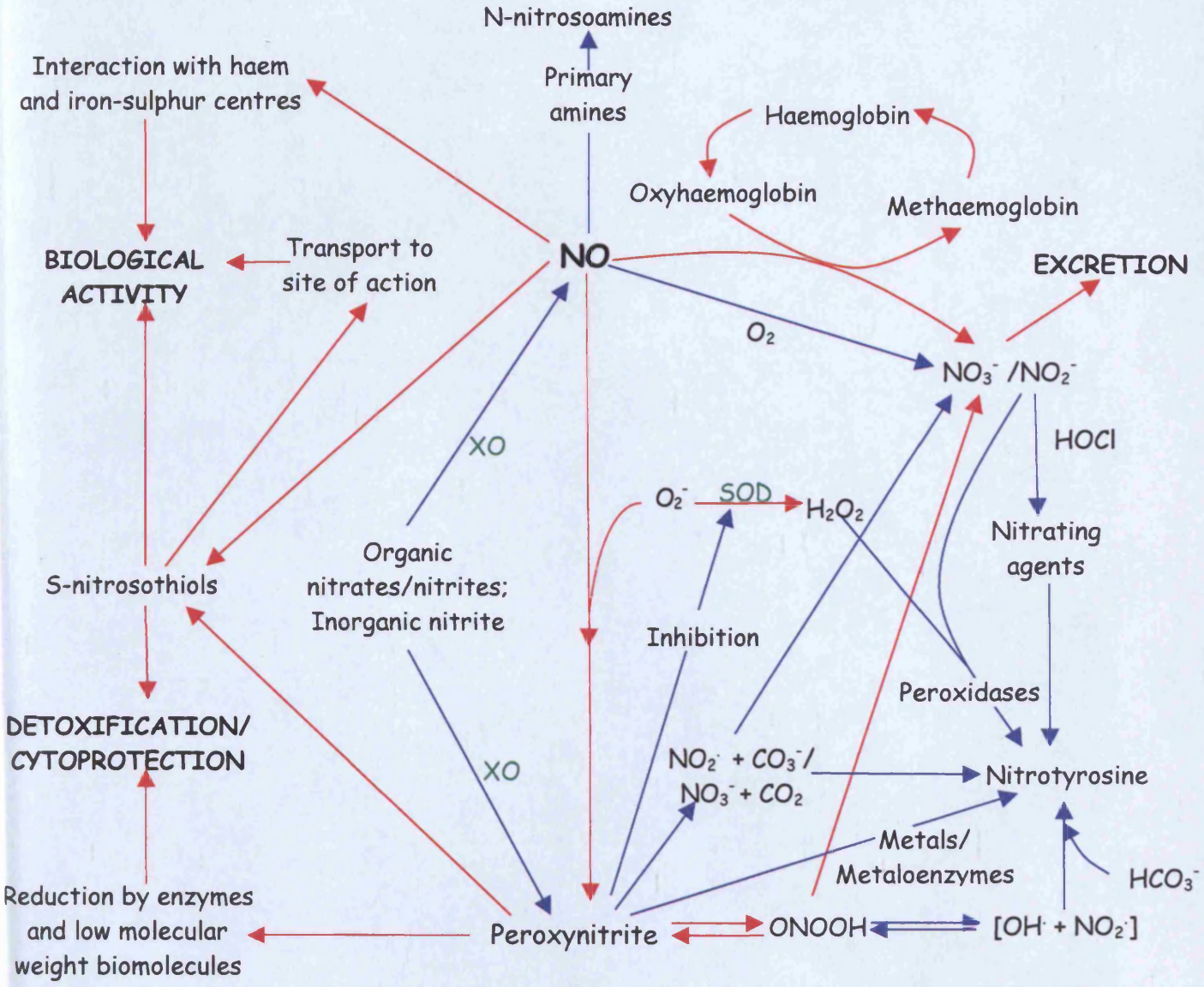

Figure 1.2. The *in vivo* interactions of NO. NO undergoes an array of reactions with a diverse range of biomolecules *in vivo*. Some of these interactions are highlighted. Red arrows indicate major routes of interaction, blue arrows the minor pathways.

The reaction of NO with oxyhaemoglobin to form methaemaglobin and nitrite is a major route of NO degradation. A reductase present in red blood cells is responsible for the regeneration of haemoglobin, but deficiencies in this enzyme, or exposure to high levels of NO, such as those encountered during inhaled NO therapy (Kinsella and Abman, 1999), can result in the methaemaglobinemia, a condition characterised by a reduction in the capacity of haemoglobin to carry oxygen. The generation of S-

nitrosothiols is an additional mechanism by which the activity of NO is regulated, with the free radical being 'mopped up' by the thiol groups of cysteine residues. Further to their cytoprotective functions, nitrosothiols are stable products capable of being transported to sites where NO is required, effectively acting as a pool for NO storage *in vivo* (Stamler et al., 1997). In contrast, the N-nitrosation, and the formation of nitrosoamines, can occur when NO reacts with primary amines. The metabolism of nitrosoamines can give rise to alkylating electrophiles that damage with DNA (Lewis et al., 1995).

Much of the oxidative damage initiated by NO can be attributed to the products of its reaction with oxidants. Peroxynitrite, nitrogen dioxide, dinitrogen trioxide and other harmful RNS are derived form the reaction of NO with oxygen-derived species. Peroxynitrite is a highly reactive anion that causes tissue damage through its interaction with a number of biomolecules (Figure 1.2). The formation of this species is derived primarily from the extremely rapid reaction of NO with superoxide (Goldstein and Czapski, 1995), although other mechanisms for the production of this reactive species are known (Godber et al., 2000). The removal of superoxide by SOD is approximately two orders of magnitude slower than the rate of peroxynitrite formation by the reaction of NO with superoxide (Groves, 1999); consequently, as opposed to being metabolised to hydrogen peroxide, superoxide will react preferentially with NO to generate peroxynitrite. In addition, by preventing the metabolism of superoxide through the inhibition of SOD (MacMillan-Crow et al., 1998; Yamakura et al., 1998), and cytochrome oxidase (Brown, 1995), peroxynitrite potentiates its own formation.

Peroxynitrite will be formed predominantly at sites of superoxide production due to the ready diffusion of NO and the highly reactive nature of superoxide. Peroxynitrite has a half-life of approximately 1 second (Groves, 1999), therefore, once formed peroxynitrite is capable of diffusing between intra and extracellular compartments. It is at the site of an inflammatory response that peroxynitrite formation is particularly prevalent, with macrophages producing large amounts of both NO and superoxide. Limiting the hydroxylation, oxidation and nitration reactions triggered by peroxynitrite through its removal is critical in minimising biomolecular and cellular damage caused by this species.

The cell possess a number of inherent detoxifying mechanisms capable of preventing peroxynitrite's deleterious effects. These include reaction with low molecular weight antioxidants, such as ascorbate (Bartlett et al., 1995) and glutathione (Quijano et al., 1997). In addition, peroxynitrite has been shown to undergo reduction by glutathione peroxidase, other selenoproteins (Seis et al., 1997), cytochrome C (Pearce et al., 1999), myoglobin (Bourassa et al., 2001) and peroxiredoxins (Byrk et al., 2000). The glutathione peroxidase mediated reduction of peroxynitrite has a rate constant which is higher than any between the reactive nitrogen species and any of its known cellular targets (8×10^6 M^{-1} s^{-1}; Sies et al., 1997), making this system an important defence mechanism against peroxynitrite mediated damage. In addition to the cell's antioxidant armoury, at physiological pH peroxynitrite becomes protonated to form the unstable peroxynitrous acid, which rapidly isomerises to nitrate. However, the formation of peroxynitrous acid can lead to the nitration and hydroxylation of cellular targets (Pfeiffer et al., 1999; Tuo et al., 2000).

The consequences of the interactions described above can vary from subtle changes in the activity of specific groups of biological molecules that do not threaten the existence of the cell, to more drastic effects that ultimately result in cell death (Figure 1.3). RNS have been shown to damage DNA. The lesions induced by RNS attack on DNA range from deamination caused by NO (Nguyen et al., 1992), to the oxidative damage and single strand breaks induced by both peroxynitrite and NO (Szabo et al., 1996; Tuo et al., 2000). The latter damage stimulates Poly ADP ribosyl synthetase, an enzyme whose activation can deplete the intracellular pool of NAD+, thus retarding production of ATP, resulting in cell dysfunction and death (Szabo, 1996). Another mechanism through which RNS can induce cell death is by generating mitochondrial permeability transition (Packer and Murphy, 1995). The MPT is a pore formed on the inner membrane of the mitochondria that enables pro-apoptotic proteins such as cytochrome C to be released into the cytosol. Peroxynitrite's ability to initiate lipid peroxidation is one of the mechanism by which this species is believed to induce MPT formation. RNS have been shown to initiate lipid oxidation, a mechanism believed to play a role in the genesis of athlerosclerotic plaques (Ischiropoulos, 1998). Conversely, NO is known to inhibit the propagation of lipid peroxidation (reviewed by Eiserich et al., 1998) Moreover, the termination of lipid peroxidation, leading to

the formation of nitrated lipid adducts, occurs at near diffusion rates, and is postulated as being a mechanism by which harmful effects of lipid oxidation are limited in *vivo*.

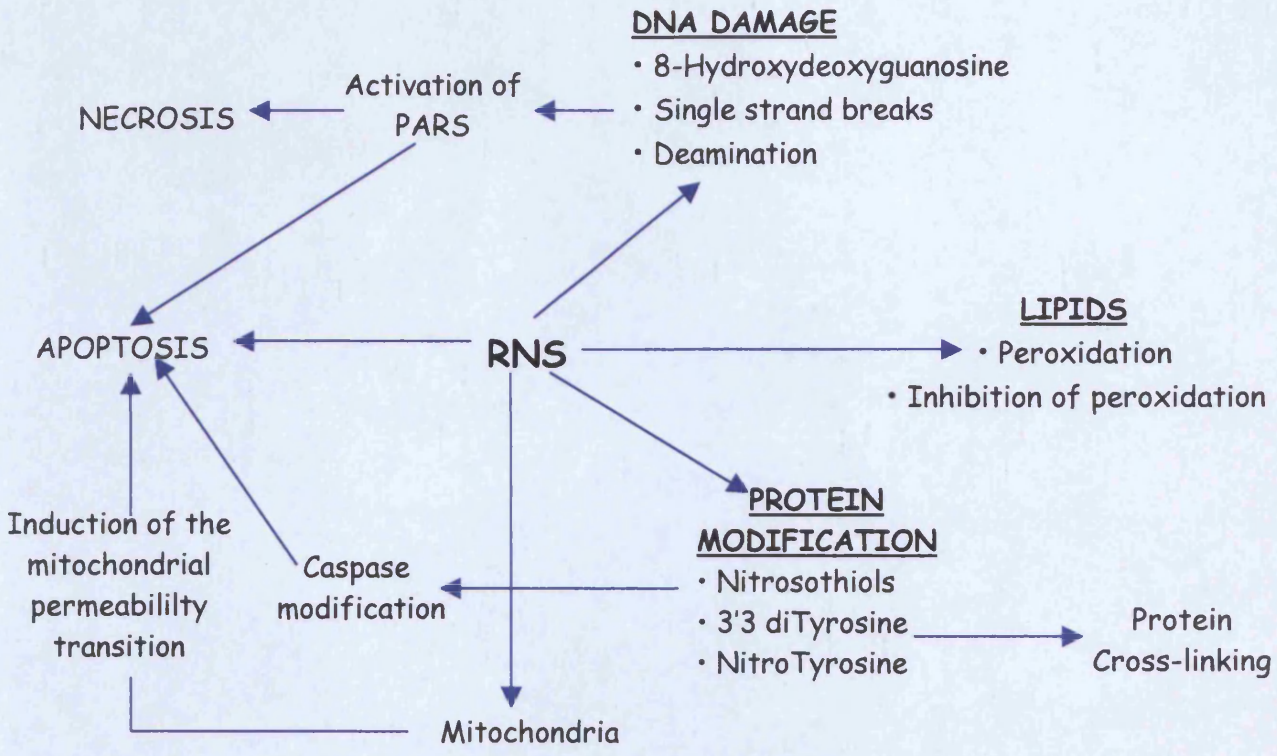

Figure 1.3. The biological consequences of RNS exposure. The figure outlines the some of the consequences of RNS interaction with three major classes of biomolecules.

RNS are known to react with methionine (Pryor and Squadrito, 1995), tryptophan and cysteine residues (Van der Vleit et al., 1994), phenylalanine and tyrosine residues (Van der Vleit et al., 1994) in proteins and peptides. The biological consequences of the formation of 4-nitrophenylalanine and the oxidised derivative of tryptophan and methionine have not been extensively studied. Nitrosothiols have a number of physiological roles *in vivo* ranging from cytoprotection to the activation of signalling proteins. By contrast, the modifications produced on tyrosine residues on their exposure to RNS have thus far been documented as having limited physiological benefit to the cell. Tyrosine residues play a key role in the functioning of an array of enzymes, in signal transduction mechanisms, and have a number of additional roles

within the cell. The exposure of tyrosine residues to RNS results in a number of modifications on the phenolic ring, including mono- and 3,3' di-nitration (Curcuruto et al., 1999), the formation of 3-chlorotyrosine (Eiserich et al., 1998), and 3,5 dityrosine crosslinks (van der Vleit et al., 1994). The mono-nitration of tyrosine has been extensively detected in a number of human diseases and pathologies (Greenacre and Ischiropoulus, 2001; Ischiropoulos, 1998 and Oldrieve and Rice-Evans, 2001), yet the role of nTyr in the diseased tissue remains poorly understood.

In summary, NO, peroxynitrite and other RNS are highly reactive species capable of interacting with a diverse range of biomolecules. Regulating the production and detoxification of RNS is critical in maintaining the fine balance between the benefits these species confer on biological systems, against the detrimental effects of their actions such as biomolecular modification.

THE *IN VIVO* FORMATION OF NITROTYROSINE

Potential nitrating agents

A number of RNS have been shown to nitrate tyrosine by direct or indirect mechanisms (Table 1.2, Figure 1.5) (Eiserich et al., 1999, Halliwell, 1997; Ischiropoulos, 1998). The mechanisms that predominate *in vivo* will depend on the organ in which nitration occurs, and the underlying physiological/pathological environment. The homolytic fission of peroxynitrous acid produces both hydroxyl and nitrogen dioxide radicals, the latter being a potent nitrating agent. Another nitrating agent, nitrosoperoxycarbonate, on reaction of peroxynitrite with carbon dioxide, and is a more potent nitrating agent than peroxynitrite itself (Gow et al., 1996). Furthermore, peroxynitrous acid, the protonated form of peroxynitrite, can react directly with tyrosine residues to form nTyr through the generation, and subsequent direct reaction of nitrogen dioxide and tyrosineosyl radicals.

An additional mechanism by which peroxynitrite is believed to be involved in tyrosine nitration is through the generation of the nitrosonium ion. This positively charged species is generated on interaction of peroxynitrite with transition metals such as iron. With the phenolic ring of Tyrosine being susceptible to the nucleophilic substitution, residues in the vicinity of the generated nitrosonium electrophile would

be potential targets of nitration. The metal centres in peroxidases also play a key role in this enzyme's ability to facilitate nitration of tyrosine residues in the presence of hydrogen peroxide and nitrite ions. The iron (III) centre of the enzyme is initially oxidised to iron (IV) by hydrogen peroxide. In regenerating the enzyme back to its ferric state, nitrite is oxidised to nitrogen dioxide, the tyrosine nitrating species.

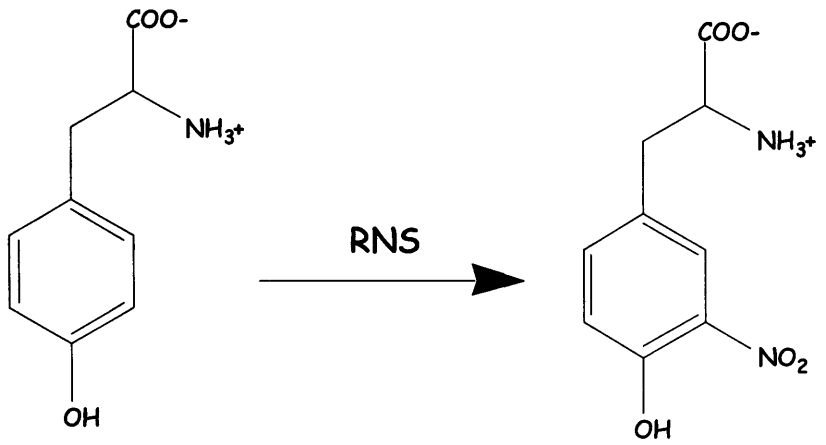

Figure 1.4. The formation of nTyr on exposure of Tyrosine to reactive nitrogen species. *On exposure of Tyrosine to RNS one of the prominent modifications that occurs is the meta substitution with a nitro group.*

Inflammatory cells generate hypochlorous acid (HOCl) in addition to a battery of agents that assist in the destruction of invading pathogens or cell debris. Reaction of nitrite with hypochlorous acid generates, nitryl chloride (NO_2Cl), a potent nitrating agent whose formation in a simulated inflammatory environment has been shown to induce tyrosine nitration (Eiserich et al., 1998). In addition to those RNS derived from endogenous sources, the nitrite derived from dietary sources is likely to contribute to the body's nTyr burden. The nitration of tyrosine residues by dietary derived nitrite is likely to be prevalent in the stomach, where the low pH promotes the formation and degradation of nitric acid into nitrating agents such as nitrogen dioxide and dinitrogen trioxide.

Table 1.2. Reactive nitrogen species speculated to mediate Tyrosine nitration.

Nitrating Agent	Substrate	Reference
Peroxynitrite/CO_2	Plasma proteins, BSA	Gow et al., 1996.
And HCO_3^-	HPA,Tyrosine, tryptophan	Denicola et al., 1996.
Nitrite/Peroxidases/H_2O_2	Tyrosine, BSA, HPA	Van der Vleit, 1997
Nitryl chloride (NO_2Cl)	BSA	Eiserich et al., 1996
	Tyrosine containing peptides	Eiserich et al., 1998
NO/Tyrosinosyl radical	Prostaglandin endoperoxide synthase	Goodwin et al., 1998
Peroxynitrite/metaloproteins	Neurofilament L	Crow et al., 1997
and metal centres	Lysosome, histones	Beckman et al., 1992
Peroxynitrite/ Peroxynitrous acid	Tyrosine	Van der Vleit et al., 1994

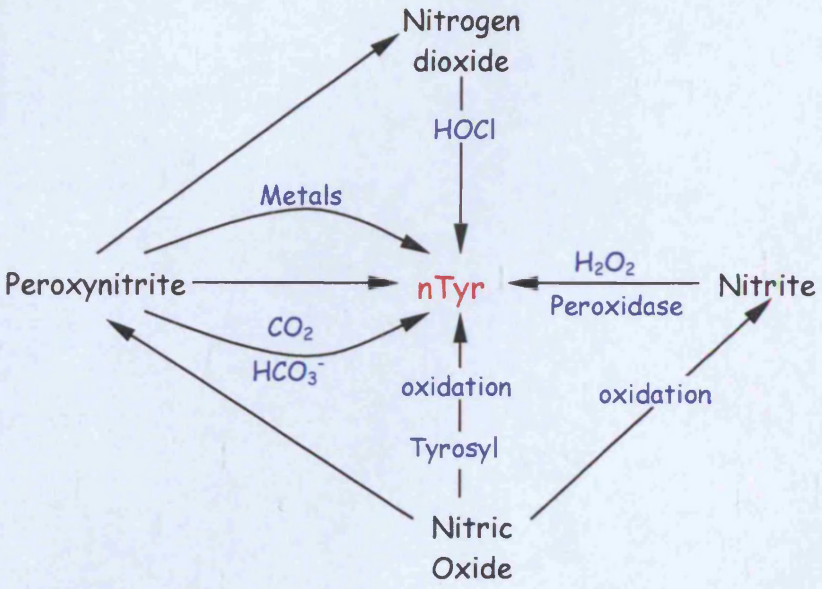

Figure 1.5. Summary of the mechanisms by which nTyr is formed *in vivo*. A number of reactive nitrogen species are capable of directly, in the case of peroxynitrite, and indirectly inducing nTyr *in vivo*.

Factors affecting formation of Nitrotyrosine

Although a number of agents are capable of nitrating tyrosine, it is apparent that some residues are more susceptible to nitration than others. The factors that underlie this susceptibility have not been fully clarified. Using both cell culture and *in vivo* models, Aulak et al., (2001) utilised a proteomic approach to establish that of the entire cell's protein complement, only a limited number (over 40) underwent nitration in simulated inflammatory conditions. The proteins identified as having undergone nitration included those involved in protecting against oxidative stress, in energy production, apoptosis, fatty acid metabolism, and structural proteins amongst others. Interestingly, over one third of the nitrated proteins identified were found in the major site of superoxide generation, the mitochondrion, with MnSOD being identified as having the most anti-nitrotyrosine immunoreactivity. The results of this study suggest it is location within the cell and intrinsic properties of the proteins that govern the intracellular targets of tyrosine nitration. In addition to SOD (MacMillian-Crow et al., 1998), tyrosine hydroxylase (Ara et al., 1998), neurofilament (Crow et al., 1997), synatophysin (Di Stasi et al., 1999), and prostacyclin synthase (Zhou et al., 1997) have also been found to be targets of peroxynitrite-mediated nitration.

In a study conducted by Souza and co-workers (1999) the modifications induced by a number of nitrating agents on three proteins (ribonuclease A, phospholipase A_2 and lysozyme) were investigated. The rationale for choosing these three proteins was that they have similar size, but differ in their tyrosine content and secondary structures. The main findings of the studies were:

- The exposure of the residues on the surface of proteins was not the sole determinant of nitration; some exposed residues did not undergo nitration, although all residues that underwent nitration were solvent accessible.
- The electrostatic environment surrounding the tyrosine residue influenced nitration. In the case of peroxynitrite, proximal to acidic negatively charged residues, such as a glutamic acid, were targeted for nitration, (a hypothesis also proposed by Crow et al., 1997). Basic amino acids, methionine and cysteine act as alternative targets for the modifying agent, thus limiting the nitration of tyrosine in the vicinity of these residues.

- Steric factors such as disulphide bridges were shown to impede tyrosine nitration.
- The secondary make-up of the protein was shown to be important determining the accessibility nitrating agents, as tyrosine found in the loop structures were preferentially nitrated.
- And finally, the nature of the nitrating agent can also determine the tyrosine residues that undergo modification, as was the case with RNAse nitration by myeloperoxidase; this finding believe to be due to the favourable protein-protein interactions.

In addition to factors that influence the formation of nTyr, the antioxidant mechanisms previously described will also have a bearing on whether nTyr residues are formed *in vivo*. Furthermore, dietary derived antioxidants may also impede the formation of nTyr formation *in vivo* (Oldrieve et al., 1998; Pannala et al., 1998). Taken together, the two studies described above indicate that *in vivo* formation of nTyr is dependent on a number of factors that result in the selective nitration of specific tyrosine residues, on specific proteins. The challenge for researchers lies in identifying these proteins and establishing the role they play in the functioning (or dysfunctioning) cell.

DETECTION OF NITROTYROSINE IN DISEASE AND IN VITRO

The formation of nTyr has been investigated both *in vivo* and *in vitro*. The *in vitro* work has primarily focused on exposing specific proteins to nitrating agents and monitoring a change in function (Table 1.3), or exposing biological media to the modifying agents and noting the presence of nTyr. *In vivo*, biopsies, biological fluids and tissue section have all been probed for the presence nTyr in specific disease states (Table 1.4; Eiserich et al., 1999; Ischiropoulos, 1998; Oldreive and Rice-Evans, 2001), and indeed under physiological conditions (Greenacre and Ischiropoulos, 2001).

Table 1.3. Some of the consequences of biomolecular exposure to either reactive nitrogen species or the specific Tyrosine nitrating agent, tetranitromethane.

Modification/Exposure	Consequence	Reference
Incorporation of nTyr into α-tubulin	• Alterations in cell morphology • Alterations in microtubule organisation • Loss of epithelial barrier function • Intracellular redistrubution of motor protein	Eiserich et al., 1996
Nitration of Tyrosine in glutamine synthase	Tyrosine nitration mimics posttranslational adenylation	Berlett et al., 1996
Nitration of fibrinogen	Increase in the rate of thrombin-catalysed fibrinolysis	Gole et al., 2000
Inhibition of specific enzymes through nTyr formation		
• Exposure of cyclooxygenase to peroxynitrite	Inhibition of enzymic activity and the production inflammatory mediators	Boulos et al., 2000
• Exposure of SOD to $ONOO^-$	Inhibition of enzymic activity	MacMillan-Crow et al., 1998
• Exposure of DNA gyrase to tetranitromethane	Inactivation of enzyme and cessation of DNA supercoiling	Klevan et al., 1983
• Exposure of cytochrome P450 2B1 to peroxynitrite	Inactivation of enzymic metabolism	Roberts et al., 1998

The *in vitro* studies generally show exposure of biomolecules either to the specific nitrating agent TNM, or RNS, resulted in a loss of biological function of the protein being studied (in the case of enzymes, an extensive list can be found in Neilsen,

1995). These functional loses may occur due to steric hindrance, allosteric modification, or the change in pKa of the hydroxl group on addition of a meta nitro group (the pKa of the hydroxyl group in tyrosine being ~10.0, whilst in the nitro-derivative the value is ~7.5). In two instances, however, a gain of protein function and an ability to mimic the endogenous posttranslational modification have been documented. Gole et al (2000) observed an increased rate of thrombin catalysed clot formation on exposure of fibrinogen to the nitrating agent nitrosoperoxycarbonate. The basis for this increased rate of clot formation is likely to lie in the introduction of additional negative charge on the fibrin peptides. Negatively charged fibrin peptides are a necessary in the formation and stabilisation of clots, this being facilitated *in vivo* by the presence of the negatively charged tyrosine sulphate (Stryer, 1988).

Table 1.4. The detection of Nitrotyrosine in various pathologic states.

Condition	Reference
• Pancreatic ductal adenocarcinoma	MacMillan-Crow et al., 2000
• Athlerosclerotic plaques of coronary vessels.	Abdalla and Moriel., 1997
• Parkinson's disease	Good et al., 1997
• Multiple sclerosis plaques	Cross et al., 1998
• Alzheimers lesions	Smith et al., 1997
• Rejected renal allografts	MacMillan-Crow et al., 1996
• Rheumatoid arthritis	Kaur et al., 1994

Berlett et al (1996) demonstrated that exposure of glutamine synthase to peroxynitrite converted the enzyme to an active form that exhibited regulatory characteristics similar to that of the *in vivo* protein. Glutamine synthase is regulated by adenylation. Adenylation, the addition of adenosine mono phosphate, occurs on the hydroxyl group of tyrosine via a phosphodiester bond (figure 1.6), unlike nitration, which is an ortho substitution. The ability of tyrosine nitration to activate glutamine synthase poses the question of whether nTyr formation in proteins can mimic the allosteric changes in protein induced by adenylation. Further to this, adenylation is a reversible post-

translational modification: adenylyl transferase regulating both the addition and removal of the adenosine monophosphate group. In contrast, the evidence suggesting the nitro group can be removed from the tyrosine ring is limited (see below). Therefore, once nitrated and 'switched on' there is potentially no means of turning off the activity of glutamine synthases.

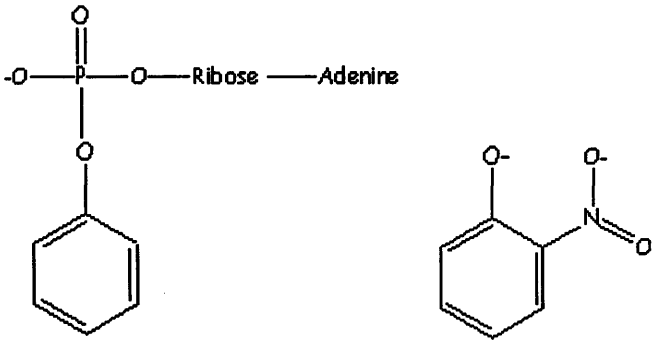

Figure 1.6. The adenylated phenolic ring of the Tyrosine residue and its comparison to the nTyr residue. Although structurally different, nTyr has been shown to mimic adenylated Tyrosine in its ability to activate glutamine synthase by allosteric means (Berlett et al., 1996).

Ntyr has been detected in the tissues and biological fluids in a number of disease conditions ranging from inflammatory to neurodegenerative disorders (a summary table can be found in Halliwell et al., 1999 and Greenacre and Ischiropoulus, 2001, although since the publication of these articles nitrated tyrosine residues may have been detected in other pathologies). In the diseased milieu, a key question is whether nTyr is merely indicative of oxidative and nitrosative insults, or are these modified residues playing a role in the onset and/or the progression of the disease. Can the prevention of nTyr formation avert the genesis or propagation of these detrimental ailments? Much is known about the function tyrosine residues plays in normal physiology, however, there is still much to be established on the role nTyr residues play in the biology of the cell. It is known that nTyr can cause cellular damage through redox cycling (Krainev et al., 1998), and that aminophenols, the possible products of nTyr metabolism, are toxic in their own right (Valentovic and Ball, 1999). *In vitro* studies can be used to dissect molecularly the function that nitropeptides and

proteins play *in vivo*, yet these experiments provide only partial insight into the function of the modified proteins *in situ*, as the cell's response to the nTyr formation is equally important in determining the role of the modified residues *in vivo*.

THE FATE OF NITROTYROSINE

Inflammation is an ancient, adaptive response used by animals to protect themselves from invading pathogens and cellular damage. Consequently, man's exposure to reactive oxygen and nitrogen species derived from internal sources is as old as the response itself. Have cells therefore evolved mechanisms to protect themselves from the potential deleterious effects of nTyr formation? Or a more intriguing notion is that the cell has incorporated tyrosine nitration into the plethora of intracellular pathways and mechanisms that regulate the functioning of the cell under physiological or pathological conditions. The cell seldom utilises a protein once before ubiquitination, consigns it to the degradation pathways present in cells. Rather, the modification of a protein utilised for physiological benefits are usually reversible, regulatable processes. A large amount of energy would be required to break a carbon-nitrogen (ΔH at 298 K, ~60 kcal/mole, Politzer et al., 1998) if the nitro group was to be completely removed from tyrosine's phenolic ring, which has been proposed as being the case (Kuo et al., 1999). An alternative to the complete removal of the nitro group would instead be to reduce it to its aminated derivative. A meta-positioned amino group on the phenolic ring of tyrosine does not alter the pKa of the hydroxyl group, unlike a nitro group. Additionally, an amino group has a smaller atomic radius than a nitro, so steric hindrance would be less prominent. Kamisaki and co-workers demonstrated the presence of a factor in rat tissue homogenates that modified nitrated proteins (Kamisaki et al., 1999). These authors established this 'nitrotyrosine denitrase' activity was inducible, protein concentration dependent, heat and trypsin labile. This group went on to demonstrate the non-protein dependent reduction of nTyr to aminotyrosine (aTyr) in the presence of haem and thiol groups, and speculated that the protein dependent 'denitrase' activity was in fact a reductive process (Balabanli et al., 1999). An additional mechanism through which aTyr is formed *in vivo* is through the exposure of the nitroalkanes found in cigarette smoke. These agents are believed to undergo activation *in vivo* to form an aminating species likely to be the unsubstituted nitrenium ion (Sodum and Fiala, 1997).

In addition to the removal or reduction of the nitro group, the extracellular clearance of nitrated proteins may be important in regulating the amounts of nTyr present at its site of formation. However, nitrated proteins may have a slower plasma clearance than the non-modified derivatives (Greenacre et al., 1999). In contrast, the intracellular proteolytic degradation of nTyr containing proteins appears to occur at a greater rate than that of the non-modified derivatives (Berlett et al., 1996; Gow et al., 1996), although extensive modification can inhibit protein breakdown (Grune et al., 1998). Once liberated from proteins nitrotyrosine is metabolised to 3-nitro-4-hydroxyphenylacetic acid and 3-nitro-4-hydroxyphenyllactic acid and excreted in urine (Ohshima et al., 1990).

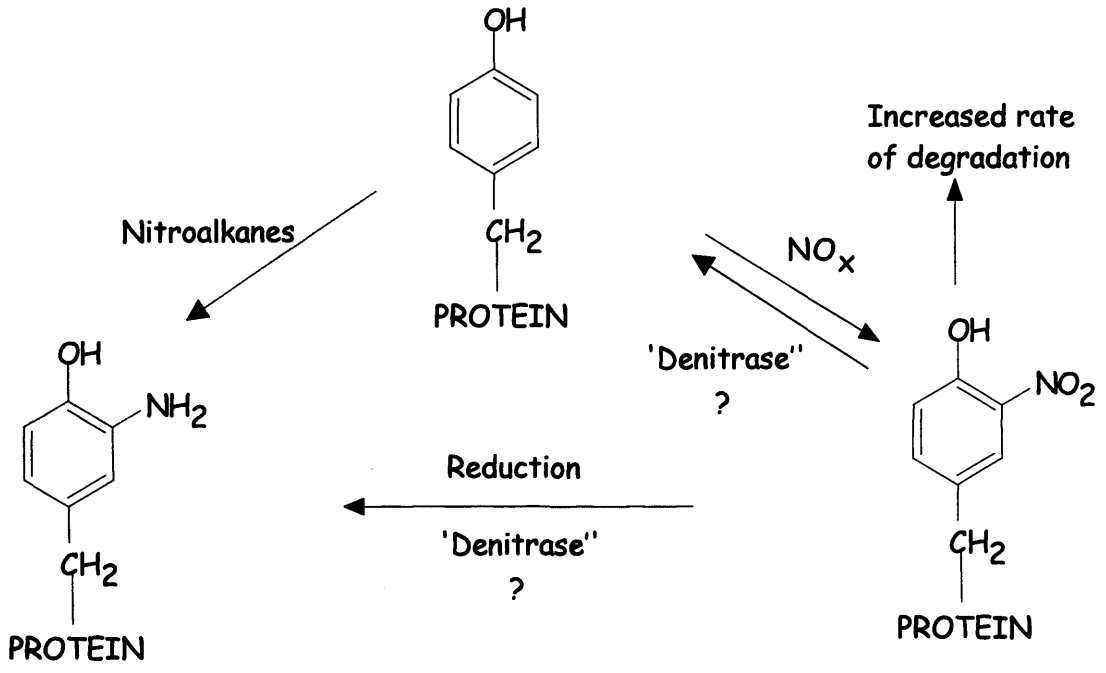

Figure 1.7. The *in vivo* fate of nitroTyrosine. In addition to the mechanisms described in the text, nTyrosine may be formed *in vivo* by exposure to nitroalkanes found in cigarette smoke (Sodum and Fiala, 1997).

It is feasible that nitration of tyrosine residues is utilised as a 'one shot' modification analogous to tyrosine sulphation (Huttner, 1987). Conversely, if tyrosine nitration is a modification utilised to modulate aspects of cell function, it must be specific and regulated, in a manner analogous to tyrosine phosphorylation. The specificity of

action would be partially achieved by the factors previously stated that steer RNS towards tyrosine residues in designated proteins. The regulation of nitration could be achieved by the removal or modification of the nTyr moiety. Can nTyr be considered a putative *in vivo* signalling entity, analogous to nitrosothiols or phosphotyrosines?

REACTIVE NITROGEN SPECIES IN SIGNAL TRANSDUCTION

Redox based modulation of cell signalling is well documented, however, the mechanisms through which oxidative entities exert their effects remain largely unknown. In the case of RNS, the nitrosation of cysteine residues is now recognised as modulating the activity of a number of intracellular proteins (Stamler et al., 2001). S-nitrosylation is a ubiquitous post-translational modification associated with the stimulation of the three isoforms of NOS (Gow et al., 2002). The S-nitrosation of cysteine residues is not mediated by protein-protein interactions, but like the phosphorylation of tyrosine residues, the specificity of nitrosylation targets is influenced by the of the residues surrounding the thiol group (Hess et al., 2001; Stamler et al., 1997). Cysteines targeted for nitrosylation are located between acidic and basic residues, and in hydrophobic motifs, analogous, in part, to the presence of acidic residues proximal to tyrosines nitrated by peroxynitrite. Further to this, it has been demonstrated that the denitrosylation of thiols is mediated by glutathione-dependant formaldehyde dehydrogenase (Liu et al., 2001), introducing a means of regulating this post-translational modification.

The activity of a number of proteins is altered on their S-nitrosylation (Stamler et al., 1997). These include haemoglobin, the NMDA receptor and caspases (Hess et al., 2001). The nitrosylation of the oncogene product $p21^{ras}$ has been well characterised (Lander et al., 1995a and 1996). $p21^{ras}$ is a pivotal mediator of mitogen activated signalling cascades and the cell's response to oxidative stress (Lander et al., 1995b). Indeed, ras is speculated to be a sensor of oxidative insult. This protein contains three cysteine residues, but Cys 118 is the most solvent accessible of the three and the only residue that undergoes nitrosylation. The modification of ras results in the structural changes that mediate's guanine nucleotide exchange activity, with GDP being exchange for GTP.

Thiols are more susceptible to nitrosylation than tyrosine is to nitration (Mirza et al., 1995; Simon et al., 1996). Therefore, *in vivo*, signal mediation through nitrosothiols is likely to predominate over nTyr, if indeed the latter residue is a mediator of signal transduction. Although comprising less than 0.1% of the cell's phosphoamino acid content (Hancock, 1997), the importance of pTyr residues *in vivo* is highlighted by approximately 1% (or over 1000 proteins) of the human genome coding for protein tyrosine kinases (Williams et al., 1998). Therefore, despite the low numbers of tyrosine residues that are likely to undergo nitration *in vivo*, their modification may be significant. One mechanism through which nTyr residues could modulate signalling pathways has been demonstrated in the inability of a nitropeptide (Kong et al., 1996) and nitrated proteins (Gow et al., 1996; Mondoro et al., 1997) to undergo phosphorylation when exposed to RNS. The consequences of this inhibition will depend on the system in which tyrosine phosphorylation is being utilised for signalling purposes.

Growth factor signal transduction

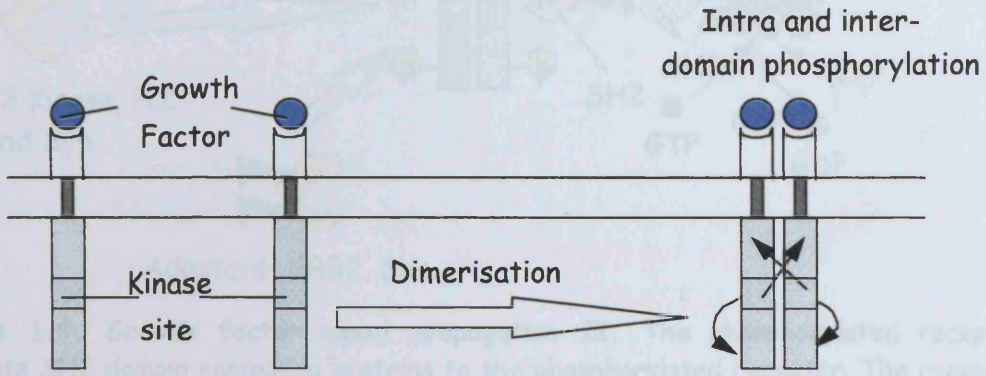

Figure 1.8. Growth factor signal propagation I. On binding of growth factors to the receptor dimerisation occurs followed by intra and inter-domain tyrosine phosphorylation.

Growth factors are important regulators of cell division and differentiation. These hormones play a key role in regulating tissue size, and moulding its architecture throughout the body. The mechanism of growth factor signal propagation has been outlined (Kavanaugh and Williams, 1999; Lodish et al., 1995). Briefly, the binding of growth factors to the extracellular domain of the growth factor receptor induces the

formation of receptor homo and heterodimers. Once formed, the dimerised receptor then undergoes autophosphorylation through inter-domain kinase activity, phosphorylating tyrosine residues located at specific positions on the intracellular segment of the receptor (Figure 1.8).

The phosphorylated tyrosine residues then act as a beacon, recruiting, and binding, specific proteins containing SH2 or PTB domains. These domains are modular proteins that bind to pTyr residues in specific amino acid motifs. Enzymes such as phosphatidylinositol 3 -kinase, phospholipase C-γ, cytoplasmic protein kinases, such as Src and Fyn, protein tyrosine phosphatases, like PTP1D and Syp; in addition to the adaptor proteins Shc and Grb2, are all recruited to the receptor due to the presence of SH2 or PTB domains in their structures.

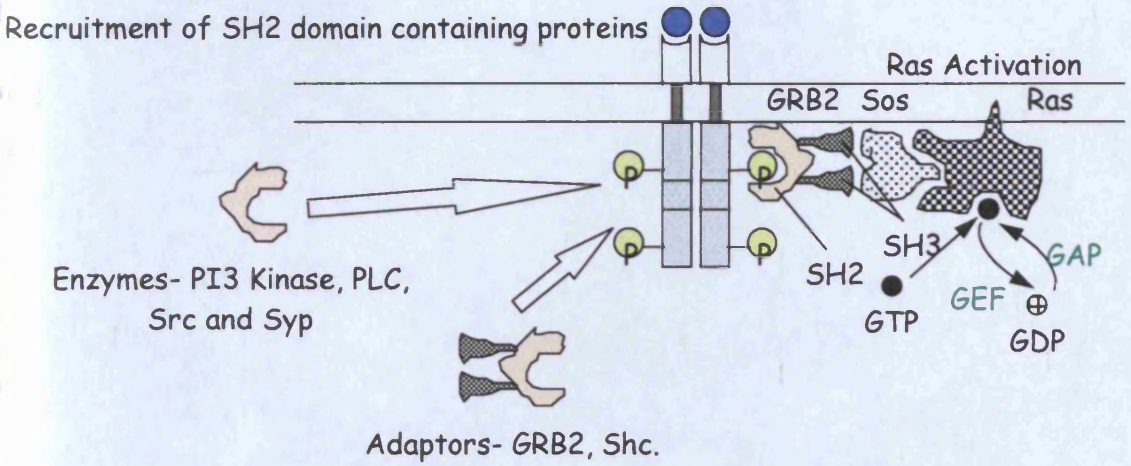

Figure 1.9. Growth factor signal propagation II. The phosphorylated receptor recruits SH2 domain containing proteins to the phosphorylated receptor. The receptor then activates ras via GRB2 and Sos

Binding of Grb2 via its SH2 domain to the phosphorylated RTK elicits a conformational change within this protein, enabling the Sos protein to bind to it via its two SH3 domains (Figure 1.9). SH3 domain recognises proline rich motifs, such as those found in Sos. The binding of Sos to Grb2 activates the guanine exchange activity of this protein, which in turn activates the membrane associated GTPase, Ras, by inducing the exchange of GDP with GTP from a binding site located on the

protein.

Acitvated Ras then relocates the serine/threonine kinase Raf from the cytosol to the plasma membrane. The binding of the dual-specificity kinase MEK to the C-terminal of Raf leads to its phosphorylation, and subsequent activaton. MEK in turn activates MAP by phosphorylating specific threonine and tyrosine residues within the enzyme. MAP kinases are composed of three distinct subgroups including ERK, c-Jun NH2-terminal kinase and p38 MAP kinase. The serine/threonine kinase activity of MAP kinases alters the activity of cytosolic proteins such as PLA_2, other kinases and transcription factors, such as c-Fos, which ultimately leads to the differentiation and proliferation of cells (Figure 1.10).

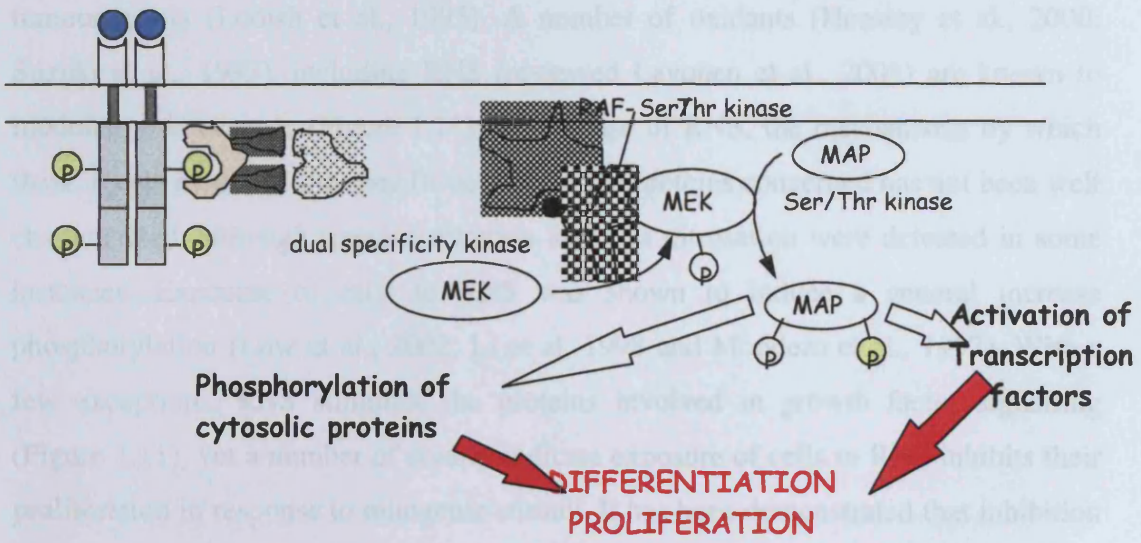

Figure 1.10. Growth factor signal propagation III. Ras leads to alterations in gene expression by through the activation of MEK and MAPK that ultimately leads to alterations cell proliferation and differentiation.

The binding of proteins to the phosphorylated receptor is critical for two reasons. Firstly, it is this binding that transduces the external signal to the intracellular cascade. Secondly, transduction pathways do not exist as isolated cascades within cells, rather, a number of cascades may be disseminated from a single receptor. Further to this, networks are formed by the cross-talk between individual components of different

cascades. Autophosphorylation, and subsequent protein binding to the phosphorylated receptor, acts as a molecular switch, activating a network of protein cascades responsible controlling of gene expression, DNA synthesis, cytoskeletal architechiture, protein sorting and cellular metabolism (Pawson, 1994), disruption of which may have deleterious effects on the cell, such as uncoupling the extracellular signal from the internal cascade, or activating the cascade in the absence of external signal. Exposure of cells containing growth factor receptors to non-toxic levels of $ONOO^-$ was shown to induce receptor dimerisation, which subsequently increased receptor autophosphorylation (van der Vleit et al., 1998). In the absence of growth factor the increase in phosphorylation and receptor cross-linking was marginal, but increased significantly in the presence of mitogen.

The Grb2-Sos system plays a key role embryonic development, postnatal function and tumourgenisis (Lodish et al., 1995). A number of oxidants (Hensley et al., 2000; Suzuki et al., 1997), including RNS (reviewed Levonen et al., 2001) are known to modulate this cascade (Figure 1.11). In the case of RNS, the mechanisms by which these agents modulate the specific activity of the proteins concerned has not been well characterised, although tyrosine nitration and Cys nitrosation were detected in some instances. Exposure of cells to RNS was shown to induce a general increase phosphorylation (Low et al., 2002; Li et al, 1998 and Mondero et al., 1997). With a few exceptions, RNS stimulate the proteins involved in growth factor signalling (Figure 1.11), yet a number of studies indicate exposure of cells to RNS inhibits their proliferation in response to mitogenic stimuli. It has been demonstrated that inhibition of growth factor induced proliferation of Swiss 3T3 fibroblasts on exposure of the cells to TNM, the specific tyrosine nitrating agent, was coupled with a dose dependent increase and decrease in nTyr and pTyr, respectively (Huntley et al., unpublished results). In addition to this growth arrest, both apoptosis and cell survival are associated with RNS modulating the activity of transduction biomolecules (reviewed Boyd and Cadenas, 2002). So rather than stimulating cell proliferation, as might be expected, RNS modulation of the growth factor/MAPK signalling may be involved with cell/tissue survival in response to oxidative insults.

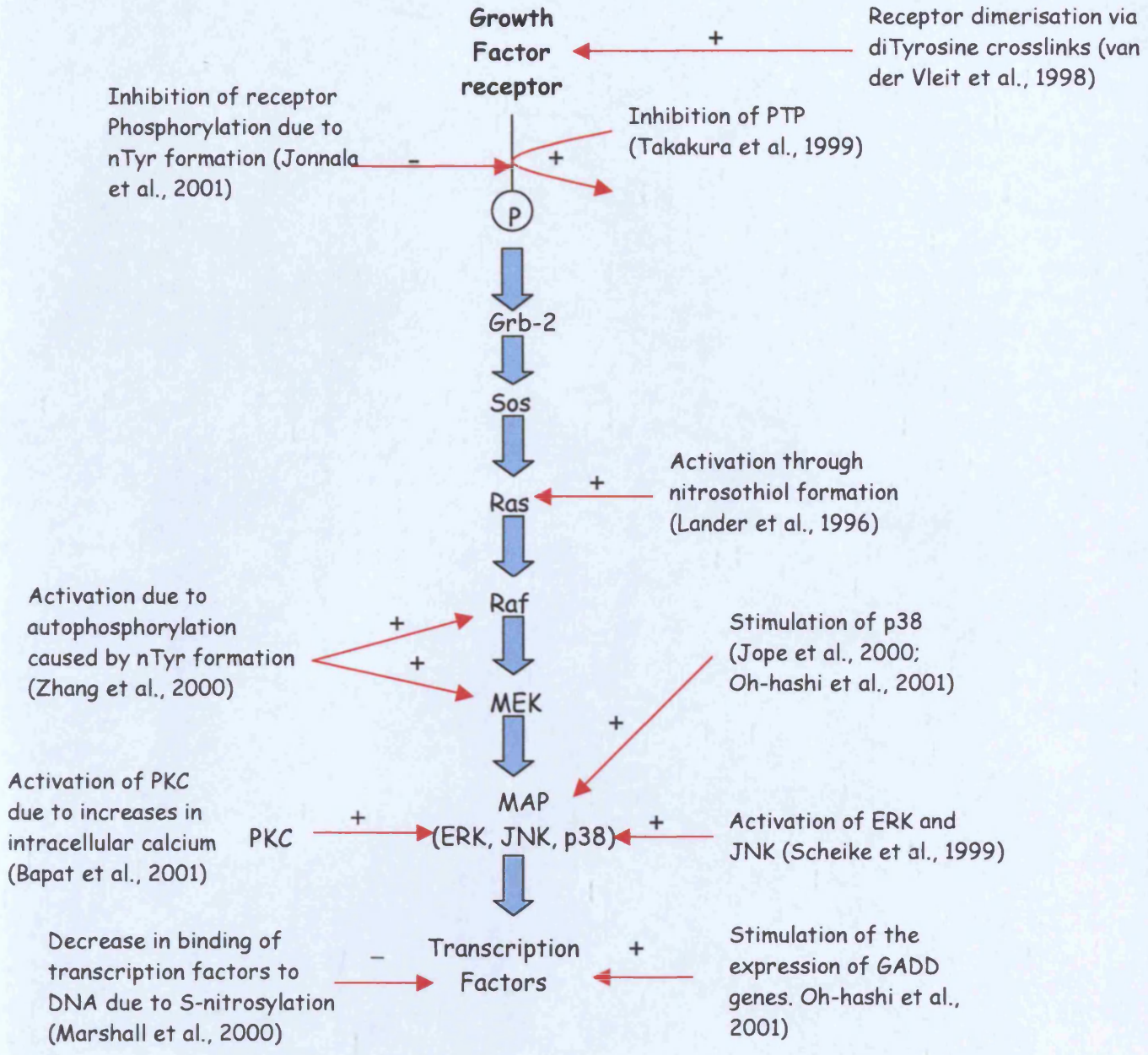

Figure 1.11. The modulation of growth factor signalling by reactive nitrogen species. RNS have been demonstrated as modulating growth factor signalling by their interaction with specific proteins in the cascade, ranging from the receptor to the transcription factors.

Src Kinases

Src kinases are a group of nine structurally related non receptor tyrosine kinases that mediate cell growth and differentiation in response to the activation of a number of cell surface receptors (reviewed Brown and Cooper, 1996). The sequence of these proteins is highly conserved, as is their structural architecture (Figure 1.12; Williams et al., 1998). The N-terminus of these proteins, known as the SH4 region, is comprised of the 9-12 amino acids that contain myristylation and palmitoylation sites. Following this region is a sequence of 40-70 residues unique to each enzyme, which may confer distinct localisation properties to each protein. SH3 and SH2 domains recognise proline rich sequences and pTyr residues within specific amino acid motifs, respectively, and are important in regulating the activity of the enzyme. The SH2 kinase linker sequence contains a proline rich consensus sequence to which the SH3 domain binds in an intramolecular manner. The importance of this interaction has been demonstrated by mutagenesis studies that indicated the SH3 domain to be critical for kinase activity (Erpel et al., 1995). A second means by which the activity of src kinases is regulated is through an intramolecular interaction between the C-terminal and the SH2 domain. Phosphorylation of tyrosine 527, in Src, by the C-terminal src kinase (Csk; Brown and Copper, 1996) causes the tail region of the protein fold back on itself, thus enclosing the kinase domain within the protein. The un-folding and activation of the protein is mediated by intracellular binding partners for the SH2/3 modules, which bind with greater affinity than the intra-protein ligands. The activity of src kinases is further increased by the autophosphorylation of a tyrosine residue located within the catalytic site (residue 416 in src), whose phosphorylation alters the conformation of the protein through interaction of the phosphate with two arginine residues (Scheri and Kuriyan, 1997).

Reactive nitrogen species have been documented as interacting with src kinases. Minetti and colleagues have conducted a number of studies on the effects of peroxynitrite on src kinase activity and shown the activity of these enzymes to increase on exposure to the reactive nitrogen species. The mechanisms by which this activity was modulated being both dependent on and independent of cysteine oxidation (Di Stasi et al., 1999; Mallozzi et al., 1999; and Mallozzi et al., 2001). Human pancreatic ductal adenocarcinoma tissue was shown to contain c-src that was both nitrated and phosphorylated, whilst *in vitro* studies demonstrated an increase in

kinase activity on exposure of peroxynitrite to the protein (MacMillan-Crow, 2000). Aberrant src proteins are know to be key mediators in oncogenesis (Brown and Cooper, 1996). The possible role that RNS play in this process is discussed in chapter 7 in light of some of the findings of this thesis.

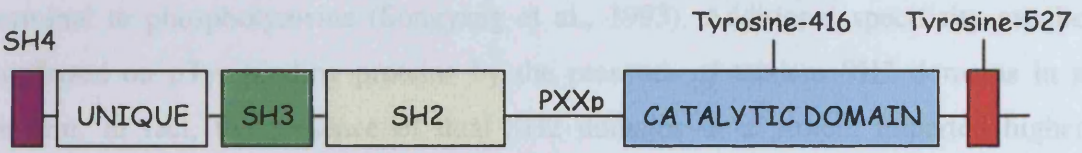

Figure 1.12. Structure of Src family Tyrosine kinases. SH2, 3 and 4 modules are found in all src kinases, as are the catalytic domain and the C-terminal regions. The unique region located in the N-terminus of the polypeptide is believed to play an important role in the localisation of individual kinases. The proline rich consensus sequence located between the SH2 and catalytic domains is important in the intramolecular binding of SH3 domain, an interaction important in regulating the proteins activity. The phosphorylation of Tyrosines 416 and 527 are key mediators of increasing the catalytic activity of the enzyme and shutting down the activity of the enzyme respectively.

THE PHOSPHOTYROSINE-SH2 DOMAIN INTERACTION

The two examples above used to illustrate the importance of tyrosine residues in cell signalling, highlight the importance of the interaction between pTyr residues and SH2 domains. Two distinct protein domains are known to bind phosphotyrosine residues (Cohen and Baltimore, 1995). The PTB domain is composed of 100-150 amino acids and is found in insulin receptor substrates 1 and 2, and the adaptor protein Shc (Harrison, 1996). This domain has been shown to be an important mediator of growth factor signal transduction (O'Bryan et al., 1998). Comprised of around 100 amino acids, SH2 domains are found in a number of intracellular proteins. These modules bind with high affinity (K_d = 10-100 nM; Pawson, 1995) to pTyr residues in specific protein motifs (Songyang et al., 1995), although the interaction also exhibits rapid association/dissociation kinetics (Felder et al., 1993).

SH2 domains are found in within a number of functionally diverse proteins ranging from enzymes and adaptors proteins (Pawson et al., 2001). The binding of these

modular proteins to pTyr containing motifs serves to relocate or activate proteins within cells, and may also activate them. As SH2 domains have no significant affinity for non-phosphorylated peptides, the phosphorylation of tyrosine regulates the binding of proteins to SH2 modules, with the sequence surrounding the pTyr residue dictating the specificity of protein binding, and thus the biochemical pathways triggered. All SH2 domains show selectivity for the amino acids immediately C-terminal to phosphotyrosine (Songyang et al., 1993). Additional specificity can be conferred on pTyr binding proteins by the presence of tandem SH2 domains in a protein. In fact, the presence of dual SH2 domains in a protein imparted higher affinity and greater specificity on pTyr-binding proteins (Ottinger et al., 1998).

The primary sequences of SH2 domains indicate a shared homology between members of this protein family. The general architecture is shared by all SH2 protein (Figure 1.13). The domains are divided into two functionally distinct regions by an antiparallel β sheet. This structure acts as the core for the protein and consists of strands A, B, C, D, and G. The region of protein concerned with phosphotyrosine binding is flanked by helix αA; the other, flanked by helix αB and the BG and EF loops, is involved in binding the residues C-terminal to the phosphotyrosine. A smaller sheet, comprising of strands D', E, and F, closes off one part of this side. Protein sequences containing the phosphotyrosine lie across the upper binding surface of the SH2 domain, orthogonal to the central β sheet. The N- and C-terminals of the domain lie on the side opposite the binding surface, allowing for the attachment to proteins without disrupting phosphotyrosine binding (Kuriyan and Cowburn, 1997).

Residues in the αA, βB, βD structures, and the BC loop are responsible for phosphotyrosine binding. The SH2 signature sequence ('FLVRES'), located in the βB sheet, is intimately involved in the binding of phosphotyrosine through hydrogen bonding and electrostatic interaction. The basic nature of these residues within this cleft is indicative of the pTyr-binding pocket being a cationic cavity, capable of binding the negatively charged phosphate group. The 'FLVRES' signature sequence, conserved throughout the SH2 domain family, contains an arginine located in position 5 of the βB sheet. This residue is the most critical residue involved with phosphopeptide-SH2 interactions, as studies have shown that mutation of this site

completely abolishes phosphopeptide binding to SH2 domain proteins (Bradshaw et al., 1999; Mayer et al., 1992). The archetypal model for the binding of phosphopeptides to src SH2 domains was established on the elucidation of the crystal structure of the Src SH2 domain complexed with an 11 residue phosphopeptide (Waksman et al., 1993). The phosphate group forms a bidentate ion pair with ArgβB5, which protrudes out of the internal structure to meet the phosphate moiety. Binding of the phosphate to ArgβB5 induces minor conformational changes within the domain which may in turn activate the protein and in so doing localise the protein of which the SH2 is part. The position of the 'FLVRES' arginine within the phosphotyrosine pocket makes it inaccessible to water, therefore, only the extended conformation of a phosphotyrosine, and not serine or threonine phosphates, allows it to form the ionic interactions with ArgβB5. Further to this interaction, a number of hydrogen bonds are formed between the phosphate oxygens interacting with ThrBC2, GluBC1, and SerβB7. LysβB6 and HisβB6 form hydrophobic interactions between, the side chains of these residues and the aromatic ring of tyrosine. An amino-aromatic interaction involving ArgαA2 is also believed to be involved in phosphotyrosine binding (Figure 1.13, Kuriyan and Crowburn, 1997; Waksman et al., 1993).

The binding of the residues C-terminal to phosphotyrosine defines the selectivity of SH2 domain binding partners. Src kinases binds the sequence: YEEI, in what has been described a 'two pronged plug, two holed socket' interaction, due to another clearly defined cavity existing on the surface of the domain for a hydrophobic residue +3 to phosphotyrosine, in addition to the phosphotyrosine pocket (Waksman et al., 1993). The residues in the EF and BG loops that form this pocket are highly variable and differences in sequence account for the differential ligand specificity of SH2 domains. Furthermore, instead of a distinct hydrophobic pocket, some SH2s, such as that of PLCγ, have an extended groove (Kuriyan and Crowburn, 1997).

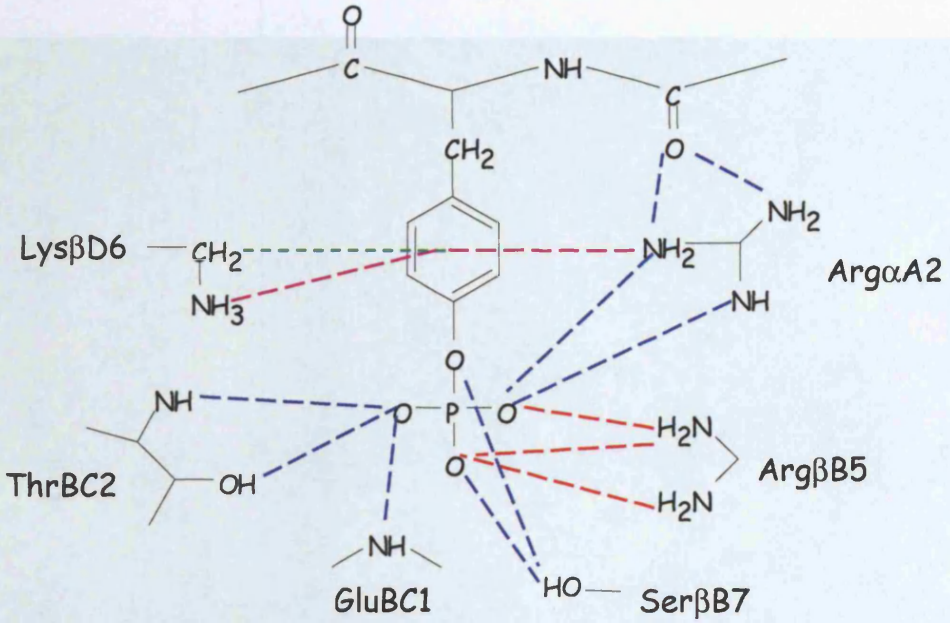

Figure 1.13. Schematic representation of the phosphotyrosine/SH2 domain interaction in src kinase. The pTyr residue forms a number of hydrogen bonds (blue) with the residues that make up the pTyr-binding pocket. Additionally van der waal (green) and amino aromatic interactions (purple) are formed. The key interaction is the bidentate interaction between the guanidium group of ArgβB5 and the phosphate oxygens (Adapted form Waksman et al., 1993).

The solution structure of the src kinase Fyn complexed to a phosphopeptide has been solved. The structure showed the distinct interaction common to other src kinases. The phosphotyrosine binding pocket being formed by residues SerβD7, ThrBC2, SerβC3, HisβD4, tyrosineβD5 and LysβD6, with through space proton-proton interactions being detected between the phosphate group and all of these residues, with the except SerβD7. Salt bridges were detected between the phosphate group and ArgβB5, and, although poorly defined, there was evidence for the amino-aromatic interaction involving ArgαA2 and tyrosine (Mulhern et al., 1997).

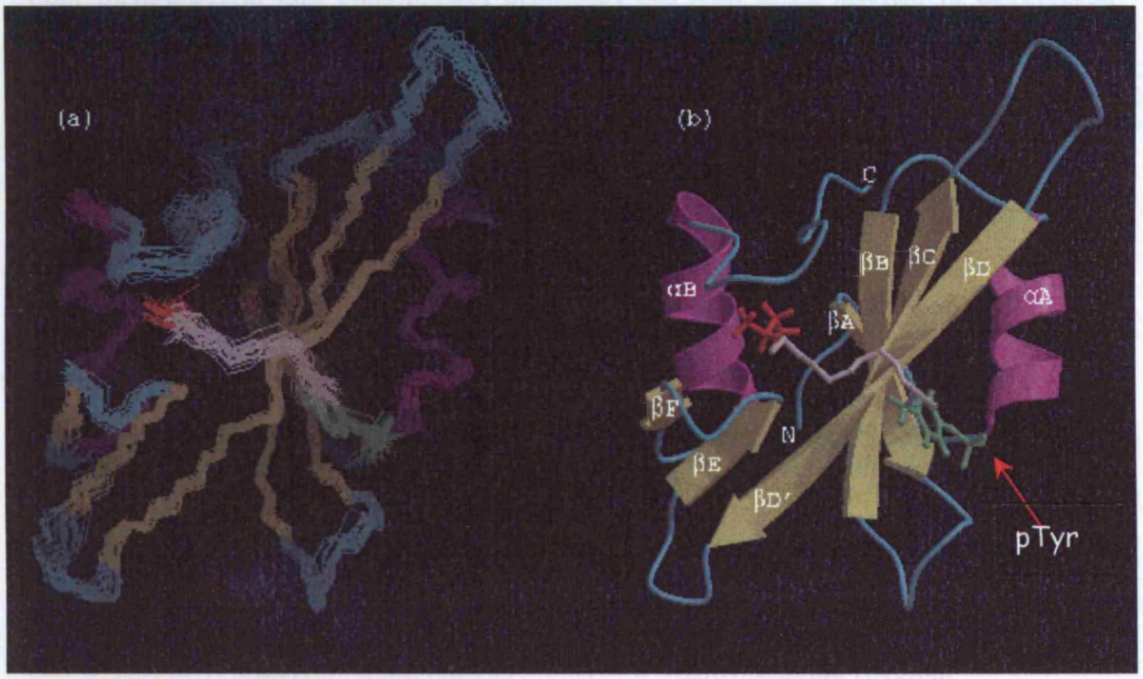

Figure 1.14. The NMR structure of the Fyn SH2-peptide complex. (a) Superposition of the 22 final structures showing the backbone N, C^{α} and C' atoms of the SH2 and the backbone N, C^{α} and C' atoms of peptide pY (green) and +3I (red) sidechains. **(b)** The secondary structural elements defined from the energy minimised average coordinates (Mulhern et al., 1997).

As well as activating and localising proteins, SH2 domains may play a role in protecting phosphotyrosine residues in cells, thus maintaining the pTyr content of the cell (Brunati et al., 1998). Tyrosine phosphatases are some of the most efficient enzymes known with the K_{cat}/K_m ratios approaching the efficiency limited by diffusion (reviewed Barford, 1995). The binding of phosphotyrosine to SH2 domains has been shown to protect the low phosphotyrosine content of the cell against dephosphorylation. Further to this, the mechanism of phosphotyrosine-SH2 dissociation may not merely depend on the equilibrium displacement by phosphatases and other agents such as inositol phosphates may be important (Rameh, 1995).

In summary, the structure of SH2 domains provides a selective means of phosphorylation dependant protein association, which is critical in initiating the

intracellular segment of growth factor signalling, the regulation of src kinase activity, as well as maintaining the cell's phosphotyrosine status. The fundamental role played by the phosphotyrosine-SH2 domain interaction in transduction pathways involved in both physiological and pathological processes has lead to an interest in developing therapeutic agents that specifically inhibit this interaction (Table 1.5). Interestingly, some prototypes have been based on the nTyr moiety, with a dinitrotyrosine based inhibitor being shown to have significant affinity for the SH2 of Syk, although the same inhibitor showed no affinity for src (Anonymous, 1998), suggesting the make up of the pTyr-binding pocket is critical in determining the binding of non-pTyr ligands.

Table 1.5 SH2 domain inhibitor targets in disease states (Sawyer, 1998).

Protein	Disease
Src	Cancer, Osteoporosis
Hck	AIDS
Syk	Allergy, Asthma
Zap70	Autoimmune disease
Syp	Aneamia
STATs	Inflammatory
Grb2	Cancer, chronic mylogenous leukaemia
Shc	Cancer, erythroleukemia
P85/PI3K	Cancer
Gap	Cancer
Bcr/Abl	Chronic mylogenous leukaemia

AIMS AND OBJECTIVES

Establishing the role that nTyr plays in cell biology is a challenge that will shed light on the harmful effects of RNS produced endogenously, exposures to RNS via other routes, in addition to the toxicity of inhaled nitric oxide therapy. One hypothesis is that nTyr mimics the post-translational actions of pTyr and may act as a permanent 'on' switch *in vivo*. The aim of the work detailed in this thesis is to determine the consequences tyrosine nitration on specific aspects of cell signalling. To this end a peptide motif consisting of residues 321-329 of the hamster polyomavirus

oncoprotein, (DS4: Glu-Pro-Gln-**Tyr**-Glu-Glu-Ile-Pro-Ile) was synthesised and used as a model.

The specific aims of this thesis are:

- To fully characterise DS4, its derivatives and to determine the consequences of tyrosine nitration peptide structure.
- To determine the extent to which nitrated DS4 binds to the SH2 domain of Fyn.
- To rationalise the binding of nDS4 to the SH2 at the molecular level.
- To observe the effects of nDS4 binding to the SH2 domain of Fyn in the cellular context.
- To establish whether aminotyrosine is a substrate for protein tyrosine kinases.

The approaches and methodologies used to achieve these objectives will be outlined in chapters 2 to 6, with the findings of these 5 chapters, along with the biological significance and implications being discussed in chapter 7.

CHAPTER 2:

SYNTHESIS AND CHARACTERISATION OF DERIVATIVES OF DS4 AND FYN SH2 DOMAIN

INTRODUCTION

The following chapter describes the synthesis and characterisation of DS4, its derivatives, and of Fyn SH2 domain, the raw materials around which all work in this thesis is based. Generation of the nitropeptide was achieved initially by nitrating DS4 using TNM. In order to save the valuable peptide, the procedure was initially optimised on Ang II. Not only does this peptide resemble DS4 in size, the nitrated derivative was of interest to colleagues at the department of Child Health, Leicester Royal Infirmary, who were investigating in the nitropeptide because of its potential role in modulating cardiovascular function. The full characterisation of both peptide and SH2 domain established biophysical properties that were used as a starting point in studies described in the following chapters.

The phosphorylated derivative of DS4 is a high affinity ligand for all Src kinase SH2 domains (Cantley et al., 1991), and was therefore utilised to study the effect of tyrosine modification on peptide-SH2 domain interactions. The rationale for selecting Fyn as a model SH2 domain for the studies was, firstly, its availability; Professor I Campbell of Oxford University of was kind enough to provide the plasmid expressing the SH2 domain protein. Additionally, the publication of the solution structure of Fyn SH2 bound to an analogue of DS4 (Mulhern et al., 1997), the availability of the backbone assignments for the ^{15}N labelled SH2 domain (personal communication, Professor I. D. Campbell, University of Oxford), and access to coordinates that would enable a model of pDS4 bound to the SH2 domain of Fyn to be constructed (Brookhaven Protein database, accession numbers: 1AOU and 1AOT), all meant a detailed molecular analysis of the interaction between the SH2 domain and derivatives of DS4 could be conducted.

PRINCIPLES AND TECHNIQUES

The following section is intended to outline briefly of the some of the techniques employed to characterise the materials that were used throughout this thesis. More detailed explanations of these techniques can be found in the following texts: for HPLC the reader is referred to Weston and Brown (1997); for NMR, Rattle (1995); and for mass spectrometry Smyth (1999), Bakhaitar and Tse (2000), and Burlingame et al., (1996).

Reverse Phase High Performance Liquid Chromatography

Chromatography can be described as a method in which the components of a mixture are separated on an adsorbent column in a flowing system. The flowing system can be either liquid or gaseous, and the adsorbent material solid particles, immobilised liquids and gels. High performance liquid chromatography (HPLC) is a technique in which a solution containing a mixture of solutes is pumped onto a stationary phase, and its components separated according to their affinity for the stationary phase. In reverse phase (RP) HPLC a polar mobile phase is pumped across a non-polar stationary phase, and solutes are retained and eluted based on their solvent solubility and their interactions with the stationary phase. The stationary phase in RP-HPLC is usually made up of silica beads to which aliphatic chains of varying length are chemically bonded.

Two mechanisms have been put forward as to the modes of solute retention on a RP column, the partitioning and solvophobic models. In the partitioning model the solute molecules are believed to bind to the stationary phase via hydrophobic interactions, whilst the solvophobic model suggests column retention is achieved due to the phobicity of the solute for the mobile phase. On replacement of a polar solvent, such as water, by a less polar solvent, such as acetonitrile, the solute is liberated from the column due to the combination of disruption of the hydrophobic interactions and its increased solubility in the mobile phase. Based on these simple principles, RP HPLC was used to separate and characterise DS4 and its derivatives.

Collision Induced Dissociation Electrospray Mass Spectrometry

The production, differentiation, and detections of ions in the gas phase are the principles on which mass spectrometry is based (Siuzdak, 1994). In fast atom bombardment (FAB) the energy to achieve these processes is delivered in 'one package' over a short period of time, which can result in sample fragmentation. By contrast, in electrospray ionisation (ESI) generation of gas ions is achieved gradually at lower temperatures. This reduces the propensity of ions to fragment, making this technique amenable to study biological materials and non-covalent interactions.

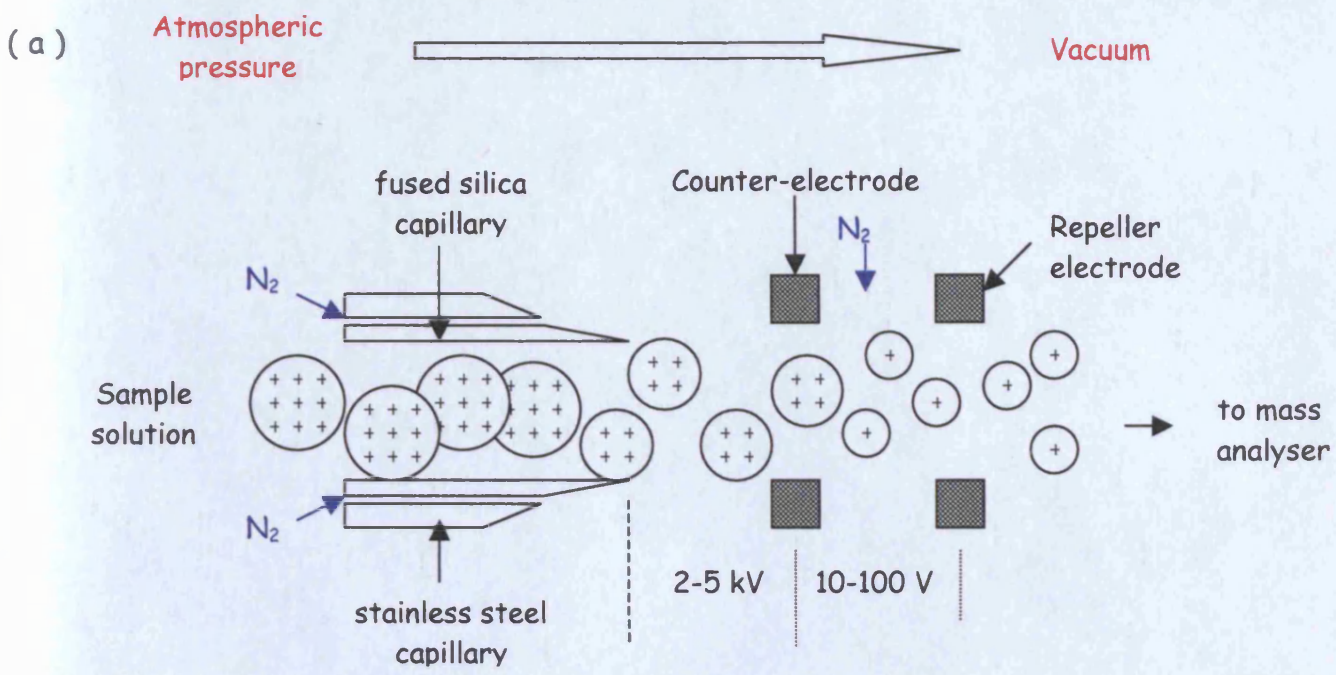

Figure 2.1 Schematic representation of Electrospray ionisation (adapted from Przybylski and Glocker, 1996). (a)The sample solution is pumped into the ionisation chamber, with the flow of nitrogen gas along the capillary aiding sample nebulisation. The generated aerosol droplets become charged by means of the electric field generated between the capillary tip and the counter-electrode. The charged droplets then undergo a rapid reduction in size eventually leading to the disintegration of the droplet and the generation of gas ions. (b) Diagrammatic representation of tandem mass spectrometry: a peptide mixture is ionised. The parent ion of a peptide is selected by the first mass spectrometer then fragmented by collision with a neutral gas such as argon or helium. These fragments can then be scanned by another mass spectrometer.

Three steps are involved in the generation of gas phase ions in ESI. Firstly, positively charged ions are generated by application of a potential difference (~4000 V) to the steel capillary, from which the sample solution is sprayed. Next, droplet size is

reduced and the charge density increases due to solvent evaporation, a process facilitated by the application of dry gas and/or heat. Finally, as the electrostaic repulsion of the positive charges exceeds that of the droplet surface tension, the droplets disintegrate generating gas phase ions, which are then separated according to mass/charge ratio (Figure 2.1a).

A further development to ESI has been to use two mass spectrometers in tandem to generate a series of fragments that characterise a pre-selected ion. The first spectrometer serves to separate the individual components of a mixture and select an ion (the 'precursor' or 'parent' ion), which is subsequently fragmented by collision with an inert gas, such as helium. The second mass spectrometer then detects the generated 'daughter', which is in effect a signature the original 'parent' ion. This technique has been applied to sequence short peptides, where fragmentation generally occurs in the peptide's backbone leading to the formation of characteristic ions (Figure 2.2).

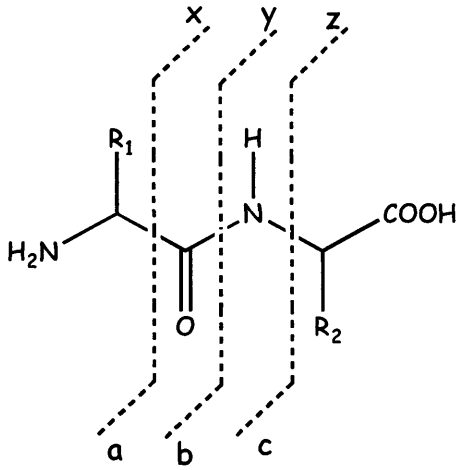

Figure 2.2 Common fragments generated on peptide fragmentation. Fragmentation of the peptides can occur at various positions on the backbone, giving rise to specific fragment ions.

Nuclear Magnetic Resonance

In the quantum mechanical world, both the nucleus and the electrons orbiting it possess spin angular momentum. Moreover, both the magnitude and the number of permitted orientations in space of this vector quantity are fixed, governed the nucleus-

specific angular momentum quantum number (j) and the spin quantum number (I). Nuclei with I values of ½ (^{1}H, ^{13}C, ^{15}N, ^{31}P, to name but a few) have two values for their angular momentum giving two orientations of the magnetic moment vector. On application of an external magnetic field (B_0) to a ½ spin nucleus the otherwise degenerate angular momentum is split into its two possible orientations, as the nucleus aligns itself within the magnetic field. The two orientations are associated with fixed energy levels- a low energy level (α), associated with the orientation that tends to line up in the direction of the externally applied field, and a high energy level (β), whose alignment is most opposed to the direction of the magnetic field. Slightly more nuclei populate the lower energy state than the upper, consequently, a net magnetic moment is generated along the z axis (M_z), in the same direction as the applied magnetic field. Secondly, the nucleus begins to precess about B_0 due to the interaction between the spinning magnet and B_0 (Figure 2.3). The frequency of this precessional motion (the Larmor frequency) is a function of the type of nucleus, and the net local magnetic field it experiences. As the magnetic flux experienced by a nucleus will be influenced not only by the externally applied field but also by the orbit of its electrons, the frequency at which a nucleus precesses will be characteristic of the chemical environment in which it resides. Additionally, magnetic fields such as those generated by aromatic rings will also affect the rate at which a nucleus precesses.

Exposure of a nucleus to electromagnetic radiation at the Larmor frequency of the nucleus of interest (this will reside in radio-frequency range of the electromagnetic spectrum) will generate an additional magnetic field (B_1) perpendicular to B_0. B_1 will also rotate at the Larmor frequency of the nucleus, and is thus stationary with respect to it. As nuclei precess about stationary magnetic fields, precession about B_1 will induce the spins to undergo transitions between its lower and upper energy levels, leading to a reduction or inversion of M_z. The length of the radio-frequency pulse applied determines the number of transitions that occur, hence the size of M_z.

Individual nuclei do not precess in concert on application of B_0, rather their precessional motion is randomly arranged and occurs at different rates. As a result of this phenomenon, there is no net magnetism in the xy plane on application of B_0 as

the sum of the individual spins is averaged to zero. However, the application of B_1, has the effect of synchronising presession about B_0 (the nuclei are said to have been brought into 'phase' or possess phase coherence), consequently, net magnetisation is induced in the xy plane. At the end of the radio frequency pulse, and hence B_1, this precessional coherence is lost, as the nuclei loose energy due to molecular interactions and motion (dephasing). The decay of the M_{xy} component of magnetism is exponential (The Free Induction Decay, FID), and, importantly, the frequency at which the magnetism rotates in the xy plane is a label of the Larmor frequency of nucleus. Put simply, the FID is a measure of the Larmor frequency of a nucleus, and therefore an indicator of the chemical environment in which the nucleus resides. The FID measures the displacement of magnetism in the xy plane on applying a pulse of a given frequency as a function of time. A mathematical algorithm (the Fourier transformation) can be applied to interconvert these time and frequency functions into a solitary peak (Figure 2.3). As nuclei of the same element will reside in a differing chemical environment within a biomolecule, Fourier transformation of the generated FID will give rise to a characteristic peaks at specific frequencies (chemical shifts), enabling the different chemical environments of the same nuclei to be distinguished (Figure 2.2).

Electrons that form a covalent bond between nucleus A and B will spend time orbiting both. As nucleus A has two orientations (α and β), each with an associated energy, nucleus B will experience two slightly different magnetic fields, as transmitted by their shared electrons. Consequently, nucleus B precesses at two different Larmor frequencies. This phenomenon, known as scalar coupling, gives rise to the splitting of an individual resonance in the NMR spectrum and is important in the identification of the different functional groups.

When dealing with larger biomolecules such as proteins, one-dimensional NMR will give rise to extensive signal overlap due a number of similar chemical shifts. However, by spreading the signals over two-dimensions protein spectra can be simplified, making interpretation easier. Moreover, 2D NMR can provide information on spins linked through covalent bonds, or those that are within close enough proximity to be linked by through space interactions. The basis that underlies two-

dimensional NMR is that phase coherence can be exchanged between two nuclei. For instance, parameters can be set such that coherence is transferred between nuclei of two different elements, such as ^{15}N nuclei and protons to which it is directly bound (a process known as Heteronuclear Single Quantum Coherence, HSQC). Additionally, COSY (**CO**rrelation **S**pectroscop**Y**) and TOCSY (**TO**tal **C**orrelation **S**pectroscop**Y**) methods can be applied to characterise through bond nuclear connectivities. In proteins, these techniques can be applied to identify amino acid spin systems, with COSY identifying those protons linked by up to three covalent bonds, whilst TOCSY couples the entire amino acid proton complement, without being transmitted through the amide bond. NOESY (**N**uclear **O**verhauser **E**ffect **S**pectroscop**Y**) identifies those protons close enough (<5Å) to be coupled via through space interactions, and is key in determining biomolecular structure by NMR.

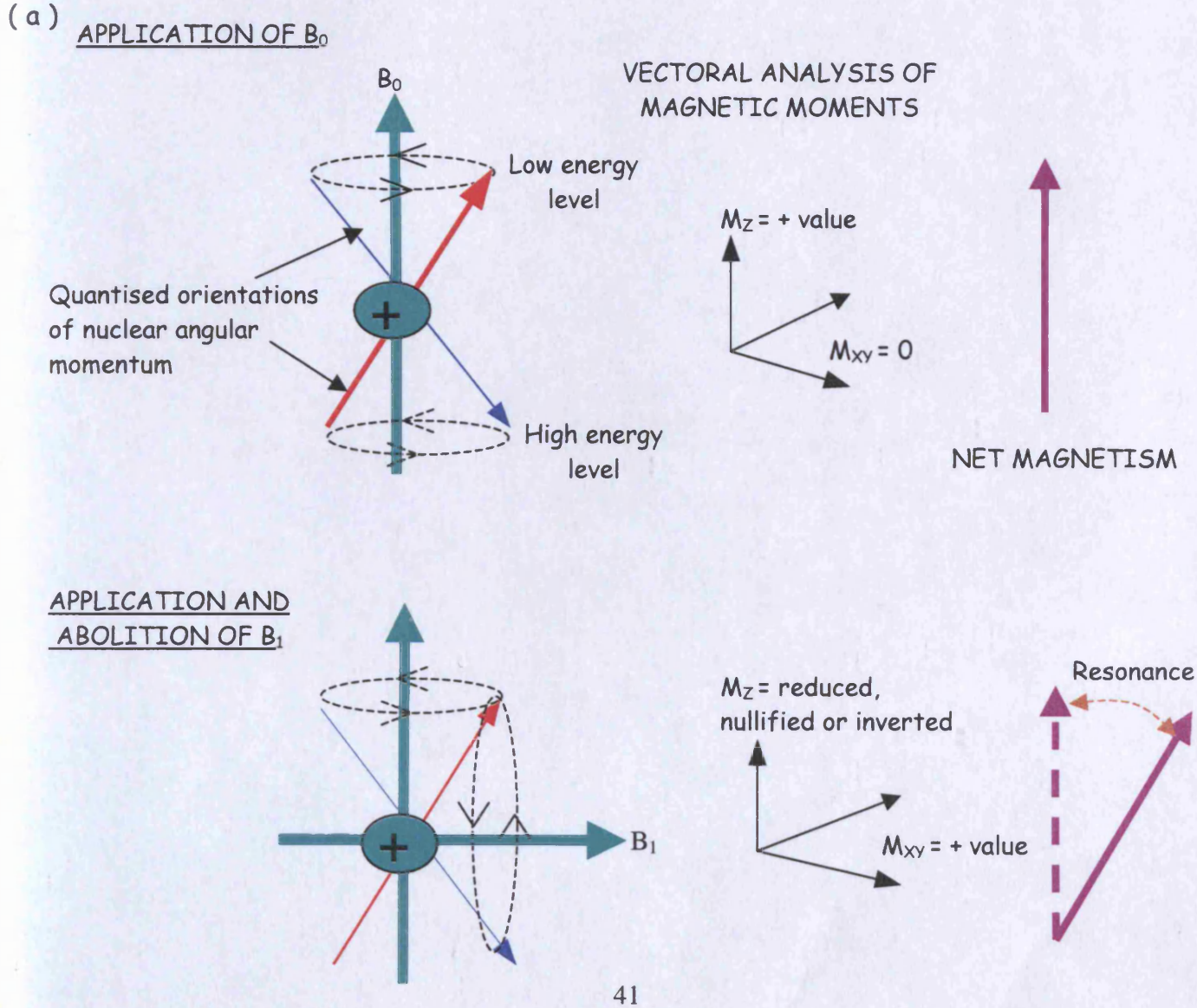

Detection and Mathematical treatment of magnetic resonance

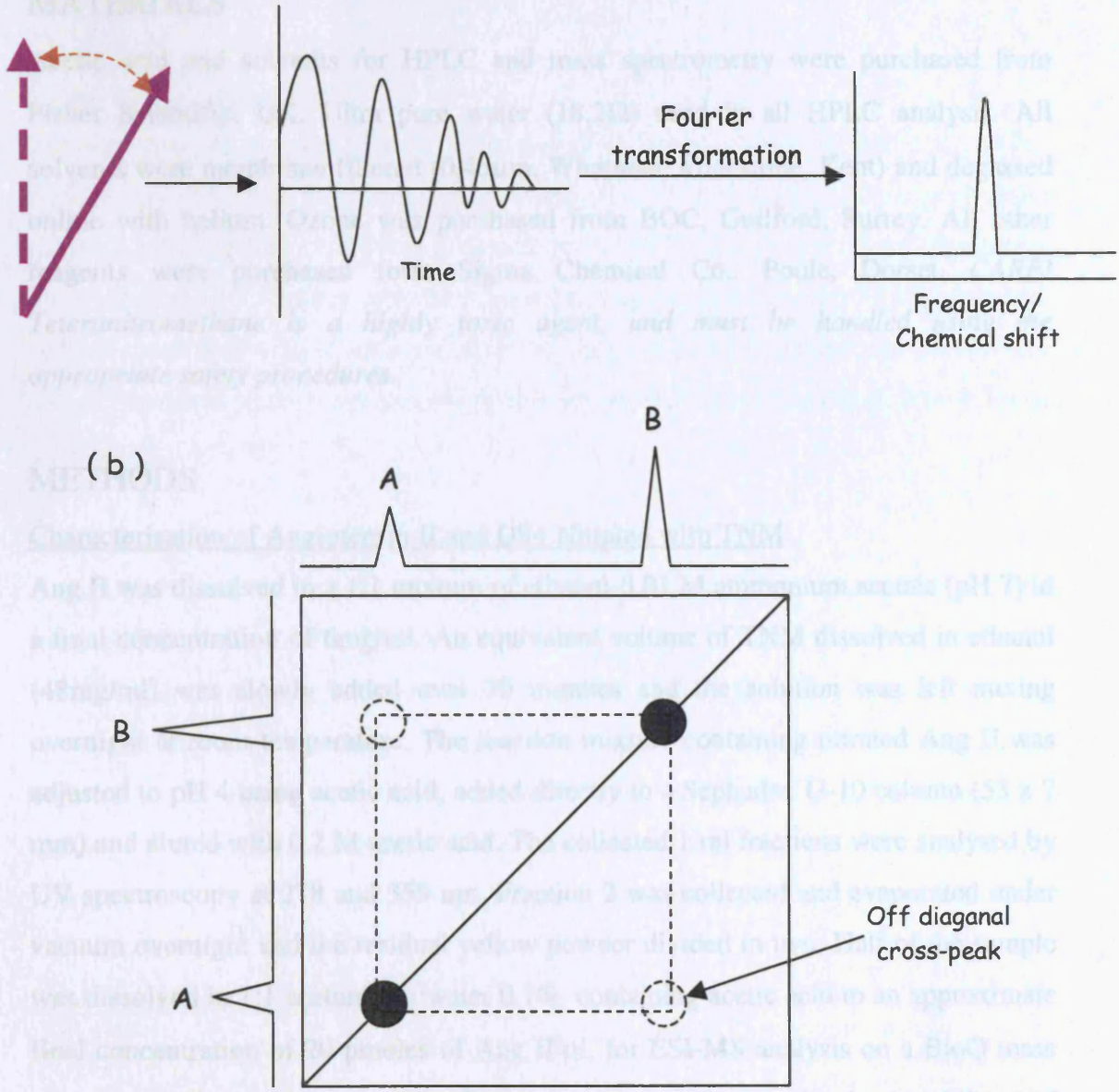

Figure 2.3. (a) Schematic representation of the generation and detection of nuclear magnetic resonance. When placed in a magnetic field the otherwise degenerate magnetic moments associated with orbiting electrons are split into high and low energy levels. Application of a second magnetic field perpendicular to the original field causes the magnetism in the z plane to be reduced and, as a result of phase coherence, magnetism to be induced in the xy plane. Once the application of B_1 is halted the net magnetic moment oscillates at the Larmor frequency of the nucleus, whilst continually losing energy, giving rise to the free induction decay. **(b) Schematic representation of a 2D spectrum.** Resonance A is coupled to resonance B as indicated by the off diagonal cross-peaks linking the two resonances.

EXPERIMENTAL PROCEDURES

MATERIALS

Acetic acid and solvents for HPLC and mass spectrometry were purchased from Fisher Scientific, UK. Ultra pure water (18.2Ω) used in all HPLC analysis. All solvents were membrane filtered (0.45μm, Whatman, Miadstone, Kent) and degassed online with helium. Ozone was purchased from BOC, Guilford, Surrey. All other reagents were purchased form Sigma Chemical Co., Poole, Dorset. *CARE! Teteranitromethane is a highly toxic agent, and must be handled using the appropriate safety procedures.*

METHODS

Characterisation of Angiotensin II and DS4 Nitrated with TNM

Ang II was dissolved in a 1:1 mixture of ethanol-0.01 M ammonium acetate (pH 7) to a final concentration of 6mg/ml. An equivalent volume of TNM dissolved in ethanol (48mg/ml) was slowly added over 30 minutes and the solution was left mixing overnight at room temperature. The reaction mixture containing nitrated Ang II was adjusted to pH 4 using acetic acid, added directly to a Sephadex G-10 column (53 x 7 mm) and eluted with 0.2 M acetic acid. The collected 1 ml fractions were analysed by UV spectroscopy at 278 and 359 nm. Fraction 2 was collected and evaporated under vacuum overnight and the residual yellow powder divided in two. Half of the sample was dissolved in 1:1 acetonitrile:water 0.1% containing acetic acid to an approximate final concentration of 20 pmoles of Ang II/μl, for ESI-MS analysis on a BioQ mass spectrometer in positive ion mode. The remaining sample was dissolved in 100 μ l of water for HPLC analysis, which was conducted on a Waters model 600 multi-solvent delivery system. The analysis of Ang II and its nitrated derivative was conducted on a Brownlee C_4 (220 x 4.6 mm) column. Solvent A was 18% MeCN, 0.05% TFA in ultrapure water, and solvent B was 30% MeCN, 0.05% TFA in ultrapure water. Peptides were eluted using an increasing linear gradient of solvent B from 0 to 45% in 45 min with a flow rate of 0.5 ml/min. For DS4 samples were analysed on a Hypersil 5 μm C_{18} semi-preparative column (250 x 10 mm), at a flow rate of 2 ml/min. Solvent compositions was as for Ang II. Peptides were eluted using an increasing linear gradient of solvent B from 0 to 100% in 100 min. Detection of eluted peptides utilised

a Shimadzu UV detector (model SPD-6A) at a wavelength of 215 for Ang II and 260nm for derivatives of DS4.

Preparation of peroxynitrite

Peroxynitrite was prepared by the ozonation of an azide solution (Pryor et al., 1995). Briefly, dry oxygen (166 ml/min) was passed through a Wallace & Tiernan ozonator (Type BA.023) undergoing electric discharge at 150 V. The stream of gas, containing approximately 0.5% ozone, was then passed through a glass-frit into 50 ml ice-cooled sodium azide (previously adjusted to pH 12 with 5M NaOH) and left for 1 hour. The concentration of peroxynitrite was determined spectrophotometrically in 0.1 M NaOH (ε: 302 nm, 1670 M^{-1} cm^{-1}).

Characterisation of DS4 Nitrated by peroxynitrite

A peroxynitrite solution (24mM) was added progressively (final concentration 50µM per addition) to DS4 (50µM) and vigorously mixed for 15 mins at room temperature. HPLC analysis was conducted on a Gilson-gradient controlled system equipped with Gilson 486 UV detector using a Hypersil BDS 5 µm C_{18} column (250 x 4.6 mm), at a flow rate of 1 ml/min. Solvent compositions was: A was 0.1 % TFA in ultrapure water, and solvent B was 100% MeCN containing 0.1% TFA. Peptides were eluted using an increasing linear gradient of solvent B from 30 to 35 % in 20 min.

Solid phase peptide synthesis

All peptide synthesis was conducted in house at the Protein and Nucleic Acid Laboratory (PNACL), University of Leicester. All HPLC analysis was conducted using the conditions utilised for analysis of DS4 nitrated by peroxynitrite.

Mass Spectral Analysis

The electrospray ionisation mass spectra were obtained on a VG Quattro-BQ tandem quadrupole instrument (Micromass, Manchester, UK). Peptide samples were electrosprayed from acidified (0.1% acetic acid) 50% acetonitrile solution at a sample concentration of 20 pmoles/µl. The analyte solutions were infused into the mass spectrometer source, using a Harvard system pump (model 55-2222) at a flow rate of 5 µl/min through a 75 µm (inner diameter) fused silica capillary, and positive ion spectra obtained. Tandem mass spectrometry measurements were performed using the

first quadrupole to transmit the singly protonated peptide to a collision cell containing research-grade argon, while a second quadrupole was used to analyse the product scan of the protonated peptide precursor.

Transformation of *E.coli* with Fyn expression plasmid

The Fyn construct, based on the pRK172 plasmid, was a kind gift from I Campbell (Oxford Centre for Molecular Science, University of Oxford). The plasmids, extracted using a Qiagen mini purification protocol (Qiagen, GmbH, Germany), were transfected into *E. coli* BL21 (DE3) (a kind gift from Dr R Badii, Biological NMR, University of Leicester) using the following protocol: A 50 ml culture of *E.coli* BL21 (DE3) was incubated at 37°C until the OD_{600} of approximately of 0.5 units. The bacteria were pelleted at 4°C at 12000 g for 5 min. The bacteria were then resuspended in 50 ml of 100 mM of calcium chloride and left on ice for 15 min. The bacteria were then repelleted and resuspended in 5ml 100 mM calcium chloride and kept on ice. 1 μg of the Fyn expression in 100 μl in TEN buffer (see appendix I), was added to 200 μl of the treated bacteria and left on ice for 30 mins, then placed in a 37°C water bath for 5 min. 300 μl L-Broth was added to the bacteria, and allowed to incubate at 37°C for 1hr.

Fyn expression and purification

The expression and purification of Fyn was based on the protocol described by Mulhern et al (1997). Breifly, transformed *E. coli* BL21 (DE3) were grown at 37°C in Terrific Broth containing ampicillin (100 μg/ml), to an OD_{260} between 0.5-1.0. Fyn expression was induced for 4 h by the addition of 0.1 mM IPTG, prior to harvesting the cells (15 min, 20000g centrifugation at 4°C). Cells were then either stored at -20°C or resuspended in TTBS (Tris-HCl, pH 8.5, 150mM NaCl, 0.1% (v/v) Triton X-100) containing 2mM PMSF, at a ratio of 10 ml/g of cells. Lysis of the cells was effected by triplicate use of a French press. Cell debris was removed by centrifugation (20,000 g for 30 min), and the ice-chilled supernatant pumped slowly onto a phosphotyrosine agarose column source. After extensive washing of the column with TTBS and TBS (TTBS without NaCl) Fyn was eluted with TBS containing 1.15M NaCl. The elution was monitored at 254nm using a Gilson UV/vis detector (model 112). The protein

was then exchanged into the appropriate buffer using a PD10 column (Pharmacia, Uppsala, Sweden), prior to SDS-PAGE, and mass spectral analysis.

NMR Analyses of DS4 and Derivatives

Peptides were dissolved in NMR buffer (1ml, see appendix) containing D_2O (10 % v/v) to a final concentration of 16.7 mM. All ^1H NMR analyses were conducted at 600 MHz on a Bruker DRX 600 instrument. All spectra were acquired at 293 K. Parameters for data acquisition and processing are provided in the table below. Suppression of the water signal in TOCSY and NOESY experiments was achieved using the WATERGATE method, whilst suppression for COSY spectra was achieved by PRESAT.

	Time domain size (points)		Spectral widths (Hz)		Proceeded points		Number of scans
	t_1	t_2	ω_1	ω_2	t_1	t_2	
1D	8192		10000				16
COSY	4092	512	10000	10000	2048	1024	8
NOESY	4096	512	10000	10000	4096	1024	48
TOCSY	4096	512	10000	10000	4096	2048	18

RESULTS

Nitration, purification and characterisation of Angiotensin II

The nitration procedure involving tetranitromethane (TNM) was initially optimised using AngII. The rationale for using this peptide as a surrogate for DS4 was the comparable lengths of the two, and the presence of solitary tyrosine residues in both (Figure 2.4). Interestingly, the nitration of Ang II renders this hormone biologically inactive (Kooy and Lewis 1996), and might therefore be an additional mechanism by which RNS can modulate cardiovascular function.

DS4:	Glu	Pro	Gln	Tyr	Glu	Glu	Ile	Pro	Ile
Ang II:	Asp	Arg	Val	Tyr	Ile	His	Pro	Phe	

Figure 2.4. The peptide sequences of DS4 and Ang II.

Figure 2.5a shows the elution of the Ang II nitration reaction mixture from a Sephadex G-10 mini column. Mass spectral analysis of the first eluting peak identified both the nitrated and the non-modified derivatives of Ang II within this fraction (Figure 2.5b), as also confirmed by HPLC/MS analysis (Figure 2.5c). The material eluting after the 12th fraction absorbing at 278 nm is likely to be a derivative of trinitromethane. Approximately 70% of the Ang II underwent nitration, as determined by the area under the peaks on the HPLC trace* (Figure 2.5c). Increasing concentrations of TNM in the original reaction mixture had no effect on the proportion of peptide nitrated (data not shown).

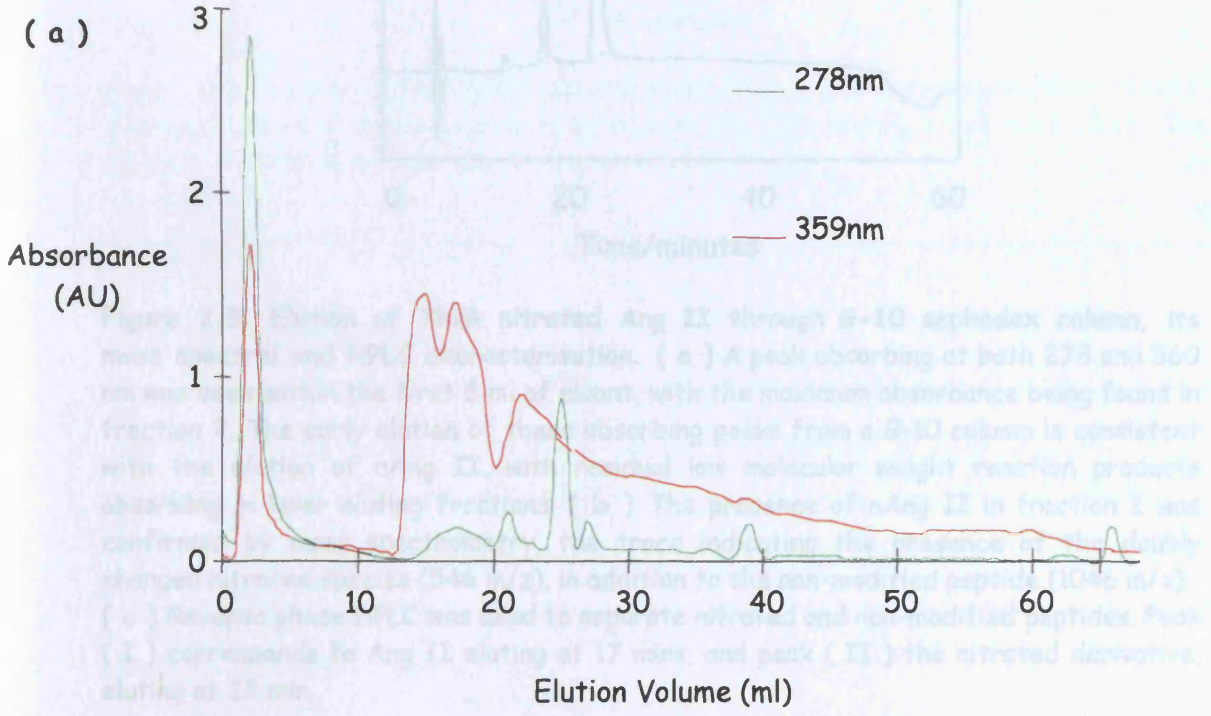

* based on the assumption that Ang II and nAng II have the same molar extinction coeffecient at 215 nm.

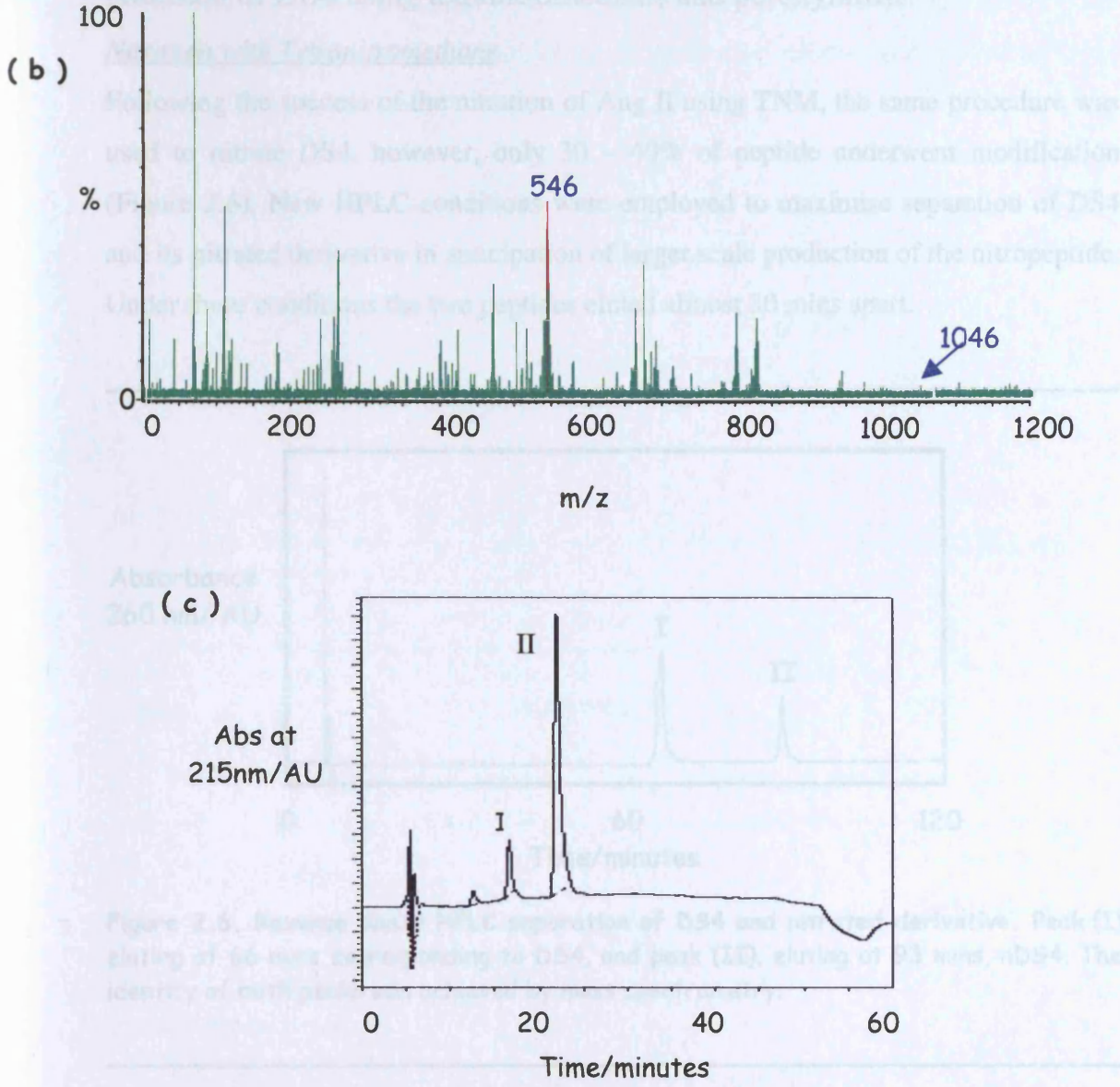

Figure 2.5. Elution of TNM nitrated Ang II through G-10 sephadex column, its mass spectral and HPLC characterisation. (a) A peak absorbing at both 278 and 360 nm was seen within the first 5 ml of eluant, with the maximum absorbance being found in fraction 2. The early elution of these absorbing peaks from a G-10 column is consistent with the elution of nAng II, with residual low molecular weight reaction products absorbing in later eluting fractions. (b) The presence of nAng II in fraction 2 was confirmed by mass spectrometry, the trace indicating the presence of the doubly charged nitrated species (546 m/z), in addition to the non-modified peptide (1046 m/z). (c) Reverse phase HPLC was used to separate nitrated and non-modified peptides. Peak (I) corresponds to Ang II eluting at 17 mins, and peak (II) the nitrated derivative, eluting at 22 min.

Nitration of DS4 using tetranitromethane and peroxynitrite

Nitration with Tetranitromethane

Following the success of the nitration of Ang II using TNM, the same procedure was used to nitrate DS4, however, only 30 – 40% of peptide underwent modification (Figure 2.6). New HPLC conditions were employed to maximise separation of DS4 and its nitrated derivative in anticipation of larger scale production of the nitropeptide. Under these conditions the two peptides eluted almost 30 mins apart.

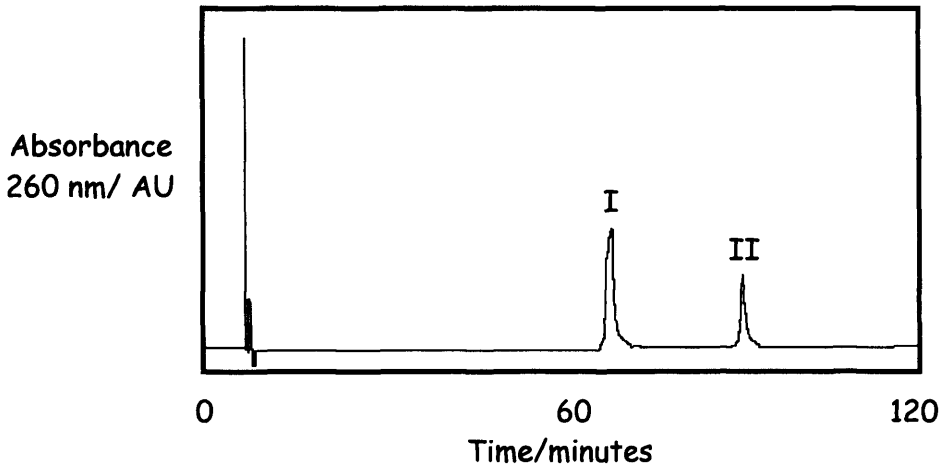

Figure 2.6. Reverse phase HPLC separation of DS4 and nitrated derivative. Peak (I) eluting at 66 mins corresponding to DS4, and peak (II), eluting at 93 mins, nDS4. The identity of both peaks was achieved by mass spectrometry.

Nitration with Peroxynitrite

The inherent danger of handling TNM prompted peroxynitrite to be investigated as a tyrosine-nitrating agent. Bolus additions of peroxynitrite to DS4 resulted in the formation of two distinct products absorbing at 360 nm, identified by ESI-MS as being the mono- and di-nitrated (dnDS4) species' of DS4 (Figures 2.9). Mass spectral analysis confirmed the tyrosine residue alone underwent modification on addition of the nitrating agent (Figure 2.10).

Formation and depletion of the derivatives of DS4 were monitored by HPLC at 215 nm. On additions of up to 10 molar equivalents of peroxynitrite, levels of DS4 decreased, whilst the levels of the mono- and di-nitrated species increased. Above 10

molar equivalents levels of both DS4 and nDS4 began to decrease, whilst the *de novo* formation of dnDS4 continued. Finally, at 20 molar equivalents the levels of all three peptides remained relatively constant.

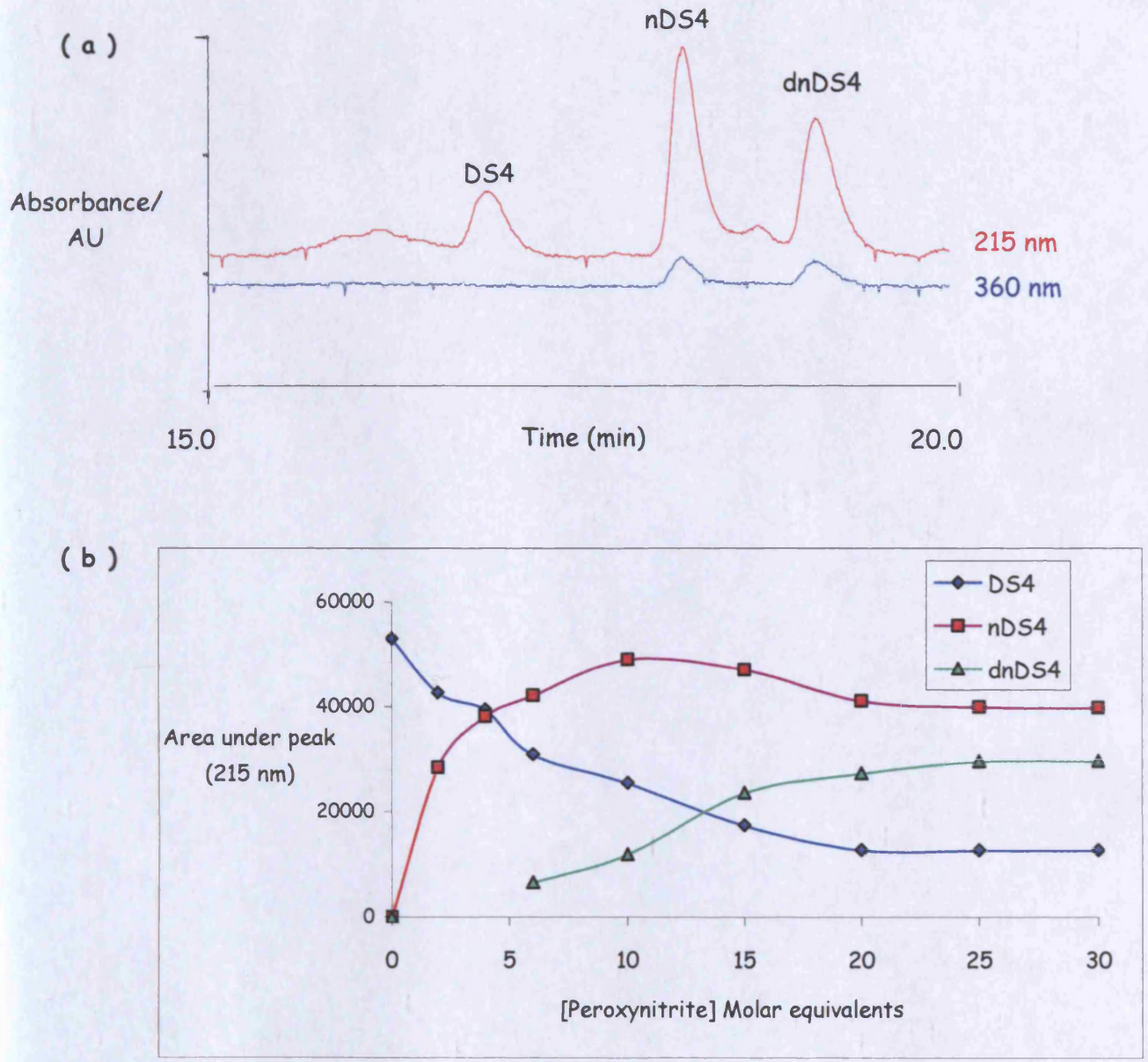

Figure 2.7. The formation of mono- and di-nitrated DS4 using peroxynitrite as a nitrating agent. (a) The above trace shows the addition and incubation of 30 molar equivalents of peroxynitrite to 50 μM DS4. The two products (nDS4 and dnDS4) as well as the starting material (DS4) were identified by mass spectrometry. (b) A comparison of the formation of dnDS4 and nDS4, as well as the depletion of DS4 with respects to peroxynitrite additions was conducted by monitoring the areas under the peaks of the 3 peptides at 215 nm.

Preparation of derivatives DS4 by solid phase peptide synthesis

Towards the end of the first year of work it was noted that an F-moc derivative of nTyr was commercially available. Solid phase peptide synthesis was subsequently utilised to produce the nDS4 motif. UV and HPLC analysis of peptide synthesised by the solid phase method were identical to nDS4 synthesised using TNM and peroxynitrite (data not shown). Unless otherwise stated all subsequent mention to nDS4 in this thesis refers to peptide prepared by the solid phase method. The phosphorylated derivative of DS4 was also synthesised by the solid phase method, utilising the Fmoc derivative of pTyr.

Characterisation of Derivatives of DS4

UV Characterisation of derivatives DS4

UV-visible spectroscopic analysis of the derivatives of DS4 yielded characteristic spectra. All peptides showed high absorbance at wavelengths less than 230 nm, wavelengths at which amide bonds are known to show high absorbance. Neither DS4 nor the phosphopeptide showed significant absorbance in the visible region (>400 nm), with the maximum absorbance above 250 nm for pDS4 being 271 nm, and for DS4 being 276 nm.

The colouration of nTyr is derived from the conjugation of the nitro group to the phenol moiety of trosine. Furthermore, this modification shifts the pKa of the phenoxy group from approximately 10 to 7.5. De-protonation of the phenoxy group of nTyr has the effect of extending the conjugation of the aromatic ring, shifting the maximum absorbance from ~360 nm to ~430 nm. Consequently, in acidic conditions, the UV-visible spectrum of nTyr has a peak situated at 360 nm, giving rise to its yellow colouration, whilst the orange colouration under alkali conditions arises because of a secondary peak found at 430 nm.

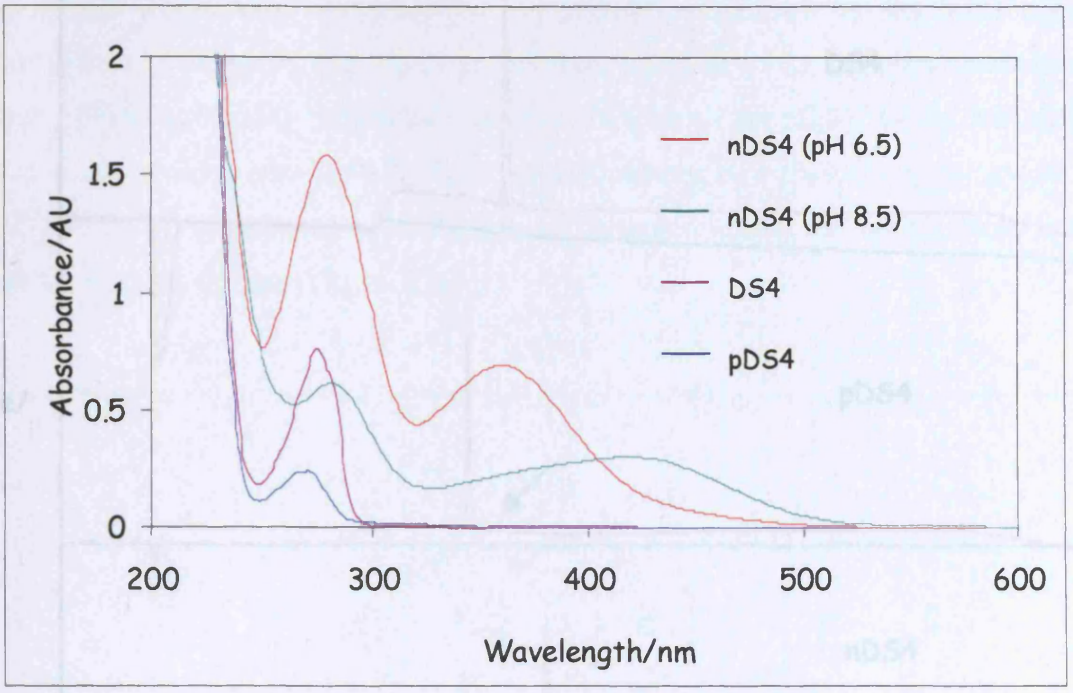

Figure 2.8. UV-visible characterisation of DS4 and its derivatives. The peptides (1mg/ml) were dissolved in phosphate buffer (pH 6.5) and a scan taken from 200 to 600nm. An additional scan was taken of nDS4 in and Tris (pH 8.5).

HPLC characterisation of DS4 Derivatives

HPLC was used to characterise the three peptides synthesised by solid phase synthesis and to check their purity. With the exception of pDS4, all peptides produced single peaks on the HPLC profiles. An additional minor peak with a retention time identical to that of DS4 was found in the phosphopeptide trace. Concomitant synthesis of DS4 along side pDS4 might have arisen due to the contamination of the F-moc-pTyr by F-moc-Tyr. However, it is also possible that the high concentrations of Trifluoroacetic acid used during the deprotection/release phase of the solid phase synthesis might have brought about cleavage of some of the phosphoester bonds that link the phosphate group through the tyrosine hydroxyl. For the purposes of any studies described herein, pDS4 was purified by the semi-preparative procedure described in the methods section.

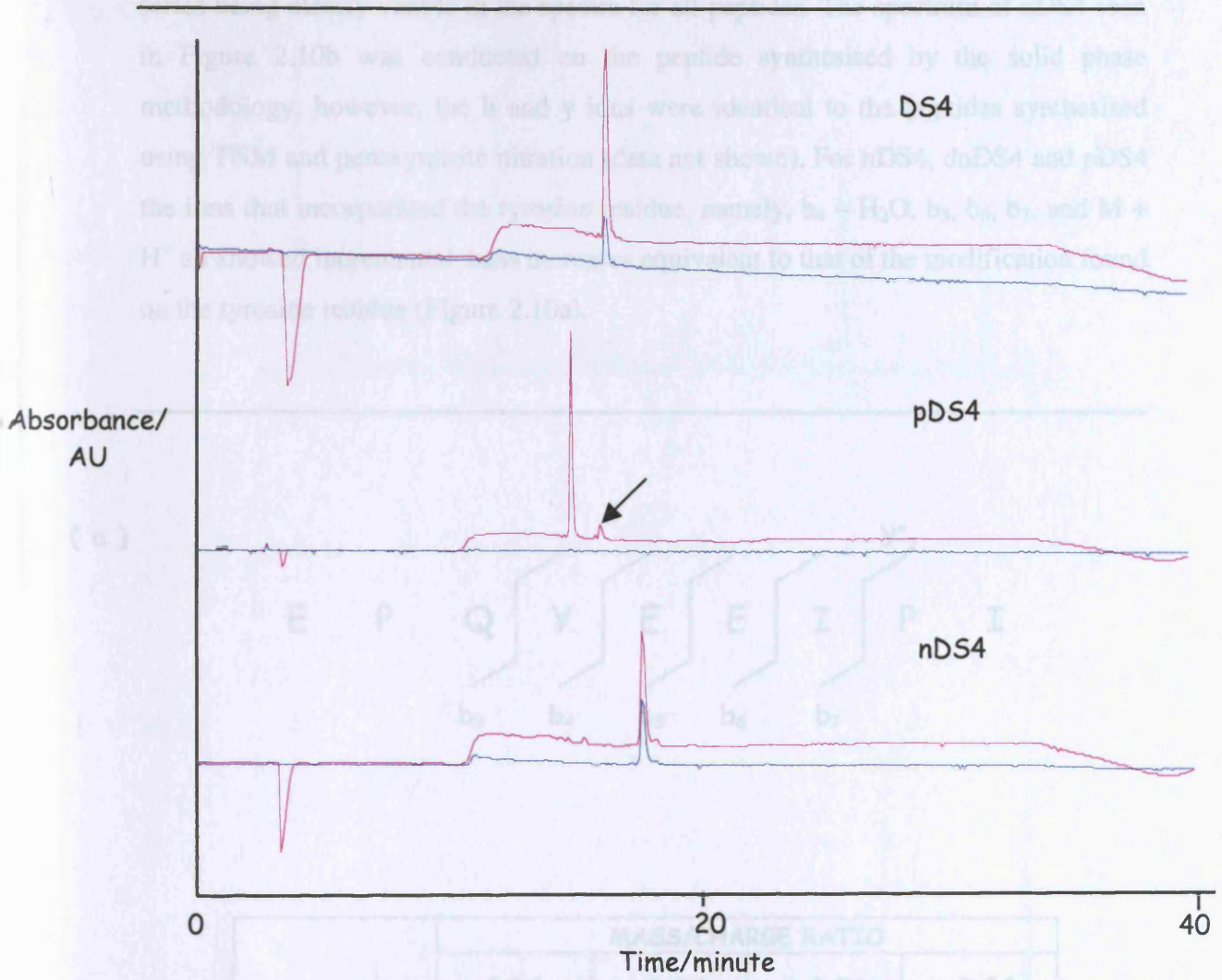

Figure 2.9. Reverse phase HPLC traces of the derivatives of DS4. Two wavelengths were used follow peptide elution: 215 nm (pink) and 280 nm (blue). The retention times of the peptides were: DS4, 16.02; pDS4, 14.88; and nDS4, 17.70 minutes. The arrow on the pDS4 trace suggests there was a residual amount of DS4 formed during the synthesis of the phosphopeptide.

MS-MS characterisation of DS4 and derivatives

ESI-MS/MS was used to characterise DS4 and its derivatives. Specifically, this technique was used to confirm that the nitration occurred on the tyrosine residue only when using TNM and peroxynitrite as nitrating agents. Additionally, this procedure was used to characterise the peptides synthesised the by solid phase procedure. The singularly charged parent ion was analysed in all peptides, with five characteristic b series ions, including two in which water had been lost, and a solitary ion from the y''

series being clearly visible in the spectra for all peptides. The spectrum of nDS4 seen in Figure 2.10b was conducted on the peptide synthesised by the solid phase methodology, however, the b and y ions were identical to the peptides synthesised using TNM and peroxynitrite nitration (data not shown). For nDS4, dnDS4 and pDS4 the ions that incorporated the tyrosine residue, namely, $b_4 - H_2O$, b_5, b_6, b_7, and $M + H^+$ all showed incremental mass increases equivalent to that of the modification found on the tyrosine residue (Figure 2.10a).

(a)

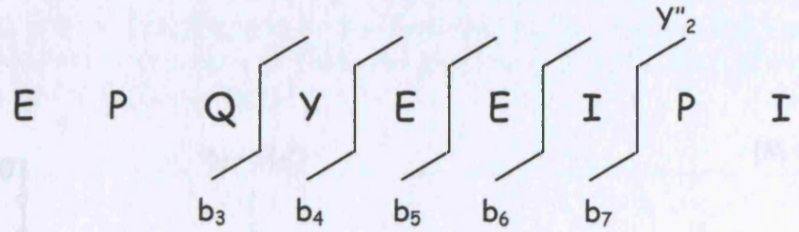

Fragment	MASS/CHARGE RATIO			
	DS4	nDS4	dnDS4	pDS4
y''_2	229.3	229.3	229.5	229.3
$b_3 - H_2O$	337.0	337.4	337.2	337.2
$b_4 - H_2O$	500.0	545.6	590.1	579.8
b_5	647.2	692.4	737.6	709.3
b_6	776.6	821.6	867.5	956.1
b_7	889.2	934.4	979.4	969.4
$[M+H]^+$	1117.8	1162.5	1208.2	1197.8

(b)

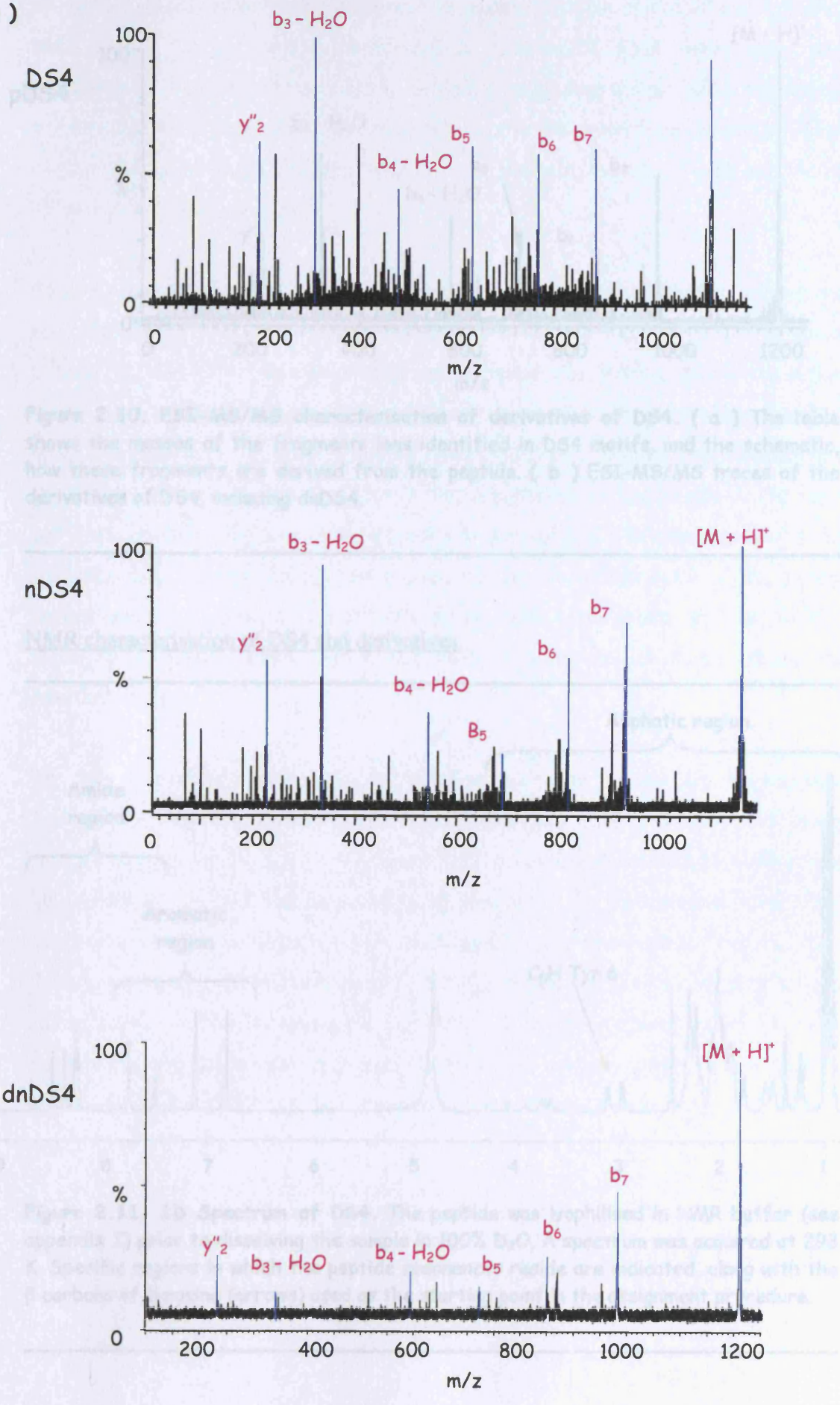
DS4
100
%
0
$b_3 - H_2O$
y''_2
$b_4 - H_2O$
b_5
b_6
b_7
0
200
400
600
800
1000
m/z
nDS4
100
%
0
$b_3 - H_2O$
y''_2
$b_4 - H_2O$
B_5
b_6
b_7
$[M + H]^+$
0
200
400
600
800
1000
m/z
dnDS4
100
%
0
y''_2
$b_3 - H_2O$
$b_4 - H_2O$
b_5
b_6
b_7
$[M + H]^+$
200
400
600
800
1000
1200
m/z

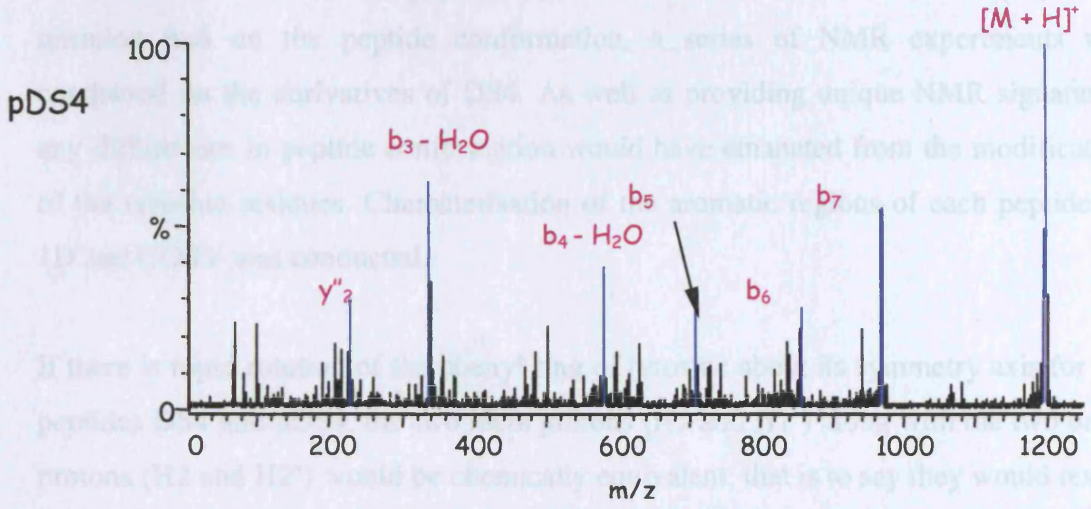

Figure 2.10. ESI-MS/MS characterisation of derivatives of DS4. (**a**) The table shows the masses of the fragments ions identified in DS4 motifs, and the schematic, how these fragments are derived from the peptide. (**b**) ESI-MS/MS traces of the derivatives of DS4, including dnDS4.

NMR characterisation of DS4 and derivatives

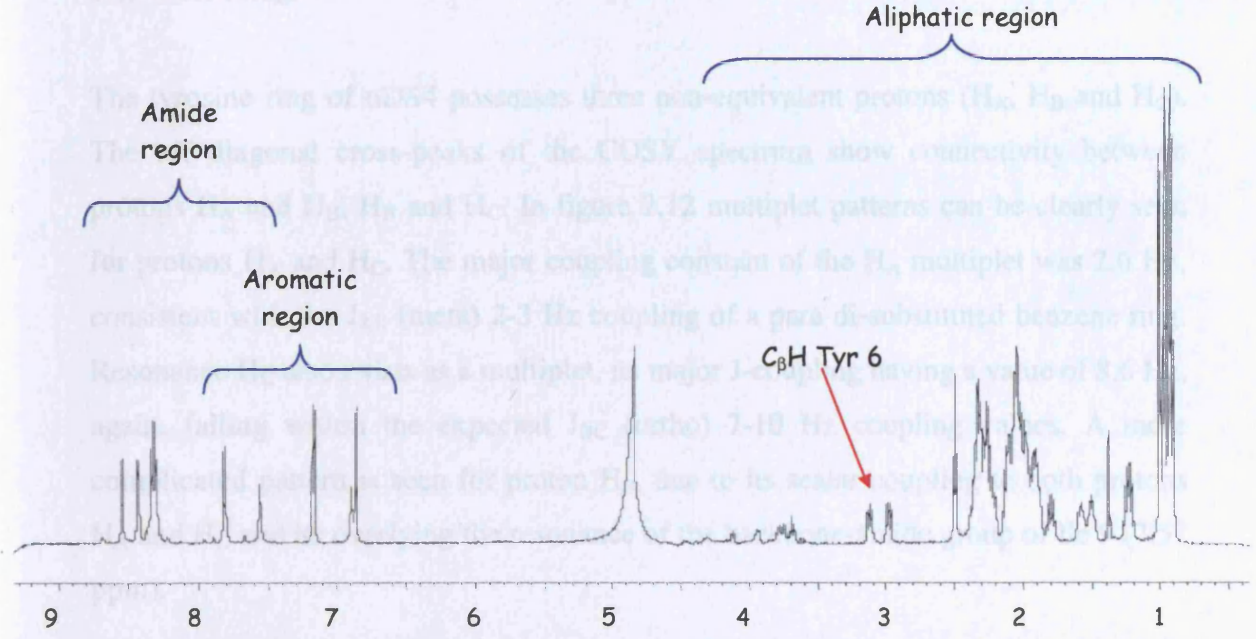

Figure 2.11. 1D Spectrum of DS4. The peptide was lyophilised in NMR buffer (see appendix I) prior to dissolving the sample in 100% D_2O. A spectrum was acquired at 293 K. Specific regions in which the peptide resonances reside are indicated, along with the β carbons of tyrosine (arrows) used as the starting point in the assignment procedure.

To further characterise the peptides and to determine what effect, if any, tyrosine nitration had on the peptide conformation, a series of NMR experiments was conducted on the derivatives of DS4. As well as providing unique NMR signatures, any differences in peptide conformation would have emanated from the modification of the tyrosine residues. Characterisation of the aromatic regions of each peptide by 1D and COSY was conducted.

If there is rapid rotation of the phenyl ring of tyrosine about its symmetry axis for the peptides DS4 and pDS4, the two meta protons (H1 and H1') along with the two ortho protons (H2 and H2') would be chemically equivalent, that is to say they would reside in the same magnetic environment and, consequently, will have the same chemical shifts and experience the same coupling effects (although, through space interactions might have a bearing these parameters). The resonances for the protons in the meta and ortho positions exist as multiplets, due to their coupling to other protons in the aromatic ring (Figure 2.12). The reason for the downfield shift of the proton resonances on substitution of the OH group with a phosphate was the latter's increased electronegativity, which effectively reduced the shielding effects the delocalised ring.

The tyrosine ring of nDS4 possesses three non-equivalent protons (H_A, H_B and H_C). The off diagonal cross-peaks of the COSY spectrum show connectivity between protons H_A and H_B, H_B and H_C. In figure 2.12 multiplet patterns can be clearly seen for protons H_A and H_C. The major coupling constant of the H_A multiplet was 2.6 Hz, consistent with the J_{AB} (meta) 2-3 Hz coupling of a para di-substituted benzene ring. Resonance H_C also exists as a multiplet, its major J-coupling having a value of 8.6 Hz, again, falling within the expected J_{BC} (ortho) 7-10 Hz coupling values. A more complicated pattern is seen for proton H_B, due to its scalar coupling to both protons H_A and H_C and its overlying the resonance of the backbone-amide group of Ile 9 (7.57 ppm).

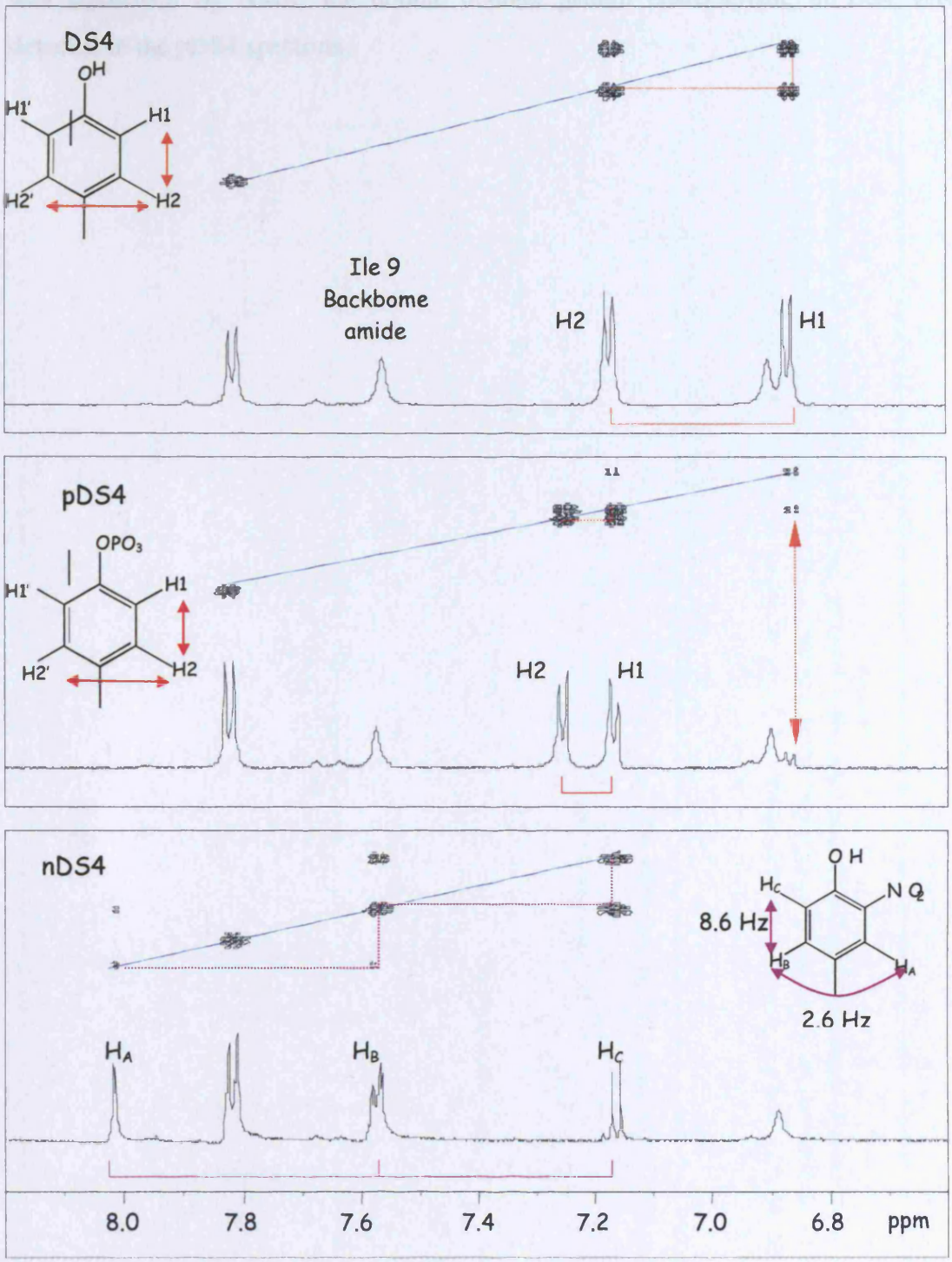

Figure 2.12. 1D and COSY spectra of the aromatic region of derivatives of DS4. Spectra of DS4 and derivatives were taken in NMR buffer. Arrows on chemical structure denote coupled protons. The brown arrow in the spectrum of pDS4 indicated the presence of DS4.

Finally, the contamination of pDS4 by DS4 observed in the HPLC characterisation, was confirmed by NMR: the double doublet pattern characteristic of DS4 was detected in the pDS4 spectrum.

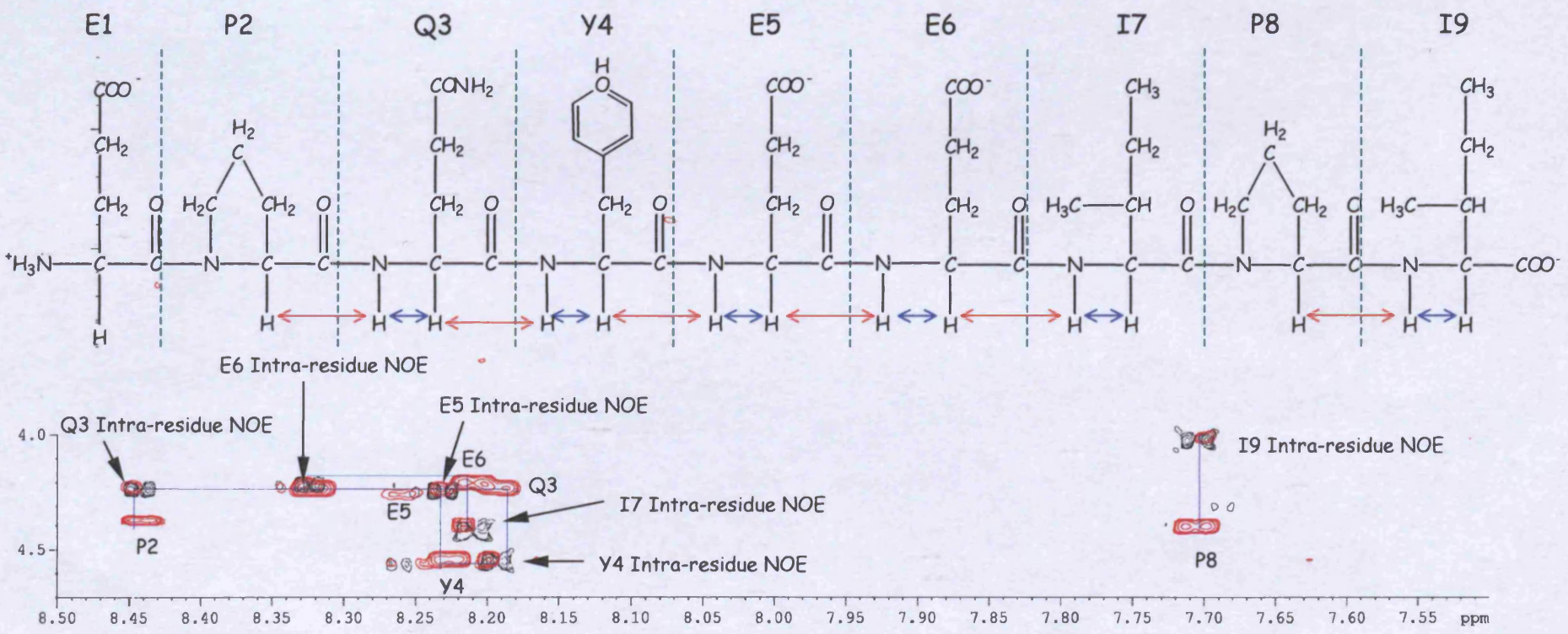

Figure 2.13. The structure of DS4 and its backbone connectivities. (a) The structure of the DS4 is shown along with intra-residue NOEs that occur between NH CαH (blue arrows) and the inter-residue NOEs that occur between the NH CαH protons **(b)** The NH/ CαH region of the NOESY spectrum of DS4 showing the sequential assignments of the peptide's backbone protons. The inter-residue NOEs are indicated in red and labelled.

In order to compare the effect of tyrosine modification on the structure of DS4 the peptide was fully assigned using COSY, TOCSY and NOESY spectra (a table of the assignment can be found in appendix II). Figure 2.13 shows NOESY and TOCSY spectra of DS4, indicating the region in which the backbone connectivities were mapped. Intra-amino acid $C_\alpha H$-NH connectivities can be detected by both TOCSY and NOESY spectroscopy, whilst the inter-residue NH-$C_\alpha H$ can only be detected by NOESY. Armed with this information, the proton resonnances in individual amino acid can first be identified using the specific spin patterns they generate in TOCSY and COSY spectra, then on identifying the $C_\alpha H$ of the amino acid, the NOE to the neighbouring NH can be identified, and the spin pattern of this amino acid can be identified. The $C_\beta H$ proton resonances of Tyr were easy to identify (δ: 3.018, 2.878 ppm; see Figure 2.11) and so were used as the starting point in the assignment procedure. Subsequently, the tyrosine spin system was identified enabling resonances in the amino acids both N- and C-terminal to be identified.

Proline residues do not contain NH protons, consequently the 'walk through' procedure that enables sequential residue identification is halted on encountering this amino acid. Two proline residues are present in the DS4 sequence: residues 2 and 8. The isoleucine residue N-terminal to proline 8, and the glututamine C-terminal proline residue 2, were identified on the basis that inter-residue NOEs were detected between the proline $C_\alpha H$ and the NH proton the neighbouring isoleucine and glutamine, respectively, but no further through bond or through space connectivities were detected from the proline $C_\alpha H$. N-terminal protonated amino groups are not detected in an NMR spectrum, so no Glu NH-$C_\alpha H$ connectivities were detected in either TOCSY or NOESY spectra for the N-terminal residue.

Peptide backbones are composed of three types of bond (Figure, 2.14 a), each with a dihedral angle associated with it: the amide bond (ω), the α-carbon-nitrogen bond (ϕ), α-carbon-carbonyl carbon bond (ψ). Rotation is possible in all of these bonds, although in the amide bond rotation is largely restricted due to its partial double-bond nature. As a result of this free rotation, short peptides tend not to possess secondary structure, although inter-residue hydrogen-bonding can confer limited structural features on short peptides (Figure 2.14 b). To determine whether any of the peptides

possessed secondary structure the NOE map of the three peptides were compared and showed no indication of protons, other than those residing in the peptide backbone, having inter-residue through space interactions. Amide protons involved in hydrogen bonds would be expected to reside in a characteristic area of a spectrum (9-10 ppm), downfield of the 'amide region' (~8.2 ppm). The lack of peaks downfield of 8.5 ppm suggests a lack of hydrogen bond formation within the peptide. Additionally, hydrogen bonds emanating from the side chain amide group of Gln 7 were not detected.

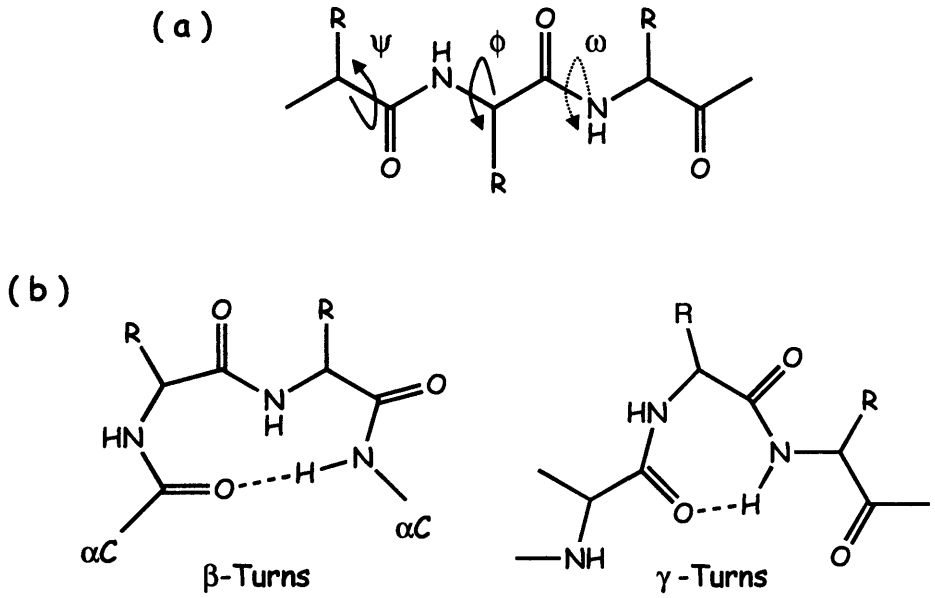

Figure 2.14. Peptide backbone structure. (a) Indicated is the backbone structure of three amino acids. Also shown are three bonds about which rotation can occur, the dotted arrow of the amide (ω) bond signifies the limited degree of freedom which this bond experiences. (b) The secondary structures that can be adopted by short peptides. In both β-turns and γ -turns the peptide turns back on itself and a hydrogen bond is formed between the amide hydrogen and the carbonyl oxygen. In a β-turn the hydrogen if formed over four residues, in γ -turns over three.

Expression and Characterisation of Fyn SH2 Domain

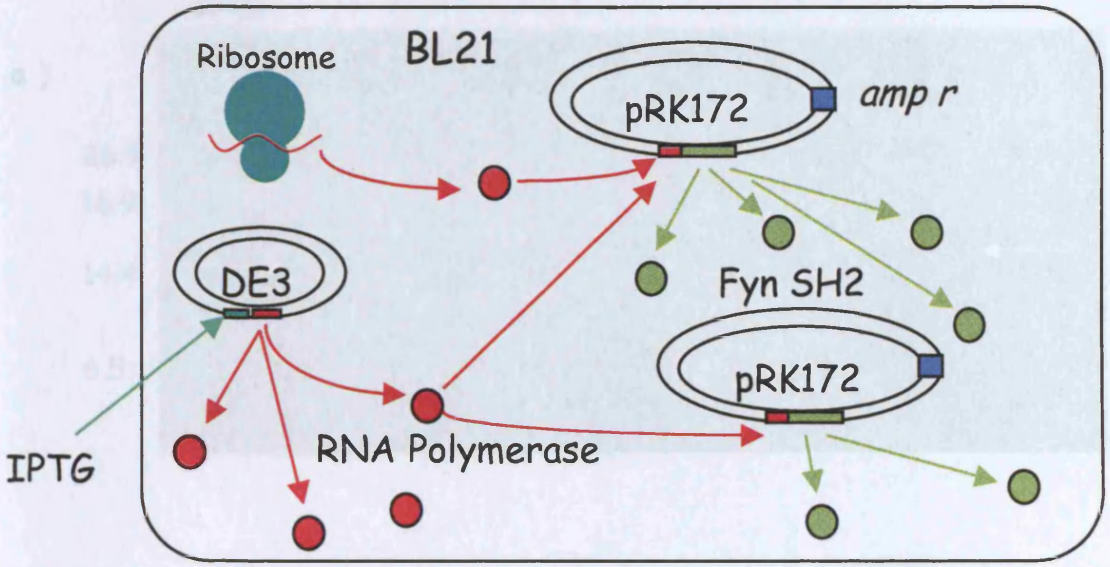

Figure 2.15. Expression of Fyn SH2 domain in E.coli BL21 (DE3). The binding of IPTG to the constitutive DE3 plasmid induces the expression RNA polymerase, which in turn binds to the modified pRK172 plasmid, containing the Fyn expression sequence. The binding of RNA polymerase to the pRK172 plasmid leads to the induction of the Fyn SH2 domain protein. The constitutive nature of RNA polymerase in dividing cells, explains why Fyn was expressed in the absence of IPTG.

The expression of Fyn in E.coli BL21 (DE3) was determined in the presence or absence of IPTG, in three different media (Figure 2.16a). The dense band indicated on the gel was assumed to be Fyn SH2; its running above the expected 12.2 kDa being an anomaly of the gel. High expression levels of Fyn were demonstrated in all media in the absence of IPTG, with the exception of 2YT, where expression was lower than in the other two media. The expression of Fyn in the absence of IPTG was due to RNA polymerase being a constitutive component of dividing cells (Figure 2.15).

After extensive washing of the phosphotyrosine column, Fyn was eluted with TBS containing 1.15 M NaCl. The elution of protein from the phosphotyrosine column was monitored by UV, and confirmed by SDS-PAGE analysis (Figure 2.16a). All three of the fractions collected all contained high levels of protein running at above the expected weight, as previously encountered.

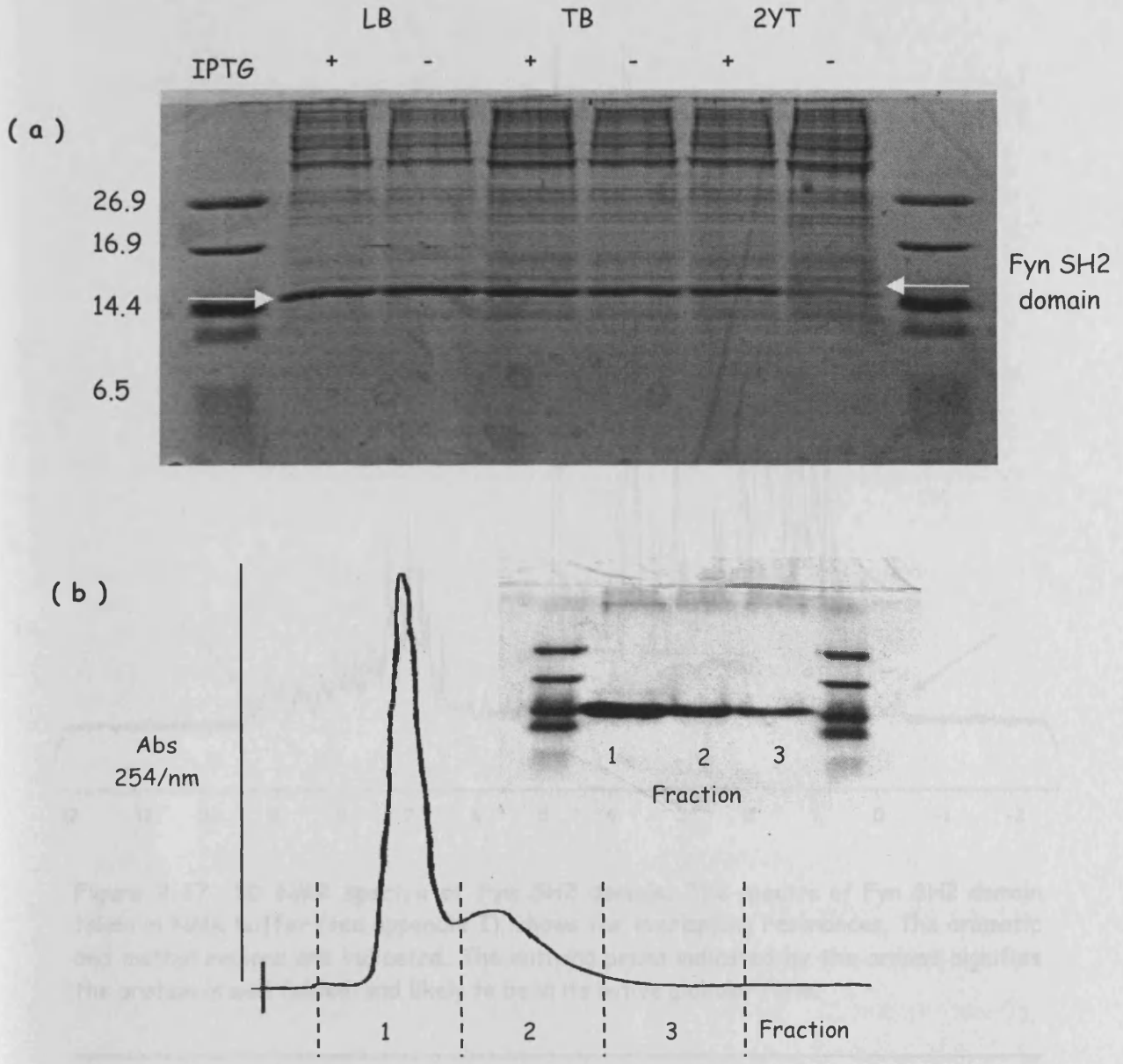

Figure 2.16. Expression and elution of Fyn SH2 domain. (a) The expression of Fyn SH2 domain was determined in three different media in the presence or absence of IPTG. (b) The elution of Fyn from a phosphotyrosine column by TBS containing 1.15M NaCl was followed by UV spectrometry and SDS-Page gel.

NMR Characterisation of Fyn SH2 domain

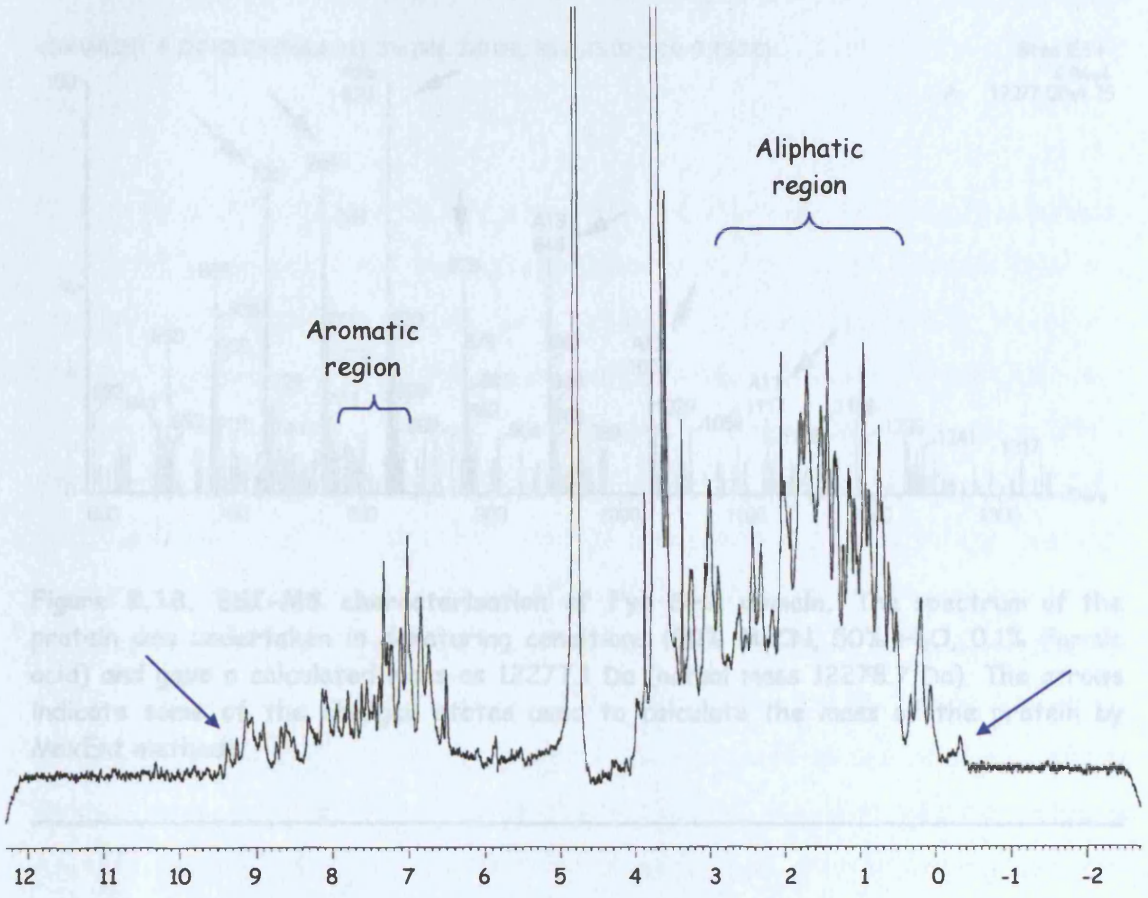

Figure 2.17. 1D NMR spectra of Fyn SH2 domain. The spectra of Fyn SH2 domain taken in NMR buffer (see appendix I), shows the overlapping resonances. The aromatic and methyl regions are indicated. The outlying peaks indicated by the arrows signifies the protein is well folded, and likely to be in its native globular form.

The expressed SH2 was exchanged into the NMR buffer and a 1D spectrum collected. Figure 2.17 shows a spectrum of Fyn SH2, illustrating the overlapping resonances characteristic of a biomolecules containing a large number of protons. Indicated on spectrum are the aliphatic and aromatic regions of the proteins, which were important in determining the binding of peptides to the SH2 protein (see chapter 3).

Mass spectral Analysis of Fyn SH2 domain

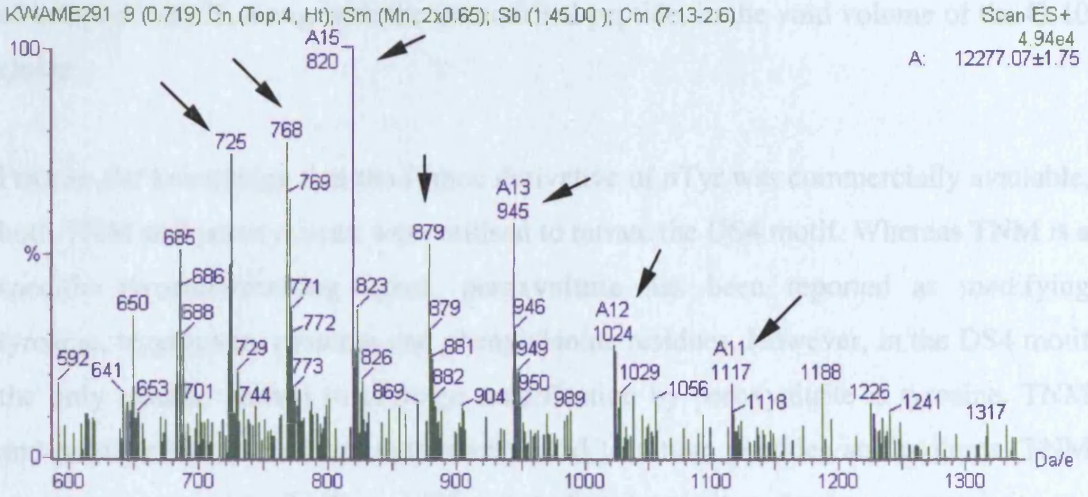

Figure 2.18. ESI-MS characterisation of Fyn SH2 domain. The spectrum of the protein was undertaken in denaturing conditions (50% MeCN, 50% H_2O, 0.1% Formic acid) and gave a calculated mass as 12277.1 Da (actual mass 12278.7 Da). The arrows indicate some of the charged states used to calculate the mass of the protein by MaxEnt methods.

Additional characterisation of the SH2 was achieved by ESI-MS anlaysis of the eluted protein. Figure 2.18 shows the ESI-MS spectrum of Fyn SH2 domain obtained in a 0.1% concentration of Formic acid and a 50% acetonitrile solution. A number of the protein's charged states were detected in the spectra. Maximum entropy transformation of the generated spectrum determined the mass of the protein to be 12277, 1 Da less than its calculated mass, determined by its amino acid sequence.

DISCUSSION

A combination of size exclusion and UV-visible spectroscopy were utilised to identify the elution of nitrated Ang II from the G-10 mini-column. Angiotensin II having a molecular weight greater than the 700 Da exclusion limit of Sephadex G-10, eluted in the void volume (approximately 2.5 ml). Confirmation of peptide elution was achieved by monitoring the eluent at both 278 and 360 nm. A wavelength of 280 nm is routinely used monitor peptides and protein containing aromatic amino acids, whilst

the rational for using 360 nm lay in the nTyr moiety having an absorbance maximum at this wavelength in acidic conditions, due to the conjugation of the nitro group to phenol moiety of tyrosine. Both HPLC and mass spectrometry confirmed the presence of nitrated Ang II, along with the unmodified peptide, in the void volume of the G-10 eluent.

Prior to the knowledge that the F-moc derivative of nTyr was commercially available, both TNM and peroxynitrite were utilised to nitrate the DS4 motif. Whereas TNM is a specific tyrosine-nitrating agent, peroxynitrite has been reported as modifying tyrosine, tryptophan, cysteine and phenylalanine residues. However, in the DS4 motif the only residue known to undergo modification by peroxynitrite is tyrosine. TNM and peroxynitrite have been extensively used to nitrate peptides and proteins (TNM nitration reviewed by Neilsen, 1995; a list of proteins nitrated using peroxynitrite can be found in Oldreive and Rice-evans, 2001), with TNM having been previously used to nitrate the peptide Ang II (Petersson et al., 2001). Using a 50 molar excess of TNM, Peterson and colleagues generated both the mono- and di-nitrated derivatives of Ang II. No information was forwarded on the yields of the nitro-substituents formed, or on whether any of the unmodified peptide remained after the nitration reaction. Despite a 40 molar excess of the nitrating agent, there was no indication of dnDS4 formation on nitrating DS4 using TNM, however the mono-nitrated species was produced in reasonable yields. The mono-substitution of phenol with a nitro group decreases the propensity of the aromatic ring to undergo a second substitution, as such, significant levels of the di-nitrated species are likely to be formed only when levels of the mono-nitrated derivative exceed those of the non-modified peptide. Surprisingly increasing the concentration of TNM had no effect on the formation of the di-nitrated substituent, or the yield of mono-nitrated species for both Ang II and DS4. TNM-mediated tyrosine nitration proceeds through the formation of a complex between the tyrosine residue and the nitrating agent. Factors that, therefore, affect the interaction between tyrosine and TNM, such as salt and solvent composition of the buffer, are known to influence the formation of nitrated tyrosine residues (Neilsen, 1995), and might explain the lack of formation of the di-nitrated species and the inability to exceed the 40 % yields.

In optimising the TNM nitration procedure using Ang II, a yield of 70 % was achieved for the mono-nitrated peptide, as opposed to the 30 – 40 % obtained for DS4. As the nitrating conditions for both DS4 and Ang II were the same, the significant difference in the yields can only be ascribed to the variation in peptide sequence. One possibility is that TNM is capable of interacting with the polar amino acids (Gln and Glu) surrounding the Tyr residue in DS4 via electrostatic forces, thus partially inhibiting the complex formation between TNM and Tyr. Conversely, the hydrophobic residues (Ile and Val) surrounding the Tyr in Ang II would not attract the highly charged TNM, leaving the nitrating agent free to form a complex and the amino acid.

Peroxynitrite was also used as a nitrating agent. Yi et al., (1997) and Curcurouto et al., (1999) have previously conducted investigations on the nitration of an array of peptides using peroxynitrite. In both studies the formation of mono- and di-nitrated tyrosine substituents was observed, analogous to the nitration of DS4 by peroxynitrite. The formation of mono- and di-nitrated derivatives of DS4 was followed by monitoring the area under the peaks at 215 nm on the HPLC traces, as expected, there was a concomitant increase in levels of nDS4 as DS4 was depleted. Levels of nDS4 would be dependent on the level of peroxynitrite additions, levels of DS4, as well as the rate of formation of dnDS4. At 10 molar equivalents of peroxynitrite and below, the rate of nDS4 formation was greater than that of the di-nitrated species. The formation of the di-nitrated peptide occurred at all levels of peroxynitrite addition, however, at concentrations above 10 molar equivalents the rate of formation of the di-nitrated peptide exceeded that of the mono-nitrated derivative, although the continued depletion of DS4 above this concentration confirmed *de novo* synthesis of nDS4 at these levels. These trends continued up to 20 molar equivalents, above which levels of all three peptides remain unaffected by increased additions of peroxynitrite.

The use of TNM and peroxynitrite in nitrating DS4 has both advantages and limitations. The reasonable yields and the lack of formation of the di-nitrated substituent were advantageous when using TNM, however, the potential risk of handling this toxic agent must be taken into consideration when assessing the its benefits as a nitrating species. In contrast, the toxicity of peroxynitrite is minimal; the

limitations of using this species as a nitrating agent lay in the production of dnDS4, an analogue from which nDS4 cannot be generated.

The commercial availability of the F-moc derivative of nTyr meant solid phase synthesis could be used to prepare both the nDS4 and pDS4 motif. The yields obtained by this synthetic procedure were superior to the methods used in the chemical nitration of DS4, in so much as, one round of solid phase synthesis produced approximately 200 mg of pure peptide, under non-hazardous conditions, without the generation of contaminating products. All experiments carried out in subsequent chapters were out on nDS4 prepared by the solid phase method.

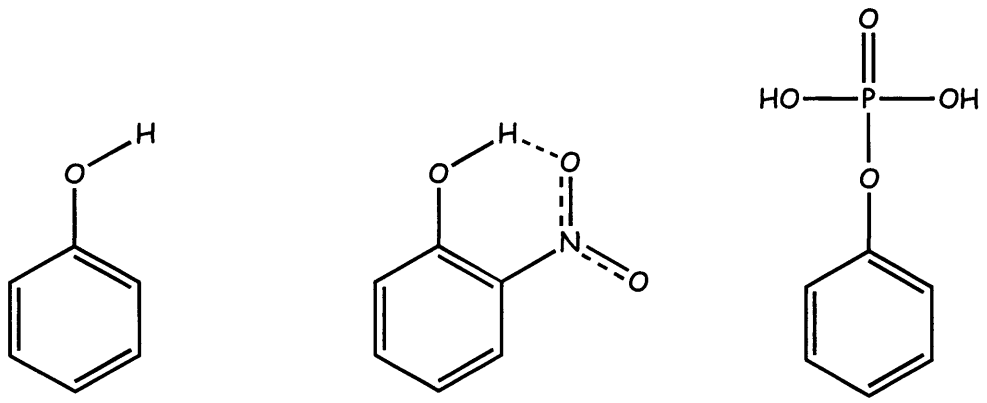

Figure 2.19. The modifications of the aromatic ring of DS4's derivatives. The chemical structures of the aromatic modifications of DS4, from left to right: the non-modified Tyr; the ortho phosphate substitution; the amino meta substitution; and the nitro meta substituent.

High performance liquid chromatography was used to characterise the derivatives of DS4. Even on a relatively shallow gradient all peptides were eluted within 3 minutes of one another, with the phosphopeptide eluting first, and the nitropeptide last. The differences in retention times reflect the differences in peptide solubility for the mobile phase, and its affinity for the column, both mediated by the modifications on the aromatic ring of tyrosine (Figure 2.19). Under the acidic conditions employed during the HPLC analysis (0.1% TFA, pH: 2), the phenoxy group of tyrosine and nTyr will be protonated, along with the phosphate oxygens, negating their negative

charge (the pk_a value of the phosphate group of pTyr being 5.7, and the phenoxy group of Tyr and nTyr 10 and 7.5, respectively). The initial elution of pDS4 can be attributed to the presence of the polar phosphate group reducing the peptide's hydrophobicity. Conversely, increasing the number of nitro groups on the tyrosine led to an increase in peptide retention (retention time DS4, 16.02; nDS4, 17.70 and dnDS4 18.45 mins).

The aim of conducting ESI-MS/MS on the derivatives of DS4 was to confirm the modification of the tyrosine residue after the use of TNM and peroxynitrite as nitrating agents. ESI-MS/MS fragmentation has been successfully used to identify the site of tyrosine nitration on large proteins (Greis et al., 1996, and MacMillan-Crow et al., 1998), as well as peptides (Curcuruto et al., 1999; Petersson et al., 2001; Yi et al., 1997). The identification of modified residues by MS/MS relies on the sequential fragmentation of the peptide around the amino acid of interest. A near complete B series confirmed tyrosine as the site of modification for both the mono-nitrated and di-nitrated peptides synthesised using TNM and peroxynitrite. In addition, DS4 and the other analogues fragmented to produce identical B series and the Y''_2 fragment, highlighting the presence of the different chemical groups (nitro, di-nitro, and phospho) on the tyrosine residue.

Interestingly, water loss was detected in the B_3 and B_4 fragments on analysis of all four peptides, suggesting a common mechanism was occurring during peptide fragmentation. Three pathways have been forwarded to account for the dehydration sometimes encountered during the mass spectrometry of peptides (Reid et al., 1998): the loss of water from the C-terminus carboxylic acid or the side chains of aspartic glutamic acid (type A); dehydration from the side chain hydroxyl Ser or Thr (type B); or the loss of water from amide carbonyl of the peptide backbone (type C). Type A mechanisms involving Glu side chains, and type B mechanisms were discounted due to the absence of Ser and Thr residues in the DS4 motif, and water loss being exclusive to fragments b_3 and b_4 and not involving fragments b_5 to b_7 that would have also contained Glu residues. Additionally, water loss from the side-chain of Glu residue 1, was also discounted as water loss by this mechanism would be expected to have registered in all the b fragments. Therefore, two possible mechanisms might account for the loss of water from fragments b_3 and b_4. The first possibility is that

once the b fragment is generated the newly formed carboxylic acid group then undergoes type A dehydration to form the corresponding oxazolone (Figure 2.17, scheme I). The second possibility is that water is lost from the amide carbonyl backbone, resulting in the formation of a nitrilium ion (Figure 2.20, scheme II). Based on the thermodynamic calculation Reid et al. (1998) suggests the later mechanism is the more likely to occur. As to why dehydration only occurs in the b_3 and b_4 is unclear, however, in terms of characterising the tyrosine modification, the fragmentation patterns generated were adequate.

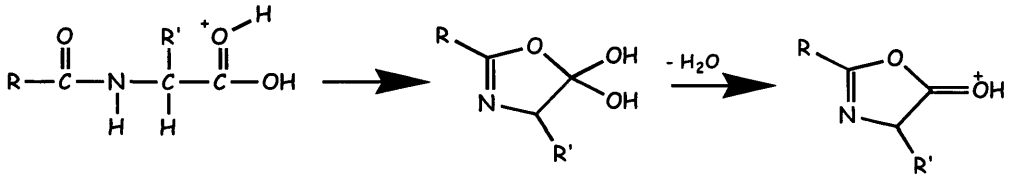

Scheme I

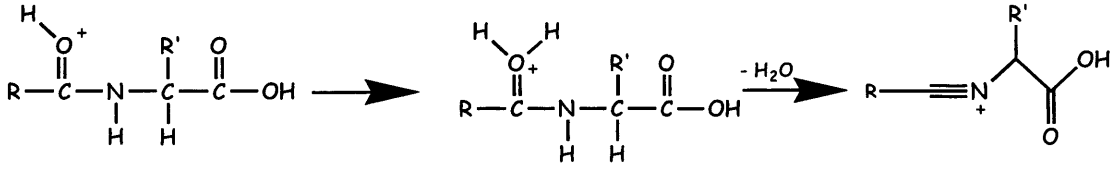

Scheme II

Figure 2.20. The proposed mechanism of water loss from DS4. Two mechanisms are proposed for the loss of water from fragments B_3 and B_4 on MS/MS analysis of DS4 and its derivatives. Scheme I: protonation of the hydroxyl group of the carboxylic acid results in the loss of water and the formation of a cyclic oxazolone derivative. Scheme II: protonation of the amide carbonyl and subsequent dehydration results in the formation of a nitrilium ion (adapted Reid et al., 1998).

The characterisation of the derivatives of DS4 by NMR was conducted in order to assess the effect of tyrosine modification on peptide conformation, and its effect on chemical shifts of protons in surrounding residues. To achieve this goal the peptide was fully assigned using COSY, TOCSY, and NOESY spectrometry (see appendix II). Tyrosine phosphorylation modulates protein function by allosteric (Johnson, 1992) and electrostatic (Hurley et al., 1989) mechanisms. The long-range electrostatic effects of phosphorylation have previously been demonstrated in short peptide sequences (Chavanieau et al., 1994). Based on this previous study the ability of

nitrated tyrosine residues to induce charge-relay effects was determined, and in so doing the hypothesis that nTyr may act as a pTyr mimetic was investigated. By simply analysing the chemical shift patterns of the protons in the surrounding residues, the charge-relay effects of tyrosine modification were compared. Neither para phosphate substitution, nor meta nitro substitution had any effect on the chemical shifts of protons in amino acids surrounding the tyrosine residue (see appendix II for actual proton chemical shifts), suggesting neither modification had any charge-relay effects in the DS4 motif. The inability of tyrosine nitration to induce electrostatic-relay in DS4 does not lead one to conclude that this post-translational modification is incapable of inducing this effect. Charge-relay effects are not distributed over random peptide sequences, rather, they are transferred through specific motifs. The lack of any accompanying resonance shifts on the phosphorylation of DS4 suggests it is the sequence of the motif rather than the nature of the tyrosine modifications that accounts for the lack of chemical shift pertubations. In the study conducted by Chavanieu and co-workers, chemical shift changes were observed in the side-chains of basic residues and not acidic ones (Chavanieau et al., 1994). No chemical shift changes were noted in any of the protons on modification of tyrosine.

The hamster middle T antigen, on which the DS4 motif is based, binds exclusively to the SH2 domain of Fyn (Dunant et al., 1997) through specific interactions between the sequence surrounding the pTyr residue, and the SH2 domains (see chapter 1). Consequently, the DS4 motif contains residues to which the surface of the SH2 binds optimally (EEI), but these residues do not necessarily transfer charge on modification of the tyrosine.

The growth of bacteria in Terrific broth, with additional protein induction for 4 hr in the presence of IPTG was determined as being the optimal conditions for protein expression. The expression of Fyn in E.coli BL21 (DE3) was determined in the presence or absence of IPTG, in three different media (Figure 2.16 a). The dense band indicated on the gel in Figure 2.15 was assumed to be Fyn SH2, although it ran at around 14.5 kDa. Confirmation that the band running at 14.5 kDa was indeed the SH2 domain was achieved by the analysis of fractions eluted from the phosphotyrosine column after extensive washing (Figure 2.16 b). Although prokaryotic cells rely on phosphorylation of proteins to trigger cellular events (Lodish et al., 1995) and might

therefore contain proteins that bind to pTyr residues, Fyn SH2 would be expected the major protein eluted after column washing. The protein fractions eluted from the phosphotyrosine column ran at approximately 14.5 kDa, yet mass spectral analysis confirmed the mass of the protein at 12277, consistent with it being Fyn.

The expression of Fyn appeared similar in all media, both in the presence or absence of IPTG, with the exception of 2YT media, where in the absence of IPTG, levels of expression were reduced, even though the volume of protein solution loaded onto the PAGE gel was the same in all cases. A possible reason for this finding might have been the composition of 2YT not being as conducive to the expression of Fyn as the other media, a process which could be overcome by inducing protein expression with IPTG. Also, as RNA polymerase is a constitutive component of dividing cells, the induction of Fyn SH2 did not require the presence of IPTG; the constitutive enzyme capable of binding to the response elements in the pRK172 plasmid and inducing SH2 domain expression, although the binding of IPTG to the DE3 plasmid would amplify the amount of RNA polymerase in the cell.

The protein eluted from the pTyr column was well folded, as indicated by the outlying methyl and amide resonances (indicated by the arrows in Figure 2.17). The methyl resonances are shifted upfield when in close proximity to an aromatic residues, as would be found in the packed core of a protein, whilst amide resonances in secondary structure formation would be shifted downfield. Confirmation that the SH2 domain was well folded meant subsequent studies could be conducted in the knowledge that the protein was likely to be in its native folded state.

In summary, a number of parameters in both peptide and SH2 have been defined in the work described above. Many of the characteristics established here were used as the starting points of studies described in subsequent chapters. In addition, analysis of proton chemical shifts of residues flanking the tyrosine indicated the modification of tyrosine had no effect on these resonances, indicating the nitration of tyrosine could not induce a charge-relay effect in the DS4 motif. Furthermore, analysis of the NOE maps of the three peptides suggested none possessed an unusual conformation.

CHAPTER 3:

QUALITATIVE AND QUANTITATIVE STUDIES OF THE BINDING OF DS4' DERIVATIVES TO FYN SH2 DOMAIN

INTRODUCTION

Protein-Protein Interactions in Signal Transduction

At any one time, a vast number of proteins are expressed within the cell, therefore, mechanisms are required that enable proteins to specifically recognise those biomolecules that propagate signalling pathways, distinguishing them from those that play no part in the transduction process. Sub-cellular localisation of proteins facilitates the formation of the protein-protein interactions, however, it is the intricate molecular contacts that accounts for the specificity of biomolecular interactions in transduction cascades. Table 3.1 highlights some of the common modular proteins involved in signal transduction, and the motifs they recognise in their binding partners.

Table 3.1 Modular proteins involved in signal transduction. (Adapted from Mayer, 1999).

DOMAIN	RECOGNITION SEQUENCE	K_D/μM	REGULATION	REFERENCE
SH2	Y(p)ααα	0.01- 0.1	Y phosphorylation	Ladbury et al (1995); Pawson (1995) [a]
SH3	αβγPβγP or γPβγβPβα	0.003 - 0.4	Not direct	Pawson (1995) [a]; Tu et al., (2001)
PTB	NPβY(p)	6	Y phosphorylation	Li et al., (1997)
PDZ	(S/T)βV-*COO*$^-$ or (Y/F)(Y/F)γ-*COO*$^-$	0.1	Phosphorylation	Songyang et al., (1997)
WW	βPββPY	10	Phosphorylated ?	Chen and Sudol (1995)
PH	Inositol phosphates	0.2	b	Harlan et al., (1994)

[a] Review article;
b Regulatory mechanisms as yet not established;
α variable amino acid involved in specificity;
β any amino acid;
γ hydrophobic amino acid.

Protein-protein interactions in transduction cascades can be defined in terms of the affinity that one protein has with another, with K_d determinations being a measure of this parameter. The dissociation constants of proteins involved in signalling cascades are generally in the nanomolar to micromolar ranges. In the case of the SH2-phosphopeptide associations, K_d values are in the nanomolar range (Pawson, 1995), yet these SH2 modules exhibit rapid on/off kinetics, enabling rapid exchange to occur between phosphotyrosine containing motifs and SH2 domains (Felder et al., 1993).

Elucidation of the mechanisms of signalling pathways continues to aid our understanding of the cell's functioning under normal and pathological conditions. Determination of the proteome will further facilitate our understanding of these processes. In addition, the proteins involved in signalling are key targets for the development of pharmaceuticals. The determination of dissociation constants has enabled researchers to establish the role proteins play in the propagation and modulation of signalling pathways, and in so doing, these simple measurements continue to facilitate our understanding of cell biology and assist in the development of new drugs.

Quantitation of the Phosphopeptide-SH2 Domain interaction

An array of techniques has been used to probe the protein-protein interactions, these include the displacement of radiolabelled ligands, to the more recent use of yeast two hybrid techniques (Aronhein, 2000; Mendelsohn and Brent, 1999; Michnick, 2001) and atomic force microscopy (Viani et al., 2000). The key role that SH2 domains play in initiating the intracellular component of growth factor and cytokine signalling has led to extensive study of the interactions between these modular proteins with their phosphoprotein ligands. As only a few amino acids from the phosphoprotein actually make direct contact with SH2 module (Waksman et al., 1993), binding studies have primarily been based on phosphopeptide-SH2 interactions. A number of techniques have been used to probe and quantitate SH2-peptide interactions (Table. 3.2).

Table 3.2 Techniques used to probe SH2 domain phosphopeptide binding.

TECHNIQUE	SH2	PEPTIDE	K_d (μM)	REFERENCE
SPR	Src PI3-Kinase p85	hmT PDGF	0.67 0.24	Ladbury et al., 1995
ITC	Src PI3-Kinase p85	hmT PDGF	0.55 0.47	Ladbury et al., 1995
FLUORESCENCE	Grb2/Ash	EGFR	2.9	Tsuchiya et al., 1999.
RADIO-LABEL DISPLACEMENT	PI3-Kinase p85 Lck	PGDF β Lck	1.1 [a] 8.2 [a]	Piccione et al., 1993. Payne et al., 1993.
ESI-MS	Src	hmT	1.8	Loo et al., 1997
FRET	PI 3-kinase	IRS-1	-	Sato et al., 1997
NANOSPRAY-MS	Fyn	hmT	-	Chung et al., 1999

[a] IC_{50} values.

The aim of the work detailed in this chapter was to determine the extent to which nDS4 bound to the SH2 domain of Fyn, with pDS4 and DS4 peptides being positive and negative controls, respectively. The direct binding of nitropeptides to SH2 domains has not, to my knowledge, been previously measured, and as such there was no specific methodology available. However, a number of techniques have been employed to study phosphopeptide-SH2 interactions. Three such techniques were utilised to examine the binding of derivatives of DS4 to Fyn SH2 domain: nanospray mass spectrometry, a FRET assay, and 1D NMR. The following section gives an overview of the principles of the three techniques and their application in binding studies.

Principles and Techniques

Nanospray Mass spectrometry

Electrospray ionisation mass spectrometry (ESI-MS) has been extensively used to probe non-covalent biomolecular complexes (reviewed Przybylski and Glocker, 1996; the principles underlying ESI-MS have been previously described in Chapter 1). Unlike other 'harder' forms of ionisation, ESI tends not to fragment the biomolecule under investigation, making this technique more amenable to the analysis of complexes in the gas phase However, the desorption and ionisation processes employed in ESI can result in significant dissociation of weakly bound ligands from proteins (Loo et al., 1997). The advent of nanoES (Wilm and Mann, 1994) has overcome the many of the problems of ligand dissociation presented by ESI. The key difference between the two techniques, which might account for the differences in ligand dissociation, lies in the size of the droplets formed during the two processes. Two mechanisms have been forwarded for droplet formation in conventional ESI. The first involves a series of evaporations eventually leading to the formation of the gas ion phase. The second suggests the electric field is sufficient to 'pull' the analyte out of an electrospray droplet (Chung et al., 1999). What is clear is that in ESI the initial size of the droplets is in the 1-2 μm range. These droplets then undergo processes (fission, desorption and evaporation) that result in a reduction in their size prior to analysis. Although the loss of solvent, and the subsequent reduction in droplet size leads to an increase in analyte concentration, there is a concomitant increase in salt concentration, which can disrupt ligand-receptor binding in addition to suppressing ion signal intensity. In nanoES the droplet size is much smaller (nanometres instead of micrometres), due to the smaller capillary orifice and the reliance on electrostatic dispersion of analyte rather than external pumping. The larger surface-area-volume ratio makes more analyte molecules available for desorption. Flow rates of 20-40 nl/min allow for longer analysis time. Moreover, the tolerance of nanoES to salt (up to 100 mM, Wilm and Mann, 1996), and the non-denaturing conditions employed in nanospray (spraying from an aqueous matrix as opposed to a water/acetonitrile mixture) means biomolecular complexes can be analysed in biological fluids (Juraschek et al., 1999; Wilm and Mann, 1996). The rationale for selecting nanospray to probe the peptide-protein interaction was prompted by a recent paper (Chung et al.,

1999), which described the binding of residues 321-331 of hamster middle T oncoprotein to the SH2 domain of fyn.

Fluoresence Resonance Energy Transfer (FRET)

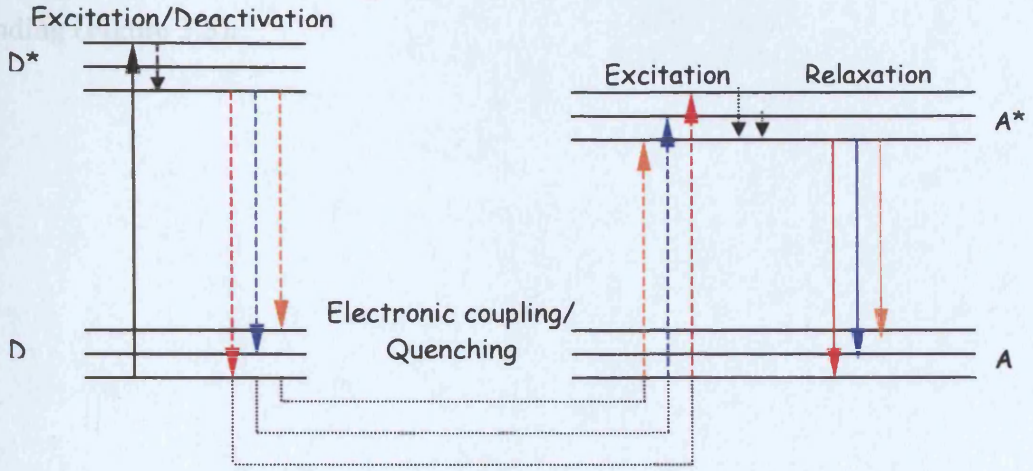

Figure 3.2. The depiction of FRET using quantised energy levels. Hashed lines indicate to non-radioative processes, the filled radioative procedures. Electrons in the donor fluorophore (D) absorb light and are excited to higher energy states (D*). If an acceptor (A) fluorophore is in close proximity to the donor, and has a favourable orientation, the two moieties can become energetically coupled through dipole-dipole interaction. Subsequent quenching of the donor by the acceptor occurs if the energetic transition of donor relaxation processes corresponds to those capable of causing electronic excitation in the acceptor. Relaxation processes in the acceptor leads to characteristic emission of electromagnetic radiation (adapted from Forster, 1959).

Fluorescence resonance energy transfer (FRET) was first reported in 1922 by Cario and Franck, when the transfer of fluorescence from mercury to thallium vapour was observed (Cario and Franck, 1922). FRET can be defined as the transfer of energy from an excited donor to a nearby acceptor fluorophore. This phenomenon can only occur when a donor's emission spectrum overlaps the excitation spectrum of an acceptor (Figure 3.2), and the transition dipoles of the fluorophores align in the correct orientation. This spectral overlap results in a shift from donor to acceptor emission spectra, on excitation at donor wavelength. The efficiency of energy transfer is inversely proportional to the sixth power distance between donor and acceptor (Equation 3.1), and, efficient energy transfer will thus only occur when the two fluorescent moieties are approximately 30 Ångstroms, or less, apart (Forster, 1959;

Szollosi et al, 2002, equation 3.1). Such distances are within the region of biomolecular interactions, and subsequently, FRET has been applied to monitor changes in biomolecular conformation, as well as the interactions between receptors and their ligands (Selvin, 2000; Weiss, 2000). Based on a protocol previously described (Sato et al., 1999) an assay was set up to monitor peptide-SH2 domain binding (Figure 3.3).

SPECIAL NOTE

This item is tightly bound and while every effort has been made to reproduce the centres force would result in damage.

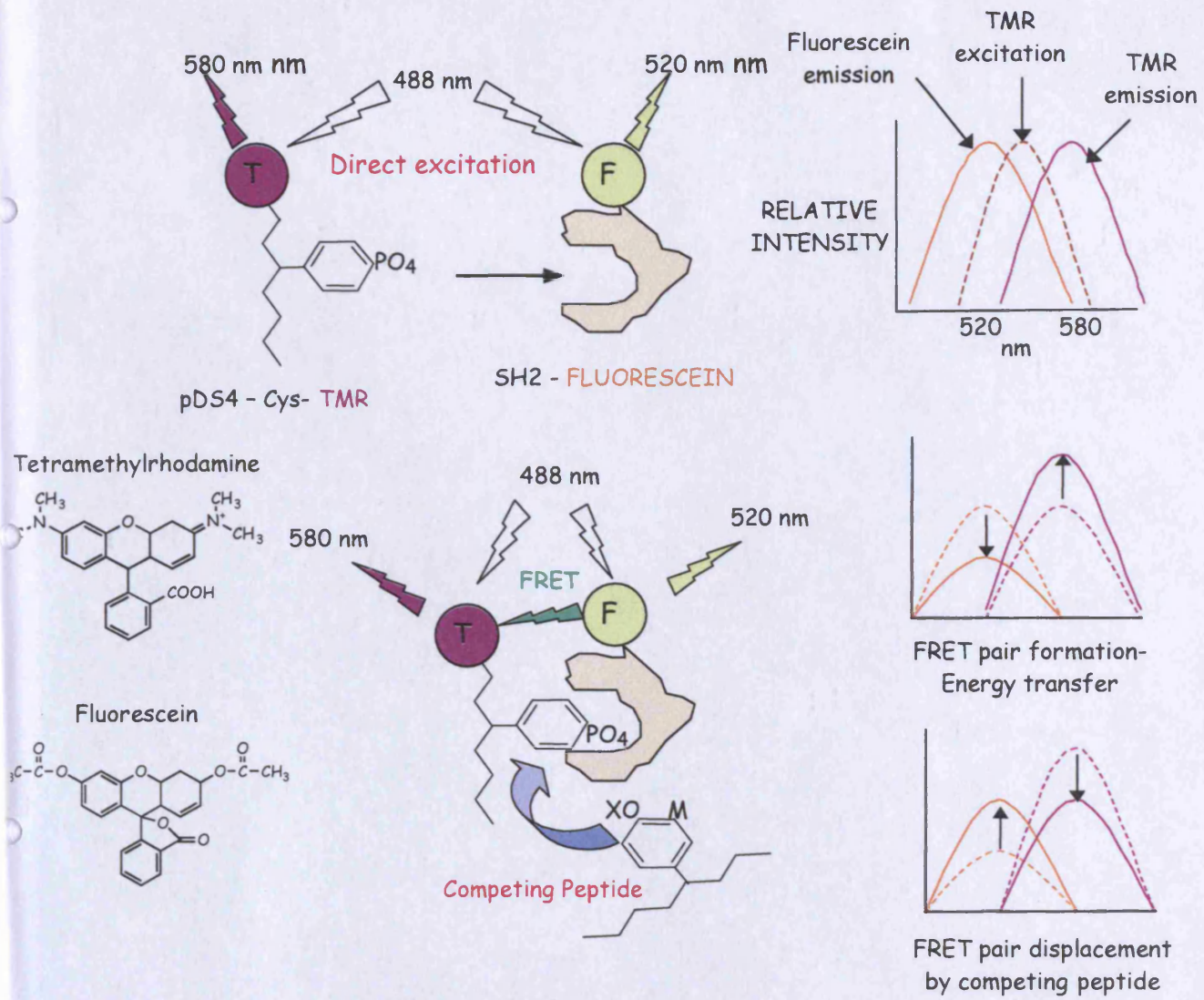

Figure 3.3 The application of FRET in monitoring the binding of derivatives of DS4 to Fyn SH2. Both Fluorescein (F) and Tetramethylrhodamine (T, TMR) are directly excited at 488nm (excitation max fluorescein) resulting in emission maxima at 520 and 580nm respectively. On binding of the labelled peptide to labelled protein, and subsequent fluorophore activation, a proportion of the energy absorbed by fluorescein is transferred directly to TMR without lose of photons (FRET). Thus, FRET pair formation results in an increased TMR emission at the expense of fluorescein. The disruption of a FRET pair by derivatives of DS4 can be visualised and is therefore an indicator the peptides ability to bind to the SH2 domain of Fyn.

Equation 3.1. Derivation of the rate of energy transfer in FRET.

$$K_T = \text{constant}\ K_F\ J n^{-4} R^{-6} \kappa^2 \qquad (1)$$

$$E = \frac{K_T}{K_T + K_F + K_D} \qquad (2)$$

$$E = \frac{R^{-6}}{R^{-6} + R_0^{-6}} \qquad (3)$$

$$K_T = \frac{1}{\tau}\left(\frac{R_0}{R}\right)^6 \qquad (4)$$

Where: K_T is the rate of energy transfer.
K_F is the rate constant of fluorescence emission of the donor.
J is the spectral overlap integral.
n is the refractive index of the medium.
R is the distance between the nuclei.
κ is an orientation factor.
K_D is the sum of the rate constants of all other de-activation processes of the donor.
τ is the donor's lifetime in the absence of the acceptor.
R_0 is the distance at which half the energy is transferred.

A number of factors influence the rate of energy transfer from donor to acceptor. Equation (4) is derived from equations (1), (2) and (3), and takes into account these factors.

Nuclear Magnetic Resonance

Nuclear magnetic resonance has been extensively used to map changes invoked in both ligands and receptors on their binding. Chemical shifts, scalar coupling, and relaxation times of a biomolecule, can differ between its free and bound states, and can all be monitored and quantitated using NMR. Chemical exchange is any process in which the parameter being followed differs between two environments. Exchange processes, such as those previously listed, vary according to affinity of a ligand to receptor, and the rate of the ligand's exchange between its free and bound states. An exchange rate of >1000 sec^{-1} is considered as fast on the 'NMR time scale', one of

~250 sec^{-1} intermediate, and those exchanges occurring at <100 sec^{-1} considered slow exchange (Roberts, 1993). A ligand in fast exchange is generally associated with weak binding, and can be followed by monitoring a single resonance, whose chemical shift is the weighted average of its proportion of ligand in its free and bound states. By fitting the data obtained in the titration experiments into equation 3.2, using a non-linear regression program, the K_d value of a fast exchanging ligand can be determined. This principle was applied to monitor the shift of the nitropeptide resonance in its free and complexed forms, and to generate a K_d value.

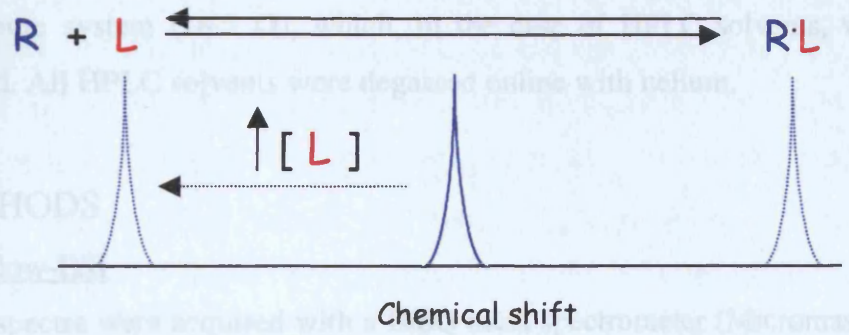

Figure 3.4 Representative NMR spectrum of a fast exchanging complex. Both free ligand and ligand complexed with receptor will have resonances with specific chemical shifts. However, the rapid exchange of ligand between free and complexed states leads to the observation of a single resonance, whose chemical shift is the weighted average of the two states. By titrating in increasing concentrations of ligand, the averaged resonance shifts towards that of free ligand. A plot of chemical shift v_s [ligand] can be analysed to determine K_d (see text).

Equation 3.2 Determination of K_d using a rectangular hyperbola curve fit.

$$\delta_{obs} - \delta_L = \frac{(\delta_{EL} - \delta_L)\{(E_T + L_T + K_d) - \sqrt{(E_T + L_T + K_d)^2 + E_T L_T}\}}{2E_T}$$

Where:
δ_{obs} is the observed chemical shift;
δ_L is the chemical shift of free ligand;
δ_{EL} is the chemical shift of the receptor/ligand complex;
E_T is the concentration of receptor;
L_T concentration of ligand;
K_d dissociation constant.

EXPERIMENTAL PROCEDURES

MATERIALS

Bicine, DMSO, TFA, sephedex, ammonium bicarbonate, guanidine hydrochloride, Tween and ovalbumin were all obtained from Sigma Chemical Co, Poole, Dorset; concentrated ammonia, acetic acid, acetonitrile and formic acid were obtained from Fisher, Loughborough, Leicetershire; Fluorescein isothiocyanate and TMR-maleimide were obtained from Molecular Probes, Eugene, Oregon; Glu-C was obtained from New England Biolabs, Hitchin, Hertfordshire; and Bradford reagent was obtained from Bio-rad, Hemel Hempsted, Hertfordshire. All water used was from the Millipore ultra pure system (18.2 Ω), which, in the case of HPLC solvents, was membrane filtered. All HPLC solvents were degassed online with helium.

METHODS

Nanoflow-ESI

Mass spectra were acquired with a BioQ mass spectrometer (Micromass, Manchester, UK) fitted with a nanoflow ESI probe. All experiments were conducted in water unless otherwise stated. In all experiments 1-3µl of protein/peptide were loaded into gold-coated borosilicate capillaries (Micromass, Manchester, UK) such that the final concentration of SH2 was 20µM. The capillary voltage was set to 1.1kV. The cone voltage was varied according to experiment, as was pH (adjusted using concentrated ammonia and formic acid) and peptide concentration. All analyses were conducted in aqueous conditions. Each spectrum corresponds to a single scan in the mass range 300 to 2000m/z. For binding studies peptide was equilibrated with SH2 for 30 mins at room temperature prior to mass spectral analysis. Maximum entropy calculations were carried out on the spectra using the Masslynx (version 2.3) software.

Fluorescein labelling of SH2 domain

Fyn SH2 was exchanged into 400nM Bicine buffer (pH 8.0) by passing it through a pre-equilibrated Sephadex G-25 column (250 x 30 mm). Eluted protein was then concentrated to 5-10mg/ml using an Amicon concentrator. Fluorescein-5-isothiocyanate (FITC, 35mM) in DMSO, was added in 20µl aliquots to the gently

stirring SH2 to a final Fluorescein:SH2 ratio of 1:25 (v/v). The solution was left gently stirring for 2 hr at room temperature. Excess label was removed by passing the reaction mixture through a G-25 column (250 x 30 mm) pre-equilibrated with PBS. The eluted SH2 was concentrated to final volume of 10-12ml and dialysed for 24hrs in PBS, prior to quantitation by Bradford and spectrophotometry at 494nm. Aliquoted labelled protein was then flash freezed and stored at –80°C.

Glu-C digestion of Fluorescein labelled SH2 domain

Glu-C digestion of fluorescein labelled SH2 domain was conducted in digestion buffer (25mM ammonium bicarbonate, pH 7.8, 0.5M guanidine hydrochloride) such that the final concentration of enzyme was 1/20 of the SH2 domain by weight. LC-MS was conducted directly on the digest using a Hypersil BDS 5µm, C18, reversed phase column (25 x 4.6). A linear gradient of 0% acetonitrile/formic acid (0.3%), 100% formic acid (0.3%) to 70% acetonitrile/ formic acid, 30% formic acid was delivered over 35 min at a flow rate of 1ml min^{-1}. MS was carried out on a Quattro BQ quadropole with an electrospray source. All acquisitions were made in positive mode with a cone voltage of 38V. The eluent from the HPLC, flowing at a rate of 1ml min^{-1} was split in the ratio 6.66:1 allowing 150 µl min^{-1} flow into the mass spectrometer. The source temperature was set at 90°C and acquisitions were made over the range m/z 300-2000, using a scan rate of 4s in continuum mode.

Tetramethylrhodamine labelling of peptides

TMR-5-maleimide (20mM, 80µl) in DMSO, was added to DS4-C or pDS4-C (1 mg) dissolved in 200 µl of PBS and left turning end-over-end overnight at room temperature. Un-reacted label was removed by passage of the reaction mixture through a sephedex G-10 column (50 x 8 mm) and subjected to a further purification/characterisation step on HPLC. Peptides were eluted on a Hypersil BDS 5µm, C18, reversed phase column (25 x 4.6) for analytical purposes or a ( ) semi-preparative column for purification purposes. A linear gradient of 0% acetonitrile/TFA (0.1%), 100% TFA (0.1%) to 70% acetonitrile/ TFA, 30% TFA was delivered over 75 min at a flow rate of 1ml min^{-1}. The elution of peptides was monitored by UV (215 and 280 nm) and fluorescence (excitation: 520nm; emission

580nm) spectrophotometry. Peaks were collected dried down and mass spectrometry conducted on a Quattro BQ quadropole with an electrospray source, or lyophilised.

Dependence of FRET on pDS4-C-TMR Concentration

Acrylic curvettes (3 ml) were pre-coated with ovalbumin (1.5ml of a 0.1% m/v solution) by drying in a 70°C oven overnight. Pre-coating cuvettes with ovalbumin had no effect on fluorescence intensity. After an initial 5mins soak in PBS-Tween, cuvettes were washed thoroughly in PBS and dried in a 40°C oven. All scans and emission measurements were conducted in 1ml of PBS. SH2 concentration was set at 250nM (as determined by the Bradford Assay), and for displacement studies the concentration of pDS4-Cys-TMR was also set at 250nM (determined using the molar extinction coefficient of TMR). Samples were incubated at 4°C for 90mins, prior to a 10mins equilibration at 25°C. The excitation wavelength was 488nm, excitation and emission slits set at 5nm. All scans were conducted between 500 and 600 nm. All readings were made on a Perkin & Elmer luminescence spectrophotometer LS50B.

Binding of derivatives of DS4 to Fyn SH2

Ninety six well microtitre plates were pre-coated with ovalbumin (200µl of a 0.1% solution) and dried overnight. Plates were then washed and dried as previously with the cuvettes. All measurements were conducted in 100 µl of PBS. The concentration of the FRET pair was set at 250nM for both the fluorescein labelled SH2 domain and pDS4-C-TMR. Competing peptide was added to each FRET pair such that the final concentration in the 100 µl ranged from 5 to 500µM. Quadropulet samples were taken at all peptide concentrations. Samples were left shaking at 4°C for 90mins, prior to a 10mins equilibration at 25°C. Readings were taken on a Wallac Victor 1420 multilabel counter. Fluorescein was used as the excitation filter (488 nm, bandwidth 10 nm), with TMR (580 nm, bandwidth 10 nm) and fluorescein (520 nm, bandwidth 10 nm) filters used to take emission readings. Controls (SH2 + pDS4-C-TMR and SH2 + DS4-C-TMR) absent of any competing peptides were used to calculate the percentage of pDS4-C-TMR bound to the SH2 domain.

Nuclear Magnetic Resonance

Fyn was exchanged into a NMR buffer (pH 6.5), containing 10% D_2O, such that the final concentration of protein was 90μM in. Nitrated DS4, in 2 μl of NMR buffer (pH 6.5) was added to 500μl of protein and spectra acquired. Resonance shifts in the methyl and aromatic regions were observed. All experiments consisted of 256 scans conducted on a Bruker 600 MHz NMR spectrometer at 25°C.

RESULTS

Determination of Peptide Binding by Nanospray-ESI

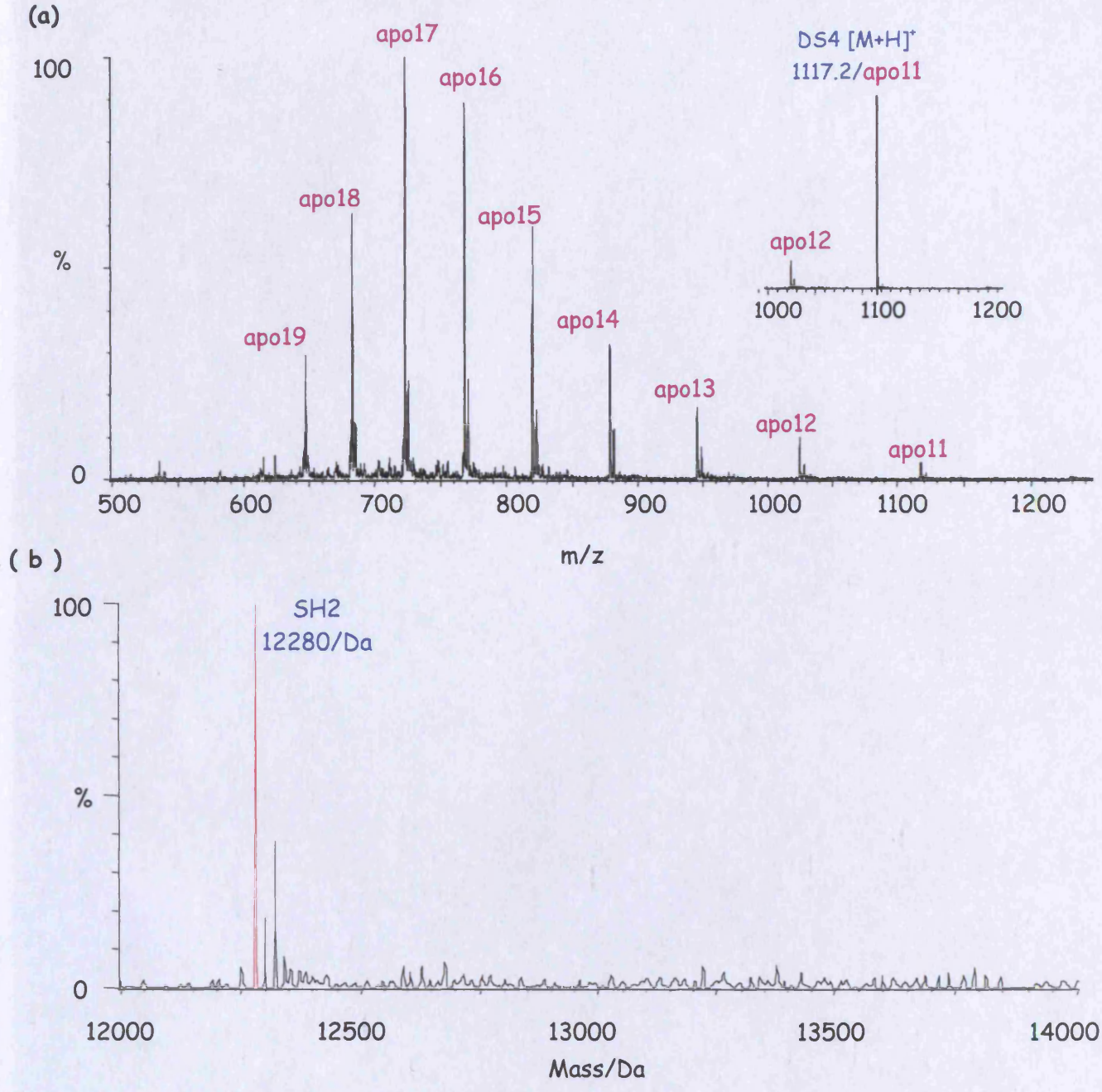

Figure 3.5. Nanoflow-ESI spectra of Fyn SH2. (a) The spectrum showing the multiply charged peaks of the protein. The spectrum is identical to that of the SH2 in the presence of DS4 (inset), it is coincidence that the apo11 value of the protein corresponds to the $[M+H]^+$ of the peptide. (b) The de-convoluted spectrum gives a theoretical calculated value of Fyn SH2 as 12280, compared to the calculated value of 12278 Da. There was no indication of an SH2-DS4 complex (theoretical mass 13395).

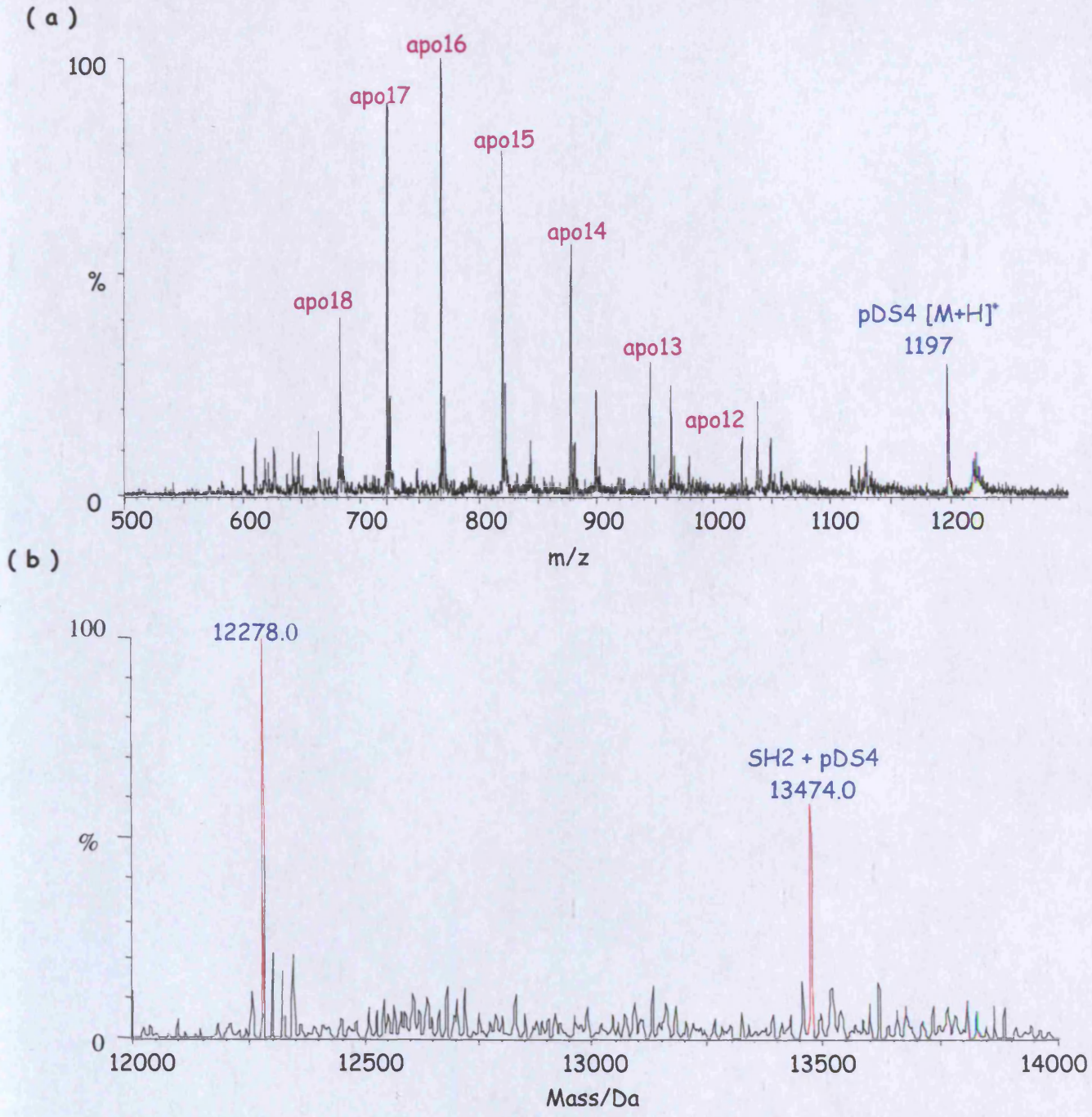

Figure 3.6. Nanoflow-ESI of spectra of Fyn SH2 equilibrated with pDS4. (a) The spectrum showing the multiply charged peaks of the protein in addition to a peak corresponding to the singly charged peptide (m/z 1197) is also present. (b) The de-convoluted spectrum shows two major peaks: one corresponding to Fyn, the other to a complex of SH2 domain and protein (theoretical value 13475, actual 13474 Da).

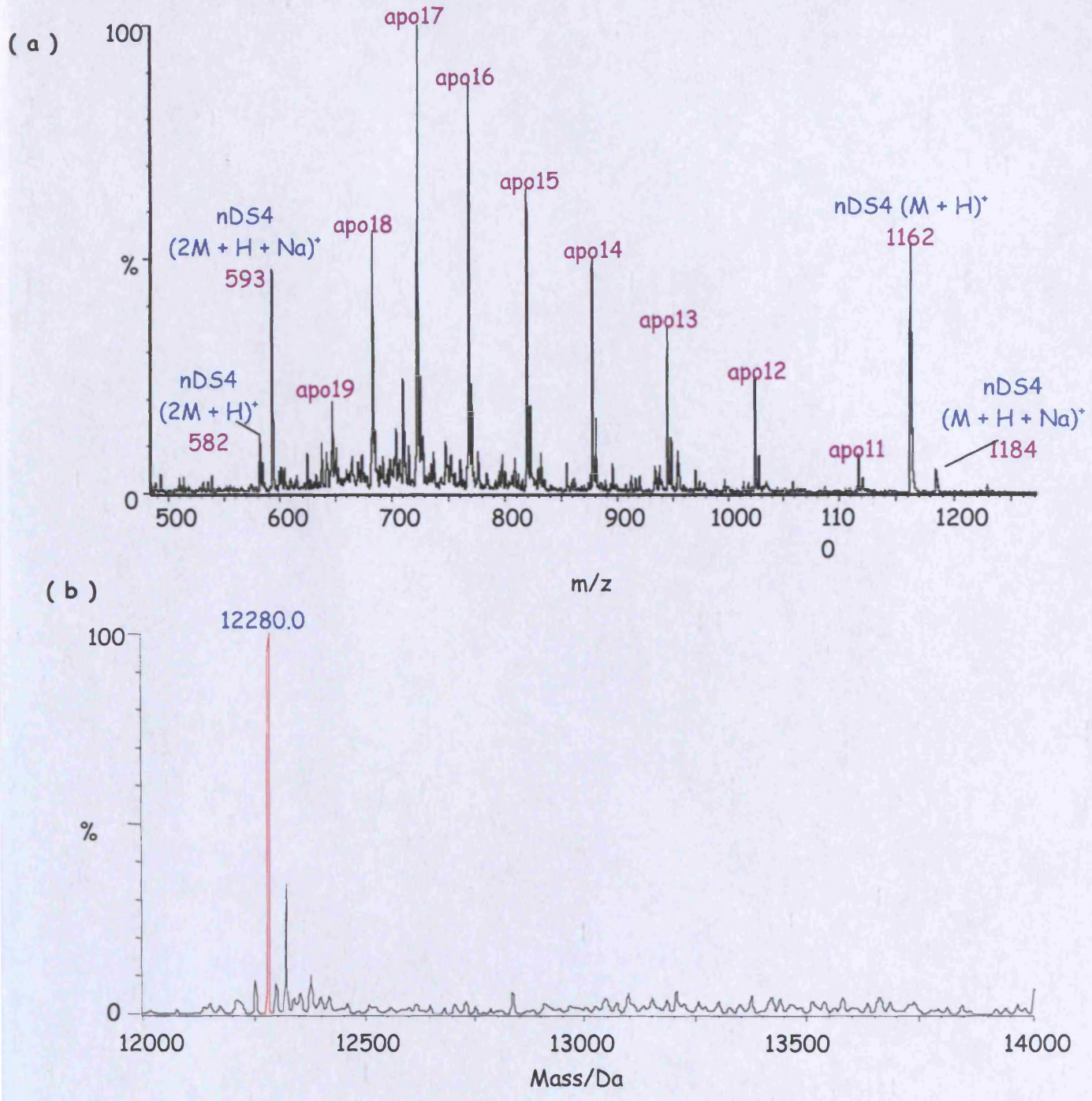

Figure 3.7. Nanoflow-ESI of spectra of Fyn SH2 equilibrated with nDS4. (a) The spectrum shows the multiply charged peaks of the protein, plus those peaks corresponding to the singly and doubly charged peptide (m/z: 1162 and 582, respectively) are present. (b) The de-convoluted spectrum of the SH2 in the presence nDS4 shows one major peak corresponding to Fyn SH2 domain, with no indication of an SH2-nDS4 complex (theoretical mass 13440). There were, however, indications that the peptide could form multimeric complexes.

Figure 3.5a shows the ESI trace of Fyn SH2 domain, with the different charge states producing the statistical bell-shaped distribution. The nine charged states from +11 to +19 confirm the mass of the apo-protein to be 12280 (Figure 3.5b), which is 2Da off the calculated mass of 12278. On addition of a 1.5 molar excess of DS4 to the SH2 domain there was no indication of peptide binding (Figure 3.5b). In contrast, transformation of the spectrum generated on addition of 1.5 molar equivalents of pDS4 to the SH2 domain (3.6 a) produced two distinct masses: 12278 Da, corresponding to the mass of the free protein, and 13474 Da in agreement of the phosphorylated derivative of DS4 bound to the SH2. Nanospray mass spectrometry has previously been used to probe the binding of the analogue of DS4, middle T antigen, to Fyn SH2 (Chung et al., 1999). In this study addition of an equimolar equivalent of phosphopeptide to SH2 domain resulted in the formation of a 1:1 complex, with no subsequent detection of free protein or peptide. In our study a 1.5 molar excess of peptide was not sufficient to saturate the SH2 domain, suggesting the differences in the conditions employed in the two studies, such as cone voltage and pH, had a bearing on the extent of peptide binding. However, the nanospray experiment clearly demonstrated the affinity of the phosphopeptide for the SH2 domain.

In the Chung study 8 charged states were detected for apo-protein, from +7 to + 14, corresponding to the protonation of side chains of basic amino acids (Lys, His and Arg). The imidazole ring of the HisβD4 side chain has a pKa of around 6.5 (Stryer, 1988), consequently, at pH 7 this group would exist primarily in its non-charged form, whereas at pH 5 the majority of the group would be in its charged state. The discrepancy between the number and distrubution of charge on analysis of the apo-proteins in the two studies can be attributed to the pH at which the experiments were conducted; pH 5 in the Chung study, 7 in our subsequent study. On the binding of phosphorylated derivative of middle T antigen to the SH2 there was a reduction in charge of –3, attributed to the peptide directly interacting with the side chains of basic residues ArgβB5, HisβD4 and LysβD6 (Chung et al., 1999; Mulhern et al., 1997), thus preventing their protonation.

Analysis of the SH2 domain in the presence nDS4 showed the peptide did not bind to the protein under the conditions employed (Figure 3.8b). Alterations to the cone voltage, pH and peptide concentration had no effect on binding (data not shown).

Determination of Peptide Binding Using Fluorescence Resonance Energy Transfer Assay

The application of FRET in sensing and quantitating biomolecular interactions is dependant on the ability to detect the loss or gain of fluorophore emission. The donor/acceptor stoichiometry is critical, therefore, as an excess of either would compromise the sensitivity of the technique. There was a single labelling site on the peptides for TMR (the terminal cysteine group), however, there were potentially nine labelling sites for fluorescein on the SH2: eight ε–amino groups on lysine residues and the N-terminal α-amino group of serine (Table 3.3). To overcome the potential of multiple additions, the dependence of the fluorescein labelling reaction on pH was successfully employed to selectively label the SH2 of Fyn. Figure 3.8 shows the LC-MS traces of Glu-C digested labelled and non-labelled SH2. Glu-C is a protein endoprotease that cleaves at the C- terminus of glutamic acid residues. This enzyme was used to characterise Fyn SH2 because the theoretical fragments produced after digestion were, sufficiently sized, yet varied in composition to be retained and resolved by reverse phase HPLC. All theoretical fragments were detected, with the exception of G2 and 5, due to their low masses. It was not possible to predict the sequence of fragment elution (elution sequence: G1, 8, 6, 3, 7 and 4).

Table 3.3. Theoretical products of Glu-C digested Fyn SH2 domain.

Fragment	Fyn SH2 domain sequence	Residue	Theoretical Molecular Weight/Da
G1	1-5	SIQAE	546.26
G2	6-6	E	147.05
G3	7-18	WYFGKLGRKDAE	1468.75
G4	19-35	RQLLSFGNPRGTFLIRE	2003.11
G5	36-37	SE	234.09
G6	38-80	TTKGAYSLSIRDWDDMKGDHV KHYKIRKLDNGGYYITTRAQFE	5076.53
G7	81-91	TLQQLVQHYSE	1344.67
G8	92-106	RAAGLSSRLVVPSHK	1576.92

The unique labelling of the N-terminal amino group was indicative of the success of pH regulating the selection of the nucleophilic amino moiety: the pKa of the of the N-terminal being less than that of the ε–groups of lysine making this group susceptible to nucleophilic attack. There was no indication of the labelling of ε–amino group of Lysines in any peptide sequence (data not shown). The mass- to-charge ratio of the detected fragments varied from the six charges detected in G6 to the solitary charge detected in G1, reflecting the proportion of residues capable of being protonated in each fragment. As expected, addition of the hydrophobic fluorescein moiety to the N-terminal amino group increased G1's retention time by some 12 minutes; and, interestingly, there was no indication of any residual G1 after the labelling process. This was unexpected as a previously reported selective N-terminal labelling of an SH2 domain presented stoichiometries of between 0.4 and 0.63 fluoresceins per SH2 domain (Sato et al., 1999).

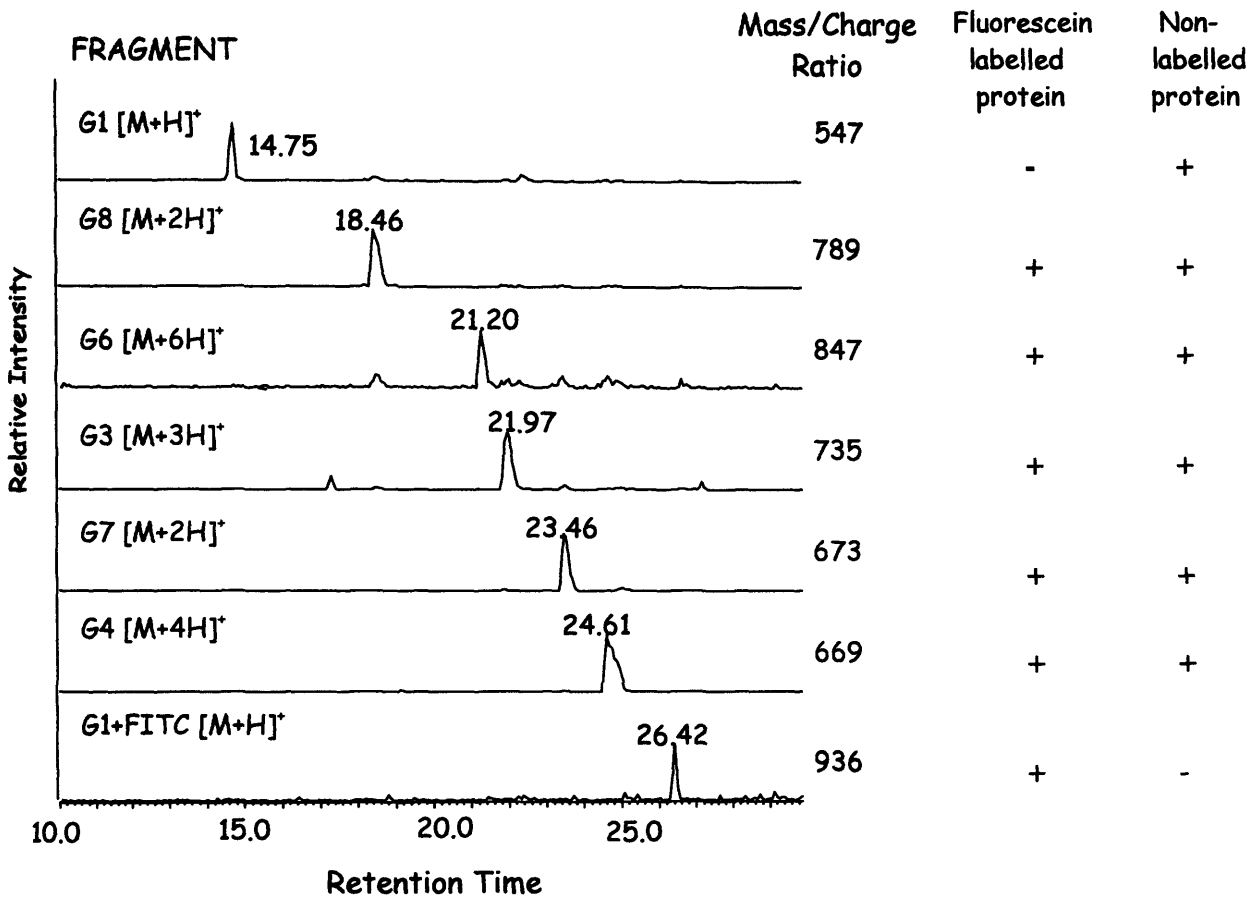

Figure 3.8. LC-MS traces of Glu-C digested fluorescein labelled and non-labelled SH2 domain. All the peaks corresponding to the SH2 digestion fragments were detected, with the exception of G2 and 5. The retention times, mass/charge ratio and their presence in labelled or non-labelled digestion products are indicated.

Both phosphorylated and non-phosphorylated peptides were successfully labelled with TMR, as confirmed by ESI-MS. Synthesis of the phosphorylated TMR peptide derivative was confirmed by the detection of the doubly charged species, whilst both doubly and triply charged species were detected for the non-phosphorylated peptide (Figure 3.9), with both peptides having similar retention time.

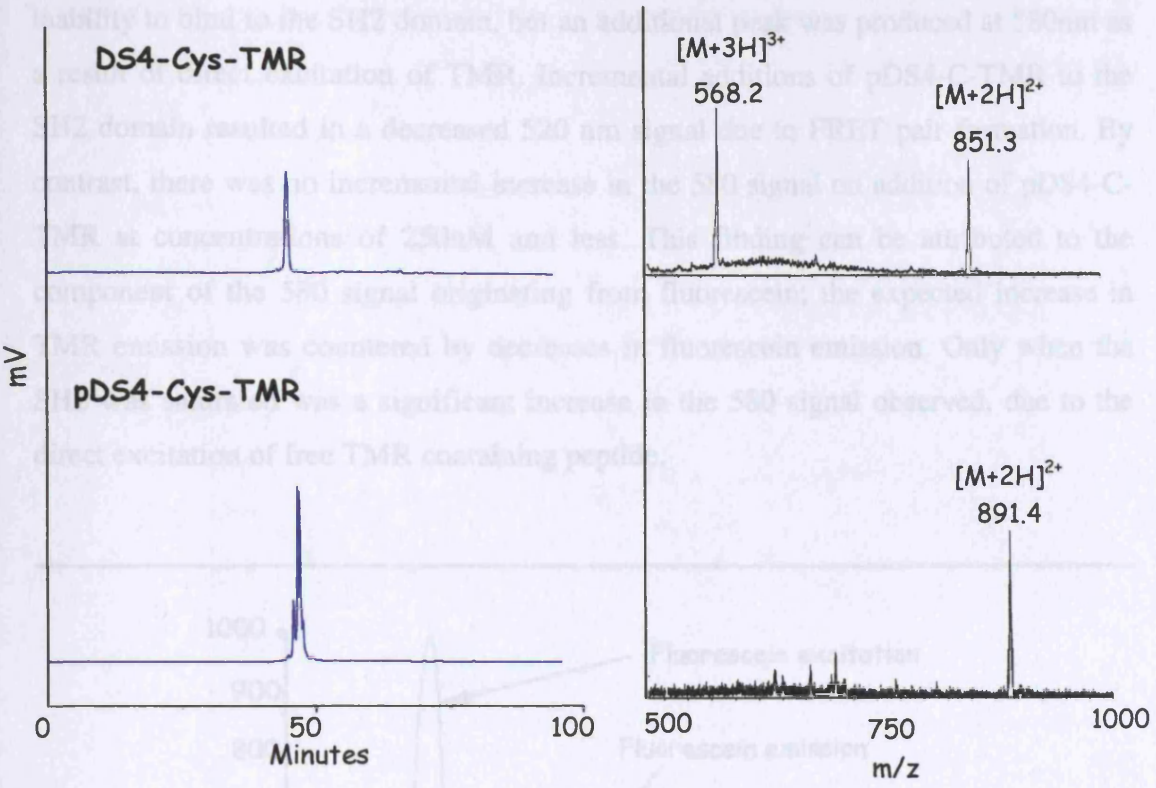

Figure 3.9. HPLC/mass-spectrometric characterisation of TMR labelled derivatives of DS4. The HPLC traces (left panel) show the retention times of both phosphorylated and non-phosphorylated peptide are very similar. Confirmation of the sucessful labelling and purification of the peptides is seen in the traces with peaks corresponding to multiply charged peptides.

Figure 3.10 shows the excitation and emission spectra of Fluorescein and TMR, indicating the overlap of Fluorescein emission spectrum with the excitation spectrum of TMR that makes these two fluorophores a FRET pair. Having characterised both labelled peptides and protein the formation of FRET pair on the binding of the labeled protein to the labelled peptide was determined (3.11). The decrease in 520nm intensity on subsequent additions of pDS4-C-TMR was indicative of efficient binding of peptide to SH2, suggesting the labelling of the binding partners did not impede their interaction. On excitation at 488nm (excitation maximum of fluorescein), the emission spectra of labelled SH2 domain only shows a peak maximum at 520nm, this wavelength being the emission maximum of Fluorescein, although, there was significant signal intensity at 580nm. The presence of DS4-C-TMR has no effect on

the Fluorescein signal at 520nm, confirming a lack of FRET, due to the peptide's inability to bind to the SH2 domain, but an additional peak was produced at 580nm as a result of direct excitation of TMR. Incremental additions of pDS4-C-TMR to the SH2 domain resulted in a decreased 520 nm signal due to FRET pair formation. By contrast, there was no incremental increase in the 580 signal on addition of pDS4-C-TMR at concentrations of 250nM and less. This finding can be attributed to the component of the 580 signal originating from fluorescein; the expected increase in TMR emission was countered by decreases in fluorescein emission. Only when the SH2 was saturated was a significant increase in the 580 signal observed, due to the direct excitation of free TMR containing peptide.

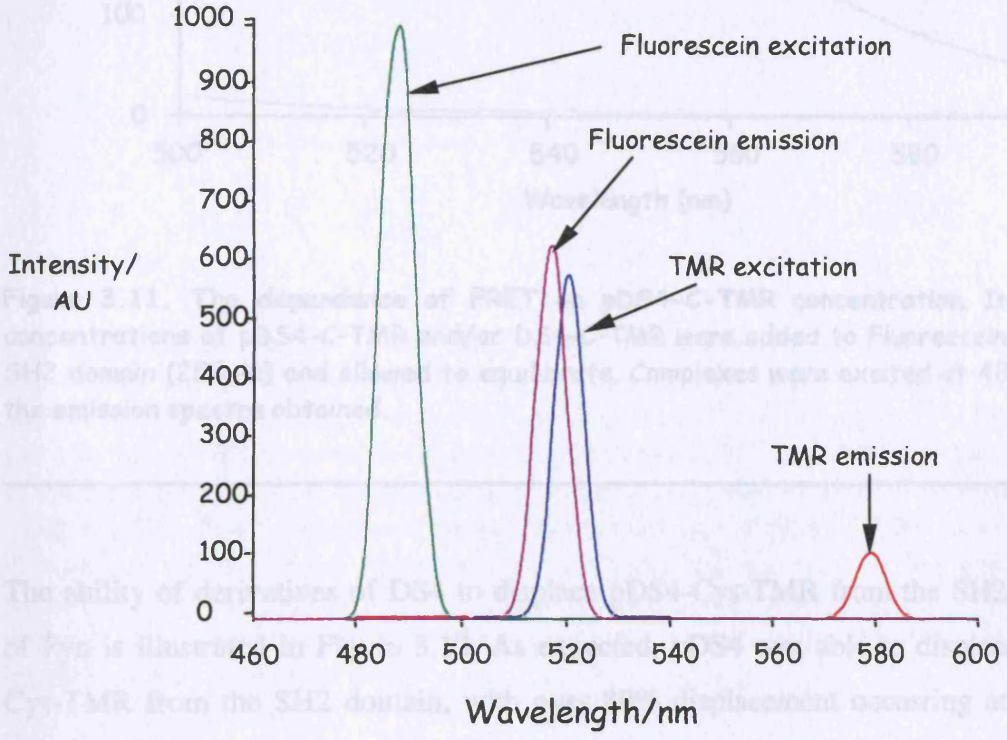

Figure 3.10. Excitation and emission spectra of Flourescein and TMR. The excitation and emission spectra was conducted on 1 mg/ml of each fluorphore in PBS. The figure clearly demonstrates the overlap of the emission spectra of Fluorescein with the excitation spectrum of TMR. Additionally, exciting the fluorophores at 488 nm (the emission maximum of Fluorescein) would lead to the excitation of TMR.

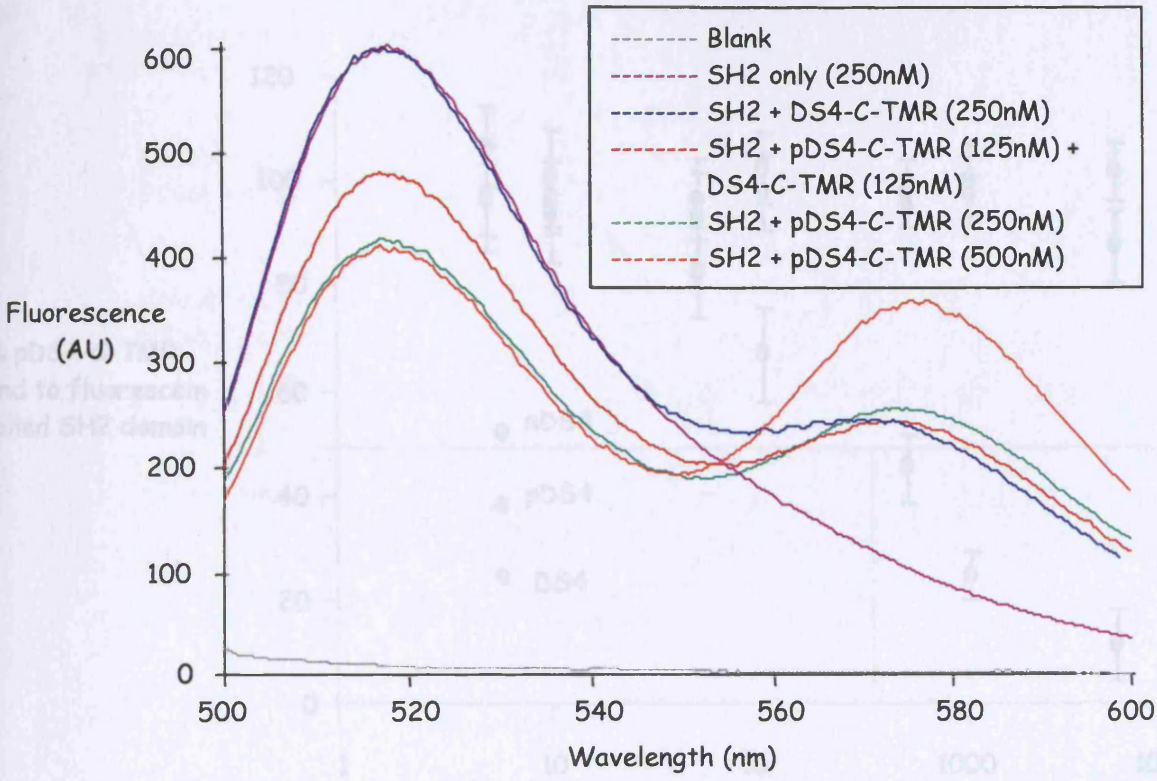

Figure 3.11. The dependence of FRET on pDS4-C-TMR concentration. Increasing concentrations of pDS4-C-TMR and/or DS4-C-TMR were added to Fluorescein labelled SH2 domain (250nM) and allowed to equilibrate. Complexes were excited at 488nm and the emission spectra obtained.

The ability of derivatives of DS4 to displace pDS4-Cys-TMR from the SH2 domain of Fyn is illustrated in Figure 3.12. As expected, pDS4 was able to displace pDS4-Cys-TMR from the SH2 domain, with over 80% displacement occurring at peptide concentrations of over 5 μM and above. An IC_{50} value of approximately 250nM was obtained, which was concentration at which displacing peptide and labelled peptide were equivalent. No displacement was noted for either nDS4 or DS4 over the studied peptide range, and an inability to extend the peptide concentration beyond 100μM due to non-specific quenching of the signal meant IC_{50} values for these peptides could not be obtained by this method.

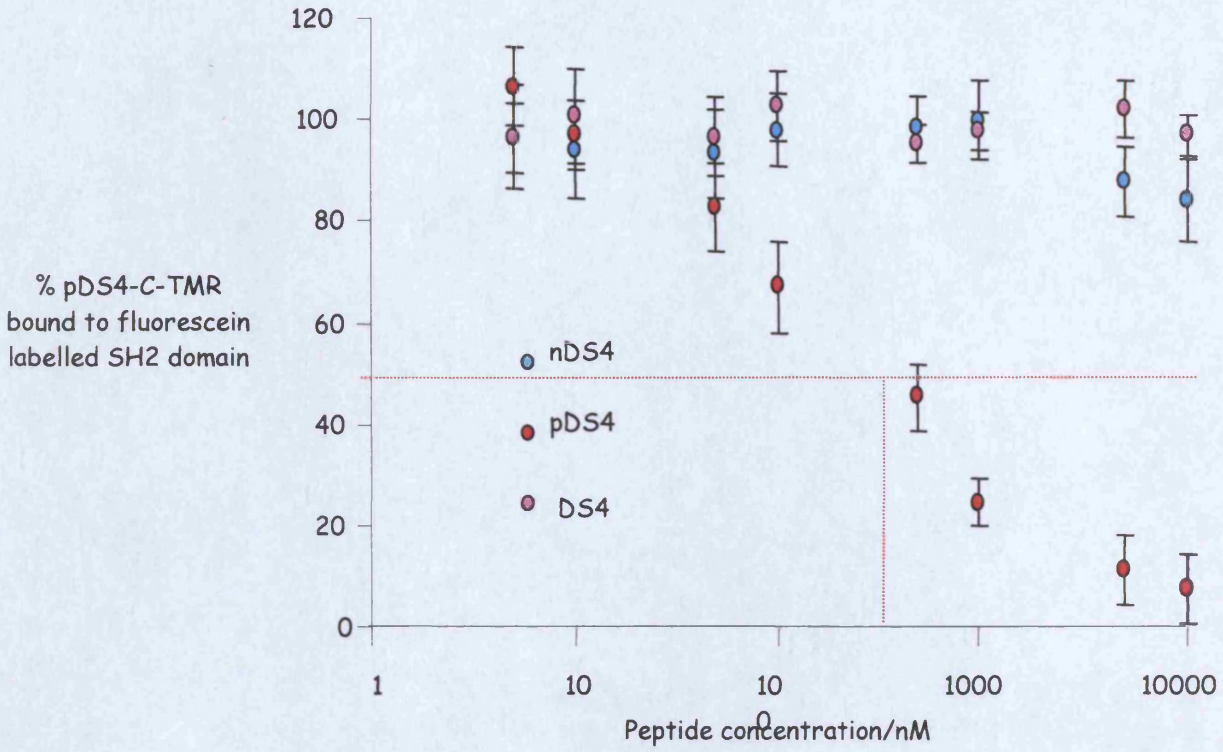

Figure 3.12. The ability of derivative DS4 to displacement of pDS4-C-TMR from fluorescein labelled SH2 domain. Derivatives of DS4 were incubated at varying concentrations (5nM - 10μM) with FRET pairs (SH2 250 nM and pDS4-C-TMR 250 nM) and the 520 nm/580 nm ratios determined. The control 520 nm/580 nm values obtained at maximal pDS4-C-TMR binding (SH2 + pDS4-C-TMR) and at minimal peptide binding (SH2 + DS4-C-TMR) were also obtained. The percentage of pDS4-C-TMR bound to SH2 domain was calculated be comparing the 520 nm/580 nm ratio in the presence of derivatives of DS4 (peptide + SH2 + pDS4-C-TMR) to the ratios obtained in the control analysis. The dotted line indicates the approximate concentration of pDS4 that reduced labelled peptide binding by 50%.

Determination of Peptide Binding By Nuclear Magnetic Resonance

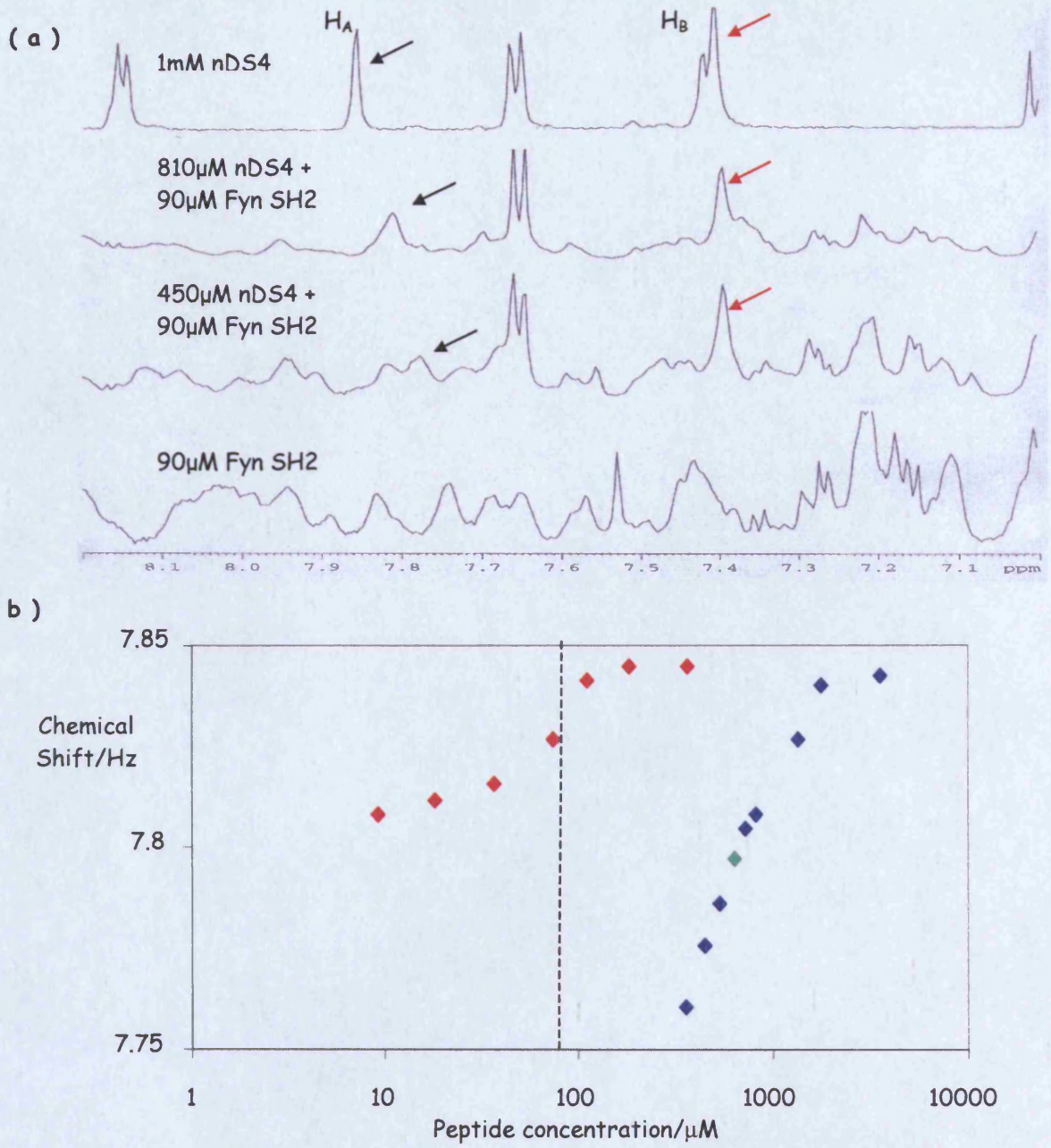

Figure 3.13. The ability of pDS4 to displace nDS4 from Fyn SH2 domain. (a) The meta proton adjacent to the nitro group (H_A) of nTyr is indicated by the black arrows, the red arrows indicates the shift of the other meta proton (H_B, see Ch.2, p.___). The shift of the meta proton was monitored in the SH2 domain peptide/complex. (b) Increasing concentrations of nDS4 were added to the SH2 domain (90 μM, indicated by the dotted line) to determine a suitable concentration to be used in the pDS4 displacement study (blue diamonds). The green diamond indicates the shift corresponding to 630 μM of nDS4, the concentration used in the pDS4 displacement study. pDS4 was added iteratively to a sample containing Fyn (90μM) and nDS4 and the shift of the nTyr meta proton was monitored (red diamonds).

An approximate value for the K_d of nDS4 could not be determined using the FRET assay, due to the weak binding and non-specific quenching of fluorescence signal at higher peptide concentrations. NMR was, therefore, used to, firstly, characterise the kinetics of the binding between the peptide and the SH2 domain, and to estimate a K_d value for this interaction. On titration of the nitropeptide against the SH2 domain a resonance, previously identified as the meta proton of nDS4 (see chapter 3 and appendix II), was observed to shift downfield towards the chemical shift in the free state (Figure 3.12 a), whilst the chemical shift of the opposing proton was unaffected by tritrations of the nitropeptide. This finding suggests the chemical environment of the meta proton was altered on binding of the peptide to the SH2 domain, unlike the para proton, whose chemical shift remained largely unchanged. At the lower concentrations of nDS4 the resonance for the para proton appears as a singlet resonance as opposed the multiplet found in the free peptide, most probably due to the increased relaxation rate on interaction with the pTyr-binding pocket.

The observed shift is the result of the weakly binding ligand rapidly exchanging between its free and bound states. To confirm that the peptide had a weak affinity for the SH2 domain, the ability of pDS4 to displace nDS4 from the SH2 domain was investigated. A concentration of 630μM of nDS4 was selected as the amount of peptide to be displaced by pDS4 for two reasons: firstly, this concentration of nitropeptide was not sufficient to saturate the protein; secondly, at this concentration of peptide, the resonance could be easily distinguished in the peptide-SH2 complex (the resonance followed could not be discerned at concentrations below 360μM). Figure 3.13 b shows the ability of pDS4 to displace nDS4 from the SH2 domain. A concentration of just over 100μM pDS4 was capable of displacing nDS4 from the SH2 domain. This finding is consistent the FRET data, which predicts the amount of pDS4 required to completely displace the nitropeptide to be approximately the same concentration as the SH2 (90 μM). Based on the findings of the experiments shown in Figure 3.12, and knowledge that SH2 domains contain a solitary pTyr-binding site, it was concluded that nDS4 and pDS4 share the same binding site.

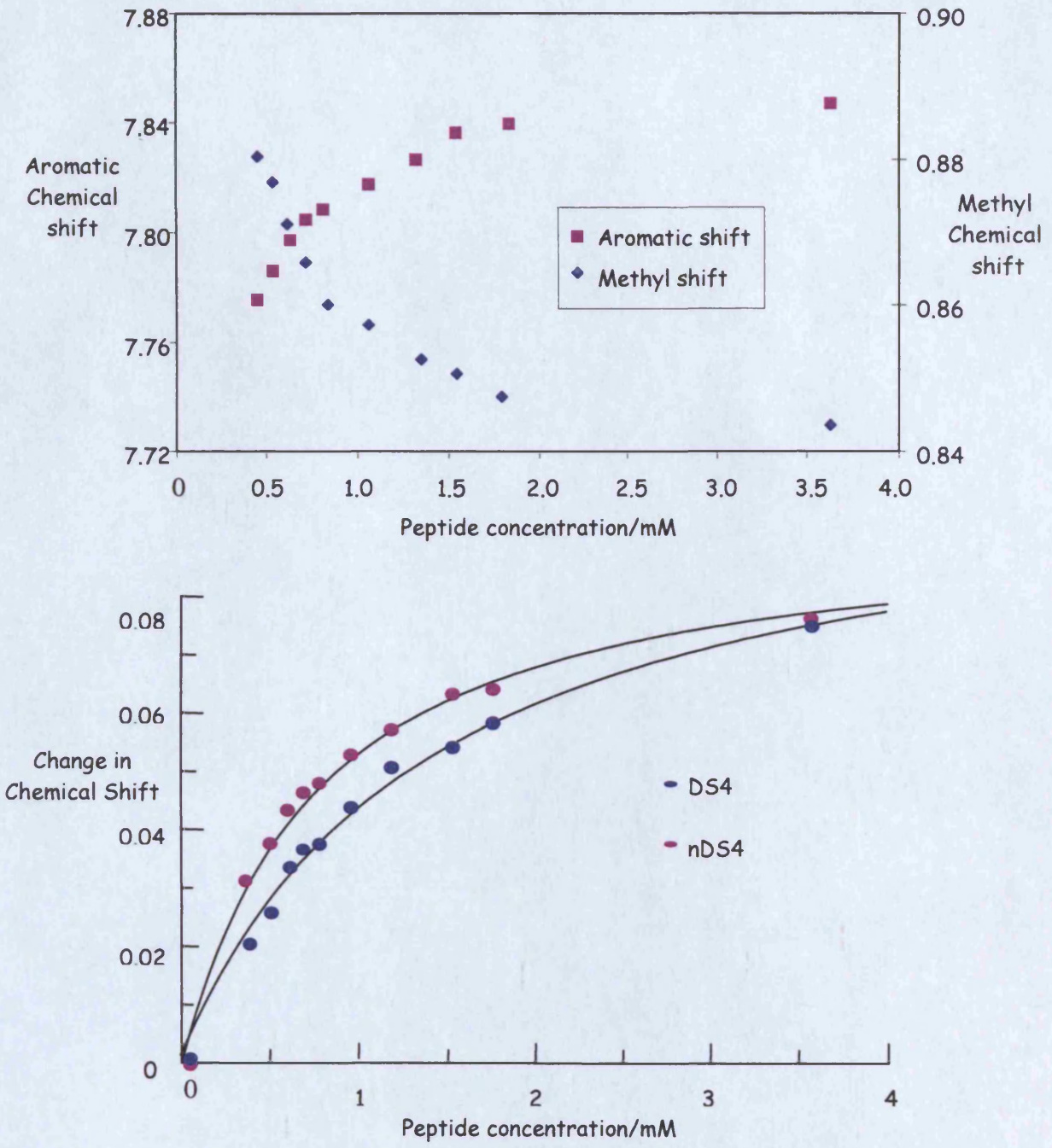

Figure 3.12. The chemical shift changes observed on the binding of DS4 and nDS4 on binding to the SH2 domain. (a) The binding of DS4 and nDS4 to Fyn SH2 domain (90μM) was observed by moitoring the shift of specific resonance in the aromatic and methyl regions, respectively. (b) The change in chemical shift was plotted as a function of peptide concentration and K_d values obtained.

In order to obtain K_d values for DS4 and nDS4 the peptides were titrated against a fixed concentration of SH2 protein, and the chemical shifts of aromatic and methyl resonances of the protein were followed, until near saturation was achieved (Figure 3.13 a). For both peptides, saturation appeared to be achieved at a concentration of over 4mM. By plotting the change in chemical shift against peptide concentration (Figure 3.14 b), and by fitting the data obtained into equation 3.2, K_d values of 0.7 ± 0.1 mM, and 1.4 ± 0.2 mM were obtained for nDS4 and DS4 respectively.

DISCUSSION

The ability of solution-phase interactions to be maintained in the gaseous phase has enabled ESI-MS to be utilised to probe non-covalent interactions (Przybylski and Glocker, 1996). Indeed, both relative and absolute affinities for phosphopeptide/SH2 domain interactions have been determined by this method (Loo et al., 1997). A refinement on this procedure is to use nanoES, which reduces the propensity of ligands to detach from the receptor during the phase change. Nanospray has been previously used to qualitatively assess the extent to which middle T antigen bound to the SH2 domain of Fyn (Chung et al., 1998). Using the same technique, the ability of nDS4 to bind to the SH2 domain of Fyn was assessed. Both the nitropeptide and DS4 had affinities for the SH2 domain some three orders of magnitude less than the phosphopeptide. These data suggest that either nDS4 is not a ligand for the SH2 domain of Fyn, or that the weakly bound peptide was displaced from the protein during the dispersion of complex from solution to gaseous phases. Loo and colleagues (1997) determined the best conditions for analysing phosphopeptide/src SH2 domain interactions by ESI-MS were typically to use an acidified solution containing a high proportion of organic solvent. An organic phase was not utilised in the nanospray experiments to avoid denaturing the SH2 domain, whilst adjusting the pH, source temperature and collision energy did not facilitate nDS4's binding.

To try and quantitate the binding of the derivatives of DS4 to Fyn SH2 domain a FRET based assay adapted from previous described procedure (Sato et al., 1999). The SH2 domain was selectively N-terminally labelled with Fluorescein, and the Glu-C digestion products of the protein analysed by LC-MS. The N-terminal fragment (G1) and those containing lysine residues (G3, 6 and 8) were of interest, as these peptides

contained the potential sites of fluorescein labelling. FITC labelling of amino groups is a neucleophilic attack of the amino group on the thiocyanate moiety of the fluorphore. For the reaction to proceed the amino must be in its non-protonated, uncharged form (Little et al., 1997). The pKa of the ε–amino of lysine is approximately 10.5, which is 1-1.5 pH units greater than α–amino groups (Stryer, 1988). Therefore, at lower pH values, a greater proportion of α–amino groups will be in the uncharged form and are, thus, more likely to act as nucleophiles. This principle has previously been used to specifically label the α–amino group of peptides containing lysine residues, with the optimal pH for this procedure being 8.5 (Little et al., 1997). The same methodology was used to selectively and completely label fragment G1 of Fyn SH2 domain. Using the same principles, the N-terminal labelling of PI 3-kinase SH2 domain with Fluorescein produced stoichiometries ranging from 0.4 to 0.63 FITCs per SH2 (Sato et al., 1999). The differences in the labelling efficiency of the two processes is likely to be due to temperatures that each of the experiments was conducted: 2 hr at room temperature for the labelling of Fyn, as opposed to the overnight incubation at 4°C conducted by Sato and colleagues (1999). Kinetically, conducting the labelling at a higher temperature would favour the reaction going to completion, akin to the complete and selective labelling of the N-terminal α–amino group of peptides under similar conditions (Little et al., 1997), yet by conducting the labelling at 4°C the risk of microbial contamination is diminished. The potential bacterial contamination was weighed against an increase in assay sensitivity; by completely labelling all the SH2 proteins, the sensitivity of the assay would be, in theory at least, improved. As the labelled SH2 protein was utilised on a one-off strategy, and the incubations for displacement studies were no more than 90 mins at 4°C, the trade off between sensitivity and microbial contamination was deemed justified.

The binding of pDS4-TMR to Fluorescein labelled SH2 domain, and subsequent FRET pair formation, were characterised and sufficiently sensitive for the quantitative studies of peptide displacement. An IC_{50} value of 250 nM for the displacement of pDS4-TMR by pDS4 was determined. From this value a K_d of 40nM was calculated, which is consistent published values of other SH2 domain phosphopeptide interactions (10-100nM; Pawson, 1995). Neither DS4 nor nDS4 showed any affinity

for the SH2 domain over the studied peptide concentration range, confirming, for DS4, and suggesting in the case nDS4, their K_d values were in the micromolar range or above.

Equation 3.2 Determination of dissociation constant.

$$K_i = \frac{[I_{50}]}{1 + \frac{[L]}{K_L}}$$

Where: K_i is the dissociation constant of DS4 derivative.
I_{50} is the concentration of peptide that brought about 50% displacement of pDS4-C-TMR (250 nM).
L is the concentration of pDS4-C-TMR (250 nM).
K_L is the dissociation constant of a phosphopeptide bound to an SH2 domain (50 nM, derived from the 1-100 nM quoted in Pawson, 1995).

For the quantitative determinations of nDS4's binding to the SH2 domain of Fyn, the FRET assay and the NMR studies complemented each other in the peptide concentration for which binding could be measured using the respective techniques: nanomolar to low micromolar amounts of peptide measured in the FRET assay, compared to the micromolar to millimolar quantities measured by NMR. When measured by NMR, the chemical shift of ligands in fast exchange with a receptor is proportional to the weighted average of the amount of ligand in its free and bound states. K_d values for both DS4 and nDS4 were obtained from the binding curves generated on titrating the peptides against a fixed concentration of SH2. The 1.4 mM value obtained for the K_d of DS4 is consistent with those reported elsewhere (Bradshaw et al., 1999), whilst the value for nDS4 was of the same magnitude (0.7mM). When using NMR (and indeed FRET) to determine dissociation constants one of the major limitations is the assumption that the receptor/ligand complex exists in one conformation, which is not necessarily the case; it is feasible that the complex might exist in more than one conformation, but these would be averages across all the states (Roberts, 1993). Previous analysis of the binding a phosphopeptide to an SH2 domain showed that the only structural changes that occurred were at the pTyr and hydrophobic binding pockets, which close-up and open, respectively, on peptide binding (Waksman et al., 1993). With this in mind, it was assumed that the binding of nDS4 to the SH2 domain of Fyn results in only one conformation for the receptor/ligand complex. Further to this, the spectra produced on titrating nDS4

against the SH2 shows the line-width of the some of the ligand resonances to decrease on peptide addition, suggesting the peptide was in very fast exchange with the protein (Figure 3.10 a), vindicating the use of equation 3.2 for K_d determinations.

The experiments presented here provide K_d values for the interaction of a nitropeptide with an SH2 domain. Such values have not been previously published. A simple technique such as the generation of a fluorescence-binding curve would have been a useful accompaniment to the NMR data, however nTyr is a potent quencher of tryptophan fluorescence, the dominating fluorophore in proteins (Prigodich and Sanaulla, 1991). NMR is a good method for determining weak binding, however, more accurate determination of the K_d values of nitropeptide/SH2 interactions would be expected using ITC or SPR.

The three techniques employed to determine the binding of nDS4 to the SH2 domain of Fyn have their benefits and their limitations. Both nanospray and the FRET assay were limited in their inability to detect weakly bound ligands, whilst NMR is limited by the assumptions that have to be made in calculating K_d. On the other hand, nanospray is a quick means of either quantitatively or qualitatively determining peptide binding using small amounts of both receptor and ligand; the FRET assay is a sensitive means of quantitatively determining peptide/SH2 domain interactions; and NMR provides values for the weakly bound ligands in fast exchange with the receptor.

CHAPTER 4:

PROBING THE MOLECULAR INTERACTIONS BETWEEN THE DERIVATIVES OF DS4 AND FYN SH2 DOMAIN

INTRODUCTION

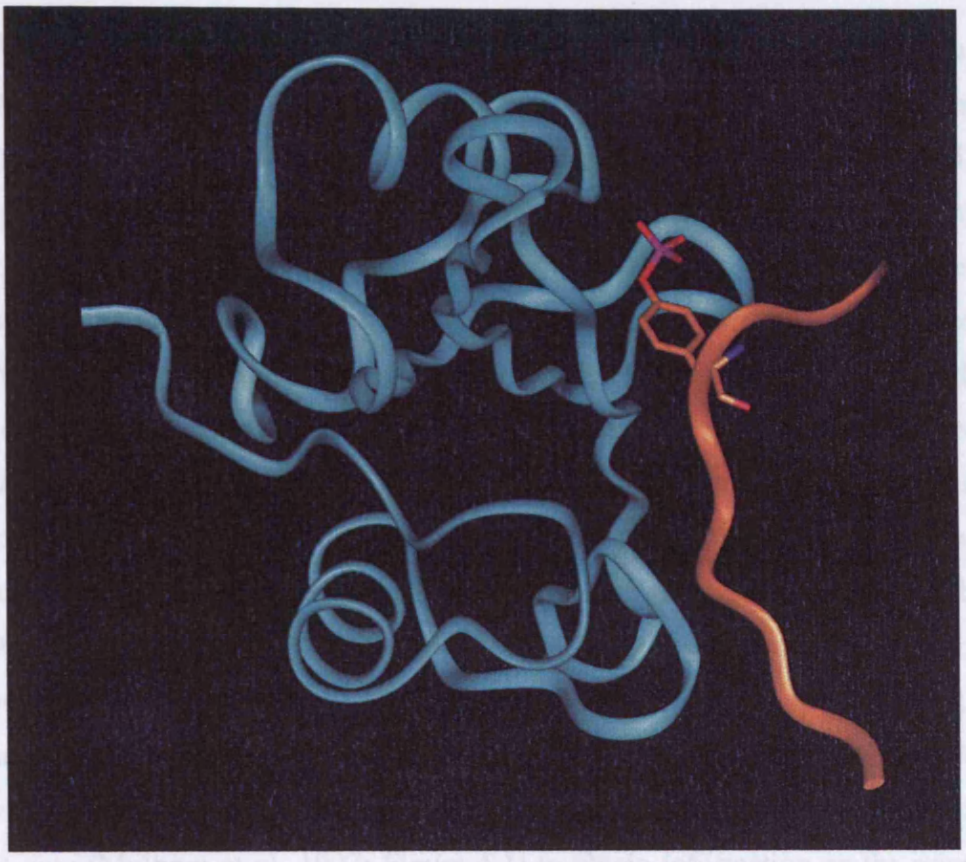

Figure 4.1. A ribbon drawing of the C-C backbone of Fyn SH2 domain bound to the residues 321-331 from hamster middle T antigen. The SH2 protein is highlighted in blue and the peptide brown. Also highlighted are the molecules of the phosophotyrosine residue.

The findings of chapter 3 showed the affinity of the nitropeptide to be approximately 1000 fold less than that of the phosphopeptide for Fyn SH2 domain. To rationalise this finding the interactions between Fyn SH2 domain and derivatives of DS4 were probed using NMR and computational modelling. Interestingly, in a recent study, nitropeptides were shown to be capable of binding to the SH2 domain of the src kinase Lyn, and in so doing activate this enzyme (Mallozzi et al., 2001). The differences in the ability of nitropeptides to bind to the SH2 domains of Fyn and Lyn suggest it is the interactions made by each of the nTyr moieties in the respective pTyr-binding pockets that govern whether binding occurs or not. The subsequent molecular studies are therefore pertinent in relating the molecular and topological make-up of

the pTyr-binding pocket to (in the case of Fyn) nitrotyrosine's lack of affinity to the SH2 domain.

NMR has become a valuable tool in probing the interaction between ligands and the receptors to which they bind. The structure of biomolecular complexes and the determinants that underlie their molecular recognition can all be established using high resolution NMR, although, these procedures can be time consuming and laborious due to the amount of data that requires analysis. However, in a process known as chemical shift mapping, simple 2D NMR experiments can monitor and quantitate the interactions between an isotopically labelled receptor with both high and low affinity ligands (Rajagopal et al., 1997). The binding of a ligand to a receptor will alter the local chemical environment at the point of interaction, and may induce conformational changes within the protein receptor. Both these effects will result in perturbations in HSQC chemical shifts. Using these principles, changes in the NH backbone chemical shifts of ^{15}N labelled SH2 domain were monitored by (^{1}H, ^{15}N)-HSQC NMR, on titration of nDS4, and on the addition of pDS4. A comparison of the global effects of peptide binding on the labelled protein, as well as the effect on individual residues, was conducted. Further to this, a model was built using existing NMR data (Mulhern et al, 1997; Figure 4.1) to obtain information on the orientation and topology of the nitrotyrosine residue in the pTyr-binding pocket.

EXPERIMENTAL PROCEDURES

MATERIALS

With the exception of ^{15}N labelled ammonium chloride, which was obtained from Cambridge Isotopes, all the components of the minimal media and NMR buffer were obtained from Sigma. Peptides were synthesised in house (see chapter 2). The SH2 domain expression plasmid was a kindly provided by Professor I Campbell (University of Oxford). Details of the expression plasmid can be found in Mulhern et al., (1997).

METHODS

Expression of ^{15}N Labelled Fyn

The plasmid expressing Fyn was derived from the pRK172 expression plasmid. The DNA sequence expressing Fyn was inserted and subsequently mutated generating the Fyn expression system (Mulhern et al., 1997). The plasmid was subsequently transformed into competent *E.Coli* (see chapter 2). Bacteria were grown in a M9 minimal medium (see appendix I) containing $^{15}NH_4Cl$ as the only source of nitrogen. Gene expression was induced by the addition of 0.1mM IPTG. Four hours after induction, cells were harvested at 4°C by centrifugation at 10000g. Cells were resuspended in TTBS containing 2mM PMSF, at an approximate ratio of 10ml/g of cells, and lysed by French Press. Cell debris was removed by centrifugation at 20000g for 30 min at 4°C, and the supernatant applied directly to a pTyr agarose column, pre-equilibrated with TTBS. After an extensive wash with first TTBS and then TBS, Fyn SH2 domain was eluted with TBS containing 1.15M NaCl. The eluted protein was concentrated with a Centriprep device (Amicon), then desalted using a PD10 column that had been previously pre-equilibrated with NMR buffer (see appendix). Fractions containing the protein were pooled and concentrated to 0.5ml using a Centricon devise (Amicon). The final solution (approximately 250-600μM) was made up to 10% D_2O and transferred a Shigemi NMR tube.

NMR Spectroscopy

The final 500 μl NMR sample of ^{15}N labelled Fyn SH2 domain in NMR buffer (see appendix I) had a concentration of 250 μM. All experiments were conducted in 5 mm Shigemi tubes and preformed at 20°C on a Bruker 600 MHz spectrometer.

Experiments consisted of 32 scans, with scan width in the ^{1}H dimension being 13.0 ppm and in the ^{15}N 41.1 ppm. Suppression of the water signal was achieved using the pulsed-field gradient-based WATERGATE method.

Chemical Shift Mapping by (^{1}H, ^{15}N)-HSQC NMR

The ^{15}N labelled protein (250μM) was complexed with 2 molar equivalents of pDS4 and HSQC analysis conducted on the sample. For nDS4, 1 molar equivalents of peptide in 10μl of NMR buffer was added incrementally to the labelled protein and the spectra acquired after each addition.

Computational Modelling

The interaction between pTyr and the pTyr-binding pocket was calculated based on the NMR coordinates of Fyn SH2 domain with residues 321-331 of hamster middle T antigen (Mulhern et al, 1997) implemented in the Brookhaven Protein Databank (accession code 1AOU). A model of the interaction was then generated Insight (Molecular Simulation Inc.), and subsequently manipulated to produce a model of the nTyr/pTyr-binding pocket interaction.

RESULTS

HSQC Analysis of Peptide Binding To ^{15}N labelled SH2 Domain

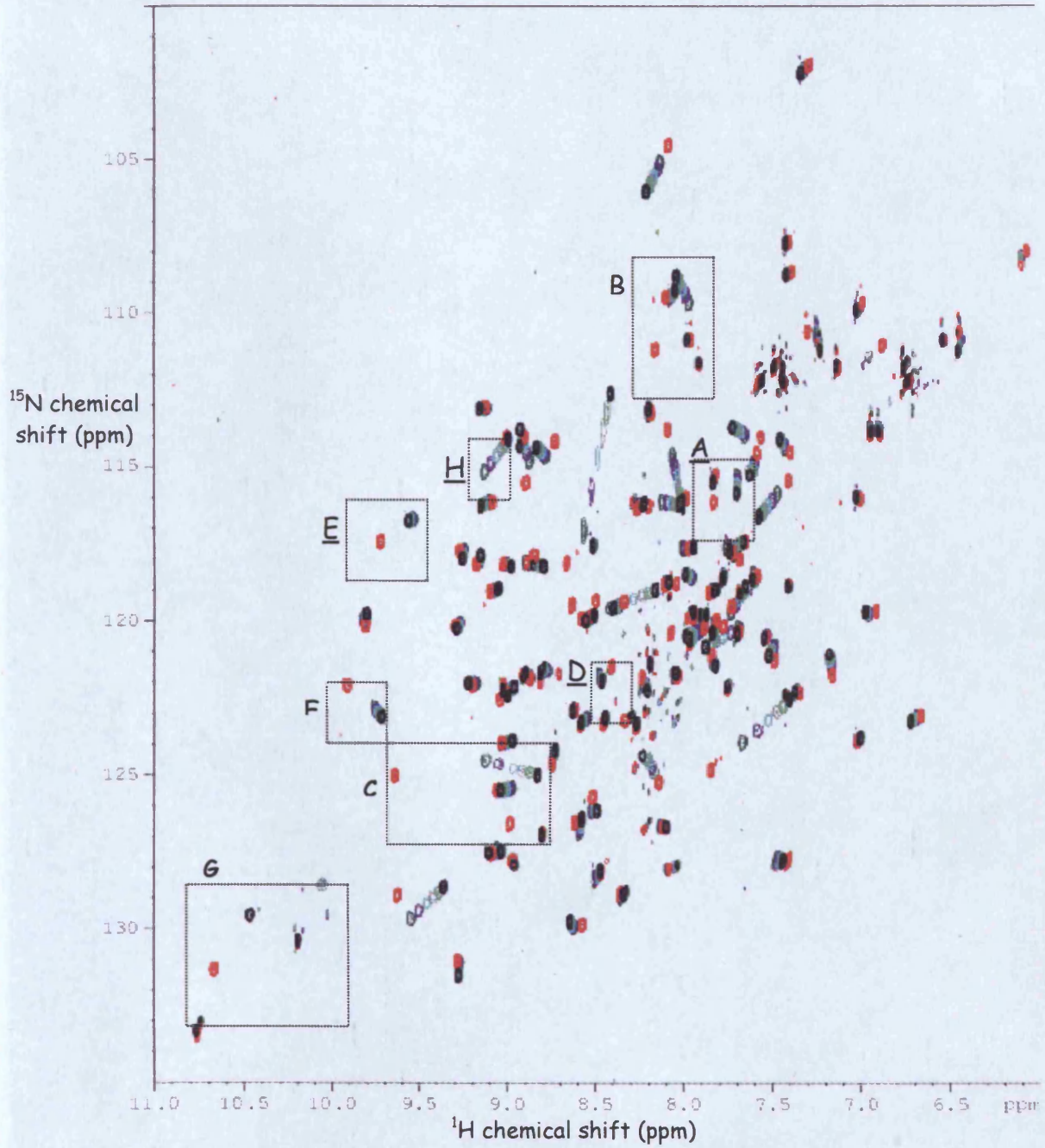

Figure 4.2. The ^{15}N-^{1}H HSQC contour maps of Fyn SH2 domain in the presence of pDS4, and various concentrations of nDS4. HSQC analysis was conducted on labelled protein (250μM) in the absence of peptide (black), in the presence 2 molar equivalents of pDS4 (red), and increasing concentrations of nDS4. The black boxes highlight the residues analysed in subsequent figures. Side chain amide peaks were not assigned.

The consequences of peptide binding to Fyn SH2 domain were investigated by comparing the HN backbone chemical shifts of the ^{15}N labelled protein before and after binding. The assignments for labelled SH2 domain in the free form and phosphopeptide-bound forms were kindly provided by I Campbell (University of Oxford), however, the cross peaks were reassigned to take into account the temperature differences at which the two experiments were conducted: 20°C in the original assignment process, 25°C in the subsequent experiments. The majority of cross peaks were assigned using this procedure, but those peaks whose identification remained ambiguous were left unassigned. A table of the new chemical shifts can be found in the appendix. The chemical shift map of labelled protein in the presence of pDS4 and nDS4 is shown in Figure 4.2.

Figure 4.3 shows the effects of peptide binding on the protein backbone chemical shifts. The values presented were calculated using the following equation, which takes into account both shifts in the ^{1}H and ^{15}N dimensions, as well as the gyromagnetic ratio of ^{15}N being approximately ten times that of ^{1}H.

Equation 4.1 Determination of Chemical Shift Change in ^{1}H-^{15}N HSQC.

$$\sqrt{\delta H^2 + \left[\frac{\delta N}{10}\right]^2}$$

Qualitatively, the binding of the two peptides are similar, in so much as, the residue the affect are largely the same, as the competition study in chapter 3 would suggest (Figure 3.13). The nitropeptide's relatively low affinity for the SH2 domain did not prevent significant perturbations of backbone shifts on binding. In general, however, binding of the phosphopeptide to the SH2 domain produced slightly larger shifts than those produceded by the nitropeptide (Figures 4.3, 4.4, see appendix II). This trend cannot be ascribed to non-saturation of the SH2 receptor as previous experiments had shown a 5 molar excess of peptide over protein (250 μM), to be sufficient for 100% occupancy (see chapter 3). These findings may be interpreted as the two peptides binding differently to the SH2 protein (Medek et al., 2000), however, the observed changes, as well as the quantitative differences in affinity of the two peptides, might simply be due to the differences in the magnetic anisotropy of nitro compared to

phosphotyrosine, whilst the mode of binding of these two peptides might be very similar. The in the chemical shift patterns on binding of the two peptides can only be attributed to the orthogonal orientation of the nitro group in relation to the phosphate on nTyr and pTyr, respectively; and the respective lengths of the two moieties. So along with differences in the ring shift currents, the direct interactions formed by the two modified residues may have resulted in the different shift patterns seen on the binding of the two peptides. The general difference in the backbone shifts observed on the binding of each the peptides is illustrated by the residues that form the pTyr-binding pocket, where the magnitude of the backbone shifts on the binding of nDS4 were 50%, or less, of those induced on pDS4 binding.

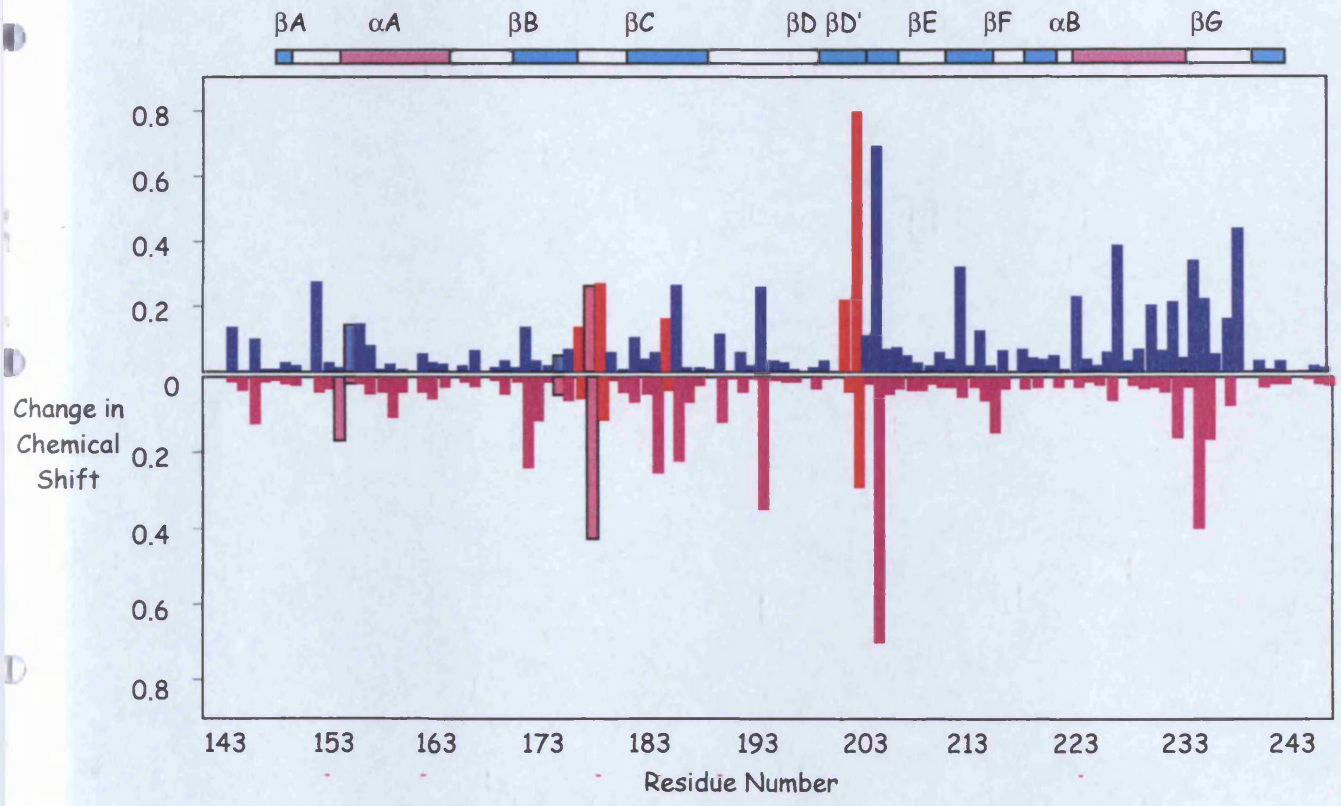

Figure 4.3. Chemical shift change on binding of derivatives of DS4 to ^{15}N labelled SH2 domain. The binding of 2 molar equivalents of pDS4 is shown (blue, pointing up) and 5 molar equivalents of nDS4 (burgundy, pointing down). Unassigned resonances are not indicated. The red bars indicate those residues that make up the pTyr-binding pocket, that are visible on the chemical shift scale. Those residues that are hashed with a black border are studied in more detail (Figure 4.4), along with binding pocket residues. Secondary structural elements are indicated above the plot: α helices in pink, β sheets in blue.

The βB, C, and D sheets, the BC loop, along with the αB helix showed the largest regional changes in chemical shift on peptide binding (Figure 4.3). The aforementioned β sheets form part of the spine of the SH2 domain (Kuriyan and Crowburn, 1997), and contain residues that make up the pTyr-binding pocket. The αB helix, as well as the BG loop structures also shows sizeable shifts. These regions possess the residues that interact with the side-chains of the amino acids C-terminal to phosophotyrosine in the peptide (Kuriyan and Crowburn, 1997), therefore, the shifts observed in these segments of the protein would have emanated from direct contact of the peptide with SH2 protein.

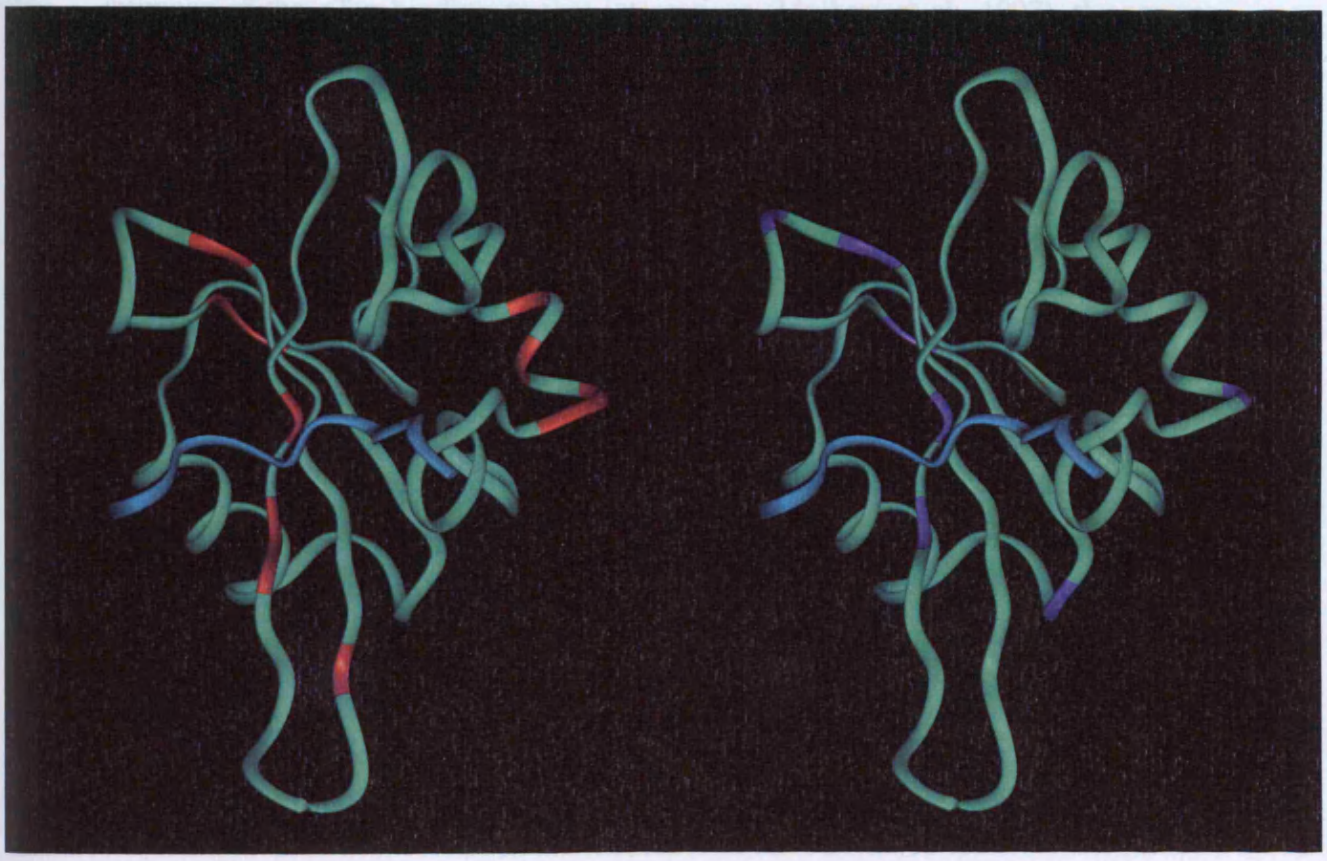

Figure 4.4. The regional chemical shift changes observed on binding of derivatives of DS4 to ^{15}N labelled SH2 domain. The residues that showed ^{1}H-^{15}N chemical shift changes of greater than 0.2 on peptide (turquoise) binding were mapped onto the C-C SH2 domain backbone (green). The red bands indicate those changes that occurred on the nitropeptide binding and mauve those that occur on phosphopeptide binding.

All the residues that make up pTyr-binding pocket were identified on the chemical shift map, with the exception of His 202. Figure 4.5 shows the expanded regions of backbone shifts of residues that make up the binding pocket, as well as residues that are located within the vicinity of the cavity. Of the five identified pTyr-binding pocket chemical shifts, only the resonance of tyrosine 203 shifted in the same direction on binding of both peptides, although the magnitude of the shift at the highest concentration of nDS4 was approximately half of that produced on pDS4's binding. This suggesting that, either through direct or indirect contacts, nTyr induces similar directional changes to the backbones of tyrosine 203 as pTyr. The remaining four identified backbone shifts show directional differences on nDS4 binding compared pDS4. For Thr 180 and Lys 204 the difference in direction was small, in comparison with Ser 178 and 186, where the effects were marked. Based on knowledge of the intimacy of the pTyr-binding pocket interactions (Mulhern et al., 1997), the reasons underlying these vectoral differences in chemical shift are likely to be due to the contacts made between the modified tyrosine moieties and these four residues. Also, differences in the ring shift currents generated by the aromatic rings of the two peptides might also account for these directional differences. The inability to identify His 202 on the chemical shift map precluded conclusions from being drawn the effect of peptide binding on this residue's chemical shift.

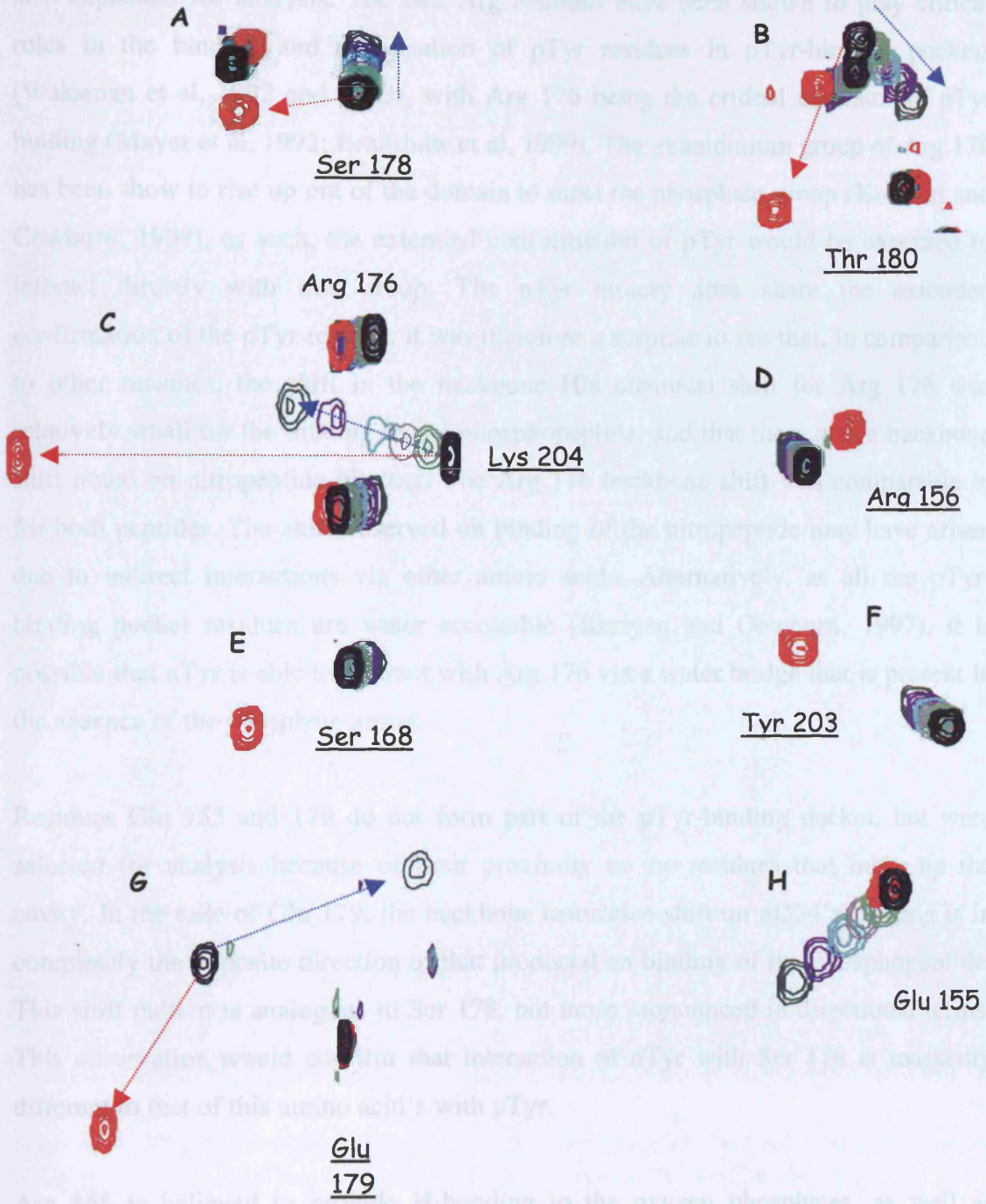

Figure 4.5. The ^{15}N-^{1}H HSQC peak shifts of the pTyr binding pocket and related residues. The labelled SH2 protein is shown the absence of peptide (black), and in the presence of 2 molar equivalents pDS4 (red). Nitrated DS4 at 0.25 (light green), 0.5 (grey), 1 (Turquoise), 2 (purple) and 5 molar equivalents (dark green) of protein was titrated against labelled SH2 domain. Red arrows indicate the direction of pDS4 shift, blue the nDS4 shift. The residues that form the pTyr-binding pocket are underlined.

The shift map regions containing Arg 156 and 176, along with Glu 179 and 155 where also expanded for analysis. The two Arg residues have been shown to play critical roles in the binding and stabilisation of pTyr residues in pTyr-binding pockets (Waksman et al, 1992 and 1993), with Arg 176 being the critical mediator of pTyr binding (Mayer et al, 1992; Bradshaw et al, 1999). The guanidinium group of Arg 176 has been show to rise up out of the domain to meet the phosphate group (Kuriyan and Cowburn, 1997), as such, the extended conformation of pTyr would be expected to interact directly with this group. The nTyr moiety does share the extended confirmation of the pTyr residue, it was therefore a surprise to see that, in comparison to other residues, the shift in the backbone HN chemical shift for Arg 176 was relatively small for the binding of the phosphopeptide, and that there was a backbone shift noted on nitropeptide binding. The Arg 176 backbone shift was comparable in for both peptides. The shift observed on binding of the nitropeptide may have arisen due to indirect interactions via other amino acids. Alternatively, as all the pTyr-binding pocket residues are water accessible (Kuriyan and Cowburn, 1997), it is possible that nTyr is able to interact with Arg 176 via a water bridge that is present in the absence of the phosphate group.

Residues Glu 155 and 179 do not form part of the pTyr-binding pocket, but were selected for analysis because of their proximity to the residues that make-up the cavity. In the case of Glu 179, the backbone resonance shift on nDS4's binding is in completely the opposite direction to that produced on binding of the phosphopeptide. This shift pattern is analogous to Ser 178, but more pronounced in directional terms. This observation would confirm that interaction of nTyr with Ser 178 is markedly different to that of this amino acid's with pTyr.

Arg 156 is believed to provide H-bonding to the oxygen phosphates, as well as stabilising the orientation of the aromatic ring of Tyr through guanidino interactions (Waksman et al, 1992 and 1993). On binding of the phosphopeptide to the SH2 domain there is a slight shift in the backbone resonance. A shift comparable in size was produced on binding of nDS4, although the direction is different to that produced on pDS4 binding. Unlike most of the resonances found on the HSQC map, Glu 155 exhibits minimal shift on the binding of pDS4, whilst there is significant movement

on binding of nDS4. This finding might have arisen due to the direct contact being made with this residue and nTyr, or the indirect interaction of with via other amino acids, possibly Arg 156.

Computational Modelling Analysis of Peptide SH2 Domain Interaction

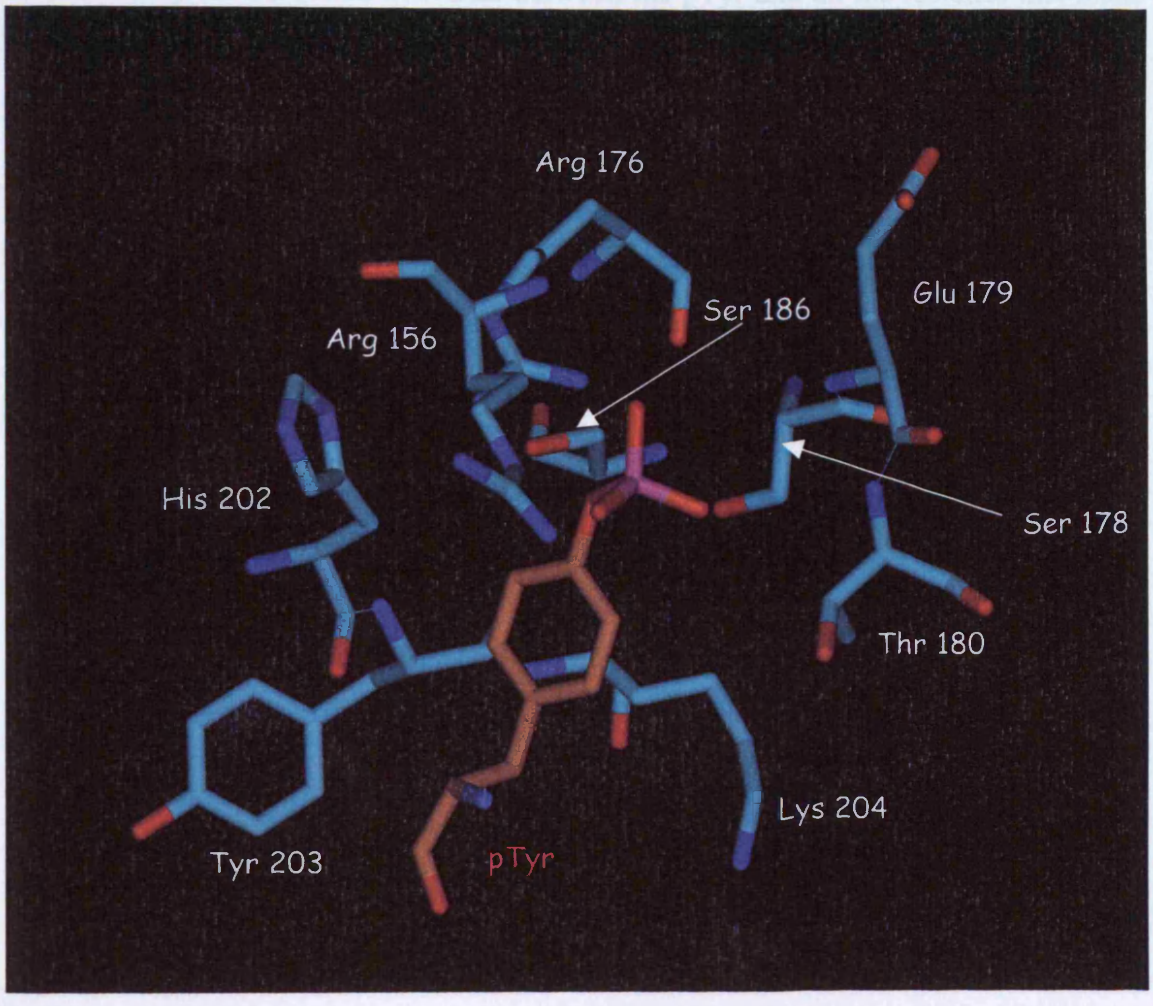

Figure 4.6. The pTyr-SH2 domain interaction. Residues of the SH2 domain that form the pTyr binding pocket are indicated (light blue) along with the pTyr residue.

Although information on the location of a ligand binding site can be deduced by HSQC, this technique provides no topological information on receptor/ligand interactions. The solution structure of Fyn bound to an extended equivalent of pDS4 had been previously determined, enabling a model to be built and the topology of the modified Tyr residues to be explored. 4.5 shows a model of the residues that make up

the phosphotyrosine binding pocket of Fyn SH2 domain, with an intact phosphotyrosine residue. This molecular picture was built using the coordinates obtained from the Brookhaven Protein Database (Acession number 1AOU), and from the information of the published NMR structure (Mulhern et al, 1997). The sides of the pTyr binding pocket are made up of 6 residues: Ser 178, Thr 180, Ser 186, His 202, Tyr 203 and Lys 204. In the NMR structure, the intimacy of the pTyr fit was illustrated by the detection of NOEs between the pTyr and all the residues that make up the pocket, with the exception of Ser 178. Additionally, the guandinium group of Arg 176, situated at the base of the pTyr pocket, was shown to form salt bridges with the phosphate group of the pTyr in the NMR structure, although no NOEs were detected (Mulhern et al, 1997). The binding of pTyr residues to the SH2 domain is mediated, primarily, through a series of hydrogen bonds to the negatively charged phosphate group, with the bidentate interaction between the guanidium group of Arg βB5 (Arg 176 of Fyn) with the phosphate oxygens being the critical mediator (Figure 1.13; Mayer et al, 1992; Bradshaw et al, 1999). A network of hydrogen bonds was formed between the phosphate moiety and a number of residues found in the binding pocket (Table 4.1). The critical interaction between the guanidium group of Arg 176 and the phosphate oxygens was detected. Also, although this interaction was poorly defined in the NMR structure, two hydrogen bonds were formed between Arg 156 and the phosphate group.

Table 4.1. Proposed hydrogen bonds form between pTyr-binding pocket and the nitro and phosophotyrosine residues established from the computer model

Binding Pocket Residue	N/O-H Distance/ Angstroms	
	pTyr	nTyr
Ser 186	4.01	1.73 (backbone)
Thr 180	3.15 (backbone)	
Ser 178		
His 202		
Tyr 203		
Lys 204		
Arg 156	2.24, 3.82	
Arg 176	3.40, 3.45	2.26, 2.27

Tyr residues are capable of rotating about the carbon-carbon that links the aromatic ring to the aliphatic part of the residue (see figure 4.6). The meta and ortho nuclei of a free rotating ring system in a biological complex are equivalent, as each species in the 2', 6' (and 3', 5' postions) encounter the same chemical environment on ring rotation. However, if the rotation of the aromatic ring is fixed or restricted, the nuclei in the meta and ortho positions are likely to be non-equivalent, due to the asymmetric nature of the environment in which the ring is likely to be found (Roberts, 1993). In the case of SH2 domains, the aromatic ring of pTyr is anchored by two interactions. Firstly, the delocalised π electrons of the ring system can interact the carbon side chain of a Lys residue in the βD structure (Lys 204 of Fyn) via van der Waals forces. Secondly, the amino groups of the βD Lys and the αA Arg (residue 156 in Fyn) form amino aromatic interactions, which are akin to hydrogen bonds (Burley and Petsko, 1988; Waksman et al, 1992; Figure 1.13). Once the pTyr moiety has inserted into the binding cavity the ring is stabilised by these interactions, although limited rotation is still possible. Owing to this effect, the ortho and meta protons likely to be non-

equivalent due to the asymmetric nature of the cavity. In the case of the nTyr moiety, the anisotropic effects of the ortho nitro group is likely to be more pronounced, due to the size of the moiety and the charge it carries. The model suggests the orthogonal orientation of the nitro group would limit the rotation of this residue within the binding pocket, therefore, he orientation adopted by the nTyr moiety in the binding pocket must be determined prior to its entrance into the cavity. Surprisingly, interactions were visualised between Arg 176 and the nTyr species. However, the number of theoretical hydrogen bonds formed between the nTyr moiety and the pTyr-binding pocket residues was limited (Table 4.1).

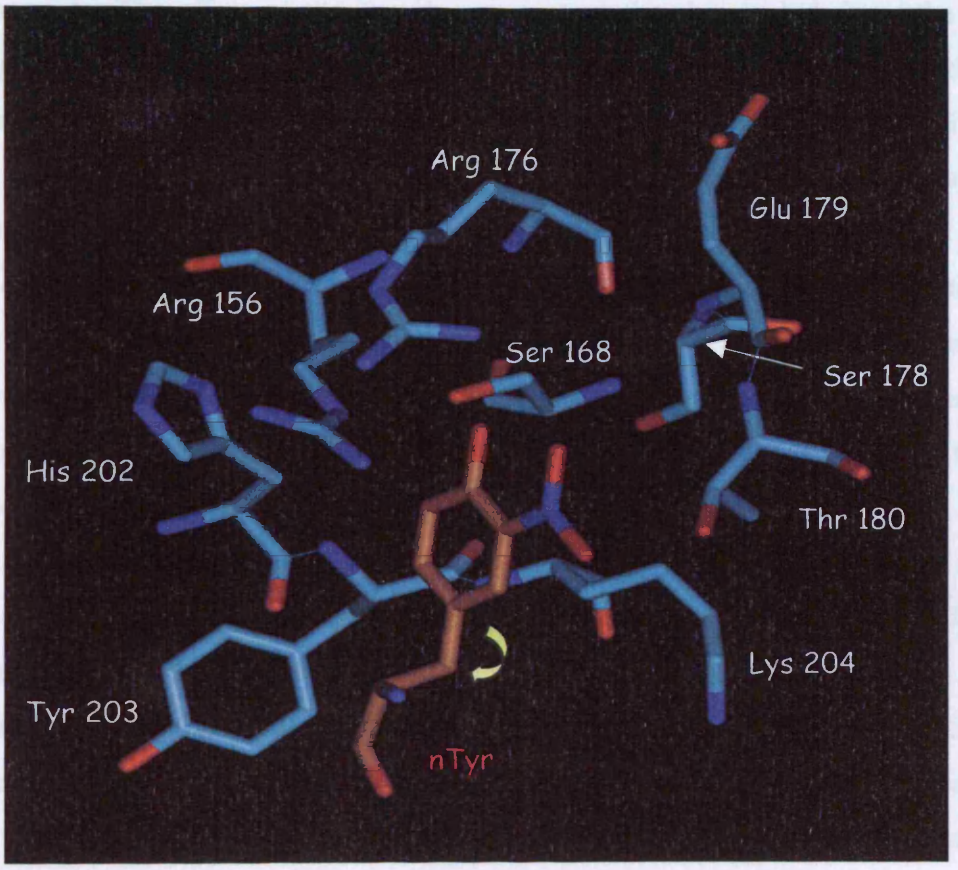

Figure 4.7. The nTyr-SH2 domain interaction. The two possible orientations of nTyr are shown. The nTyr (brown) moiety was fitted into the pTyr-binding pocket (blue). Rotation about which the nitrophenol moiety can occur is also indicated (yellow arrow).

Discussion

The data presented in this chapter provide evidence of differences in the pTyr-binding pocket backbone chemical shifts, and the protein backbone resonances in general, on the binding of pDS4 and nDS4 to the SH2 domain. These differences were visualised by HSQC NMR and the topology of the interactions between the tyrosine residues of the peptides and the amino acids of the pTyr-binding pocket rationalised using computer modelling. It is difficult to extrapolate the backbone chemical shifts to structural information, due to the number factors (hydrogen-bonding, ring current shift and dihedral angles) that influence chemical shift changes. In spite of this, one can conclude that the differences in the binding pocket chemical shifts observed on the interaction of the two peptides are due to the protons being in different chemical environments. The effect of the Tyr ring-current on the chemical shifts of the pTyr-binding pocket side chain protons is likely to be marked, along with those backbone NH resonances (Tyr 203, Lys 204) likely to be influenced by this magnetic field. With this in mind, the highly electronegative nitro group would be expected to reduce the Tyr ring-current effect in comparison to the phosphate group of pTyr. This effect might explain why the total chemical shift for all residues that form the pTyr-binding pocket were reduced on binding of nDS4 in comparison to pDS4. However, the differences in the direction of the backbone chemical shifts also suggest the peptides bind to the SH2 protein in slightly different manners, which might also account for the reduced chemical shifts.

Of the residues forming the pTyr-binding pocket that were identified on the HSQC spectra, Ser 178 and 186, Thr 180, and Lys 204 showed directional differences in the resonance shifts on peptide binding, whilst Tyr 203 showed no vectoral change (Figure 4.4). Tyr 203, a highly conserved residue in SH2 domain structures, plays no role in anchoring the pTyr moiety, but interacts with the Glu immediately C-terminal (+1) to the pTyr residue in the peptide (Waksman et al, 1993). The shift observed for this residue was likely to have resulted from its interaction with the Glu immediately C-terminal to the pTyr residue, the difference in affinity of the respective peptides accounting for extent of the backbone shift.

The Ser in the βC3 (residue 186) position of SH2 domains is situated at the base of the binding cavity, where it forms a hydrogen bond with Nε of ArgβB5 (Waksman et al, 1992). In addition, this Ser residue has been shown to interact with the phosphate oxygen of pTyr residues bound in the pTyr-binding cavity (Mulhern et al., 1997; Rahuel et al., 1998). The proximity of the nTyr residue to Ser 186 in the static model suggests interaction between the nTyr residue and the amino acid might be made. The observed difference in the direction of the chemical shift of Ser 168 on nDS4 binding might therefore be due to indirect interactions via the polypeptide backbone or water/salt bridge formation between the residue and the nTyr moiety.

Interestingly, from our computer model, Arg 176 forms 2 H-bonds with the para oxygen of the nTyr residue (the assumption being that this residue is in its non-protonated state). The bidentate ion-pair interaction of the phosphate group and Arg 176 is critical for phosphopeptide/SH2 domain binding, yet, in the case of the nTyr moiety, the formation of two hydrogen bonds with this residue mediated weak peptide binding. Three H-bonds are believed to be formed between the guanidinium group of Arg 176 and the phosphate group (Figure 1.13; Waksman et al., 1993), whilst only two are postulated as being formed with the nTyr. Additionally, the distance between the two phosphate oxygens and the two guanidinium amino groups may be similarly spaced to facilitate the formation colinear hydrogen bonds, which is unlikely to occur with the nTyr moiety. Despite these differences, the effect on the backbone chemical shift of Arg 176 was the same on the binding of both peptides, suggesting this resonance is unaffected by the ring currents of the two modified Tyr residues.

The chemical shift changes in the remaining three pTyr-binding residues can be attributed to their direct interaction with the nTyr moiety and the varied ring shift currents: Lys 204, by virtue its amino-aromatic and van der Waals interactions; Ser 178 because of it interaction with the hydroxyl and nitro oxygens; and Thr 180 due to its interaction with the nitro oxygen and the amino group of Lys 204. The amino-aromatic interaction, as well as the loss of the phosphate-guanidium interaction between Arg 156 and the modified Tyr residues, would account for the changes observed in the backbone chemical shifts on the binding of the two peptides to the protein.

In theory nTyr could have adopted two general orientations within the binding pocket due the rotation about the C_β-aromatic bond (Figure 4.7). The orientation adopted by the nTyr group in the binding pocket is likely be determined prior to its entering the binding pocket, as our model suggests, rotation within the pocket would be limited by steric factors. However, the intrinsic flexibility of the protein might enable rotation to occur in the pTyr pocket. Assuming protein flexibility did not permit rotation to occur in the pTyr cavity, the computer model suggests the orientation shown in figure 4.7 to be the adopted orientation than one in which the ring had 'flipped' by 180°, as the nitro moiety would be sterically hindered by Arg 156 in this orientation.

When rationalising the relative lack of affinity of the nitropeptide for the SH2 compared to the phosphopeptide, as well as looking at the interactions made by the nTyr moiety in the pTyr-binding pocket, other factors such as desolvation, and the charge carried by the nTyr and pTyr moieties respectively must be considered. The tyrosine species must undergo desolvation prior to its entry into the binding pocket (Kuriyan and Cowburn, 1997). It is unlikely that the extent to which nTyr and pTyr desolvate varies markedly, but the relative charge of the two species will differ. The approximate pKa of pTyr is 5.7, as such at physiological pH, phosphotyrosine carries a charge of –2. The hydroxyl group of nTyr has a pKa of ~7.5, consequently, at physiological pH this species will exist in approximately equal proportions of both its protonated and non-protonated forms. In addition, the protonated nTyr moieties are likely to form an intra molecular hydrogen bond with the protonated hydroxyl group (Figure 2.16), further reducing the availability of hydrogen bond formation and the peptides ability to bind to the SH2 protein, although, even in this state the nitro group will still possess a partial negative charge.

SH2 domains have evolved to recognise and intricately bind pTyr and not nTyr residues (but the inflammatory response is an ancient physiological mechanism; have SH2 domains also evolved the recognise the nTyr residues, whose presence in cells is as old as inflammation itself, in addition to pTyr?). The positioning of basic amino acids within the cationic cavity is crucial in specifying the recognition of pTyr. The development of highly affinity phosphopeptide mimetics as potential therapeutic

agents has focused on molecules based on the existing pTyr residue, or ortho-substituents of the residue (Gao et al., 2000; Sawyer, 1998). However, bi-ortho substitutions (with nitro groups, interestingly) have been shown to have high affinity interactions with the SH2 domain of Src (Anon, 1998). From our studies, mono-nitration of Tyr in the ortho position did not confer binding affinity comparable to that of pTyr, for Fyn. This was due to the number and nature of the interactions formed between the nTyr and the pTyr-binding pocket amino acids, in addition to steric factors.

One of the interesting aspects of the data presented in this chapter was the effect of the peptide binding on the global changes in chemical shift (Figure 4.3). Although the chemical shift changes show regional trends for both peptides, the nitro substitution in the ortho position of Tyr, and the removal of the phosphate group had a pronounced effect on the chemical shift profiles. The binding of two high affinity peptides to Fyn produced similar disparities in the chemical shift map (Pintar et al., 1996), yet both of the phosphpeptides are biologically active in their ability to localise the SH2 containing protein. Based on the chemical shift profile induced by nDS4, could the interaction of this peptide to Fyn SH2 domain have a similar biological outcome to phosphopeptide? The answer to this question is no, simply because it is the affinity of the peptide for the SH2 protein that governs biological effect. Changes in the backbone chemical shifts were not an indicator of a peptide's affinity for SH2 proteins, so in instances where binding alone is the prerequisite for biological effect, chemical shift maps produced on nitropeptide binding could not be used to predict biological outcome. It has been speculated that binding of pTyr to SH2 domains may alter the biological activity of enzymes through allosteric mechanisms, although this tends to occur in proteins containing tandem SH2 domains (Eck et al., 1996; Ottinger et al., 1998). Again in this instance HSQC changes could not be used a surrogate indicator of biological activity, as the link between individual, or regional protein chemical shift changes on peptide binding is qualitative and cannot define any induced conformational changes. The allosteric alteration in enzyme activity is likely to occur because of the spatial changes on binding of tandem SH2 domains and not conformational changes within the individual domains. HSQC mapping can be useful in determining K_d measurement of fast exchanging ligands, and in the determination of the location of the ligand's binding sites and orientation within the cavity (Medek

et al., 2000), but this technique provides no quantitative information on the changes in a protein's conformational changes on ligand binding.

In summary, nDS4 induced significant backbone chemical shifts on binding to the SH2 domain. Change in backbone chemical shifts on binding of nitropeptides to SH2 domains is not, therefore an indication of the peptides' affinity for the protein. There was no general pattern to the shifts observed on the binding of both nDS4 and pDS4, as residues not involved on binding also showed significant shifts. The hydrogen bonding formed between the nTyr moiety and pTyr-binding pocket residues was limited, however, hydrogen-bonding was postulated as occurring between the ortho oxygen and the the guanidinium group of Arg 176. As previously stated, others have used indirect methods to establish that nitropeptides bind to the SH2 domain of Lyn (Mallozzi et al, 2001). The solution or crystal structure of Lyn complexed to a high affinity phospopeptide is not to my knowledge available, so modelling comparisons to Fyn and Lyn cannot be made. The model presented suggests that DS4 is capable of forming limited hydrogen bonds with the residues with the residues that make-up the pTyr-binding pocket, including the invariant Arg situated at the base of cavity. However this interaction is not the bi-dentate ion-pair that mediates the high affinity association of phosphopeptides for SH2 domains.

CHAPTER 5:

DERMINATION OF THE BINDING OF DS4 DERIVATIVES TO T-CELL DERIVED FYN

INTRODUCTION

In chapters 3 and 4 it was shown that the association between the SH2 domain of Fyn derived from *E.coli* and nDS4 was of the same order of magnitude as that for DS4 and therefore much less than for pDS4. In order to explore this further a study of the binding of peptides to T-cell derived Fyn was undertaken. To achieve this, the ability of derivatives of DS4 to displace a protein bound to the SH2 domain of Fyn derived from a T-cell line was determined.

The T-cell transmembrane TCR/CD3 receptor (Figure 5.1) recognises MHC/peptide complexes on antigen presenting cells, such as macrophages. On engaging an antigen-presenting cell, the TCR/CD3 receptor initiates a series of intracellular signalling cascades within T-cells, the first step in which is the activation of the protein tyrosine kinases (PTKs) Fyn and Lck. The transmembrane phosphatase CD45 is believed to be responsible for activating these enzymes by removing a phosphate residue found on a tyrosine residue in the C-terminal tail of these proteins (see chapter 1). Subsequently, the activated PTKs are responsible for phosphorylating specific motifs in the CD3 accessory molecules (ITAMs, immunoreceptor tyrosine based activation motifs), in addition to phosphorylating members of the Syk tyrosine kinase family, including ZAP-70, which in turn bind to the phosphorylated ITAM sequences. ZAP-70 is responsible for phosphorylating the adaptor proteins LAT and SL7-76, which in addition to possessing phosphoamino acid recognition sites also possess a number of modular protein domains. The early events in T-cell signalling are characterised by the formation of multimeric protein complexes; adaptor proteins provide the matrix on which these complexes are formed, bringing substrates into the proximity of kinases, as well as localising other key proteins to the cell membrane (see Clements et al., 1999; Tomlinson et al., 2000). The formation of these proteins complexes is key in triggering downstream signalling cascades such as the Ras/MAPK and PLC/Ca^{2+} pathways, which ultimately lead to T-cell activation and differentiation (Figure 5.1; Clements et al., 1999; Kuby, 1994).

One such adaptor protein is the Fyn binding protein Fyb/SLAP-130 (Fyb). Initially identified in 1992 (da Silva et al., 1992), this protein contains 16 potential phosphorylation sites, an SH3-like domain as well as a binding motif for this domain,

in addition to a nuclear location motif (Clements et al., 1999; da Silva et al., 1997). Fyb is a hemopoietic cell-specfic adaptor protein (da Silva et al., 1997; Musci et al., 1997), which has been shown to play key roles in mast cell adhesion and mediator release (Geng et al, 2001), and in the cytoskeletal reorganisation that occurs on T-cell stimulation (Krausse et al., 2000). However, the role that Fyb plays in the integration of T-cell signalling is not entirely clear. Cell adhesion, cytoskeletal reorganisation and mediator release are not expedited through MAPK or calcium-dependent pathways (Peterson et al., 2001). Furthermore, it has been demonstrated that phosphorylated Fyb binds to SLP-76 and is believed to impede the latter's function, as demonstrated in the abrogation of the activation of the transcription factor NF-AT, suggesting Fyb is a negative regulator of T-cell signalling. Conversely, overexpression of Fyb has been shown to increase the production of IL-2, a cytokine responsible for the clonal expansion of T-cells (Clements et al., 1999). Although there are uncertainties as to the role Fyb plays in T-cells, the *in vivo* association between phosphorylayed Fyb and the SH2 domain of Fyn has been well documented (da Silva et al., 1992, 1993 and 1997). Based on this knowledge, the ability of derivatives of DS4 to displace Fyb from the SH2 domain of Fyn was investigated.

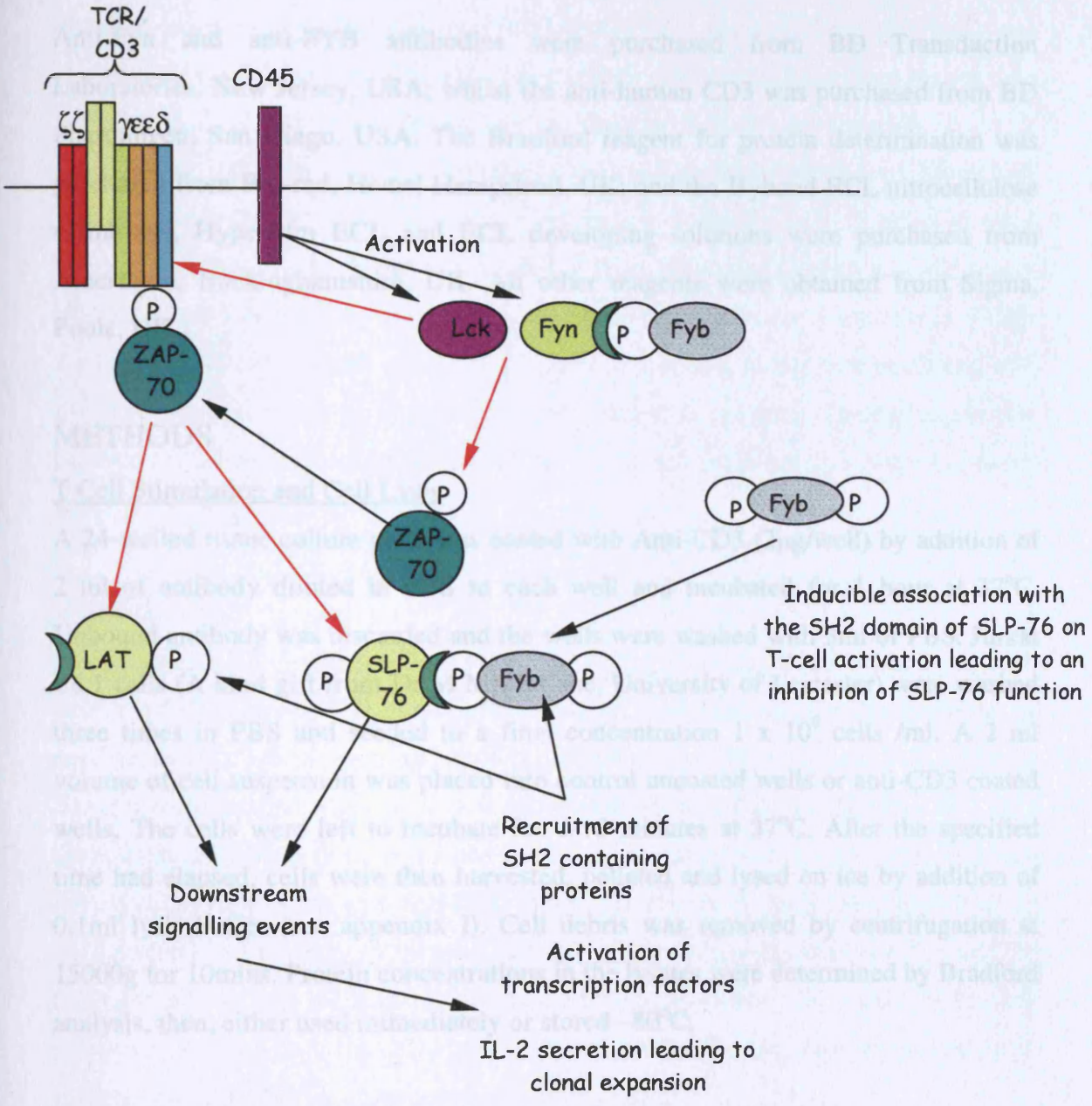

Figure 5.1. The known role of Fyb in T-cell signalling. On binding of the MHC/Peptide complex to the TCR/CD3 complex, the tyrosine kinases Fyn and Lck are activated by the phosphatase activity of the CD45. The tyrosine kinases in turn phosphorylate the tyrosine kinase from the Syk family, ZAP-70, and specific sequences on the CD3 domain, as signified by the red arrows. The phosphorylated ZAP-70 kinase is recruited and binds to the phosphorylated CD3, where it subsequently phosphorylates and activates the adaptor protein SLP-76. This protein has been shown to play a key role in coupling TCR/CD3 activation to downstream signalling events that result in T-cell division and differentiation. In both resting and activated T-cells Fyb is associated to the SH2 domain of Fyn. The protein has also been speculated as being a negative regulator of T-cell signalling by binding to SLP-76.

EXPERIMENATAL PROCEDURES

MATERIALS

Anti-Fyn and anti-FYB antibodies were purchased from BD Transduction Laboratories, New Jersey, USA; whilst the anti-human CD3 was purchased from BD Pharmingen, San Diego, USA. The Bradford reagent for protein determination was purchased from Bio-rad, Hemel Hempstead, UK; and the Hybond ECL nitrocellulose membrane, Hyperfilm ECL and ECL developing solutions were purchased from Amersham, Buckinghamshire, UK. All other reagents were obtained from Sigma, Poole, UK.

METHODS

T Cell Stimulation and Cell Lysis

A 24-welled tissue culture plate was coated with Anti-CD3 (2μg/well) by addition of 2 ml of antibody diluted in PBS to each well and incubated for 1 hour at 37°C. Unbound antibody was discarded and the wells were washed with 3ml of PBS. Jurkat E6.1 cells (A kind gift from Dr M Macfarlane, University of Leicester) were washed three times in PBS and seeded to a final concentration 1 x 10^6 cells /ml. A 2 ml volume of cell suspension was placed into control uncoated wells or anti-CD3 coated wells. The cells were left to incubate for 0-10 minutes at 37°C. After the specified time had elapsed, cells were then harvested, pelleted and lysed on ice by addition of 0.1ml lysis buffer (see appendix I). Cell debris was removed by centrifugation at 15000g for 10mins. Protein concentrations in the lysates were determined by Bradford analysis, then, either used immediately or stored –80°C.

Immunoprecipitation and Western Blot Analysis

A slurry of Protein A-sepherose beads (20μl) was washed twice in cold PBS. A volume of 5μl of antibody was added to the slurry and left mixing for 1 hour at room temperature, prior to being washed twice in cold PBS. A volume of 20 μl of protein A/Ab slurry was added to 400 μg of protein lysate, and left tumbling at 4°C for 3 hours. Immunoprecipitates were collected by centrifugation and washed twice in cold PBS. The pellet was then resuspended in 20 μl of PBS containing various concentrations of peptide and allowed to incubate at 4°C for a further 3 hours. Beads were pelleted and the supernatants removed. Beads were further washed twice in cold

high concentration PBS (350mM NaCl), followed by two additional PBS washes. Sample buffer (40µl) was added to the sample, which was heated at 95°C for 4 minutes, prior to centrifugation at 14000 rpm for 2 minutes. Sample (35 µl) was loaded onto a 7.5 % SDS-PAGE gel and run. Protein was transfered from the gel onto Hybond ECL nitrocellulose membrane in transfer buffer (see appendix I; 30 V overnight or 100 V for 2 hours, both procedures being conducted on ice). Membrane was then incubated in 25ml of blocking buffer (see appendix I) for 2 hours at room temperature. Primary antibody was diluted 1:2000 in blocking buffer and allowed to blot for 2 hours at room temperature, the washed three times for 5 minutes in TTBS. Anti-mouse peroxidase (20 µl) diluted 1:2000 in blocking buffer was incubated with the blot for 2 hours at room temperature, then washed as previous. The membrane was covered with 2 ml ECL solution and left for one minute to develop, wrapped in Saran wrap and exposed to Hyperfilm ECL.

RESULTS

Prior to determining whether the derivatives DS4 were capable of displacing Fyb from the SH2 domain of Fyn the optimal time of T-cell stimulation and the levels of peptide to be used in the displacement studies had to be established. In order to determine the optimal time for T-cell stimulation by anti-CD3 antibodies, cells were stimulated for a fixed time, lysed and immunoprecipitated with an anti-Fyn antibody, prior to immunoblotting with anti-Fyb. Figure 5.2 illustrates the binding of Fyb to the SH2 domain of Fyn over 10 minutes and shows the association between Fyb and the SH2 domain of Fyn, even in non-stimulated cells. Moreover, the extent of binding remained constant over the 10 minutes. Subsequently, T-cells were stimulated for 5 minutes prior to lysis, and immunoprecipitation.

Optimisation of the amount of phosphopeptide required to displace FYB from the SH2 domain of Fyn was achieved by incubating levels of pDS4 ranging from 1 nM to 1 mM with anti-Fyn immunoprecipitates, followed by an anti-FYB blot. At 1 mM levels of pDS4 the binding of FYB to Fyn was completely ameliorated (Figure 5.2 b), whilst micromolar and nanomolar amounts of peptide were incapable of effecting complete displacement Fyb from Fyn SH2. Based on the findings of this experiment,

1 mM of peptide was used to determine the ability of the different derivatives of DS4 to disrupt the binding of the adaptor protein to the SH2 domain.

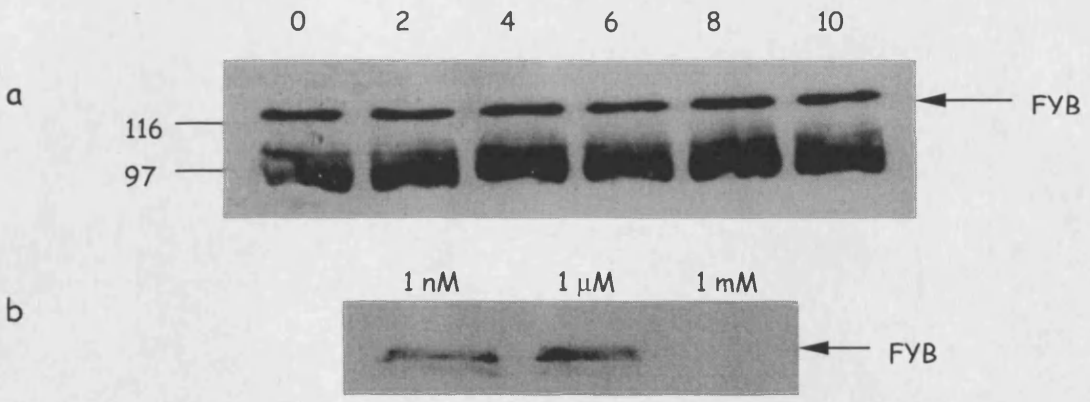

Figure 5.2. The dependency of FYB/Fyn interaction on time of jurkat stimulation by anti-CD3 and pDS4 concentration. (a) Jurkat cells were stimulated for the times indicated above the bands. Time 0 controls were non-stimulated cells. Lysates of these cells were then immunoprecipitated with anti-Fyn antibody and analysed with an anti-FYB antibody. (b) After immunoprecipitation of Jurkat cells stimulated for 5 minutes, lysates with anti-Fyn antibody, immunoprecipitates were incubated with varying concentrations of pDS4 and analysed with an anti-FYB antibody.

Having established the conditions in which pDS4 could displace FYB from the SH2 domain of Fyn the same conditions were applied to determine the effect of the nitropeptide on FYB binding to the SH2 domain of Fyn. Figure 5.3 shows the results of these experiments. As expected, and as previously demonstrated (Figure 5.2 b), after incubation of 1 mM pDS4 with anti-Fyn immunoprecipitates no FYB remained bound to the SH2 domain, whilst the nitropeptide along with the non-modified peptide failed to displace FYB from Fyn SH2 domain (Figure 5.3), consistent with findings of chapter 3, as corroborated in chapter 4.

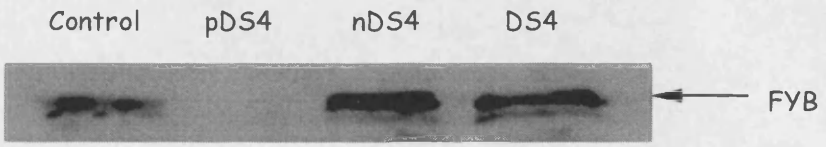

Figure 5.3. The effect of derivatives of DS4 on the FYB/Fyn SH2 domain interaction. After immunoprecipitation of stimulated Jurkat cells with an anti-Fyn antibody, cell lysates were incubated 1 mM of peptide and blotted with an anti-FYB antibody. Control lanes contained PBS only.

DISCUSSION

Although the role Fyb plays in T-cells has not been fully defined, it is known that this adaptor protein binds to the SH2 domain of Fyn when phosphorylated. To determine the extent to which the derivatives of DS4 bind to the SH2 domain of T-cell derived Fyn, the ability of the peptides to displace Fyb from Fyn was investigated. The weak binding of nDS4 to the SH2 domain, as determined in chapter 3, was corroborated in nitropeptide's inability to displace Fyb from Fyn. By contrast, and as expected, an equal concentration of phosphopeptide was sufficient to completely displace Fyb from the SH2 domain of Fyn (Figure 5.3). It is possible that by increasing the peptide concentrations, or lowering the amount of protein lysate used in the assay, non-specific binding of the nitropeptide might have effected the dissociation of Fyb from Fyn, however, achieving peptide concentrations above ~10 mM was not possible due to aggregation. It would have been possible to reduce the amounts of protein used but the 400 μg amounts is within the range used as part of a standard protocol (Personal communication Lynne Howells, University of Leicester). Under the optimised conditions, the qualitative determination of the ability of derivatives of DS4 bind to the SH2 domain of wild type Fyn was achieved.

On incubating the immumoprecipitated Fyn with three different concentrations of pDS4, the all-or-nothing binding of Fyb to the SH2 domain of Fyn was demonstrated (Figure 5.2 b). Assuming a 1:1 stoichiometric association between phosphopeptide and SH2, there must clearly have been more than 1 μM of Fyn immunoprecipitated to generate the signals at 1 nM and 1 μM; yet, such is the nature of the signal amplification that can be achieved be varying the time a blot is developed, the

concentration of Fyn in the assay sample need not have greatly exceeded 1 μM. However, there must have been 1 mM, or less, of immunoprecipitated Fyn in the assay mixture for the phosphopetide to have completely abolished binding at this concentration. For the purposes of achieving our objectives, namely to compare and confirm the relative affinities of the derivatives of DS4 for the SH2 of wild type Fyn, the use of 1 mM of peptide and 400 μg of protein lysate, was justified as our positive control (the phosphopeptide) completely abolished the binding Fyb to Fyn, whilst the negative control (the non-modified peptide) failed to displace the adaptor protein from the SH2.

As the derivatives of DS4 were added to the immunoprecipitated proteins after the removal of lysate supernatants, the results presented in this chapter demonstrate the ability of derivatives of DS4 to bind to the isolated wild type SH2 domain of Fyn, rather than their ability to bind to the protein in the context of the cellular environment. Attempts to use Streptolysin-O to introduce the peptides into T-cells prior to their stimulation, analogous to the work previously conducted by Alexander and colleagues (1989), was unsuccessful, as were attempts to optimise the methodology by introducing the peptides to the cell lysates prior to immunoprecipitation. One can only speculate on what the effect, if any, of introducing the peptide to intact cells or cell lysates might have been. In the case of the phosphopeptide, the presence of intracellular phosphatases might have rendered the peptide ineffective in displacing Fyb, although a high enough concentration of peptide and the activity of kinases might have been able to overcome phosphatase activity. In the case of the nitropeptide might there have been a reductase activity (Kamisaki et al., 1999, see Chapter 1) that converted the nitro to an amino derivative, which then underwent phosphorylation to produce a peptide derivative that was capable of displacing Fyb from Fyn SH2 domain? (This latter concept is addressed in the following two chapters). An inability to optimise the methodology in intact cells or lysates meant these questions could not be pursued.

It was interesting to note that the relative amount of Fyb bound to Fyn were unaffected by TCR/CD3 receptor cross-linking. Fyb contains a number of tyrosine phosphorylation sites (Tomlinson et al., 2000) and on T-cell stimulation the levels of

pTyr levels in Fyb rise to a maximum one minute after stimulation, after which the levels of phosphorylation fall (Musci et al., 1997). Engagement of the TCR/CD3 receptor is known to increase the activity of a number of tyrosine kinases. The kinase responsible for phosphorylating the tyrosine residue on Fyb that enables the adaptor protein to interact with the SH2 domain of Fyn is unknown, however, data in Figure 5.2 suggests it must be active in non-stimulated T-cells. Furthermore, although Fyb is known to undergo phosphorylation on T-cell activation (Musci et al., 1997) the amount associated with Fyn SH2 domain remained unaffected by the length of T-cell stimulation (Figure 5.2). These data suggest there is a constitutive association between Fyb and Fyn, analogous to the association of Fyb with another adaptor SKAP-55 (Marie-Carfine et al., 1998), yet unlike the induced association that occurs on T-cell activation between Fyb and SLP-76 (Clements et al., 1999; Liu et al, 1998).

T-cell signalling is a highly complicated process relying on the intricate temporal and spatial coordination of enzymes activity and adaptor protein localisation and modification. In addition, T-cells are key mediators in the inflammatory response, particularly chronic inflammation, and as such these cells are likely to encounter RNS. Due to the complexity of the mechanisms of T-cell signalling it is difficult to predict what effect if any the nitration T-cell signalling proteins might have on cell function. Based on our findings of nitropeptide/SH2 domain interactions, it is possible to predict that the nitration of adaptors and/or ITAMS would prevent the formation of critical protein complexes and disrupt the recruitment of PTKs to the CD3 proteins, respectively. However, whether these processes would effect the overall function of T-cells is a matter of speculation. Some adaptors such as SLP-76 and LAT are key to coupling receptor activation to downstream signalling events so tyrosine nitration in these proteins may have a significant bearing on T-cell function. By contrast, nitration of adaptors such as Fyb, whose function is not been well defined, might have a less dramatic outcome on T-cell function. Nitration of the of the C-tail tyrosines in Lck and Fyn, the critical for initiators of the intracellular cascades of T-cells, might render these enzymes permanently active by maintaining them in an open form (see chapters 1 and 7), which in immunological terms can be as detrimental as a non-functioning cell. In T-cells it is possible that apoptosis would result in the death of these overactive cells, however in normal somatic cells the outcome could be different. This is discussed further in Chapter 7.

In summary, the nitropeptide unlike the phosphopeptide failed to displace Fyb from the SH2 domain of Fyn in the immunoprecipitates of Jurkat cells. This finding corroborates the findings of chapter 3 and confirms the weak association between nDS4 and Fyn SH2 domain.

CHAPTER 6:

IS AMINOTYROSINE A SUBSTRATE FOR TYROSINE KINASES?

INTRODUCTION

Evidence has been forwarded to suggest that once formed nTyr undergoes reduction, to form the amino derivative of tyrosine (Balabanli et al., 1999; Kamisaki et al., 1999). The concept of this reaction being a means regulating the cellular effects of nTyr formation has been previously discussed (see chapter 1). However, if the tyrosine residue that has undergone reduction is to continue serve a role in cellular regulation, it must either serve this function in its reduced from, be readily converted back to its bioactive nitro equivalent, or alternatively, it must be a substrate for tyrosine kinases (PTKs). There is no current evidence to suggest aTyr regulates protein function in an analogous manner to phosphorylation or, as speculated in this thesisThe oxidation of aTyr to its nitrated equivalent could occur by chemical or biochemical mechanisms *in vivo*, providing routes through which active nitro moieties could be regenerated. To my knowledge, aTyr has not been previously investigated as being a candidate substrate for PTKs. Determining whether these residues undergo phosphorylation, in an analogous fashion to tyrosine, will aid our understandingof how the cell copes with nTyr formation. The following work describes an initial experiment conducted to establish whether aTyr is a PTK substrate.

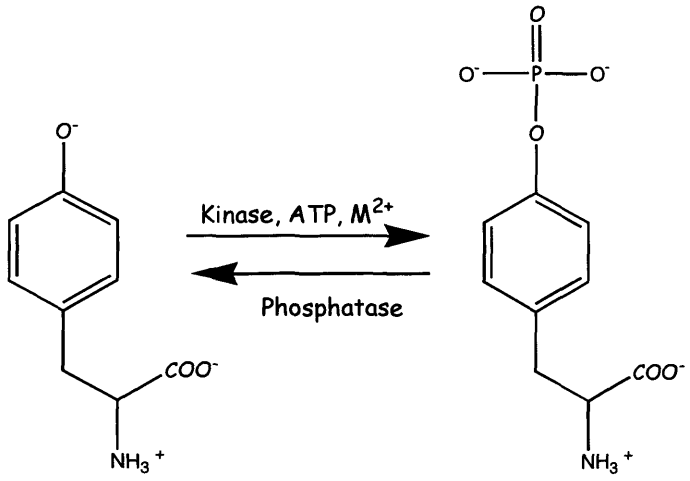

Figure 6.1. The addition and removal of phosphate from tyrosine. Tyrosine kinases mediate the transfer of ATP's γ-phosphate to the hydroxyl moiety of tyrosine in the presence of di-valent metal ions. The reverse process is mediated by tyrosine phosphatases.

The incorporation of phosphate onto the hydroxyl group oftyrosine is mediated by PTKs (Figure 6.1). These enzymes play important roles in cancer, immunology, neurobiology and endocrinology (Lodish et al., 1995). Major efforts have been made to develop inhibitors to these enzymes as pharmaceuticals (Al-Obeidi et al., 1998; Cole et al., 1999), consequently research has focused on establishing the factors that underlie the binding of enzyme to substrate (Johnson et al., 1998; Songyang and Cantley, 1995) and the mechanisms through which phosphorylation proceeds (Kim and Cole, 1997; Kim et al., 2000). The sequence in which the tyrosine residue is found (Songyang et al., 1995); Songyang and Cantley, 1995) and aryl ring substitutions (Kim et al., 2000) are factors that determine substrate binding and, inthe latter instances, influence PTK activity. PTKs require the tyrosine hydroxyl group to be protonated for phosphorylation to occur (Kim and Cole, 1997), consequently, ring substitutions that alter the pKa of the phenoxy moiety of aTyr is the same as that for tyrosine (~10.0) and would therefore be protonated at physiological pH and be able to undergo phosphorylation, analogous to a tyrosine residue. However, in addition to the pKa of the phenoxy group, the size and charge of the aryl substitutions will also have a bearing on whether tyrosine substituents are substrates for PTKs due to stericfactors and charge repulsion, respectively. The following section forwards very preliminary evidence to suggest that aTyr could indeed be a substrate for Src tyrosine kinase.

EXPERIMENTAL PROCEDURES

MATERIALS

Acetic acid and solvents for HPLC and mass spectrometry were purchased from Fisher Scientific, UK. Ultra pure water (18.2Ω) used in all HPLC analysis. All solvents were membrane filtered (0.45μm, Whatman, Miadstone, Kent) and degassed online with helium. The src kinase was purchased from Calbiochem, Nottingham, UK. All other reagents were purchased form Sigma. CARE! Teteranitromethane is a highly toxic agent, and must be handled using the appropriate safety procedures.

METHODS

Reduction of Nitrated DS4 to the Aminated Derivative

The reduction of nDS4 to aDS4 was based on the procedure previously described (Shigenaga et al, 1997). Briefly, nitrated DS4 was dissolved in water to a final concentration of 16.8 mM, to which 0.1 M sodium hydrosulfite was added at a concentration of 700 µl/ml of peptide solution. After 30 min at 25°C, concentrated HCl was added to the sample at a concentration of 100 µl/ml of solution. The resulting solution was applied directly to the reverse phase HPLC column, or, lyophilised, reconstituted in dilute acetic acid to a final concentration of 1 mg/ml and stored below 0°C.

HPLC Characterisation

HPLC analysis was conducted on a Gilson-gradient controlled system equipped with Gilson 486 UV detector using a Hypersil BDS 5 µm C_{18} column (250 x 4.6 mm), at a flow rate of 1 ml/min. Solvent compositions was: A was 0.1 % TFA in ultrapure water, and solvent B was 100% MeCN containing 0.1% TFA. Peptides were eluted using an increasing linear gradient of solvent B from 30 to 35 % in 20 min. Peaks were collected and analysed directly by ESI-MS/MS.

Phosphorylation of DS4 derivatives by src kinase

Note, all solutions used in this assay were degassed wth helium prior to use; additionally, a helium atmosphere was generated in the screw top eppendorf prior to its securing and incubation overnight to remove in an attempt to remove any dissolved oxygen that might oxidise the aminopeptide. 10µl of aDS4 in kinase assay buffer (see appendix I) was added to 10µl of src, which had been previously diluted in Kinase dilution buffer (see appendix I) at a concentration of 0.2 units of enzyme/µl of buffer, such thast the final concentration of peptide, ATP and src was 5.3 mM, 66 µM and 0.6 units, respectively. The reaction was started by adding 10 µl of ATP solution (see appendix I) and allowed to incubate overnight at 30°C and stopped by the addition of 120µl of 10% phosphoric acid. 20 µl of reaction mixture was injected directly onto a Hypersil BDS 5µm, C18, reverse phase column under the conditions described above.

Mass Spectral Analysis

The electrospray ionisation mass spectra were obtained on a VG Quattro-BQ tandem quadrupole instrument (Micromass, Manchester, UK). Peptides samples were electrosprayed from acidified (0.1% acetic acid) 50% acetonitrile solution at a sample concentration of 20 pmoles/μl. The analyte solutions were infused into the mass spectrometer source, using a Harvard system pump (model 55-2222) at a flow rate of 5 μl/min through a 75 μm (inner diameter) fused silica capillary, and positive ion spectra obtained. Tandem mass spectrometry measurements were performed using the first quadrupole to transmit the singly protonated peptide to a collision cell containing research-grade argon, while a second quadrupole was used to analyse the product scan of the protonated peptide precursor.

RESULTS

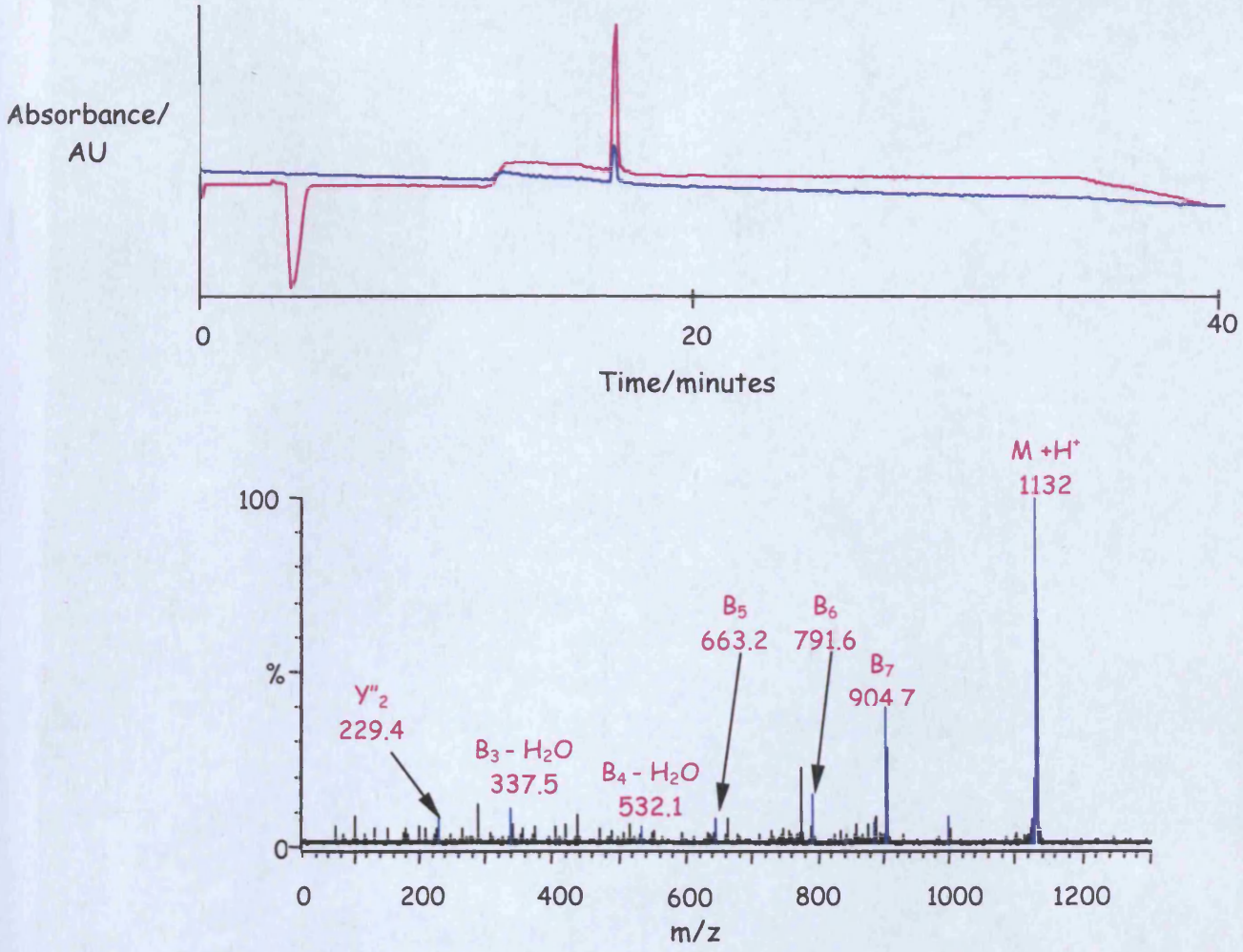

Figure 6.2. Characterisation of aminoDS4. The aminated derivative of DS4 was characterised by HPLC and ESI-MS/MS. On reduction of nDS4 a solitary product was eluted by HPLC with a retention time of 15.21, which was confirmed as being aDS4 by ESI-MS/MS.

The aminopeptide was generated by the dithionite reduction of nDS4. Prior to conducting phosphorylation reactions on aDS4 the peptide was characterised by HPLC, and ESI-MS/MS (Figure 6.2). A solitary peak was generated on the reduction of nDS4, whose retention time was approximately 2 minutes less than that of the nitropeptide (17.70 minutes compared to 15.21 minutes). A comparison of the fragments generated during MS/MS analysis of the HPLC peak generated on the reduction of the nitropeptide with those of DS4 (Figure 2.9) confirmed the complete

reduction of nDS4 to aDS4. These two techniques were deemed sufficient for the purpose of characterisation: the ESI-MS/MS confirming that tyrosine residue contained a modification resulting in an increase of 15 mass units, consistent with a amino group, with its purity being confirmed by HPLC.

The phosphorylation of DS4 and aDS4 by Src were conducted overnight at 30°C. DS4 was used as a positive control to ensure Src was capable of phosphorylating the peptide motif under the conditions used. Reaction mixtures were applied directly to the RP column (Figure 6.3) and peaks collected for mass spectral analysis. Figure 6.4 shows the mass spectral analysis of the peaks collected from the kinase reactions of aDS4. Peak I in figure 6.3 panel B was established as being pDS4 by ESI-MS/MS (see Figure 2.9), as the retention time (14.94 minutes) of the product also suggested, confirming the conditions were suitable for Src to phosphorylate the DS4 motif.

The lower spectrum in Figure 6.4 shows the ESI-MS trace of peak II collected from Figure 6.3 panel D. In addition to aDS4 ($M+H^+$ 1132, $M+2H^+$ 567), an m/z value of 1212 was also detected on MS analysis of peak I. This mass is consistent with the incorporation of a phosphate group into the peptide aDS4. The elution of the putative phosphorylated derivative before the aminopeptide was also consistent with the reduced hydrophobicity of the peptide on the incorporation of phosphate. Peak II was as expected residual aDS4 ($M+H^+$ 1132, $M+2H^+$ 567). The presence of aminopeptide in peak I can be accounted for by cross-contamination with the closely eluting peak II, or alternatively, the conditions employed during the MS analysis might have been sufficient to remove the phosphate group, which would suggest weak or unstable bond formation. To confirm it was the aminotyrosine residue that underwent phosphorylation, ESI-MS/MS was conducted on the 1212 ion. It was surprisingly, however, to find that attempts to fragment the 1212 ion were not successful. Attempts to alter the MS conditions failed to generate an MS/MS spectrum. Therefore absolute confirmation that the 1212 fragment was phosphorylated aDS4 was not possible.

SPECIAL NOTE

This item is tightly bound and while every effort has been made to reproduce the centres force would result in damage.

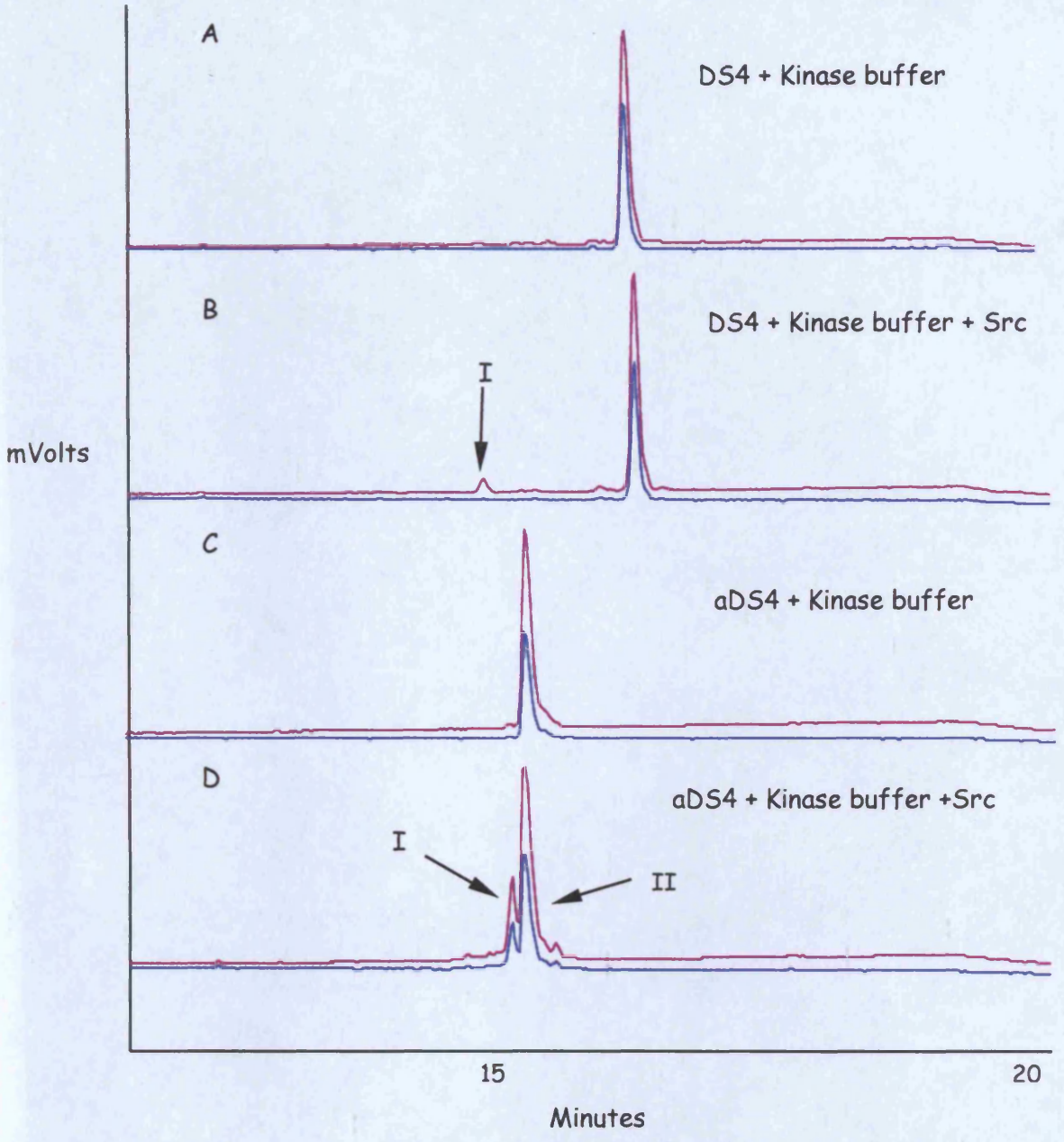

Figure 6.3. The phosphorylation of DS4 and its aminated derivative by Src. Derivatives of DS4 were incubated overnight with Src and analysed by HPLC. In the absence of enzyme there was no indication of the generation of the phosphorylated derivatives of DS4. By contrast, in the presence of Src additional peaks were detected and collected for mass spectral analysis.

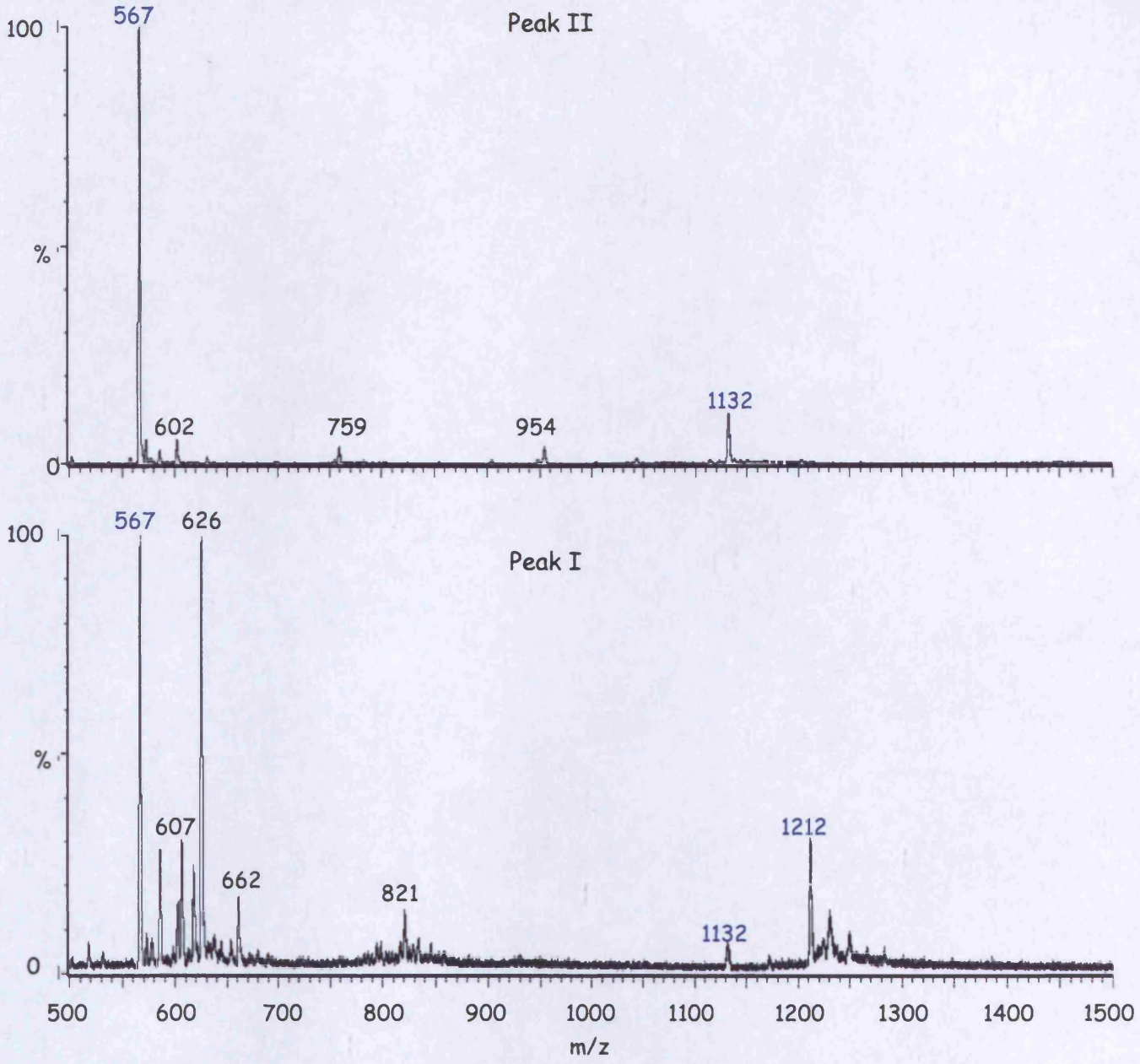

Figure 6.4. Electrospray analysis of the peaks generated in the aDS4 kinase reaction. HPLC analysis of an overnight incubation of aDS4 with Src produced two prominent peaks (I and II, Figure 6.3), which were collected and analysed by ESI-MS. The upper spectrum shows the analysis of Peak II, which as expected was unreacted aDS4 as denoted by the m/z values of 1132 and 567. Analysis of peak I (lower panel) indicated the presence of 1212, 80 mass units higher the 1132 of aDS4, which is consistent with the incorporation of a phosphate group into the aminopeptide.

DISCUSSION

In an attempt to establish whether aTyr is a substrate for PTKs aDS4 was incubated with Src and reaction products analysed. A number of peptides containing modified tyrosine residues have been shown to be substrates for TKs (Kim et al., 2000; Lee et al., 1995). Kim and colleagues demonstrated that increasing the size of ortho tyrosine-substituents, within reason, decreased the rate of phosphorylation. Yet, kinase activity was less sensitive to the size of the meta substitutions. An amino group will have a smaller atomic radius than a hydroxymethyl group (bond length C-H ~1.08 Angstroms, N-H ~ 1.48) a residue that has been shown to undergo phosphorylation (Kim et al., 2000). This finding would suggest the steric factors would not impede phosphorylation of aminotyrosine. Further, in addition to the size of ring substitutions, it was found that the presence of a negatively charged ortho substituent (a carboxylic acid group) on the tyrosine ring was sufficient to prevent phosphorylation. At physiological pH the amino group would be in its neutral uncharged state (pKa of the amino group of 2-aminophenol being 4.9, Eckert et al., 1990), and would not influence phosphorylation. Overall, the size and the charge at physiological pH of the substituted amino, along with the pKa of the phenoxy group all favoured aTyr being a substrate for Src.

A comparison of the relative height of the peaks generated in the HPLC chromatogram on phosphorylating DS4 and aDS4 indicates that either the phosphorylation product of the aminopeptide has properties that increase its extinction coefficient at 215 and 280 nm relative to that of the aminopeptide itself, or alternatively, Src phosphorylates the aminopeptide at a greater rate than the non-modified peptide. The pKa of the two peptides could not account for this difference, as the value is the same for both peptides. Also, it is unlikely that the steric influence of the amino group would make aDS4 a more proficient substrate for Src than DS4. One possibility is that the amino group might increase the affinity of the peptide for the enzyme by mediating hydrogen bonding with residue in the active site. The active site of PTKs contains acidic residues (Johnson et al., 1998). It is therefore feasible that hydrogen bonds could be formed between the amino group and the side chain oxygens of these acidic residues.

The inability to conduct ESI-MS/MS on the reaction product of aDS4 phosphorylation meant the aDS4 could not unequivocally be confirmed as being a substrate for TKs, although the ESI-MS analysis suggested this to be the case. None of the starting materials in the kinase reaction mixture have a mass 1212, so the only other source of the peak could be a peptide fragment of Src, which would also be expected to fragment on ESI-MS/MS analysis. As to why fragmentation could not be achieved was unclear. It is possible that the phosphorylated derivative of aDS4 was unstable and consequently the 1212 species did not survive long enough under the mass spectral conditions for the second fragmentation to occur. As a result of this the findings presented must be treated with caution until the 1212 peak can be characterised, and further work conducted can confirm or disprove aTyr as being a PTK substrate.

If it is indeed confirmed that aTyr is a substrate for PTKs, a number of questions would need to be answered, namely:

- Is an aTyr containing peptide a substrate for all PTKs?
- Is the phosphate group added to the hydroxyl or amino group?
- How stable is the phosphorylation product?
- Does a phosphorylated aTyr containing peptide bind to SH2 domains? If yes how avidly?
- And, would phosphatases be able to remove the phosphate group in an analogous manner to pTyr?

The presence of aDS4 in the fraction that also contained the 1212 ion suggested if formed, the product of the phosphorylation aDS4 might be unstable. As well as the hydroxyl group of tyrosine being an acceptor for phosphate, the amino could conceivably be the ultimate destination for the phosphate. Internal rearrangement of the phosphoaminotyrosine residue would lead to the formation of the phosphoramidite derivative of tyrosine (Figure 6.5). Both the phosphoester and the phosphoramidite would be stable products, therefore the more likely explanation for the presence of a 1132 ion in peak I was contamination with the closely eluting aDS4 (Figure 6.3 panel) D.

One can postulate that reduction of nTyr to aTyr serves to protect the cell from the ill effects of nTyr formation. If it transpired that phosphorylated aTyr residues function in much the same way as the pTyr, the reduction of nTyr to the corresponding innocuous amino derivative provides a more efficient means of reducing the potential harm caused by nTyr, compared with the degradation of the nitrated protein. Thus, in addition to its protective role, reduction would also conserve modified proteins by regenerating tyrosine into a form in which it could continue to serve its cellular function.

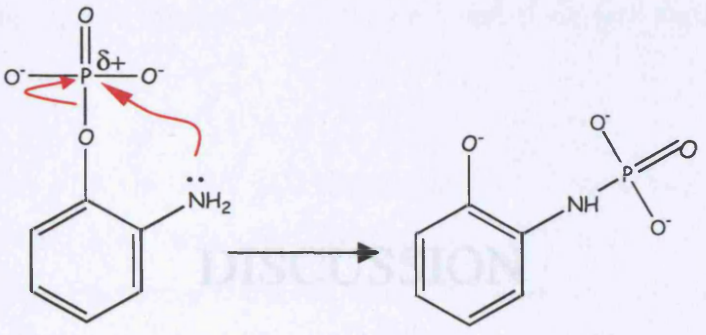

Figure 6.5. Rearrangement of phosphoaminotyrosine to its phosphoramidite derivative. The lone pair of the amino group attacks the electrophilic phosphorus centre leading to rearrangement and phosphoramidite formation.

In summary, the work outlined in this chapter provides provisional evidence based on one type of experiment that aTyr might be substrate for the TK Src. More work needs to be conducted to confirm this finding, but if confirmed, a number of other questions will need to be answered.

CHAPTER 7:

DISCUSSION

Chapter 1 of this thesis introduced the notion of nTyr being a posttranslational modification that may contribute to the mechanisms that the cell uses in regulating its own function. The first chapter also included a discussion of one way in which nTyr residues may serve this role: by mimicking pTyr in their ability to bind to SH2 domains. Having initially conducted characterisation of peptides and proteins in Chapter 2, chapters 3 to 5 utilised various techniques to provide compelling evidence that, in the case of Fyn SH2 domain, a nTyr residue does not confer high affinity binding between DS4 and the SH2 domain; rather the affinity of the nitropeptide for Fyn was comparable to that of the non-modified peptide. In addition to this, chapter 6 explored the possibility that the *in vivo* product of nTyr metabolism, aTyr, was a possible substrate for Src kinase. So what then is the biological significance of these findings?

The formation of nTyr in cells and tissues is well documented (Greenacre and Ischiropolous, 2001). It is known that the nitration of tyrosine residues impedes the activity of an array of enzymes (Neilsen, 1995) and alters the function of a number of other proteins (see introduction, Chapter 1). Furthermore, nTyr has been detected in a number of human pathologies (Eiserich et al., 1999; Ischiropolous, 1998; Oldreive and Rice-evans, 2001). Yet, it is unclear as to what role, if any, nTyr plays in these disease states and the normal function of the cell. One of the fundamental problems in trying to shed light on the role that nTyr plays in cell function is translating *in vitro* data to the *in vivo* situation. For instance, determination that an isolated enzyme that has undergone nitration and ceases to function *in vitro* can not be translated to the cellular milieu, where feedback mechanisms might ensure the system, of which the enzyme forms an integral part, is not compromised. Yet what is the alternative? Exposure of cells to RNS in an attempt to establish the role nTyr might play in disease is likely to pose more questions than provide answers: What systems have been compromised, or activated, as a result of the exposure? Is the visualised effect due to alteration of a solitary system or is it as a result of multiple system aberrations? What is the nature of the modification that has brought about change in the cell's function? The fact that there are potentially a number of systems whose function might be altered on protein nitration suggests it might be more prudent to determine the outcome of these potential modifications than to study the outcome of the exposure of whole cells to RNS, determine the end point, then work back to establish the systems,

proteins and the individual residues that might be responsible for the observed effect. As researchers continue to develop more sophisticated ways of analysing cell function, unravelling these problems will become an easier task. Currently, proteomic analysis provides a powerful tool for investigating the global effects of toxins on cell's protein complement. However, the use of this technology has not been fully explored in investigating the role that RNS play in cell function.

It might be possible to forecast the outcome of tyrosine nitration on a specific system, if it could be demonstrated that, firstly, phosphorylation of a specific tyrosine was associated with a specific cellular outcome, and secondly, if the nitration of this residue could be demonstrated *in vivo*. The latter experiment has recently been conducted in A549 cells and in rat lung and liver tissue (Aulak et al., 2001), identifying a diverse range of proteins that were shown to undergo nitration. However, analysis of a more diverse range of cells needs to be conducted to generate a extensive list of *in vivo* nitrated proteins. The mutation of tyrosine residues in growth factor receptors and the subsequent failure of SH2 domains to bind to the receptor could be used as a model of tyrosine nitration in growth factor signalling. In these systems it has been shown that the mutation of some tyrosines only partially impeded biological outcome, whereas, the mutation of other individual residues within the same receptors completely abolished the biological outcome (Mania et al., 1996; Nicholson et al., 1996). Models where it has been demonstrated that the failure of an SH2 domain to bind to a pTyr residue results in a specific biological outcome, present another situation where predicting the effect of tyrosine nitration might be possible. One such example is the failure of mutants of the SH2 domain containing protein SAP to bind to the T-cell transmembrane receptor SLAM, which renders individuals susceptible to the unregulated proliferation of EBV-infected B-cells (Sayos et al., 1998).

A further complication in extrapolating the findings of this thesis in a general way to the interactions of nitrotyrosine containing peptides with SH2 domains nTyr *in vivo* comes from work published by Mallozzi and colleagues. This group recently demonstrated that the affinity of a nitropeptide for the SH2 domain of Lyn was more akin to that of the phosphorylated equivalent than the non-modified peptide (Mallozzi et al, 2001), in contrast to the results reported here for the Fyn domain. In light of

these findings it would appear that a simple model for SH2 domain/nitropeptide interactions cannot be proposed on the basis of the work presented here, rather the ability of a nitropeptide to bind to an SH2 domain would appear to be a protein-specific phenomenom. Both Fyn and Lyn are members of the Src tyrosine kinase family and share common SH2 domain architecture, although subtle differences do exist in their structure (Kuriyan and Crowburn, 1997). In all SH2 domains there exists an invariant arginine residue (the fifth residue in the D β sheet) situated at the base of the pTyr-binding pocket to which the phosphate of pTyr forms a bi-dentate interaction (Waksman et al., 1993). This interaction has been demonstrated to be the key mediator of phosphopeptide-SH2 domain interactions (Bradshaw et al., 1999; Mayer et al, 1992). Conversely, in attempt to develop small molecules that bind to SH2 domains, the pharmaceutical industry has demonstrated that 3,5 bi-nitrated substituted tyrosines bound avidly to the SH2 domain of Csk (Anon, 1998), suggesting this arginine might not be critical in mediating nitropeptide binding to SH2 domains. In the case of Fyn, the lack of affinity of the nitropeptide for the SH2 domain was rationalised in terms of an inability to form a bi-dentate interaction with the βD5 arginine and the fewer hydrogen bonds formed between the nTyr residue and residues of the pTyr-binding pocket. One can only conclude that the ability of nDS4 to bind to the SH2 domain of Lyn lies in the subtle structural differences in the pTyr-binding pocket that enables a nitropeptide to form sufficient hydrogen bonds with the protein. It is not currently clear what features of Lyn are that enable a nitropeptide to bind to it with such high affinity.

Because of the dependency of growth factor signalling on multiple SH2 domain pTyr bindings, the vast network of intracellular biomolecular interactions initiated from the activation of a single receptor and the possibility that not all the phosphorylatable tyrosine residues will undergo nitration, predicting the consequences of the modification of a solitary, or multiple, tyrosine nitrations on the growth factor receptor is very difficult. In the growth factor signalling pathway, tyrosine phosphorylation is key in translating ligand binding to the extracellular receptor to an intracellular cascade. A number of tyrosine residues on the receptor undergo autophosphorylation on receptor stimulation. Predicting the cellular outcome of the nitration of these residues would vary according to the nitropeptide/SH2 domain

interaction model adopted (Figure 7.1). Assuming that all phosphorylatable tyrosines undergo nitration, the model based on findings of this thesis would result in the decoupling of phosphorylated receptor from the intracellular signalling cascade. Conversely, based on the Mallozzi model, one would expect initiation of the intracellular cascade in an analogous manner to receptor phosphorylation.

As well undergoing degradation at a faster rate than non-modified proteins (Berlett et al., 1996; Gow et al, 1996), nTyr-containing proteins are believed to undergo reduction *in vivo* to form aTyr (Balabanli et al., 1999; Kamisaki et al., 1999) The work described in chapter 6 provides very preliminary data to suggest that aTyr might be a substrate for PTKs; one can speculate, therefore, that the phosphorylation products of aTyr might be able to bind to SH2 domains with sufficient affinity to initiate downstream signalling. Based on these initial data and the supposition that the product of phosphorylation binds to SH2 domains with at least moderate affinity, both models could ultimately share a common final pathway that might result in downstream signal propagation, if reduction of the nitrated receptors occurred (Figure 7.1). If, in the Mallozzi model, nitration was not followed by reduction it is possible that the receptor could continue to recruit cytosolic proteins and form complexes that initiated intracellular cascades, resulting in cell over-stimulation and transformation, analogous to the expression of mutant tyrosine kinase receptors (Cantley et al., 1991).

The difficulty in trying to extrapolate the findings of peptide-SH2 domain interactions to growth factor signal transduction lies in the complexity of the cascades emanating from the receptor. On activation of growth factor receptors a number of enzymes and adaptor proteins capable of initiating specific signalling pathways bind (Claesson-Welsh, 1994). Consequently the 'inactivation' of a specific tyrosine by nitration would not necessarily disrupt the cell growth and differentiation initiated by a growth hormone. These problems are not, however, encountered on trying to predict the effect on Src kinase where extrapolation is much simpler as we are dealing with a single protein, whose activity is dependant on the phosphorylation of two key tyrosine residues and a solitary SH2 domain pTyr interaction.

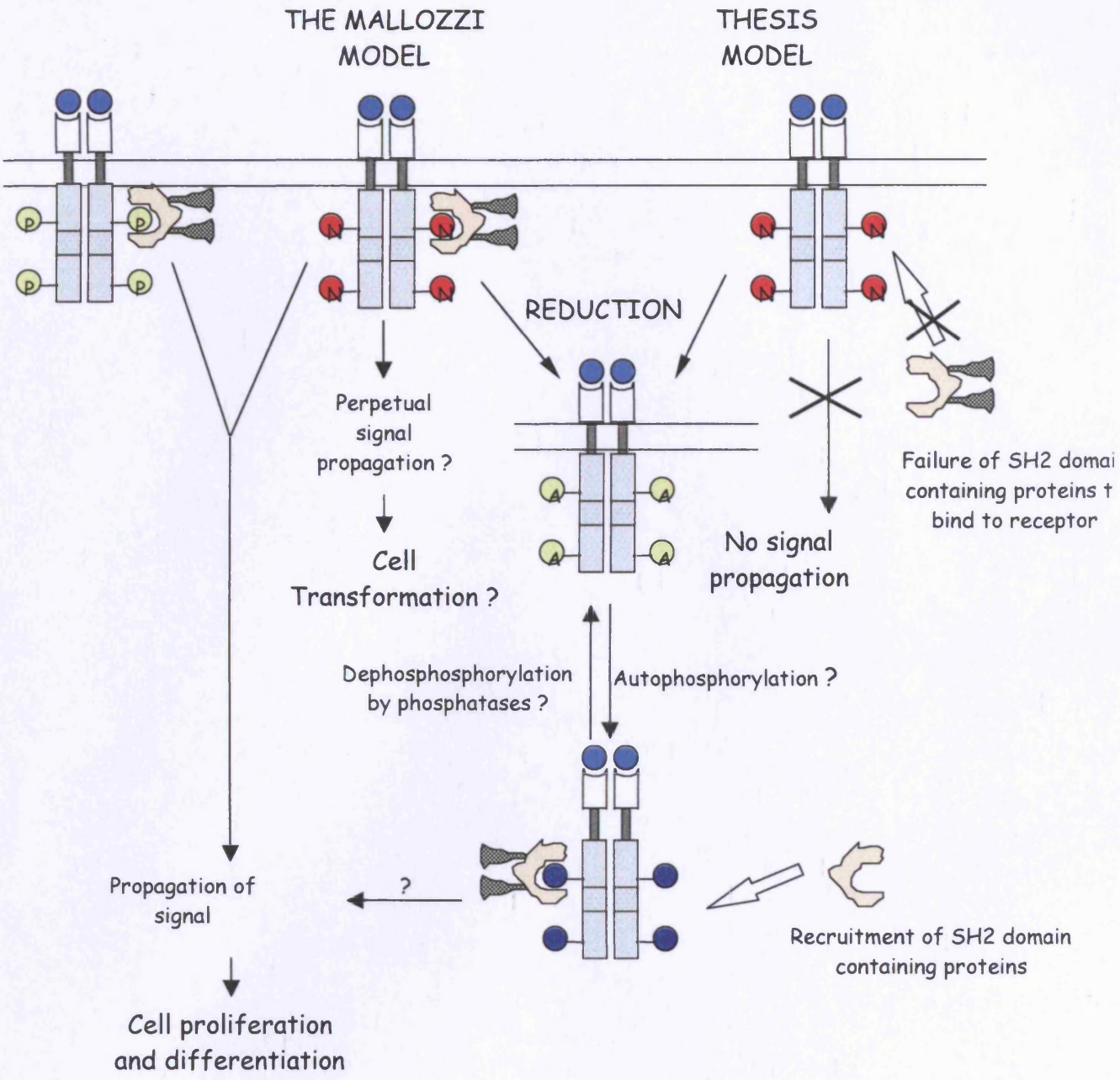

Figure 7.1. The effect of nitrotyrosine formation in the growth factor receptor on signalling. On the assumption that all phosphorylatable tyrosine residues undergo nitration on exposure of the cell to RNS, using the work outlined in this thesis the intrcellular component of this cascade would not be initiated. Conversely, using the work of Mallozzi and colleagues as a model, the signal would be transduced in an analogous manner to a receptor that had undergone tyrosine phosphorylation. For both models it is possible that the nTyr residues would undergo reduction to aTyr, which might generate a residue capable of binding to SH2 domains.

The mechanisms that regulate the activity of src kinases have been previously described (see chapter 1). Key to maintaining Src in its inactive conformation is the interaction between its phosphorylated C-terminal tail and SH2 domain, which precludes substrate binding to the enzyme's active site. If this regulatory mechanism is compromised Src is capable of transforming cells through its unregulated phosphorylation of a number of proteins (Brown and Cooper, 1996). On analysis of human biopsies of pancreatic adenocarcinomas MacMillan-Crow and colleagues (2000) discovered Src had undergone both nitration and phosphorylation. They hypothesised that exposure of pancreatic cells to RNS resulted in the activation of Src, which subsequently lead to cell transformation. Based on the findings of their SH2 domain nitropeptide study, Mallozzi and co-workers suggested the origin of transformation of the pancreatic cells lay in the ability of intracellular ligands to bind to the SH2 domain and maintain it in its open active form (Figure 7.2). Based on the data presented in this document an alternative hypothesis is proposed: exposure of Src to RNS in its active form results in the nitration of the C-terminal tyrosine (residue 527). The consequent weak affinity of the C-terminal tail for the SH2 domain maintains Src in an active form capable of transforming cells. This would be analogous Src tyrosine 527 found in human cancers (Bagrodia et al., 1991), or to the ability of polyoma virus to transform cells through its lacking the regulatory tail sequence; or finally, to the ability of middle-T antigen to form a high affinity complex with Src that also maintains it in its active form (Kaech et al., 1991). Additionally, this model also accounts for the presence of both the nitrated (tyrosine 527) and phosphorylated residues (tyrosine 416), moreover, it suggests that these modifications are a requirment for the enzyme to remain active. The ubiquitous nature of Src kinases means they are likely to be exposed to RNS. As suggested in chapter 5, the nitration of the key T-cell kinases Lyn and Fyn in a chronic inflammatory environment might transform these kinases into their overactive phenotype.

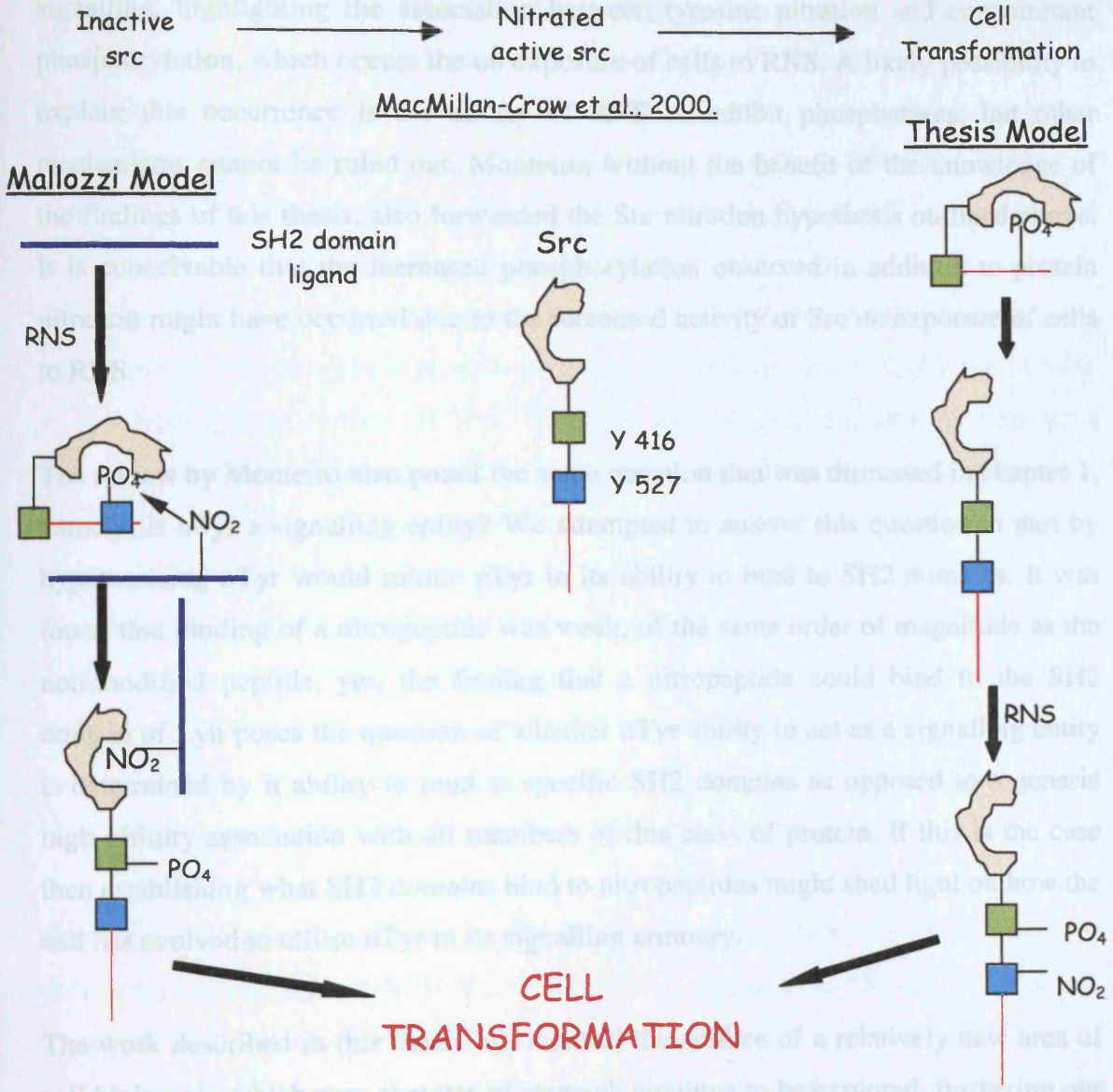

Figure 7.2. The role of reactive nitrogen species in src mediated cell transformation. MacMillan-Crow and co-workers proposed the exposure of src kinase to the RNS was responsible for the presence of pancreatic adenocarcinomas in human biopsies. Based on this hypothesis Mallozzi and colleagues (2001) proposed that exposure of src nTyr containing ligands maintained the kinase in its open active form, known to cause cell transformation. Alternative to this based on our work is that Src in its open, active state becomes nitrated on Y 527. The subsequent weak association between the regulatory tail of the enzyme and its SH2 domain is responsible for maintaining Src in its open, active state.

Monteiro (2002) recently reviewed literature on the role of RNS and nTyr in cell signalling, highlighting the association between tyrosine nitration and concomitant phosphorylation, which occurs the on exposure of cells to RNS. A likely possibility to explain this occurrence is the ability of RNS to inhibit phosphatases, but other mechanisms cannot be ruled out. Monteiro, without the benefit of the knowledge of the findings of this thesis, also forwarded the Src nitration hypothesis outlined above. It is conceivable that the increased phosphorylation observed in addition to protein nitration might have occurred due to the increased activity of Src on exposure of cells to RNS.

The review by Monteiro also posed the same question that was discussed in chapter 1, namely, is nTyr a signalling entity? We attempted to answer this question in part by hypothesising nTyr would mimic pTyr in its ability to bind to SH2 domains. It was found that binding of a nitropeptide was weak, of the same order of magnitude as the non-modified peptide, yet, the finding that a nitropeptide could bind to the SH2 domain of Lyn poses the question of whether nTyr ability to act as a signalling entity is determined by it ability to bind to specific SH2 domains as opposed to a generic high affinity association with all members of this class of protein. If this is the case then establishing what SH2 domains bind to nitropeptides might shed light on how the cell has evolved to utilise nTyr in its signalling armoury.

The work described in this thesis has touched the surface of a relatively new area of cell biology in which new avenues of research continue to be explored, furthering our understanding of cell function. Proteomics provides a powerful tool that can be utilised to determine the proteins that undergo nitration on assault from RNS in addition to determining which proteins are bound together after the *in vivo* formation of nTyr. In the immediate future it will be interesting to establish those SH2 domains capable of binding tightly to nitropeptides. On a more detailed level, establishing the structural determinants that underlie high affinity nitropeptide binding to SH2 domains using high resolution NMR or X-ray crystallography will not only further our understanding of SH2 domain mediated signalling, but will aid the pharmaceutical and biotechnology industry in developing a range of small molecule agents that disrupt the pTyr/SH2 domain interactions that have been shown to be important in the genesis of human disease, whilst avoiding the unwanted activation of Src kinases.

The data presented in chapter 6 was not wholly conclusive in establishing whether aDS4 was a substrate for Src kinase, further work must be conducted to either confirm or rule this out. Key to this work will be establishing that the tyrosine residue has undergone modification; determining the final destination of the phosphate group; establishing whether the product of the aTyr phosphorylation generates a product capable of binding the SH2 domain of Fyn with high affinity and probing, if phosphorylation occurs, whether the product is susceptible to phosphatase activity. Although the experiments conducted in chapter 6 failed to confirm absolutely the incorporation of a phosphate group onto a tyrosine residue, ESI-MS/MS can be used in this regard, with further ^{1}H and ^{31}P NMR work being conducted to determine whether the ultimate destination of the phosphate is the phenoxy group or the amino. The ability of any potential phosphorylation product of aDS4 to bind to the SH2 domain of Fyn could be established by utilising the methodology of chapter 3. Qualitatively, both nanospray and the use of a FRET pair provide a simple and quick means of determining the high affinity binding of peptides to the SH2 domain of Fyn, whilst the FRET assay described in chapter 3 or one-dimensional NMR could be used to quantitate the affinity of the peptide for the SH2 domain. The reversibility of any phosphorylation reactions could be determined by simple phosphatase assays.

The work conducted by MacMillan-Crow and colleagues (2000) on the detection of the nitrated and phosphorylated Src in pancreatic adenocarcinomas can be extended. Firstly, if the 'Thesis' hypothesis is correct then tyrosine 527 in the C-terminal tail of the protein would be expected to be nitrated. This could be determined by a protein digest followed by LC-MS analysis on the generated fragments. The identification of nitrated Src could also be sought in other tumours, as this modified protein is potentially general epigenetic mechanism through which cells could undergo transformation. Further to these studies, proteins that are known to modulate the activity of non-modified Src (e.g., Csk and proteins that alter the intramolecular SH3 binding in Srcshould also be investigated to determine their effect on ability of nitrated Src to phosphorylate known substrates.

In conclusion, the inability of nDS4 to bind to the SH2 domain of Fyn suggests a wholly new aspect of the potential harmful effects of protein tyrosine nitration, in addition to known and suggested toxicities. Of particular concern is the potential

activation of Src kinases, the unregulated control of which are known to lead to cell transformation (see above). The work presented in this thesis, particularly on the interaction of the nitropeptide/SH2 domain, has added a valuable insight into our understanding of the role that nTyr residues play in cell function, a fascinating and expanding area of biomedical research.

REFERENCES

Abdalla, D. S. P. and Moriel, P. (1997) Nitrotyrosine bound to apolipoproteins as biomarker of peroxynitrite formation in atherosclerosis. Atherosclerosis, **134**, 219-220.

Al-Obeidi, F. A., Wu, J. J., and Lam, K. S. (2001) Protein Kinases: Structure, substrate specificity and drug discovery. Biopolymers - Peptide Science Section, **47** 197-223.

Alexander, D. R., Hexham, J. M., Lucas, S. C., Graves, J. D., Cantrell, DA, and Crumpton, M. J. (1989) A protein kinase C pseudosubstrates peptide inhibits phosporylation of the CD3 antigen in Streptolysin-O-permeabilisation human T lymphocytes. Biochemical Journal **260**, 893-901.

Anonymous. (1998) New inhibitors of SH2-mediated processes. Expert Opinion on Therapeutic Patents, **8**, 333-335.

Ara, J., Przdbrski, Niani, A., B., Jackson-Lewis, V., Trifiletti, R., R., Horwitz, J. and Ischiropoulus, H. Inactivation of tyrosine hydroxylase by nitration following exposure to peroxynitrite an MPTP. Proceedings of the National Academy of Science United State of America **95**, 7659-7663.

Aronheim, A. (2000) Protein recruitment systems fir the analysis of protein-protein interactions.

Aulak, K., S., Miyagi, M., Yan, L., West, K. A., Massillon, D. and Crabb, J. W. and Stuehr, D. J. (2001) Proteomic method identifies proteins nitrated *in vivo* during inflammatory challenge. Proceedings of the National Academy of Science, United States of America **98**, 12056-12061.

Bagrodia, S., Chackalaparampil, I., Kmiecik, T. E. and Shalloway, D. (1991) Altered tyrosine 527 phosphorylation and mitotic activation of $p60^{c\text{-}src}$. Nature **349**, 172-175.

Bakhtia, R. and Tse, F. L. S. Biological mass spectrometry: a primer (2000) Mutagenesis **15**, 415-430.

Balabanli, B., Kamisaki, Y., Martin, E., and Murad, F. (1999) Requirement for heme and thiols for the nonenztymatic modification of nitrotyrosine. Proceedings of The National Academy of Sciences of The United States of America **96**, 13136-13141.

Bapat, S., Verkleij, A. and Post J. A. (2001) Peroxynitrite activates mitogen-activated protein (MAPK) via a MEK-independent pathway: a role for protein kinase C. FEBS Letters **499**, 21-26.

Bartlett, D., Church, D., F., Bounds, P., L. and Koppenol, W., H. (1995) The kinetics of the oxidation of L-ascorbic acid by peroxynitrite. Free Radical and Medicine in Biology **18**, 85-92.

Beckman, J. S., Ischiropoulos, I., Zhu, L., van der Woerd, M., Smith, C., Chen, J., Harrison, J., Martin, J. C. and Tsai, M. (1992). Kinetics of superoxide dismutase- and

iron-catalysed nitration of phenolics by peroxynitrite. Archives of Biochemistry and Biophysics **298**, 438-445.

Beckman, J. S., Ye, Y., Anderson, P. G., Chen, J., Accavitti, M. A., Tarpey, M. M. and White C. R. (1994). Extensive nitration of protein tyrosines in human athlerosclerotic plaques. Biological Chemistry **375**, 81-88.

Berlett, B. S., Friguet, B., Yim, M. B., Chock, P. B., and Stadtman, E. R. (1996) Peroxynitrite-mediated nitration of tyrosine residues in E. Coli glutamine synthetase mimics adenylylation: relevance to signal transduction. Proceedings of The National Academy of Sciences The United States of America **93**, 1776-1780

Boulos, C., Jiang, H., and Balazy, M. (2000) Diffusion of peroxynitrite into human platelet inhibits cyclooxygenase via nitration of tyrosine residues. Journal of Pharmacology & Experimental Therapeutics **293**, 222-229.

Bourassa, J., L., Ives, E., P., Marqueling, A., L., Shimanovich, R. and Grooves, T. (2001) Myoglobin catalyses its own nitration. Journal of the American Chemical Society .

Boyd and Cadenas (2002) Nitric oxide in cell signalling pathways in mitochondrial-dependant apoptosis. Biological Chemistry **383**, 411-423.

Bradshaw, J. M., Mitaxov, V., and Waksman, G. (2000) Investigation by the SH2 domain of the Src kinase. Journal of Molecular Biology **299**, 521-535.

Bradshaw, J. M., Mitaxov, V., and Waksman, G. (1999) Investigation of phosphotyrosine recognition by the SH2 domain of the Src kinase. Journal of Molecular Biology **293**, 971-985.

Bredt, D. S. and Snyder, S. H. (1994) Nitric oxide: a physiological messenger molecule Annual Review of Biochemistry **63,** 179- 195

Brown, G., C. (1995) Nitric oxide regulates mitochondrial respiration and cell functions by inhibiting cytochrome oxidase. FEBS Letters **369**, 136-139.

Brown, M. T. and Cooper, J. A. (1996) Regulation, substrate and functions of Src. Biochimica et Biophysical Acta **1287**, 121-149.

Brunati, A. M., James, P., Donella-Deana, A., Matoskova, B., Robbins, K. C., and Pinna, L. A. (1993) European Journal of Biochemistry **216**, 323-327.

Brunati, A. M., Pinna, L. A., Bergantino, E., Ruzzene, M., Cirri, P., Ramponi, G., and Donella-Deana, A. (1998) Src homology-2 doamins protect phosphotyrosyl residues against enzymatic dephosphorylation. Biochemical & Biophysical Research Communications **243**, 700-705.

Bryk, R., Griffin, P., and Nathan, C. (2000) Peroxynitrie reductase activity of bacterial peroxiredoxins. Nature **407**, 211-215.

Burley, S. K. and Petsko G. A. (1986) Amino-aromatic interactions in proteins. FEBS Letters **203**, 139

Burlingame, A. L., Boyd, R., K. and Gaskell, S. J. (1996) Mass spectrometry. Analytical chemistry **68**, 599-651.

Cantley, L. C., Auger, K. R., Carpenter, C., Duckworth, B., Graziani, A, Kapeller, R., and Soltoff, S. (1991) Oncogenes and signal transduction. Cell **64**, 281-302.

Cario and Franck (1923) Z. Physik **7**, 202.

Chavanieu, A., Keane, N. E., Quirk, P. G., Levine, B. A., Calas, B., Wei, L., and Ellis, L. (1994) Phosphorylation effects on flanking charged residues. Structural implications for signal transduction in protein kinases. European Journal of Biochemistry 224, 115-123.

Chen, H. I. and Sudol, M. (1995) The WW domain of Yes associated protein binds a proline-rich ligand that differs from the consensus established for Src homology 3-binding modules. Proceeding of the National Academy of Science, United States of America **92**, 7819-7823.

Cheng, H. I. and Sudol, M. (1995) The WW domain of Yes-associated protein binds a proline-rich ligand that differs from the consensus established for Src homology 3-binding modules. Proceedings Of The National Academy Of Sciences Of The United States Of America **92** 7810-7823.

Chung, E. W., Henriques, D. A., Renzoni, D., Morton, C. J., Mulhern, TD, Pitkeathly, M. C., Ladbury, J. E., and Robinson, C. V. (1999) Probing the nature of the interactions in SH2 binding interfaces-evidence from electrospray ionisation mass spectrometry. Protein Science **8**, 1962-1970.

Claesson-Welsh, L. (1994) Platelet-derived growth factor receptor signals. Journal of Biological Chemistry **269**, 32023-32026.

Clements, J. L., Boerth, N. J., Lee, J. R., and Koretzky, G. A. (1999) Integration of T cell receptor-dependant signalling pathways by adaptor proteins. Annual Review of Immunology **17**, 89-108

Cohen, G. B., Ren, R. and Baltimore, D. (1995) Modular binding domains in signal transduction proteins. Cell **80**, 237-248.

Cole, P. A., Sondhi, D. and Kim, K. (1999) Chemical approaches to the study protein tyrosine kinases and their implication for mechanisms and inhibitor design. Pharmacology and Therapeutics **82**, 219-229.

Crow, J., Ye, Y.Z., Strong, M., Kirk, M., Barnes, S. and Beckman, J., S. (1997) Superoxide dismutase catalyses nitration of tyrosines by peroxynitrite in the rod and head domains of neurofilament-L. Journal of Neurochemistry **69**, 1945-1953.

Cross, A. H., Manning, P., T., Keeling, R., M., Schmidt, R. E. and Misko, T., P. (1998) Peroxynitrite formation within the central nervous system in active multiple sclerosis. Journal of Neuroimmunolgy **88**, 45-56.

Curcuruto O, Rovatti L, Pastorino AM, Hamdan M. (1999) Peptide nitration by peroxynitrite: characterisation of the nitration sites by liquid chromatography tandem mass spectrometry. Rapid Communications In Mass Spectrometry **13**, 156-163.

Da Silva, A. J., Yamamoto, M., Zalvan, C. H. and Rudd, C. E. (1992) Engagement of the Tcr/CD3 complex stimulates $p59^{fyn(T)}$ activity: detection of associated proteins at 72 and 120-130 KD. Molecular Immunology **29**, 1417-1425.

Da Silva, A. J., Rosenfeild, J. M., Mueller, I., Bouton, A., Hirai, H. and Rudd, C. E. (1997) Biochemical analysis of p120/130 A protein-tyrosine kinase substrate restricted to T and myeloid cells. The Journal of Immunology **158**, 2007-2016.

Da Silva, A. J., Janssen, O., and Rudd, C. E. (1993) T cell receptor ζ/CD3-$p59^{fyn(T)}$-associated p120/130binds to the SH2 domain of $p59^{fyn(T)}$. Journal of Experimental Medicine **178,** 2107-2113.

Darley-Usmar, V. M., McAndrew, J., Patel, R., Moellering, D., Lincoln, T. M., Jo, H., Cornwell, T., Digerness, S., and White, C. R. (1997) Nitric oxide, free radicals and cell signalling in cardiovascular disease. Biochemical Society Transactions **25**, 925-929.

Denicola, A., Freeman, B. A., Trujillo, M., and Radi, R. (1996) Peroxynitrite reaction with carbon dioxide/bicarbonate kinetics and influence on peroxynitrite-mediated oxidations. Archives of Biochemistry & Biophysics **333**, 49-58.

Di Stasi, A. M. M., Mallozzi, C., Macchia, G., Petrucci, T. C., and Minetti, M. (1999) Peroxynitrite induces tyrosine nitration and modulates tyrosine phosphorylation of synaptic proteins, Journal of Neurochemistry **73**, 727-735.

Doel, J. J., Godber, B. L. J., Goult, T. A., Eisenthal, R, and Harrison, R. (2000) Reduction of organic nitrites to nitric oxide catalysed by xanthine oxidase:possible role in the metabolism of nitrovasodialators. Biochemical & Biophysical Research Communications **270**, 880-885.

Dollery, C. (1995) Nitric oxide. In Therapeutic Drugs. N109-N113. Churchill Livingstone, Edinburgh.

Dunant NM, Messerschmitt AS, BallmerHofer K. (1997) Functional interaction between the sh2 domain of fyn and tyrosine 324 of hamster polyomavirus middle-t antigen. Journal Of Virology, **71**, 199-206.

Eck, M. J., Shoelson, S. E., and Harrison, S. C. (1993) Spatial constraints on the recognition of phosphoproteins by the tandem SH2 domains of the phosphatase SH-PTP2. Nature **362**, 87-91.

Eckert, K. G. and Eyer, P. (1983) Differences in the reactions of isomeric ortho and para-aminophenols with hemoglobin. Biochemical Pharmacology **32**, 1019-1027.

Eiserich, J., P., Patel, R., P. and O'Donnell, V., B. (1999) Pathophysiology of nitric oxide and related species: free radical reactions and modifications of biomolecules. Molecular Aspects of Medicine **19**, 221-357.

Eiserich, J. P., Estevez, A. G., Bamberg, T., Ye, Y. Z., Beckman, J. S., Chumley, P., H. and Freeman, B. A (1996) Microtubule dysfunction by posttranslational nitrotyrosination of alpha-tubulin: a nitric oxide dependent mechanism of cellular injury. Proceedings of the National Academy of Science, United States of America **96**, 6365-6370

Eiserich, J. P., Cross, C. E., Jones, A. D., Halliwell, B.and van der Vleit, A. (1996) Formation of nitrating and chlorinating species by reaction of nitrite with hypochlorous acid: a novel mechanism for nitric-oxide mediated protein modification. Journal of Biological Chemistry **271**, 19199-19028

Eiserich, J. P., Hristova, M., Cross, C. E., Jones, A. D., Freeman, B. A., Halliwell, B., and Van der Vliet, A. (1998) Formation of nitric oxide-derived inflammatory oxidants by myeloperoxdase in neutrophils Nature **391**, 393-397.

Erpel, T., Superti-Furga, G. and Courtneidge, S. A. (1995) Mutational analysis of the Src SH3 domain: the same residues of the ligand binding surface are important for intra- and intermolecular interactions. The EMBO Journal **14**, 963-975.

Felder, S., Zhou, M., Hu, P., Urena, J., Ullrich, A., Chaudhuri, M, White, M., Shoelson, S. E., and Schlessinger, J. (1993) SH2 domains exhibit high-affinity binding to tyrosine-phosphorylated peptides yet also exhibit rapid dissociation and exchange. Molecular & Cellular Biology, **13**, 1449-1455.

Feldman P, L., Griffith O, W., Stuehr D, J. (1993) The surprising life of nitric oxide. C&EN **20**, 26-38.

Forster, T. (1959). Transfer mechanisms of electronic excitation. Discussions of the Faraday Society **27**, 7-17.

Gao, Y., Luo, J., Yao, Z.-J., Guo, R., Zou, H., Kelley, J., Voigt, JH, Yang, D., and Burke, T. R., Jr. (2000) Inhibition of Grb2 SH2 domain binding by non-phosphate-containing Ligands. 2.4-(2-Malonyl) phenalanine as a potent phosphotyrosyl mimetic. Journal of Medicinal Chemistry **43**, 911-920.

Geng, L., Pfister, S., Kraeft., S. and Ruud, C. E. (2001) Adapter FYB (Fyn-binding protein) regulates integrin-mediated adhesion and mediator release: differential involvement of the FYB SH3 domain. Proceeding of the National Academy Science, United States of America **98**, 11527-11532.

Godber, B. L. J., Doel, J. J., Durgan, J., Eisenthal, R. and Harrison, R. (2000) A new route to peroxynitrite: a role for xanthine oxidoreductase. FEBS Letters **475**, 93-96.

Goldstein, S. and Czapski, G. (1995) The reaction of ntric oxide with superoxide and water: a pulse radiolysis study. Free Radical Biology & Medicine **19**, 505-510

Gole, M., D., Souza, J., M., Choi, I., Hertkorn, C., Malcom, S., Foust, R. F., Finkel, B., Lanken, P. N. and Ischiroploulos (2000) Plasma proteins modified by tyrosine nitration in acute respiratory distress syndrome. American Journal of Physiology **278**, L961-L967.

Good, P. F., Hsu, P., Werner, P., Perl, D. P. and Olanow, C. W. (1998) Protein nitration in Parkinson's disease. Journal of Experimental Neuropatholgy and Neurology **57**, 338-342.

Goodwin, D. C., Gunther, M. R., His, L. C., Cresw, B. C., Eling, T. E., Manson, R. P. and Marnett, L. J. (1998) Nitric oxide trapping of tryosyl tadicals generated during prostaglandin endoperoxide synthase turnover: detection of the radical derivative of tyrosine. Journal of Biological Chemistry **273**, 8903-8909.

Gow, A., Duran, D., Thom, S. R., and Ischiropoulos, H. (1996) Carbon dioxide enhancement of peroxynitrite mediated protein tyrosine nitration. Archives of Biochemistry & Biophysics **333**, 42-48.

Gow AJ, Duran D, Malcolm S, Ischiropoulos H. (1996) Effects of peroxynitrite-induced protein modifications on tyrosine phosphorylation and degradation. FEBS Letters **385**, 63-66.

Gow, A. J., Chen, Q., Hess, D. T., Day, B. J., Ischiropoulos, I. and Stamler, J. S. (2002) Basal and stimulated protein S-nitrosoylation in multiple cell types and tissue. Journal of Biological Chemistry **277**, 9367-9640.

Greenacre, S. A. B., Evans, P., Halliwell, B. and Brain S. D. (1999) Formation and loss of nirated proteins in peroxynitrite-treated rat skin in vivo. Biochemical and Biophysical Research Communications **262**, 781-786.

Greenacre and Ischiroploulos (2001) Tyrosine nirtration: localisation, quantification, consequences for protein function and signal transduction. Free Radical Research **34**, 541-581.

Greis, K., D., Zhu, S. and Matalon. (1996) Identification of nitration sites on Surfactant protein A by tandem electrospray mass spectrometry. Archives of Biochemistry and Biophysics **335**, 396-402.

Groves, J., T. (1999) Peroxynitrite: reactive, invasive and enigmatic. Current Opinion in Chemical Biology **3**, 226-235.

Grune, T., Blasig, I. E., Sitte, N., Roloff, B., Haseloff, R., and Davies, K. J. A. (1998) Peroxynitrite increases the degradation of aconitase and other cellular proteins by proteosome.Journal Of Biological Chemistry **273**, 10857-10862.

Halliwell, B. (1997) What nitrates tyrosine? Is nitrotyrosine specific as a biomarker of peroxynitrite formation *in vivo*. FEBS Letters **411**, 157-160

Halliwell, B., Zhao, K., and Whiteman, M. (1999) Nitric oxide and peroxynitrite. The ugly, the uglier and the not so good. Free Radical Research **31**, 651-669.

Hancock, J. T. (1997) Protein Phosphorylation, Kinase and Phosphatases. Cell Signalling. Longman, Harlow.

Harlan, J. E., Hajduk, P. J., Yoon, H. S., Fesik, S. W. (1994) Plectrin homology domains bind to phosphatidylinositol 4,5-bisphosphate. Nature **371**, 168-170.

Harrison SC. (1996) Peptide-surface association: The case of PDZ and PTB domains. Cell **86**, 341-343

Hensley, K., Robison K. A., Gabbita S., P., Salsman S. and Floyd R. A. (2000) Reactive oxygen species, cell signalling and cell injury. Free Radical Biology and Medicine **28**, 1456-1456.

Hess, D. T., Matsumoto, A., Nudelman, R., and Stamler, J. S. (2001) S-nitrosylation: spectrum and specificity. Nature Cell Biology **3**, E46-E49.

Huttner (1987) Protein tyrosine sulfation. Trends in Biological Sciences **12**, 361-363.

Hurley, J., Thorsness, P., E., Ramalingnam, V., Helmers, N., H., Koshland, D., E. and Stroud, R.M. (1989) Structure of a bacterial enzyme regulated by phosphorylation, isocitrate dehydrogenase. Proceedings of the National Academy of Science United States of America **86**, 8635-8639.

Ignarro, L J., Buga, G M., Wood, K S., Byrns, R E., and Chaudhuri, G. (1987) Endotheliai-derived relaxing factor produced and released from artery and vein is nitric oxide. Proceedings of the National Academy of Science **84**, 9265-9569.

Ischiropoulos, H. (1998) Biological tyrosine nitration: a pathological function of nitric oxide and reactive oxygen species. Archives of Biochemistry And Biophysics **356**, 1-11

Johnson, L., N. (1992) Glycogen phosporylase:control by phos[]phorylation and allosteric effects. FASEB Journal 6, 2274-2282.

Johnson, L. N., Lowe, E. D., Noble, M. E. M. and Owen, D. J. (1998) The structural basis for substrate recognition and control by kinases. FEBS Letters **430**, 1-11.

Jonnala R. R. and Buccafuusco. J. J. (2001) Inhibition of nerve growth factor signalling by peroxynitrite. Journal of Neuroscience Research **63**, 27-34

Jope, R. S., Zhang, L., and Song, L. (2000) Peroxynitrite modulates the activation of p38 and extracellular regulated kinases in PC12 cells. Archives of Biochemistry & Biophysics **376**, 365-370.

Juraschek, R., Dulcks, T. and Karas M. (1999) American Society for Mass Spectrometry **10**, 300-308.

Kamisaki, Y., Wada, K., Bian, K., Balabanli, B., Davis, K., Martin, E., Behbod, F., Lee, Y.-C., and Murad, F. (1998) An activity in rats tissue that modifies nitrotyrosine containing proteins Proceedings of the National Academy of Sciences of The United States Of America **95**, 11584-11589.

Kaur, H. and Halliwell, B. (1994) Evidence for nitric oxide-mediated oxidative damage in chronic inflammation. Nitrotyrosine in the synovial fluid from rheumatoid patients. FEBS Letters **350**, 9-12.

Kavanaugh, W. M. and Williams, L. T. (1999) Signalling through receptor tyrosine kinases. In Heldin, C. and Purton, M., editors. Signal Transduction, Chapman and Hall, London.

Kikugawa, K., Kato, T. and Okamato, Y. (1994) Free Radical Biology and Medicine **16**, 373-382.

Kim, K. and Cole, P. A. (1997) Measurement of a Bronsted nucleophile coefficient and insights into the transition state for a protein tyrosine kinase. Journal of the American Chemical Society **119**, 11096-11097.

Kim, K. and Cole, P. A. (1998) Kinetic analysis of a protein tyrosine kinase reaction transition state in the forward and reverse directions. Journal of the American Chemical Society **120**, 8651-8568.

Kim, K., Parang, K., Lau, D. O. and Cole, P. A. (2000) tyrosine analogues as alternative substrates for proteintyrosine kinase Csk: insights into substrate selectivity and catalytic mechanism. Bioorganic and Medicinal Chemistry **8**, 1263-1268.

Kim, Y.-M., Kim, T.-H., Chung, H.-T., Talanian, R. V., Yin, X.-M., and Billiar, T. R. (2000) Hepatology 32, (pp 770-778)

Kim, Y.-M., Kim, T.-H., Seol, D.-W., Talanian, R. V., and Billiar, T. R. (1998) Journal Of Biological Chemistry 273, (pp 31437-31441)

Kim, Y.-M., Talanian, R. V., Li, J., and Billiar, T. R. (1998) Journal of Immunology 161, (pp 4122-4128)

Kinsella, J. P. and Abman, S. H. (1999) Recent developments in inhaled nitric oxide therapy of the newborn. Current Opinion in Pediatrics **11**, 121-125.

Kinsella, J. P., Ivy, D. D., and Abman, S. H. (1994). American Journal of Physiology **267**, H1955-H1961

Kiroycheva, M., Ahmed, F., Anthony, G. M., Szabo, C., Southan, G. J., and Bank, N. (2000) Journal of the American Society of Nephrology 11, (pp 1026-1032)

Klevan, L. and Tse, Y. C. (1983) Chemical modification of essential tyrosine residues in DNA topisomerse. Biochimica et Biophysica Acta **745**, 175-180.

Kong S, Moon Bin Yim, Stadtman ER, Chock PB. (1996) Peroxynitrite disables the tyrosine phosphorylation regulatory mechanism: Lymphocyte-specific tyrosine kinase fails to phosphorylate nitrated cdc2(6- 20)NH2 peptide. Proceedings f The National Academy of Sciences of The United States of America **93**, 3377-3382.

Kooy, N. W. and Lewis, S. J. (1996) The peroxynitrite product 3-nitrotyrosine attenuates the hemodynaic responses to angiotensin II. European Journal of Pharmacology **315**, 165-170.

Krainev, A. G., Williams, T. D., and Bigelow, D. J. (1998) Enzymatic reduction of 3-nitrotyrosine generates superoxide. Chemical Research In Toxicology **11**, 495-502.

Krausse, M., Sechi, A. S., Konradt, M., Monner, D. and Gertler, F. B. (2000) Fyn-binding protein (Fyb)/SLP-76-associated protein (SLAP), Ena/Vasodialotor-stimulated phosphoprotein (VASP) proteins and the Arp2/3 complex link T cell receptor (TCR) signalling to the actin cytoskeleton. Journal of Cell Biology **149**, 181-194.

Kuby, J. (1994) Immunology. W. H. Freeman and Company. New York.

Kuo, W., Kanadia, R. N., Shanbhag, V. P., and Toro, R. (1999) Denitration of peroxynitrite-treated proteins by 'protein nitratases' from rat brain and heart. Molecular & Cellular Biochemistry **201**, 11-16.

Kuo, W. N., Kanadia, R. N., and Shanbhag, V. P. (1999) Dentration of peroxynitrite-treated proteins by 'protein nitratases' from rat brain and heart. Biochemistry & Molecular Biology International **47**,1061-1067.

Kuriyan, J. and Cowburn, D. (1997) Modular peptide recognition domains in eukaryotic signalling. Annual Review of Biophysics & Biomolecular Structure **26**, 259-288

Ladbury, J. E., Lemmon, M. A., Zhou, M., Green, J., Botfield, M. C., and Schlessinger, J. (1995) Measurement of the binding of tyrosyl phosphpeptides to SH2 domains: a reappraisal. Proceedings of The National Academy of Sciences of The United States Of America 92, 3199-3203

Lander, H. M. (1997) FASEB Journal **11**, 118-124.

Lander, H. M., Ogiste, J. S., Teng, K. K., and Novogrodsky, A. (1995) Nitric oxide-stimulated guanine nucleotide exchange on $p21^{ras}$. Journal of Biological Chemistry **270**, 21195-21198.

Lander, H. M., Ogiste, J. S., Teng, K. K., and Novogrodsky, A. (1995) $p21^{ras}$ as a common signalling target of reactive free radical and cellular redox stress. Journal of Biological Chemistry **270**, 21195-21198.

Lander, H. M., Milbank, A. J., Tauras, J. M., Hajjar, D. P., Hempstead, BL, Schhwartz, G. D., Kraemer, R. T., Mirza, U. A., Chait, B. T., Campbell Burk, S., and Quilliam, L. A. (1996) Redox regulation nof cell signalling Nature **381**, 380-381.

Levonen, A.-L., Patel, R. P., Brookes, P., Go, Y.-M., Jo, H., Parthasarathy, S., Anderson, P. G., and Darley-Usmar, V. M. (2001) Mechanisms of cell signalling by nitric oxide and peroxynitrite : from mitochondria to MAP kinases. Antioxidants & Redox Signaling **3**, 215-229.

Lee, T. R., Niu, J. and Lawerence, D. S. (1994) Phenol kinase activity of the serine/threonine-specific cAMP-dependant protein kinase: steric and electronic effects. Biochemistry **33**, 4245-4250

Lewis, R., S., Tannenbaum, S., R. and Deen, W., M. (1995) Kinetics of N-nitrsationin oxygenated nitric oxide solutions at physiological pH: role of nitrous anhydride and effects of phosphate and chloride. Journal of the American Chemical Society **117**, 3933-3939.

Li, S., Songyang, Z., Sebastien J. F., Zwahlen, C., Wiley S., Cantley L., Kay L. E., Forman-Kay, J., Pawson T. High-affinity binding of the drosphila numb phosphotyrosine-binding domain to peptides containing a Gly-Pro-(p)Tyr motif (1997). Proceedings Of The National Academy Of Sciences Of The United States Of America **94**, 7204-7209.

Li, X., De Sarno, P., Song, L., Beckman, J. S., and Jope, R. S. (1998) Peroxynitrite modulates tyrosine phosphorylation and phosphoinositide signalling in humanneuroblastoma SH-SY5Y cells: attenuated effects in human 1321N1 astrocytoma cells. Biochemical Journal **331**, 599-606.

Little, M., J., Paquette, Paquette, D., M., Harvey, M., D.and Banks, P., R. (1997) Single-label fluourescent derivatization of peptides. Analytica Chimica Acta **339**, 279-288.

Liu, J., Kang, H., Raab, M., da Silva, A. J., Kraeft S. and Ruud, C. E. FYB (FYN binding protein) serves as a binding partner for lymphoid protein and FYN kinase substrate SKAP55 and a SKAP55-related protein in T cells. Proceedings of The National Academy of Sciences of The United States of America **95**, 8779-8784

Liu, L., Hausladen, A., Zeng, M., Que, L., Heitman, J., Stamler, and JS. (2001) A metabolic enzyme for S-nitrosothiol conserved from bacteria to humans. Nature **410**, 490-494.

Lodish, H., Baltimore, D., Berk, A., Zipursky, S. L., Matsudaria, P., and Darnell, J. (1995) Cell-to-Cell Signalling: Hormone and Receptors. Molecular Cell Biology, Scientific American Books, New York

Loo, J. A., Hu, P., McConnell, P., Mueller, W. T., Sawyer, T. K., and Thanabal, V. (1997) Study of a Src SH2 domain protein-phosphopeptide binding interactions by electrospray ionisation mass spectrometry. Journal of the American Society for Mass Spectrometry **8**, 234-243.

Low. S. Y., Sabetkar. M., Bruckdorfer K. R. and Nasseem K. M. (2002) The role of protein nitration in the inhibition of platelet activation by peroxynitrite. FEBS **511**, 59-64.

MacMillanCrow, L. A., Crow, J. P., Kerby, J. D., Beckman, J. S. and Thompson, J. A. (1996) Nitration and inactivation of manganese superoxide dismutase in chronid rejection of human renal allografts. Proceedings of the National Academy of Science, United States of America **93**, 11853-11858

MacMillanCrow, L. A., Crow, J. P., and Thompson, J. A. (1998) Peroxynitrite-mediated inactivation of manganese superoxide dismutase involves nitration and oxidation of critical tyrosine residues. Biochemistry **37**, 1613-1622

MacMillian-Crow, L. A., Greendorfer, J. S., Vickers, S. M. and Thompson, J. A. (2000) Archives of Biochemistry and Biophysics **377**, 350-356.

Mallozzi, C., Maria, A., Di Stasi, M. and Minetti, M.(1999) Activation of src tyrosine kinases by peroxynitrite. FEBS Letters **456**, 201-206.

Mallozzi, C., Maria, A., Di Stasi, M. and Minetti, M. (2001) Nitrotyrosine mimics phosphotyrosine binding to the SH2 domain of the Src family tyrosine kinase lyn. FEBS **503**, 189-195.

Mania, F., Casagranda, F., Audero, E., Simeone, A., Comoglio, P. M., Klein, R. and Ponzetto, C. (1996) Uncoupling of Grb2 from the Met receptor in vivo reveals complex roles in muscle development. Cell **87**, 531-542.

Marie-Cardine, A., Verhagen, A. M., Eckerkorn, C. and Schraven, B. (1998) SKAP-HOM, a novel adaptor protein homology to the FYN-associaion protein SKAP-55. FEBS Letters **435**, 55-60

Marshall, H. E., Merchant, K., and Stamler, J. S. (2000) Nitrosation and oxidation in the regulation gene expression. FASEB Journal **14**, 1889-1900

Mayer, B. (1999) Protein-protein interactions in signaling cascades. Molecular biotechnology **13**, 201-213.

Mayer, B. J., Jackson, P. K., Van Etten, R. A., and Baltimore, D. (1992) Point mutation in the *abl* SH2 domain co-ordinately impair phosphotyrosine binding *in vitro* and transforming activity *in vivo*. Molecular & Cellular Biology 12, (pp 609-618)

Mayer, B. J. (1999) Protein-protein interactions in signalling cascades. Molecular Biotechnology **13**, 201-213.

Medek, A., Hajuk, P., J., Mack J. and Fesik, S., W. (2000) The use o differential chemical shifts for determining the binding site location and orientation of protein-bound ligands. Journal of the American Chemical Society **122**, 1241-1242.

Mendelsohn, A. R. and Brent, R. (1999) Protein interaction methods-towards an endgame. Science **284**, 1948-1950.

Michnick, S. W. (2001) Exploring protein interaction-induced folding of proteins from complementary peptide fragments. Current Opinion in Structural Biology **11**, 472-477.

Mirza, U. A., Chait, B. T., and Lander, H. M. (1995) Monitoring reactions of nitric oxide with peptides and proteins by electrospray ionisation mass spectrometry. Journal Of Biological Chemistry **270**, 17185-17188.

Monteiro, H. P. (2002) Signal transduction by protein tyrosine nitration: competition or cooperation with tyrosine phosphorylation-dependent signalling events? Free Radical Biology and Medicine **33**, 765-773.

Moriel, P. and Abdalla, D. S. P. (1997) Nitrotyrosine bound to β-VLDL-apoproteins: a biomarker of peroxynitrite formation in experimental athlerosclerosis. Biochemical and Biophysical Research Comminucations **232**, 332-335.

Mondoro T. H., Shafer BC, Vostal JG. (1997) Peroxynitrite-induced tyrosine nitration and phosphorylation in human platelets. Free Radical Biology & Medicine **22**, 1055-1063.

Mulhern TD, Shaw GL, Morton CJ, Day AJ, Campbell ID. (1997) The SH2 domain from the tyrosine kinase Fyn in complex with a phosphotyrosyl peptide reveals insights into domain stability and binding specificity. Structure **5**, 1313-1323.

Murphy, M. P., Packer, M. A., Scarlett, J. L., and Martin, S. W. (1998) Peroxynitrite: a biologically significant oxidant. General Pharmacology **31**, 179-186.

Musci, M. A., Hendricks-Taylor, L. R., Motto, D. G., Paskind, M., Kamens, J., Turck, C. W., and Koretzky, G. A. (1997) Molecular cloning of SLAP-130, an SLP-76-associated substrate of the T cell antigen receptor-stimulated protein tyrosine kinases. Journal of Biological Chemistry **272**, 11674-11677.

Neilsen A, T. (1995) Introduction and Tetranitromethane. In: Nitrocarbons. 1-72. VCH Publishers, New York.

Nguyen, T., Brunson, D., Crespi, C. L., Penman, B., W., Wishok, J., S. and Tannenbaum, S. R. (1992) DNA damage and mutation in human cells exposed to nitric oxide. Proceedings of the National Academy of Sciences of the United States of America **89**, 3030-3034.

Nicholson, S. E., Starr, R., Novak, U., Hilton, D. J. and Layton, J. E. (1996) Tyrosine residues in the granulocyte colony-stimulating factor (G-CSF) receptor mediat G-CSF-induced differentiation of murine myeloid leukemic (M1) cells. Journal of Biological Chemistry 271, 26947-26953.

O'Bryan J. P., Lambert Q. T. and Der C. J. (1998) The Src homology 2 and phosphotyrosine binding domains of the ShcC adaptor protein function as inhibitors of mitogenic signaling by the epidermal growth factor receptor. Journal of Biological Chemistry **273**, 20431-20437.

Oh-hashi, K., Maruyama, W., and Isobe, K. (2001) Peroxynitrite induces GADD34, 45 and 153 via p38 MAPKin human neuroblastoma SH-SY5Y cells. Free Radical Biology & Medicine **30**, 213-221.

Ohshima H, Friesen M, Brouet I, Bartsch H. (1990) Nitrotyrosine as a new marker for endogenous nitrosation and nitration of proteins. Food & Chemical Toxicology, **28**, 647-652.

Oldreive, C., Zhao, K., Paganga, G., Halliwell, B., Rice-Evans, and C. (1998) Inhibition of nitrous acid-dependent tyrosine nitration and DNA base deamination by flavanoids and other phenolic compounds. Chemical Research In Toxicology **11**, 1574-1579.

Oldreive, C. and Rice-Evans, C. (2001) The mechanisms for the nitration and nitrotyrosine formation *in vitro* and *in vivo*: impact of diet. Free Radical Research **35**, 215-231.

Ottinger, E. A., Botfield, M. C., and Shoelson, S. E. (1998) Tandem SH2 domains confer high specificity in tyrosine kinase signalling. Journal of Biological Chemistry **273**, 729-735.

Packer, M. A. and Murphy, M. P. (1997) Peroxynitrite formed by the simultaneous nitric oxide and superoxide generation causes cyclosporin-A-sensitive mitochondrial calcium efflux and depolarisation. European Journal of Biochemistry **234**, 231-239.

Pannala, A., Razaq, R., Halliwell, B. and Rice-Evans, C. (1998) Inhibition of peroxynitrite dependent tyrosine nitration by hydroxycinnamates: nitration or electron donation. Free Radical Biology and Medicine **24**, 594-606.

Park, K., Moreland, R., B., Goldstein, I., Atala, A. and Traish, A. (1998) Sildenafil inhibits phosphodieasterase type 5 in human clitoral corpus smooth muscle. Biochemical and Biophysical Reseach Communications **249**, 612-617.

Patel, R., P., McAndrew, J., Sellak, H., White, C., R., Jo, H., Freeman, B., A., Darley-Usmar, V.,M. (1999) Biological aspects of reactive nitrogen species. Biochimica et Biophysica Acta **1411**, 385-400.

Pawloski, J. R., Hes, D. T., and Stamler, J. S. (2001) Nature 409, (pp 622-626)

Pawson T. (1994) SH2 and SH3 domains in signal transduction. Advances in Cancer Research **64**, 87-110.

Pawson T. (1995) Protein modules and signalling networks. Nature **373**, 573-580.

Pawson. T., Gish, G. D. and Nash, P. (2001) SH2 domains, interaction modules and cellular wiring. Trends in Cell Biology **11**, 504-511.

Payne, G., Shoelson, S. E., Gish, G. D., Pawson, T., and Walsh, C. T. (1993) Kinetics of p56lck and p60src Src homology 2 domainbinding to tyrosine-phosphorylated peptides determined by a competition assay or surface plasmon resonance. Proceedings Of The National Academy Of Sciences Of The United States Of America **90**, 4902-4906.

Pearce, L. L., Pitt, B. R., and Peterson, J. (1999) The peroxynitrite reductase activity of cytochrome c oxidase involves a two-electron redox reactionat heme a_3-Cu_B site Journal Of Biological Chemistry **274**, 35763-35767.

Peterson, E. J., Woods, M. L., Dmowski, S. A., Dermanov, G., Jordan, M. S., Wu, J. N., Myung, P. S., Liu, Q., Pribila, J. T., Freedman, B. D., Shimizu, Y. and Korestzky, G. A. (2001). Coupling of the TCR to integrin activation by SLAP-130/Fyb. Science **293**, 2263-2265.

Petersson, A., Steen, H., Kalume, D., E., Caidahl. K. and Roepstorff, P. (2001) Investigation of tyrosine nitration in proteins by mass spectrometry. Journal of Mass Spectrometry **36**, 616-625.

Pfeiffer, S., Mayer, B., and Hemmens, B. (1999) Nitric Oxide: Chemical Puzzles Posed by a Biological Messenger. Angew.Chem.Int.Ed. **38**, 1714-1731.

Piccione, E., Case, R. D., Domchek, S. M., Hu, P., Chaudhuri, M., Backer, J. M., Schlessinger, J., and Shoelson, S. E. (1993) Phosphatidylinositol 3-kinase p85 SH2 domain specificity difined by direct phosphopeptide SH2 domain binding. Biochemistry **32**, 3197-3202.

Pintar, A., Hensmann, M., Jumel, K., Pitkeathly, M., Harding, S. E., and Campbell, I. D. (1996) Solution studies of the SH2 domain from the Fyn tyrosine kinase: secondary structure, backbone dynamics and protein association. European Biophysics Journal **24**, 371-380.

Prigodich, R., V. and Sanaulla, A. (1991) Journal of Chemical Research, 66-67.

Pryor, W. A. and Squadrito, G. L. (1995) The chemistry of peroxynitrite: a product from the reactio of nitric oxide with superoxide. American Journal of Physiology - Lung Cellular & Molecular Physiology **268**, L699-L722.

Przybylski, M and Glocker, M. O. (1996) Electrospray mass spectrometry of biomolecular complexes with noncovalent interactions-new analytical perspectives for supramolecular chemistry and molecular recognition processes. Agnew. Chem. Int. Ed. Engl. **35**, 806-826.

Quijano, C., Alvarez, B., Gatti, R. M., Augusto, O., and Radi, R. (1997) Pathways of peroxynitrite oxidation of thiol groups. Biochemical Journal **322**, 167-173.

Rahuel, J., Garcia-Echeverria, C., Furet, P., Strauss, A., Caravatti, G., Fretz, H., Schoepfer, J., and Gay, B. (1998) Structural basis for the high affinity of amino-aromatic SH2 peptide ligands. Journal of Molecular Biology **279**, 1013-1022.

Rajajopal, P., Waygood, E. B., Reizer, J., Saier, M. H. and Klevit, R. E. (1992). Demonstrated of protein-protein interaction specificity by NMR chemical shift mapping. Protein Science **6**, 2624-2627.

Rameh, L. E., Chen, C., and Cantley, L. C. (1995) Phosphatidylinositol (3,4,,5)P_3 Interacts with SH2 domains and modulates PI 3-kinase association with tyrosine-phosphorylated proteins. Cell **83**, 821-830.

Rattle (1995) An NMR primer for life scientists. Partnership Press. Farenham.

Reid, G., E., Simpson, R. J. and O'Hair, R., A., J. (1998) A mass spectrometric an Ab Initio study of the pathways for dehydration of simple glycine and cysteine-containing peptide $[M+H]^+$ ions. American society for Mass Spectrometry **9**, 945-956.

Roberts, G. C. K. (1993) NMR of macromolecules a practical approach. IRL Press, Oxford.

Roberts, E. S., Lin, H. L., Crowley, J. R., Vuletich, J. L., Osawa, Y., and Hollenberg, P. F. (1998) Peroxynitrite-mediated nitration of tyrosine and inactivation of the catalytic activity of cytochrome P450 2B1. Chemical Research In Toxicology **11**, 1067-1074.

Sato M, Ozawa T, Yoshida T, Umezawa Y. (1999) A fluorescent indicator for tyrosine phosphorylation based insulin signaling pathways. Analytical Chemistry **71**, 3948-3954.

Sawyer, T. K. (1998) Src Homology-2 domains: Structure, mechanisms and drug discovery. Biopolymers **47**, 243-261.

Sayos, J., Wu, C., Morra, M., Wang, N., Zhang, X., Allen, D., van Schaik, S., Notarangelo, L., Geha, R., Roncarolo, M. G., Ottegen, H., De Vreis, J. E., Aversa, G. and Terhorst, C. (1998) The X-linked lymphoproliferative-disease gene product SAP regulates signals induced through the co-receptor SLAM. Nature **395**, 462-469.

Schieke, S. M., Briviba, K., Klotz, L.-O., and Sies, H. (1999) Activation pattern of mitogen-activated protein kinases elicited by peroxynitrite: attenuation by selenite supplementation. FEBS Letters **448**, 301-303.

Sicheri, F. and Kuriyan, J. (1997) Structures of Src-family tyrosine kinases. Current Opinion in Structural Biology **7**, 777-785.

Schmidt, H. H. H. W. and Walter, U. (1994) NO at work Cell **78**, 919-925

Seis, H., Sharov V., S., Klotz, L. and Briviba, K. (1997) Gluatathione peroxidase protects against peroxynitrite- mediated oxidations. Journal of Biological Chemistry **272**, 27812-27817.

Selvin, P. R. (2000) The renaissance of fluorescence resonance energy transfer. Nature Structural Biology **7**, 730-734.

Shigenaga MK, Lee HH, Blount BC, et al. (1997) Inflammation and NO(x)-induced nitration: Assay for 3-nitrotyrosine by HPLC with electrochemical detection. Proceedings of The National Academy of Sciences of The United States of America **94**, 3211-3216.

Simon, D. I., Mullins, M. E., Jia, L., Gaston, B., Singel, D. J., and Stamler, J. S. (1996) Polynitrosylated proteins:characterisation, bioactivity and functional consequences. Proceedings of The National Academy of Sciences of The United States of America **93**, 4736-4741

Siuzdak, G. (1994) The emergence of mass spectrometry in biochemical research.Proceedings of the National Academy of Science **91**, 11290-11297.

Smith, M. A., Harris, P. L. R. Sayre L. M., Beckman J. S. and Perry, G. (1997) Widespread peroxynitrite-mediated damage in Alzheimer's disease. Journal of Neuroscience **17**, 2653 –2657.

Smyth (1999) The use of electrospray mass spectrometry in the detection and determination of molecules of biological significance. Trends in analytical chemistry **18**, 335-346.

Sodum, R. S. and Fiala, E. S. (1997) Amination of tyrosine in liver cytosol protein of male F344 Treated with 2-nitropropane, 2-nitrobutane, 3-nitropentane, or acetoxime. Chemical Research In Toxicology **10**, 1420-1426.

Songyang, Z. and Cantley, L. C. (1995) Recognition and specificity in protein tyrosine kinase-mediated signalling. Trends in Biochemical Sciences **20**, 470-475.

Songyang, Z., Carraway, I. I. I. K., Eck, M. J., Harrison, S. C., Feldman, R. A., Mohammadi, M., Schlessinger, J., Hubbard, S. R., Smith, D. P., Eng, C., Lorenzo, M. J., Ponder, B. A. J., Mayer, B. J., and Cantley, L. C. (1995) SH2 domains recognize phosphopeptide sequences. Nature **373**, 536-539

Songyang, Z., Shoelson, S. E., Chaudhuri, M., Gish, G., Pawson, T., Haser, W. G., King, F., Roberts, T., Ratnofsky, S., Lechleider, R. J., Neel, B. G., Birge, RB, Fajardo, J. E., Chou, M. M., Hanafusa, H., Schaffhausen, B., and Cantley, L. C. (1993) SH2 domains recognise specific phosphopeptide sequences. Cell **72**, 767-778.

Songyang, Z., Fanning, A. S., Fu, C., Xu, J., Marfertia, S. M., Chishti, A. H., Cromptom, A., Chan, A. C., Anderson, J. M., Cantley, L. C. (1997). Recognition of unique carboxyl-terminal motifs by distinct PDZ domains. Science **275**, 73-77.

Souza, J. M., Daikhin, E., Yudkoff, M., Raman, C. S., Ischiropoulos, and H. (1999) Factors determining the selective nitration of protein tyrosine nitration. Archives of Biochemistry & Biophysics **371**, 169-178.

Stamler, J. S., Lamas, S. and Fang, F. C. (2001) Nitrosylation: the prototypic redox based signalling mechanism. Cell **106**, 675-683.

Stamler, J. S., Toone, E. J., Lipton, S. A., and Sucher, N. J. (1997) (S)NO signals:translocation, gegulation and a consensus motif . Neuron **8**, 691-696.

Styer (1988). Biochemistry. W. H. Freeman and Co. New York.

Suzuki, Y. J., Forman, H. J. and Sevanian, A. (1997) Oxidants as stimulators of signal transduction. Free Radical Biology and Medicine **22**, 269-285.

Szabo, C. (1996) DNA strand breakagege and activity and activation of PARS: a cytotoxic pathway triggered by peroxynitrite. Free Radical Biology & Medicine **21**, 855-869.

Takakura, K., Beckman, J. S., MacMillan-Crow, LA, and Crow, J. P. (1999) Rapid and irreversible inactivation of protein phosphatases PTP1B, CD45 and LAR by peroxynitrite. Archives of Biochemistry & Biophysics **369**, 197-207.

Tomlinson, M. G., Lin, J. and Weiss, A. Lymphocytes with a complex: adaptor proteins in antigen receptor signalling. Immunology Today **21**, 584-591.

Tsuchiya S., Ogura, K., Hatanaka, H., Nagata, K., Terasawa, H., Mandiyan, V., Schlessinger J., Aimoto, S., Ohta, H. and Inagaki, F. (1999) Solution structure of the SH2 domain of Grb2/Ash complexed with EGF receptor-derived phosphotyrosine-containing peptide. Journal of Biochemistry **125**, 1151-1159.

Tu, Y., Kucik D. F., Wu, C. (2001) Identification and kinetic analysis of the interaction between Nck-2 and DOCK 180. FEBS **491**, 193-199.

Tuo, J., Liu, L., Poulsen, H., E., Weiman, A., Svendsen, O. and Loft, S. Importance of guanine nitration and hydroxylation in DNA in vitro and in vivo. Free Radical Medicine and Biology **29**, 147-155.

Valentovic, M. A. and Ball, J. G. (1999) 2-aminophenol and 4-aminophenol toxicity I renal slices from Sprague-Deawley and Fischer 344 rats. Journal Toxicology and Environmental Health, Part A, **55** 225-240.

Van der Vleit, A., O'Neill, C.,A., Halliwell, B., Cross, C. E. and Kaur H. (1994) Aromatic hydroxylation and nitration of phenylalanine and tyrosine by peroxynitrite. FEBS Letters 339, 89-92.

Van der Vliet, A., Eiserich, JP, Halliwell, B., and Cross, C. E. (1997) Formation of reactive nitrogen species during peroxidase-catalysed oxidation of nitrite: a potential additional mechanism of nitric oxide-dependant toxicity. Journal of Biological Chemistry **272**, 7617-7625.

Van der Vleit, A., Hristova, M., Cross, C. E., Eiserich, J. P. and Goldkorn T. (1998) Peroxynitrite induces covalent dimerisation of epidermal growth factor receptors in A431 epidermoid carcinoma cells. Journal of Biological Chemistry **273**, 31860-31866.

Viani, M. B., Pietrasanta, L. I., Thompson J. B., Chand, A., Gebshuber, I. C., Kindt J. H., Richter M., Hansma H. G., and Hansma P. K. (2000) Probing protein-protein interactions in real time. Nature Structural Biology **7**, 644-647.
Virag, L., Scott, G. S., Cuzzocrea, S., Marmer, D., Salzman, A. L., and Szabo, C. (1998) Immunology 94, (pp 345-355)

Waksman G, Shoelson SE, Pant N, Cowburn D, Kuriyan J. (1993) Binding of a high affinity phosphotyrosyl peptide to the Src SH2 domain: Crystal structures of the complexed and peptide-free forms. Cell **72**, 779-790.

Waksman, G., Kominos, D., Robertson, S. C., Pant, N., Baltimore, D., Birge, R. B., Cowburn, D., Hanafusa, H., Mayer, B. J., Overduin, M., Resh, M. D., Rios, C. B., Silverman, L., and Kuriyan, J. (1992) Crystal structure of the phosphotyrosine recognition domain SH2 of v-src complexed with tyrosine-phosphorylated. Nature **358**, 646-653.

Weiss, S. (2000) Measuring conformational dynamics of biomolecules by single molecule fluorescence spectroscopy. Nature Structural Biology **7**, 724-729.

Weston, A. and Brown, P. R. (1997) HPLC and CE: principles and practice. Academic Press, London.

Williams, J. C., Wierenga, R. K., and Saraste, M. (1998) Insight into Src kinase functions: structural comparisons. Trends in Biochemical Sciences **23**, 179-184.

Wilm, M. S. and Mann M. (1994) Electrospray and Taylor-Cone theory, Dole's beam of macromolecules at last? International Journal of Mass Spectrometry and Ion Processes **136**, 167-180.

Wilm, M. S. and Mann M. (1996) Analytical properties of nanoelectrospray ion source. Analytical Chemistry **68**, 1-8.

Wink, D., A. and Mitchell, J., B. (1998) Chemical biology of nitric oxide: insight into regulatory, cytotoxic and cytoprotective mechanisms of nitric oxide. Free Radical Biology and Medicine **25**, 434-456.

Yamakura, F., Taka, H., Fujimura, T., and Murayama, K. (1998) Inactivation of human manganese-superoxide dismutase by peroxynitrite is caused by exclusive nitration of tyrosine 34 to nitrotyrosine. Journal of Biological Chemistry **273**, 14085-14089.

Yi, D., Smythe, G., A., Blount, B., C. and Duncan, M., W. (1997) Peroxynitrite-mediated nitration of peptides: characterisation of products by electrospray and combined gas chromatography-mass spectrometry. Archives of Biochemistry and Biophysics **344**, 253-259.

Zhang, P., Wang, Y.-Z., Kagan, E., and Bonner, J. C. (2000) Peroxynitrite targets the epidermal growth factor receptor, Raf-1 and MEK independently to activate MAPK. Journal of Biological Chemistry **275**, 22479-22486.

Zhang, Z.-Y., Thieme-Sefler, A. M., Maclean, D., McNamara, D. J., Dobrusin, E. M., Sawyer, T. K., and Dixon, J. E. (1993) Proceedings of The National Academy of Sciences of The United States of America 90, (pp 4446-4450)

Zhou, M., Martin, C. and Ullrich, V. (1997) Tyrosine nitration as a mechanism of selective in activation of prostacyclin synthase by peroxynitrite. Biological Chemistry **378**, 707-713.

APPENDIX I:

SOLUTIONS AND BUFFERS

ATP solution
0.2 mM ATP
30 mM $MgCl_2$
in kinase assay buffer

Blocking Buffer
TBS
0.1% Tween-20
10% m/v non-fat dry milk

Kinase assay buffer
50 mM HEPES, pH 7.5
0.1 mM EDTA
0.015% Brij 35.

Kinase dilution buffer
0.1 mg/ml BSA
0.2% β-mercaptoethanol.

Lysis Buffer
20 mM Tris (pH 7.5)
150 mM NaCl
1 mM EDTA
1 mM EDTA
1% Triton X-100
2.5 mM sodium pyrophosphate
1 mM β–Glycerolphosphate
1 mM Na_3VO_4
1 mM PMSF (add just before use).
1 in 100 dilution Mammalian protease inhibitor cocktail (add just before use).

^{15}N labelled M9 minimal media (per litre)
8.0 g Na_2HPO_4
2.0 g KH_2PO_4
3.0 g D-Glucose
0.6 g ^{15}N labelled NH_4Cl
0.5 g NaCl
10.0 ml Trace elements solution
1.0 ml 0.3 M Na_2SO_4
1.0 ml Thaimine HCl (1 mg/ml)
1.0 ml Biotin (1 mg/ml)
1.0 ml 1M $MgSO_4$
0.3 ml 1M $CaCl_2$
150 mg L-Proline
75 mg L-Leucine
50 mg Ampicillin

NMR Buffer
10 mM Phosphate buffer, pH 6.5
0.02 % Azide

Sample Buffer
0.1 M Tris-HCl, pH 6.8
24 % (v/v) Glycerol
1 % SDS
1 % β-mercaptoethanol
0.02 % Commassie G-250

TBS
Tris-HCl, pH 8.5
150mM NaCl

TEN Buffer
Tris-HCl, pH 7.4
0.5 M EDTA

Trace elements solution (100 x concentration) per litre
5 g EDTA
1.6 g $MnCl_2$
0.5 g $FeCl_3$
50 mg $ZnCl_2$
10 mg $CuCl_2$
10 mg $CoCl_2$
10 mg H_3BO_3

Transfer Buffer
25 mM Tris base
0.2 M glycine
20% methanaol (pH 8.5)

TTBS
Tris-HCl, pH 8.5
150mM NaCl
0.1% (v/v) Triton X-100

APPENDIX I:

SOLUTIONS AND BUFFERS

ATP solution
0.2 mM ATP
30 mM $MgCl_2$
in kinase assay buffer

Blocking Buffer
TBS
0.1% Tween-20
10% m/v non-fat dry milk

Kinase assay buffer
50 mM HEPES, pH 7.5
0.1 mM EDTA
0.015% Brij 35.

Kinase dilution buffer
0.1 mg/ml BSA
0.2% β-mercaptoethanol.

Lysis Buffer
20 mM Tris (pH 7.5)
150 mM NaCl
1 mM EDTA
1 mM EDTA
1% Triton X-100
2.5 mM sodium pyrophosphate
1 mM β–Glycerolphosphate
1 mM Na_3VO_4
1 mM PMSF (add just before use).
1 in 100 dilution Mammalian protease inhibitor cocktail (add just before use).

^{15}N labelled M9 minimal media (per litre)
8.0 g Na_2HPO_4
2.0 g KH_2PO_4
3.0 g D-Glucose
0.6 g ^{15}N labelled NH_4Cl
0.5 g NaCl
10.0 ml Trace elements solution
1.0 ml 0.3 M Na_2SO_4
1.0 ml Thaimine HCl (1 mg/ml)
1.0 ml Biotin (1 mg/ml)
1.0 ml 1M $MgSO_4$
0.3 ml 1M $CaCl_2$
150 mg L-Proline
75 mg L-Leucine
50 mg Ampicillin

NMR Buffer
10 mM Phosphate buffer, pH 6.5
0.02 % Azide

Sample Buffer
0.1 M Tris-HCl, pH 6.8
24 % (v/v) Glycerol
1 % SDS
1 % β-mercaptoethanol
0.02 % Commassie G-250

TBS
Tris-HCl, pH 8.5
150mM NaCl

TEN Buffer
Tris-HCl, pH 7.4
0.5 M EDTA

Trace elements solution (100 x concentration) per litre
5 g EDTA
1.6 g $MnCl_2$
0.5 g $FeCl_3$
50 mg $ZnCl_2$
10 mg $CuCl_2$
10 mg $CoCl_2$
10 mg H_3BO_3

Transfer Buffer
25 mM Tris base
0.2 M glycine
20% methanaol (pH 8.5)

TTBS
Tris-HCl, pH 8.5
150mM NaCl
0.1% (v/v) Triton X-100

APPENDIX II:

NMR ASSIGNMENTS

^{1}H ASSIGNMENTS OF DS4

Residue	HN	Hα	Hβ	Hβ'	Hγ	Hγ'	Hδ	Hδ'	Other
1 Glu	8.23	4.24	2.17	2.14	1.95	1.88			
2 Pro		4.39			1.98	1.956	3.846	3.642	
3 Gln	8.442	4.23	1.96	1.887	2.25	2.25			Hε 7.46 6.80
4 Tyr	8.19	4.55	3.02	2.90			7.02 (nDS4 7.85)	(nDS4 7.41)	Hε 6.71 (nDS4 7.00)
5 Glu	8.23	4.22	1.95	1.82	2.18	2.18			
6 Glu	8.44	4.20	2.22	2.16	2.22	2.15			
7 Ile	8.21	4.55	1.15		1.39	1.12	0.82		
8 Pro	4.41				2.01	1.92	3.84	3.65	
9 Ile	8.21	4.42	1.82		1.41	1.15	0.87		

HSQC BACKBONE ASSIGNMENTS OF ^{15}N LABELLED FYN SH2 DOMAIN BOUND TO DERIVATIVES OF DS4

Residue number	Phosphopeptide assignments			Nitropeptide assignments[a]		
	^{1}H chemical shift	*^{15}N chemical shift*	*Chemical shift change[b]*	*^{1}H chemical shift*	*^{15}N chemical shift*	*Chemical shift change[b]*
143	U	U	0	U	U	0
144	U	U	0	U	U	0
145	5.599	109.709	0.1369352	5.744	110.007	0.0111158
146	7.741	122.253	0.0039699	7.736	122.57	0.0352206
147	7.725	119.542	0.1028611	7.727	119.798	0.1214384
148	8.908	121.785	0.0115741	8.907	121.813	0.0118727
149	10.758	133.466	0.0124664	10.76	133.427	0.0082608
150	7.334	122.378	0.0293171	7.344	122.318	0.0190759
151	8.962	127.758	0.0221775	8.959	127.732	0.0226504
152	5.488	104.713	0	U	U	0
153	8.506	123.727	0.2781155	8.576	126.822	0.0406123
154	7.399	127.782	0.0310928	7.462	127.716	0.0322744
155	8.997	114.023	0.0144461	9.116	115.193	0.1660015
156	8.444	123.329	0.1419771	8.475	121.775	0.018976
157	8.659	118.127	0.1477871	8.501	117.579	0.0195489
158	8.065	120.413	0.08256	7.948	120.795	0.0451991
159	8.573	123.37	0.0093941	8.539	123.149	0.0403604
160	8.196	116.376	0.0279694	8.116	116.165	0.1078862
161	7.646	117.474	0.0100841	7.691	117.658	0.0389539
162	U	U	0	U	U	0
163	8.036	118.869	0.0569896	7.947	118.69	0.0415384
164	7.97	117.682	0.0311752	7.996	117.711	0.0573362
165	6.995	116.111	0.0262185	6.994	116.105	0.0270054
166	U	U	0	U	U	0
167	8.184	113.289	0.0178986	8.194	113.343	0.0130384
168	6.898	119.699	0.0642029	6.935	119.749	0.0270002
169	U	U	0	U	U	0
170	8.605	122.923	0.0161372	8.615	122.884	0.0084853
171	9.115	113.048	0.0342854	9.105	113.116	0.0430726
172	7.677	120.353	0.01622	7.68	120.335	0.0152398
173	8.323	123.321	0.13933	8.444	123.246	0.2392824
174	8.895	114.064	0.0345769	8.866	114.867	0.1162739
175	9.278	120.163	0.0193982	9.253	120.174	0.0150147
176	9.022	123.898	0.0530273	9.019	123.953	0.0505157
177	8.865	121.907	0.0696419	8.854	121.95	0.0606539
178	7.829	116.257	0.1360868	7.702	115.349	0.0579162
179	10.66	131.292	0.2588035	10.05	128.643	0.4301193
180	8.163	111.27	0.2716381	7.693	115.342	0.1156713
181	7.725	119.581	0.0611376	10.45	128.549	0.0069462
182	8.455	128.124	0.0087201	7.966	109.71	0.040096
183	8.723	114.226	0.1088348	7.672	119.155	0.0662966
184	7.48	121.379	0.038541	8.49	128.359	0.0447595
185	8.841	117.924	0.0614369	8.77	114.707	0.2533925
186	9.698	117.398	0.162231	7.476	120.871	0.0357329
187	9.61	128.889	0.2666927	9.535	129.689	0.219545

188	9.045	125.442	0.0163368	8.963	125.41	0.0663193
189	9.013	122.11	0.0156208	9.02	122.058	0.0205205
190	9.084	127.577	0.0080399	U	U	0
191	9.267	130.963	0.1196662	9.263	131.504	0.1190195
192	10.188	130.403	0.0010198	10.187	130.419	0.0024413
193	6.648	123.105	0.0602685	6.669	123.077	0.0408902
194	7.818	115.307	0.0217816	7.829	115.443	0.0052
195	8.101	118.869	0.2601151	8.098	118.845	0.3480002
196	9.089	119.114	0.0379415	9.062	119.036	0.010018
197	7.388	108.755	0.030024	7.404	108.777	0.0140357
198	8.793	126.905	0.0086579	8.788	126.875	0.0130599
199	8.493	119.387	0	U	U	0
200	8.517	119.875	0.0175046	8.529	119.978	0.032966
201	8.52	125.811	0.0364944	8.508	126.143	0.00402
202	8.634	119.548	0	U	U	0
203	9.891	122.106	0.2210165	9.729	122.906	0.0415727
204	9.618	125.004	0.7970014	9.111	124.636	0.2921405
205	8.975	126.539	0.1108213	9.039	127.414	0.0191471
206	8.114	126.694	0.6907187	8.118	126.626	0.6957718
207	8.331	119.403	0.0720447	8.356	119.566	0.0436492
208	8.563	129.831	0.0743494	8.607	129.896	0.0329801
209	8.736	124.67	0.0509608	8.735	124.524	0.0367744
210	8.265	116.435	0.0313904	8.246	116.32	0.0349344
211	7.403	107.756	0.0180544	7.404	107.814	0.0184619
212	8.103	109.549	0.0588371	8.067	109.531	0.0269409
213	9.269	117.685	0.0400245	9.227	117.761	0.0252389
214	9.117	113.145	0.3205996	9.088	116.213	0.0545473
215	9.783	120.098	0.0220737	9.792	120.083	0.0244131
216	8.89	115.567	0.1269132	8.867	114.391	0.0601202
217	8.57	119.956	0.020195	8.409	119.618	0.1456728
218	7.679	118.097	0.0688561	7.711	117.858	0.0320351
219	7.833	124.865	0	U	U	0
220	7.768	120.175	0.0705056	7.816	120.174	0.0307247
221	9.172	118.263	0.0456426	9.148	118.17	0.0251921
222	9.029	122.557	0.0434166	U	U	0
223	7.278	102.128	0.0503314	7.302	102.144	0.0268888
224	8.806	122.029	0.0082	8.773	121.661	0.0033
225	9.079	116.245	0.2295997	9.002	118.216	0.0272325
226	7.854	119.146	0.04245	7.827	118.999	0.0144807
227	7.002	123.922	0.0184391	7.011	123.849	0.0220429
228	7.88	120.234	0.0633937	7.901	120.328	0.061573
229	7.937	119.938	0.3897007	U	U	0
230	7.577	118.54	0.0351648	7.595	118.512	0.0233529
231	7.395	114.613	0.0694637	7.43	114.409	0.0294871
232	7.584	114.613	0.2063097	7.594	114.848	0.0255
233	7.149	121.788	0.0680089	7.157	121.534	0.0414788
234	7.403	115.521	0.2154172	7.468	115.913	0.1589552
235	8.229	121.897	0.047352	8.221	122.104	0.0263105
236	8.09	113.882	0.3438661	8.07	114.691	0.3974653
237	8.089	104.693	0.2250046	8.128	105.182	0.1629375
238	7.81	119.997	0.0550499	U	U	0
239	7.561	114.068	0.1647362	7.651	114.001	0.0756455
240	6.883	111.116	0.4422411	U	U	0
241	U	U	0	U	U	0

242	7.835	121.184	0.0373877	7.831	121.315	0.024286
243	8.986	122.354	0.0125603	8.995	122.306	0.0185699
244	7.98	116.079	0.0361519	7.996	116.165	0.0180278
245	U	U	0	U	U	0
246	8.182	121.422	0.0054781	8.183	121.514	0.0042202
247	8.256	123.499	0.0197101	8.26	123.47	0.0164
248	7.526	120.562	0.0138928	7.519	120.495	0.0231206

U signifies those resonances that were unassigned.

[a] The assignments for the nDS4 were taken at a peptide concentration of 5 molar equivalent of SH2.

[b] The equation 3.1 (p. 112) was used to determine the chemical shift change.

APPENDIX III:

LIST OF TABLES FIGURES AND EQUATIONS

FIGURES

CHAPTER 1: INTRODUCTION

CHAPTER 2: SYNTHESIS AND CHARACTERISATION OF DERIVATIVES OF DS4 AND FYN SH2 DOMAIN

CHAPTER 3: QUALITATIVE AND QUANTITATIVE STUDIES OF THE BINDING OF DS4' DERIVATIVES TO FYN SH2 DOMAIN

TABLES

EQUATIONS